THE USE OF BIOREACTORS AND A VERTICAL FLOW REACTOR IN THE TREATMENT OF CIRCUM-NEUTRAL MINE AFFECTED WATER

A thesis submitted in partial fulfilment of the requirements for the Degree of Master of Science

at the University of Canterbury

by

Stephanie R. Hayton

Department of Geological Sciences,
University of Canterbury, Christchurch, New Zealand
June 2020

Abstract

OceanaGold's Globe Progress Mine, located in the West Coast of New Zealand, is a hard rock gold mine which ceased operation in 2015 and is now in the closure phase. During operations an active water treatment plant was used to remove contaminants before release offsite. As the mine transitioned into closure, a site-wide water balance model based on sampling data identified the need for treatment of various water sources for arsenic and iron. Field trials were established to test two methods of passive treatment, sulphate reducing bioreactors and a meso-scale vertical flow reactor to determine the most appropriate passive treatment option for post-closure. To establish the most efficient substrate mixes, four bioreactors with different combinations of organic media, with the addition of either mussel shells or biosolids were constructed. The bioreactors were fed water from the sites combined Underdrains (median chemistry: 28 g/m^3 iron, 1.69g/m^3 arsenic and 430 g/m^3 sulphate). Results showed that in all cases biosolids treatments out preformed mussel shell treatments, but ratios of other materials had no effect. At 50 hours HRT biosolid treatments showed removal of iron at 60%, arsenic at 75%, and sulphate at 20%. Results also indicated that in most cases there was a positive relationship with HRT, but this was strongest for sulphate removal. An insulated tank was also trialled to reduce the effect of cold ambient air temperatures on the bacteria's activity. This showed that internal temperature was dictated more by influent temperature but using an insulted tank prevented diurnal temperature fluctuations in the outside edge of substrates, and therefore maintaining a more constant temperature throughout the reactor. The vertical flow reactor (VFR), which utilises oxidation of iron rich water to precipitate onto a non-reactive gravel bed, and then allows for adsorption of other metals such as arsenic onto precipitated iron hydroxides. Water from the waste rock underdrain (median chemistry: 7.6g/m^3 of iron, 0.17g/m^3 of arsenic, and 575g/m^3 of sulphate) was fed through the VFR. Results from this showed median iron and arsenic removal was 99.10% and 94.83%, respectively. High removal was achievable at even very low residence times, with 84% iron and 75% arsenic removal at 10.5 hrs residence time. These results showed a VFR could remove adequate iron and arsenic with a small footprint and was deemed appropriate as a full-scale system for the study site.

Acknowledgments

Charles Darwin once said "It is the long history of humankind (and animal kind, too) that those who learned to collaborate and improvise most effectively have prevailed." and this body of research couldn't have been achieved without the gracious help, and resources that I received from so many and also, a substantial amount of improvisation.

There are so many who work with me on this project to enable it to happen I would like to take this opportunity to thank each and every one of you, as this project could not have been able to happen without you time and support. I would especially like to thank the following people:

I would like to take this opportunity to first thank those who allowed me the ability to undertake this research in the first place. This includes all those at OceanaGold Corporation (OGC) who encouraged and enabled me to pursue further study, but I would especially like to thank Duncan Ross and Dale Oram who opened the door and made this possible in the first place.

I would secondly like to thank the all those the Verum Group (VG) (previously CRL Energy Ltd) and from the University of Canterbury (UC) who have given continual guidance and encouragement, especially my supervisors Dave Trumm (VG) and Travis Horton (UC) who have been so patient and supportive. I would also like to thank James Pope (VG), Alex Nicholls (UC) and Janet Warburton (UC).

I would next like to thank all those at OGC who helped to make this research a reality and continued to assist in the monitoring, maintenance, and improvements throughout the course of this study. In particular, I would like to thank Jeffery Nyenhuis, Geoff Archer and Robert Wallace who helped me build these systems and continued to come up with innovative solutions to problems we faced along the way.

I would also like to make special to Megan Williams for the continual support and assistance with sampling and monitoring of the systems, even though it was not always a pleasant or welcome task and the meticulous maintenance of the sites data base which made data analysis that much more painless. I would also like to thank Hannah Christenson (VG) for the lab assistance and continual couriering of equipment and Will Olds for the counsel and advice.

I would like to make a special thanks to Darren Lee (OGC), Mark Clarke (OGC), David Bickerton (OGC) and Mark Cadzow (OGC) for the financial assistance, resources, and time to allow me to complete this research project. Thank you, also, to Christchurch City Council for gifting me the biosolids which were used in this trial.

Thank you to all my friends and family, you provide me with support every day without even knowing it. A special thanks to Justyna Giejsztowt, who skyped me countless times and invested her precious time to talk me through and help me with a long-forgotten discipline. Finally, to Dylan Butcher and Phantom, thank you for your ongoing support and encouragement, thanks for listening and offering advice and thank you most of all for just being there.

Thank you!

Contents

List of Figures

List of Tables

List of Acronyms

AMD -Acid mine drainage
BIOIN - Bioreactor Influent
DC01 – Devils Creek downstream compliance point
DCSP – Devils creek silt pond
DCWRS – Devils Creek waste rock stack
DOC – Department of conservation
B-LC - Biosolids, less compost
B-MC - Biosolids, more compost
GPL – Globe pit lake
HRT - Hydraulic retention time
INS - Insulated
M-LC - Mussel shells, less compost
M-MC - Mussel shells, more compost
MAW - Mine affected water
NMD – Neutral mine drainage
PAG - Potentially acid/arsenic generating
RDRN - Rock drain
SMC - Spent mushroom compost
SRB - Sulphate reducing bacteria
TSF – Tailings Storage Facility
TSS – Total suspended solids
TT - Temperature treatment
VFR - Vertical flow reactor
WCRC – West Coast regional council
WRD – Waste rock drain
WRS – Waste rock stack
WTP – Water treatment plant

1. Chapter One- Introduction, Research Objectives and Thesis Layout

1.1 Introduction

Mining has many environmental impacts, one of the most notable impacts is the production of acid mine drainage (AMD) or mine affected water (MAW). (Neculita et al. 2007; Celebi and Özdemir 2015; Vasquez et al. 2016b). MAW occurs through the oxidation of minerals, often pyritic, present in the host rock during and after mining operations (Skousen et al. 2017). The acidic and metal rich water produced through mining activities cause many adverse effects to the environment, in particular to aquatic ecosystems, such as, increased acidity, suspended solids, presence of heavy metals and habitat reduction through armouring of stream beds (Gray et al. 2016; Skousen et al. 2019; Acharya and Kharel 2020). In the US alone, over 20,000km of streams have been impacted by MAW, in which the majority is from abandoned legacy sites (Skousen et al. 2019). While prevention is the best method of control for MAW (Acharya and Kharel 2020) it is not always considered or possible, therefore the treatment or control of site discharges needs to be incorporated into the closure plans for modern mining operations. Active treatment through water treatment plants is often undertaken during operation of mine sites but is often not practical to operate long-term after the closure of an operation (Nielsen et al. 2018). Passive Treatment is a far more attractive and practical solution, as it has been shown to require less ongoing maintenance and cost (Trumm 2010; Skousen et al. 2017). This research looks to investigate passive treatment options for an operation in the West Coast of New Zealand, which has several MAW sources which will require long-term treatment. The site, which has recently moved into a closure phase, has circum-neutral seepages and discharges that contain elevated arsenic and iron but has very limited space due to steep topography. Therefore, careful consideration needs to made to the type of passive treatment which will be suitable for both the predicted flows and also the chemistry (Trumm 2010; Skousen et al. 2017).

In order, to investigate the best option for the site a literature review was undertaken to establish the passive treatment systems which would be most fitted to the site (chapter 2). This established that two systems may be applicable for the sites chemistry and sizing constraints, a) a sulphate reducing bioreactor and b) a vertical flow reactor (VFR). Much of the research on bioreactors suggests that there are three main factors which influence the efficiency; substrate mixture, hydraulic retention time (HRT) and temperature (Uster et al. 2014; Trumm et al. 2015a; Vasquez et al. 2016b; Skousen et al. 2017; Nielsen et al. 2018), therefore this research aimed to look at all three factors. Four substrate mixtures were trialled, these included two treatments with biosolids, which have never been trialled as a substrate in passive treatment to the authors knowledge, and two with mussel shells, which have been shown to be effective previously (McCauley et al. 2008; Uster et al. 2014; DiLoreto et al. 2016). Substrate mixtures for treatments one and two contained: 30% sawdust, 30% bark, 20% spent mushroom compost (SMC) and either 20% biosolids or 20% mussel shells (noted as B-LC (biosolids, less compost) and M-LC (mussel shells, less compost) throughout text), while treatments three and four contained 20% sawdust, 20% bark, 40% spent mushroom compost (SMC) and either 20% biosolids or 20% mussel shells (noted as B-MC (biosolids, more compost) and M-MC (mussel shells, more compost) throughout text). HRT was measured and compared with metal and sulphate removal rates. A fifth and sixth treatment were used to test whether an insulated tank would prevent cold ambient air temperatures effecting the internal temperature, and in turn if the temperature was higher in the insulated tank, did it show better treatment

performance. A meso-scale VFR was also trialled to assess the removal rates of arsenic and iron, especially at low HRTs.

1.2 Research Objectives

Previous research has shown that both bioreactors (an anaerobic system) and Vertical Flow Reactors (aerobic) are both viable options for the passive treatment of either acid mine drainage, or circum-neutral mine drainage.

Many studies have investigated different substrates and substrate mixes in bioreactors to establish the most efficient for both metal removal and neutralisation (Zagury et al. 2006; Uster et al. 2014; Uster 2015; DiLoreto et al. 2016; Vasquez et al. 2016b), although the use of the biosolids has not been trialled, therefore the first objective of this research was to investigate metal removal efficiencies with different material compositions, including biosolids, in bioreactors to treat circum-neutral mine affected water. It is also well documented that most passive treatment systems also require a long hydraulic residence times and therefore a large foot print (Trumm 2010; Skousen et al. 2017; Vasquez et al. 2018), therefore the second objective of this research was to determine how HRT effects removal efficiency within the different substrate mixes. Temperature has been shown to impact the removal efficiency of bioreactors through bacterial growth or activity, decomposition of substrates, and solubility of hydrogen sulphide (Zagury et al. 2005; Uster 2015). Several studies have indicated that sulphate reducing bacteria (SRB) have less activity at lower temperatures and therefore sulphate reduction decreases substantially (Nevatalo et al. 2010; Van Den Brand et al. 2014; Nielsen et al. 2018). As the study site often has sub-zero temperatures during winter months, objective three of this research was to determine the mechanisms which determine internal temperature of a bioreactor and trial the use of insulated tanks to buffer low against ambient air temperatures.

It has been suggested that vertical flow reactors are able to remove metals, such as iron, arsenic and manganese with high efficiency and can require half the footprint of traditional oxidising precipitation systems such as a settling ponds (Sapsford 2013; Trumm et al. 2017; Blanco et al. 2018). As the study site has a small area available for a passive treatment system, the fourth objective of the study was to test the efficiency and HRT of a meso-scale VFR for the removal of iron. Removal of arsenic using iron products, such as ferric chloride, in active water treatment plants is a fairly common practice. It has also been shown that adsorption of arsenic onto iron hydroxides in passive systems is possible (Rait et al. 2010). It is, therefore, the fifth and last objective of this study, to investigate the potential for arsenic removal through coprecipitation and adsorption on the newly formed ochre bed within the VFR by the addition of high arsenic water from a secondary source (a tailings impoundment).

Objective summary:

1. Investigate different material compositions for bioreactors to treat mine affected water, including biosolids.
2. Investigate the effect of hydraulic retention time on the efficiency of metal and sulphate removal
3. Investigate the effect of temperature on bioreactors by using an insulated tank
4. Investigate the efficacy of a large-scale vertical flow reactor to remove iron from mine affected water
5. Investigate the removal of arsenic from tailings water as a proxy for mine pit lake water on a newly formed ochre bed within the vertical flow reactor

In order to achieve Objectives One and Two, four bioreactors were established with different substrate composition, and the influent and effluent concentration on contaminates was measured to establish the removal efficacy of each mix, and at a variety of HRTs. This research shows that substrate mixes containing biosolids had higher removal rates for iron, arsenic and sulphate than other mixes trailed. It also concludes that iron and sulphate removal for all substrate mixes is positively correlated with HRT, whereas while arsenic showed a positive correlation for most mixes, not all showed this trend. Objective Three was achieved by establishing two smaller bioreactors with the same substrate mix, one standard tank and one insulated, and measuring contaminate removal of each, as well as the large bioreactor of the same mix. All tanks were also fitted with two temperature probes, one in the middle and one to the side, to establish internal temperature dynamics. This concludes that the internal temperature of all tanks is determined more by influent water temperature than ambient air temperature, but the side of the tanks is influenced more by external temperatures with diurnal fluctuations recorded. Data also shows that the sides of the insulated tank were not affected by diurnal temperature fluctuation to the same extent as the non-insulated tanks. A meso-scale VFR was installed to achieve Objectives Four and Five. This included treatment of an underdrain with elevated iron and then the addition of higher arsenic water from the sites tailings impoundment, with analysis of the influent and effluent to establish removal efficiencies. Data from this system shows that the VFR is extremely efficient at removing high percentages of iron and arsenic at relatively low HRTs, although the removal efficacy of high arsenic water was not able to be undertaken fully due to improvement in tailings impoundment water quality.

1.3 Thesis Layout

This thesis is divided into seven chapters, including this chapter, which will not be discussed.

Chapter Two (*Literature Review*): This chapter introduces acid mine drainage and mine affected water and explores the literature around the production of this water and the various treatment options. Further detail around the two specific treatment options of interest, Bioreactors and Vertical Flow Reactors, are then presented.

Chapter Three (*Setting and Context*): This chapter gives detail of the study sites location, geology, climate and topography, along with operational details in terms of regulatory requirements and land use obligations. It also explains the sites configuration and its water sources.

Chapter Four (*Methods*): This chapter explains the methodology of the research project. This is broken down into two sections. The first section presents bioreactor methods, which includes substrate selection and mix design, bioreactor design, system operation, sampling methodology and temperature monitoring. The second presents the VFR methodology, which includes the design, system operation and sampling methodology.

Chapter Five (*Results*): This chapter presents the findings of this research project. It is broken down into five sections. The first presents the results of the bioreactor substrate analysis and removal efficiencies of the different treatments. The second section presents the results of the effect of HRT on the bioreactors removal efficacies. The third section presents data from the bioreactor's temperature probes and the removal rates of the temperature treatments. The fourth section presents data the bioreactor precipitate analysis and the fifth section present the data from the vertical flow reactor trial, including metal removal, HRT, driving head and precipitate analysis.

Chapter Six (*Discussion*): This chapter discusses the findings of this research in more detail and looks to explain the reasons and mechanisms behind the results. This is broken down into three section. The first section discusses the results from the bioreactor trials. The second section discusses the results from the VFR trial, and the third section discusses options for a full-scale system and the applications of this research.

Chapter Seven (*Conclusions*): The seventh chapter concludes the findings of this research and provides suggestions for future work.

2. Chapter Two- Literature Review

What is AMD

Acid Mine Drainage (AMD) is one of the most significant impacts of mining on the environment. Acidification and metal loading in AMD impacted water bodies occurs due to sulphide and secondary sulphate mineral weathering in waste rock dumps, tailings impoundments and pit walls (Skousen et al. 2019). Sulphide/sulphate weathering (i.e. AMD) produces aqueous forms of H^+ and metals when minerals, such as pyrite (FeS_2) or melanterite ($FeSO_4 \cdot 7H_2O$), are exposed to near-surface waters (Skousen et al. 2017). The equations for the chemical weathering of pyrite is depicted below (Acharya and Kharel 2020).

$$(1)\quad FeS_2 + 3.5\,O_2 + H_2O \rightarrow Fe^{2+} + 2\,SO_4{}^{2-} + 2H^+$$

$$(2)\quad Fe^{2+} + \tfrac{1}{4}\,O_2 + H^+ \rightarrow Fe^{3+} + \tfrac{1}{2}\,H_2O$$

$$(3)\quad Fe^{3+} + 3H_2O \rightarrow Fe\,(OH)_3 + 3H^+$$

$$(4)\quad FeS_2 + 14\,Fe^{3+} + 8\,H_2O \rightarrow 15\,Fe^{2+} + 2\,SO_4{}^{2-} + 16H^+$$

Equation (1) shows the initial weathering of pyrite with the introduction of water and oxygen, which produces ferrous iron (the reduced form of iron) in solution, sulphate and acidity. The second equation shows ferrous iron interacting with dissolved oxygen and a hydrogen ion to produce ferric iron and water. In the third equation ferric iron with water produces iron hydroxide (iron precipitates) and more acidity. The fourth equation shows more pyrite interacting with ferric iron and water to produce more ferrous iron, more sulphate, and significantly more acidity from the hydrogen ions. In areas with carbonate bedrock, carbonate weathering increases alkalinity therefore buffering the AMD discharge. AMD-produced metals remain an issue in carbonate settings (Trumm and Pope 2015) and circum-neutral discharge with elevated metal concentrations is more commonly referred to as Mine Affected Water (MAW), or neutral mine drainage (NMD). Elevated metals are released due to the weathering processes, equation 1 shows this for pyrite, although other minerals release other metals also, such as arsenic from arsenopyrite (FeAsS), or antimony from Stibnite (Sb_2S_3) (Altun et al. 2014; Trumm et al. 2015a). While these discharges don't affect the stream pH as AMD does, it does however lead to the presence of elevated metals such as aluminium, iron, nickel, lead, arsenic, antimony and zinc (Trumm and Pope 2015; Sekula et al. 2018; Acharya and Kharel 2020).

MAW waters impact terrestrial systems, human health and due to the elevated metal concentrations and potentially low pH of MAW, there is normally a negative effect on downstream aquatic ecosystem (Gray and Harding 2012; Hogsden and Harding 2012a; Cadmus et al. 2016; Acharya and Kharel 2020). The specific impacts depend on several factors, including the metals present and their concentrations, the concentration of sulphate and the alkalinity (Gray and Harding 2012; Hogsden and Harding 2012b; Jellyman and Harding 2014). Some impacts to aquatic ecosystems due to contamination of MAW include acute toxicity, disruptions to food webs, migration, uptake of heavy metals, and precipitation of minerals onto the streambed causing habitat loss (Hogsden et al. 2013; Cadmus et al. 2016; Gray et al. 2016; Champeau et al. 2017; Acharya and Kharel 2020). To prevent significant impacts on waterways, mining companies in New Zealand are given compliance limits for nearby waterways to which they plan to discharge as part of their mining consents by local and regional councils. Compliance limits are based on water use and ecological protection. To meet these conditions during operations, mining companies will commonly use an active treatment, such as a water treatment plant.

Active Treatment

Active treatment is often expensive and requires regular maintenance/restocking, and therefore is impractical after a mine has gone into closure (Trumm 2010). Active treatment for wastewater, including mine water, covers a variety of different methods and chemicals (Skousen 2014). One of

the common methods of active treatment methods for AMD follows three steps: dosing with alkalinity, oxidation and sedimentation (Trumm 2010). OceanaGold's water treatment plant (WTP) uses the same basic three steps as for AMD, although since the water they are treating is neutral, instead of dosing for alkalinity, they dose with chemicals, such as ferric chloride and flocculants, to remove metals and aid in sedimentation. Ferric chloride acts as a coagulant but also removes metals, such as arsenic, through adsorption (Hering et al. 1996). Addition of coagulants reduce the forces which repel particles while flocculants helps to join particles together to form larger particles (Skousen 2014). OceanaGold use the addition of coagulants and flocculants, at the dosing step, to enhance the removal of Total Suspended Solids (TSS) through a clarifier before being discharged to a lagoon which is used as a polishing step before the water is allowed to be discharged offsite. Active treatment while generally more reliable than passive systems, requires chemicals (such as flocculants, coagulants, lime etc), power and extensive maintenance to ensure they remain reliable (Trumm 2010; Skousen 2014). Often one of the largest costs in an active water treatment plant is power costs associated with pumping, and measuring flows and dose rates (Trumm 2010; Skousen et al. 2017). Passive treatment is a less costly, less labour-intensive alternative, which is becoming an increasingly popular option for long term treatment of MAW after the closure of a mine site.

Passive treatment options

There are many different passive treatment options and the most appropriate approaches depend on the site-specific conditions, including: metal concentrations, flow rates, pH and acidity loads (Trumm 2010). Table 2-1 lists different passive treatment systems, the condition under which they operate and what they predominantly treat. All discharges from OceanaGold's Globe Progress Mine are circum-neutral, although as there is elevated iron present, passive treatment options need to account for the production of acidity through the hydrolysis of iron (equation 3). In the case of the Globe Progress discharges, data from the site suggests that there is sufficient alkalinity to offset the production of acid from this reaction and therefore there is no need for the addition of a neutralizing agent. Therefore, there are at least six treatment system options which treat for metals that may be applicable to this site; aerobic wetland, anaerobic wetland, vertical flow reactor, low-pH iron oxidation channel, vertical flow wetland (which is also referred to as successive alkalinity producing systems (SAPS) or reducing and alkalinity producing systems (RAPS)), and sulphate reducing bioreactor. Anaerobic and aerobic wetlands require large areas that are unavailable at this site and therefore impractical to trial. Low-pH iron oxidation channels target low pH water and are therefore also not an applicable treatment method for the neutral site water (Skousen et al. 2017). Vertical flow reactors are a viable option to treat iron rich neutral water, such as the Rock Drain, as they require a small space, relatively low cost and minimal maintenance (Trumm et al. 2015b). Bioreactors and vertical flow wetlands work in a similar manner, using organic materials and sulphate reduction to remove metals, although a bioreactor's main component is organic material whereas a vertical flow wetland is made predominantly of limestone chip with a smaller organic component (Skousen et al. 2017). A bioreactor is made up of a higher proportion of organics and as the MAW does not require alkalinity through the addition of limestone, a bioreactor is a more suitable treatment system for Globe Progress.

Table 2-1: Types of Passive treatment types.

System Type	Oxidation State	Treats
Open Limestone Drain (OLD)	Oxidising	Acidity
Diversion Well (DW)		Acidity
Limestone Leaching Bed (LLB)		Acidity
Slag Leaching Bed (SLB)		Acidity
Aerobic Wetland		Metals
Mn Removal Beds		Manganese
Vertical Flow Reactor		Iron
Low-pH Iron Oxidation Channel		Iron
Dosing with Limestone Sand		Acidity
Anoxic Limestone Drain	Reducing	Acidity
Anaerobic Wetland		Metals
Vertical Flow Wetland (VFW)		Metals + Acidity
Sulphate Reducing Bioreactor		Metals

Bioreactors

A bioreactor, otherwise referred to as a sulphate reducing bioreactor is a form of passive treatment in which sulphate reducing microbes convert sulphate to hydrogen sulphide and dissociated sulphides using organic substrates (DiLoreto et al. 2016; Isosaari and Sillanpää 2017; Skousen et al. 2017). The equation for this reaction is as follows (Neculita et al. 2007; DiLoreto et al. 2016):

$$(5)\quad 2\,CH_2O + {SO_4}^{2-} \rightarrow 2HCO_3^- + H_2S$$

$$(6)\quad M^{2+} + H_2S + 2HCO^{3-} \rightarrow MS + 2H_2O + 2CO_2$$

Where, in reaction (5) a simple organic carbon is used to reduce the sulphate to bicarbonate and hydrogen sulphide then in reaction (6) a catatonic metal (M^{2+}) along with the hydrogen sulphide and bicarbonate produce a metal sulphide precipitate. Removal of metals through sulphate reduction, and formation of sulphide minerals, within bioreactors has been shown to be effective for a range metals such as iron, arsenic, antimony and zinc (Altun et al. 2014; Uster et al. 2014; Trumm et al. 2015a; Vasquez et al. 2016b).

These systems rely on readily available carbon and sufficient permeability and porosity. The efficiency of different substrates and substrate mixes has been studied extensively eg. (Zagury et al. 2006; McCauley et al. 2008; Uster et al. 2014; DiLoreto et al. 2016; Skousen et al. 2017). Materials used in these systems are often waste products to make them more financially feasible. Products typically used are animal manures, sawdust, woodchip, spent mushroom compost, mussel shells, post peel, limestone, bark and compost (McCauley et al. 2008; Uster et al. 2014; DiLoreto et al. 2016; Vasquez et al. 2016b; Isosaari and Sillanpää 2017; Muhammad et al. 2017; Skousen et al. 2017). Most research suggest that a mixture of material that breaks down at different rates to ensure a constant carbon supply is essential to long-term operation (Gibert et al. 2004; Neculita and Zagury 2008; Skousen et al. 2017). This is backed up by Zagury et al. (2006) who did batch experiments of single source substrates and mixed substrates; they found that the mixed substrates were more effective at promoting sulphate reduction. They suggest that this is likely due to different carbon compounds resulting in higher variation in the microflora. Skousen et al. (2017) states there are 3 classifications of materials; 1) easily available substances which are consumed rapidly by the sulphate reducing bacteria (SRB) and other microbes and are often depleted within the first few months (eg. soluble sugars, starch, amino acids, and proteins); 2) Cellulose and hemicellulose, which

are broken down to simpler compounds by cellulose degraders and fermenting bacteria; and 3) lignins which break down very slowly, if at all. The material make-up of these systems not only provides a carbon source, but also provides sites for adsorption, nutrients, porosity and permeability. This may not always be achieved by organic materials and it is therefore not uncommon to add non-organic materials, such as gravel or shells to add permeability and/or alkalinity (Skousen et al. 2017).

The other three major factors which are highlighted by the literature as affecting the efficiency of these systems to treat MAW are pH, hydraulic retention time (HRT) and seasonal temperature fluctuations. A pH of 5 to 8 is required for SRB to thrive, with low pH (<5) inhibiting sulphate reduction and also increasing the solubility of sulphide minerals (Zagury et al. 2005). Bioreactors require a long HRT to successfully remove target metals and sulphate (Vasquez et al. 2016a; Skousen et al. 2017). HRT not only changes the microbial communities present within the system (Aoyagi et al. 2017; Vasquez et al. 2018), but can also affect metal removal (Uster et al. 2014; Vasquez et al. 2016a). Trumm et al. (2015a) found that at residence times of <5 hours antimony removal was around 40% in a field trial whereas at >20 hours was up to 98%, and Uster et al. (2014) found that in general a longer HRT showed higher metal removal and Zagury et al. (2005) suggests that at least 3-5 days HRT is required for precipitation of metal sulphides. It has also been suggested that short HRTs may not only not provide adequate time for SRB to neutralise acidity or precipitate metal sulphide but also might result in a loss of substrates through flushing of the system (Zagury et al. 2005).

Most bioreactor trials in the literature are small scale laboratory or batch tests which are not subject to seasonal temperature variation as are larger field trials. Field trials for denitrification bioreactors have shown seasonal fluctuations in microbial communities and a decrease in the operation efficacy due to cold winter temperatures (Porter et al. 2015; Hassanpour et al. 2017). Bioreactors for treatment of MAW are also highlighted as being temperature and climate dependent (Trumm 2010; Skousen et al. 2017). Trumm et al. (2015a) found antimony removal in a field scale trial was poor in winter, likely due to suppressed biological activity. It has been shown that temperature affects bacterial growth and activity, the breakdown kinetics of the substrates and the solubility of hydrogen sulphide (Zagury et al. 2005). It has also been suggested that SRB show poor performance if exposed to cold temperatures before acclimated, although once they have established, they are less affected by cold temperatures (Zagury et al. 2005; Nevatalo et al. 2010). Altun et al. (2014) found that removal of both arsenic and iron through the formation of sulphides was possible through formation of sulphide minerals through a bioreactor. In fact, they achieved up to 96% arsenic removal given the right chemical conditions. Bioreactors may be an effective treatment system for Globe MAW although due to variations in temperatures (about -8.5 to 33.7 °C[1]) it may cause issues in the running efficiency, which needs to be investigated.

Vertical Flow Reactors

Vertical flow reactors are a compact system in which Fe^{2+} is oxygenated to Fe^{3+} (equation 2) and then precipitated onto an unreactive gravel bed (equation 3) and on the ochre surface which forms on the surface of the gravel (Sapsford et al. 2006; Trumm et al. 2015b; Blanco et al. 2018). This treatment method has been shown to be effective in circum-neutral waters by filtration through the gravel bed and ochre layer and precipitation as hydrated oxides and oxyhydroxides, and in acidic water by precipitation or aggregation of nanoparticulate iron precipitate (Blanco et al. 2018). Sapsford et al. (2006) found they could remove 10-20 g/m^3/day of iron and Trumm et al. (2015b) found they could achieve >77% removal of iron in a similar system. It is well documented in the literature that metals can be removed from solution by adsorption onto iron hydroxides or oxyhydroxides (Rait et al. 2010; Trumm et al. 2015a; Luong et al. 2018). Iron sludges formed by AMD have been utilised at several sites to remove arsenic and antimony from MAW (Rait et al. 2010; Trumm et al. 2015a). Trumm et

[1] From all air temperature data available for the Reefton area from Macara GR. 2016. The climate and weather of west coast. NIWA Science and Technology Series (72):40 pp.

al. (2015a) used an AMD sludge from an abandoned coal mine, which consisted of goethite and ferrihydrite, to removal antimony in a small field trial. They found that the sludge removed up to 95% of antimony present, although the efficiency dropped over time as adsorption sites were filled. Similar removal of arsenic was achieve by Rait et al. (2010) in an earlier study, also using AMD sludges. Arsenic in AMD discharges has been found to be naturally removed by adsorption and absorption mechanism. This is because of the affinity arsenic has to the iron oxide/hydroxide precipitates due high surface reactivity (Paikaray 2015). While sorption onto oxide and hydroxide is the most prevalent removal mechanism for arsenic in AMD, another important process for arsenic removal when iron is present is co-precipitation, with the formation of Fe-OH-As or Fe-S-OH-As precipitates (Paikaray 2015). Therefore, it may be possible to use a VFR to precipitate iron hydroxides and oxyhydroxides onto a gravel bed from the waste rock underdrain at the Globe Progress Site (high iron, low arsenic) and utilise the sludge this creates to adsorb the arsenic from the pit water (modelled to have low iron but relatively high arsenic). As noted above, when iron precipitates it creates acidity (equation 3). As this system relies on the precipitation of iron, the water being treated must contain enough alkalinity to assure that pH is not affected. Monitoring data from Globe Progress suggests that this is the case for the Globe Progress MAW.

Key findings and implications for this research

There has been a lot of research into different media substrates for bioreactors, although no trials have been done which test whether biosolids would be an effective additive. Therefore, this media is tested in this research. There is mounting literature which supports the use of mussel shells to treat AMD, but none which test how it would perform as a bioreactor substrate for the treatment of neutral mine drainage, so this is being tested here.

Temperature has been shown to affect the rate in which the SRB function and therefore the removal rates that are possible within bioreactors. There is, however, very little research on whether the temperature inside a bioreactor can be maintained by insulating it from cold ambient air temperatures, so this is investigated in this this work.

Vertical Flow Reactors have been trialled at small scale and show promising results for both iron and arsenic removal but as this concept is fairly new there is limited research on larger scales, such as meso-scale nor have full-scale systems been installed yet, so this is included in the current study.

3. Chapter Three- Setting and Context

The objective of this chapter is to provide context and setting to the study site. In this chapter there is a brief explanation of the geographical and geological location of the site, climate, and topography. There is also an explanation of the operational context in terms of regulatory requirements and land ownership obligations. It also attempts to describe the sites layout, main features and water sources, around which this research is based.

3.1 The Site

OceanaGold's Globe Progress Mine is located approximately 7 km southeast of Reefton, in the West Coast of New Zealand's South Island (figure 3.1-1). It consists of steep topography, with an elevation range of about 300m over an area of approximately 260 Ha. The area is covered by a mature beech and podocarp forest, where undisturbed by the mine footprint. The site is located within the Reefton Goldfield which is a 15km by 35km area comprised of Greywacke and Argillite which has undergone several phases of metamorphism. The Globe Progress site is comprised of a prominently interbedded metasedimentary Greenland group host rock, with sulphide mineralisation containing gold, arsenic and antimony (Johnson and Pilson (1972); (Madambik and Moore 2013). It operated as an underground mine in the late 1800's through to about 1920 (Madambik and Moore 2013). OceanaGold began open cast mining at Globe Progress in 2006 which operated until 2015 when mining completed at a total footprint of 260 Ha. The site then went into care and maintenance until closure was announced in late 2016.

OceanaGold operates under an Access Agreement with the Department of Conservation (DOC) but also under various recourse consents with the West Coast Regional Council (WCRC). A condition on one of the resource consents is to meet upstream-downstream differential compliance limits (table 3.2.1). During the course of the operation several sources of mine affected water (MAW) was produced. These consisted of seepages associated with the Fossickers Tailings Storage Facility (TSF), Potentially Acid/Arsenic Generating (PAG) Cell, and the Waste Rock underdrain (Rock Drain) and the TSF water itself. During operation, the seepages from the TSF and PAG were pumped into the TSF and discharged offsite through the Water Treatment Plant (WTP), which reduced contaminants to below the compliance limits. This is scheduled to continue until water meets discharge quality. The Rock Drain is discharged through the Devil's Creek Silt Pond (DCSP), which provides adequate retention time to precipitate and settle out a substantial portion of the iron and therefore does not need any treatment. After mining completed and the dewatering pumps were removed from the Globe Pit a new water source began to form. This consisted of the Globe Pit Lake (GPL). The GPL is currently filling and will eventually discharge to the environment unless the water is diverted to the WTP. This water has been monitored by OceanaGold through Care and Maintenance and into the closure phase. Modelling results from a site wide water balance model completed for OceanaGold by Golder (Golder 2015) showed potential non-compliance for arsenic at the downstream compliance point DC01 (shown on figure 3.1-2) post closure if water from the site was not continually treated through the WTP. Based on iron loading there was also a concern within the company that the consent requirements around macro-invertebrate health in the stream may also not be met due to armouring of the creek bed with iron hydroxides.

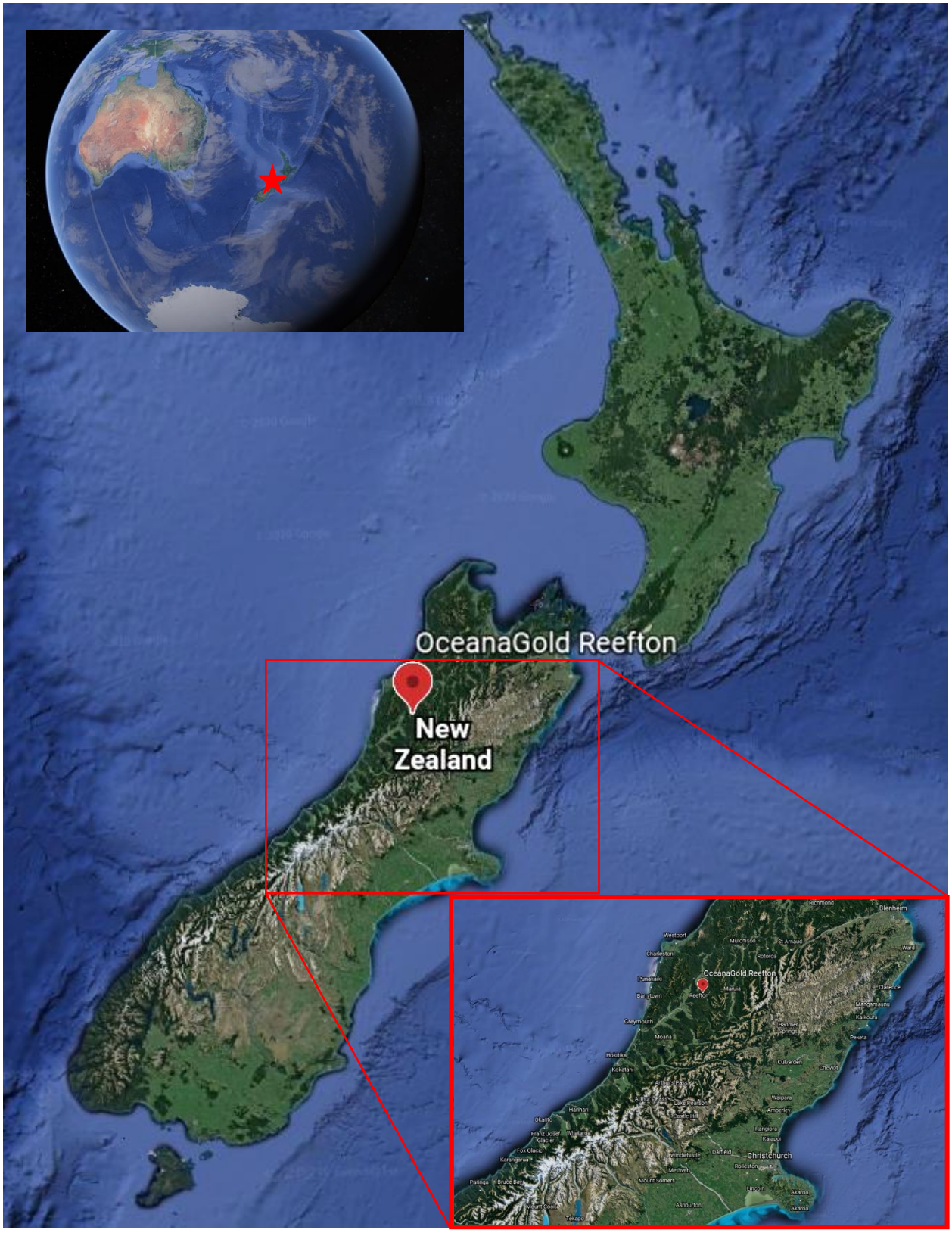

Figure 3.1-1: Google Earth image of New Zealand, showing the Globe Progress mine site as "OceanaGold Reefton".

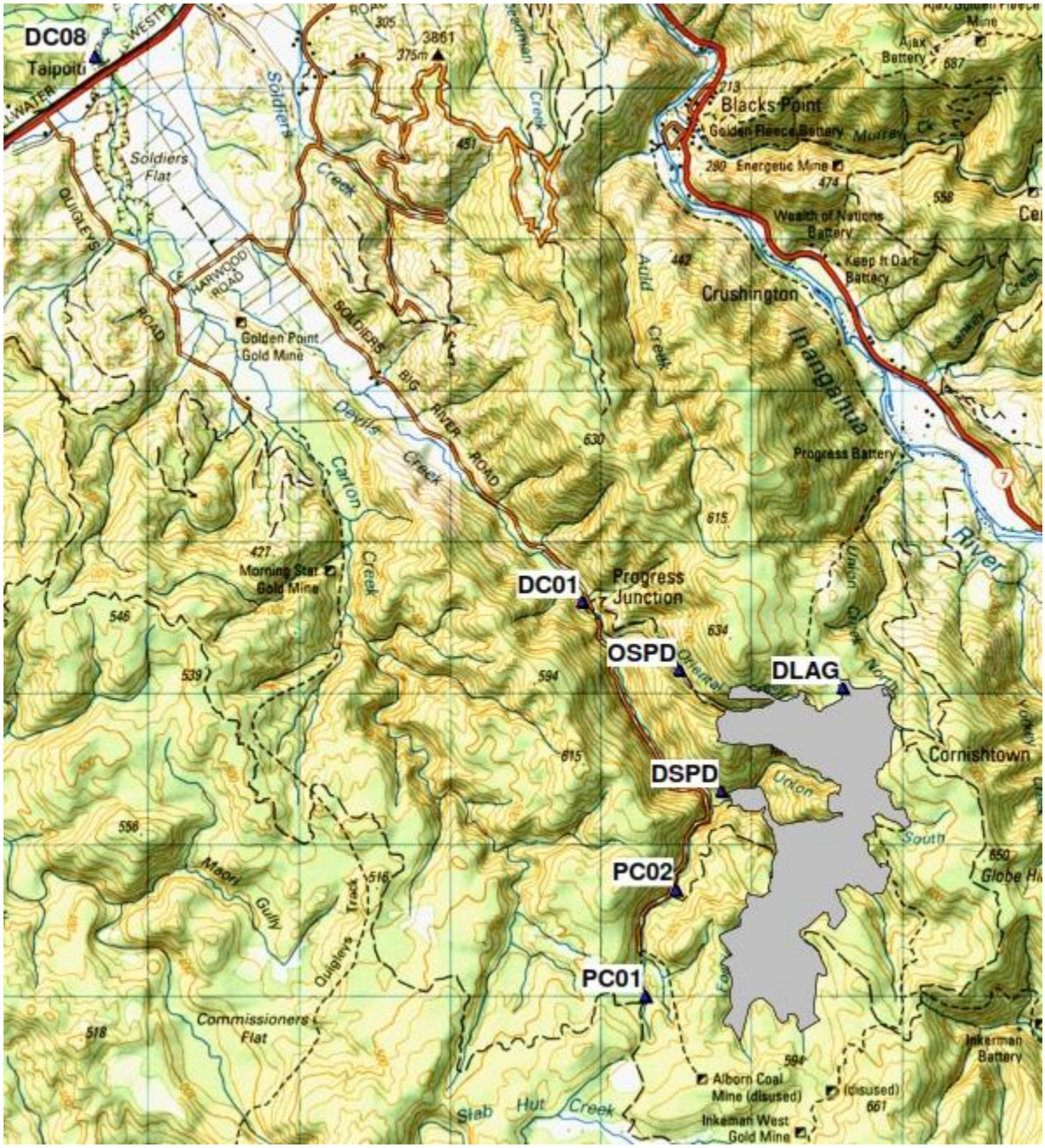

Figure 3.1-2: Approximate location of the sites compliance water quality monitoring points in relation to the site (the approximate footprint of the mine shown in grey)

3.2 Water Sources at Mine Site

There are three sources of water that will discharge from site on closure: the TSF, which currently discharges through the water treatment plant, Globe Pit Lake and the Underdrains (figure 3.2-1). Due to the presence of carbonates within the local mineralised rock (Milham and Craw 2009), all discharges are neutral to slightly basic.

The TSF water has relatively high levels of total suspended solids (TSS) (21-300 g/m^3), arsenic (0.12-1.06 g/m^3) and antimony (0.25-0.74 g/m^3)[2] compared to the downstream differential compliance

[2] Range over the last 12 months.

limits of 25 g/m^3, 0.1 g/m^3 (median) and 1.6 g/m^3 respectively. The predicted flowrate from the TSF post closure is 18 L/sec. The water treatment plant uses ferric chloride to remove arsenic and antimony from solution and then a flocculent and coagulant to settle out suspended particulates through a clarifier. The TSF is modelled (Golder, 2015) to improve in water quality over a period of 2-5 years to meet downstream compliance without any long-term treatment, with the exception of a small wetland to remove any residual TSS.

The Globe Progress Pit, the only remaining open pit, will become a pit lake on closure. Globe Pit Lake began filling from runoff water in 2015, and in mid-2019 the level began to be maintained to prevent discharge until the Globe Spillway is constructed. The natural low point of the Globe Pit is at the south west corner, which will serve as the eventual spillway that then goes down a steep valley for approximately 100m and into the DCSP. The DCSP will be removed as part of the construction of the Globe Pit spillway. Globe Pit Lake follows a stratification cycle each year, whereby it stratifies in the warmer summer months for approximately six months and becomes mixed for approximately six months. When stratified, the epilimnion has moderate concentrations of arsenic (approximately 0.3 g/m^3) and antimony (approximately 0.25 g/m^3), whereas the hypolimnion has higher concentrations (approximately 0.7 g/m^3 of arsenic and 0.7 g/m^3 of antimony). Levels of sulphate are moderate (200 g/m^3) in all levels, whereas concentrations of dissolved and total iron are below the detection limit of 0.02 g/m^3. Golder Associates predicted, in a report to OceanaGold in 2017, that arsenic concentrations may breach downstream median compliance limits (0.1 g/m^3) once the lake elevation reaches the spill-over elevation and the predicated flow rates (median flow of 35 L/sec)[3] eventuate.

The third type of water which is produced by the Globe Progress site is the combined Underdrain water. The Underdrains have a variety of sources and chemistries but report to one area (with the exception of the Saddle Embankment seepages). The Underdrains can be put into two categories: 1) the Potentially Acid/Arsenic Generating (PAG) Cell and the Fossickers TSF Underdrains, and 2) the WRD underdrain (referred to as Rock Drain). The TSF and PAG seeps daylight at a collection sump at the toe of the Devil's Creek Waste Rock Stack (DCWRS) (see figure 3.2-1) which from there are combined and pumped over 100m vertically to the TSF. Post closure all power will be removed from site and therefore these will no longer be able to be pumped. Without being pumped this water would flow out into the DCSP (figure 3.2-1) and be discharged through the decant structure. There are elevated levels of arsenic (1.5 g/m^3), sulphate (430 g/m^3) and iron (34 g/m^3)[4] present in this water which make it unacceptable for discharge. The median flow over 2017 for the combined Underdrains at this sump is about 3.5 L/sec. The Rock Drain daylights and flows into the DCSP approximately 50m downstream of the combined underdrain collection sump. It then discharges to Devils Creek (downstream of the mine site), via the DCSP, which is controlled by a manual valve. The Rock Drain has moderate levels of iron (9.3 g/m^3) and elevated levels of sulphate (555 g/m^3)[5] and flows from around 5 L/sec to >60 L/sec. The Water Treatment Plant, which currently treats the TSF and the PAG/TSF Underdrains is an expensive and labour-intensive process. If the Pit Lake water is to follow the predicted water quality when it reaches the spillway level, it would currently have to be pumped up to the water treatment plant for treatment before discharge for a number of years until the water chemistry improves to meet all downstream compliance limits. An alternative passive treatment system would be a far more practical solution for long term (Trumm 2010).

Passive Treatment reduces the need for power and for chemicals when compared to the use of the WTP. Therefore, passive treatment is preferred over active treatment. It is also an expectation from DOC that the WTP and associated infrastructure, such as power lines, will be removed as part of closure to reduce the long-term liability of assets left onsite. In order to remove the WTP and

[3] Golder predicted in 2015 a median daily flow rate of 3100 m^3/day with an upper quartile of 8860 m^3/day and a lower of 1410 m^3/day.

[4] Median values from combined Underdrains taken February 2018-March 2018.

[5] Median concentrations over the previous year.

continue to meet compliance limits and minimise downstream impacts post closure, a passive treatment system is necessary to decrease contaminate concentrations. The objective of a passive treatment system is to achieve concentrations below that of the differential downstream compliance limit for the Globe Progress site of 0.01 g/m^3 (median) for arsenic, 1.6 g/m^3 for antimony, and 25 g/m^3 for iron. As Globe Progress does not have a compliance limit for sulphate, the ANZECC (2000) guideline for recreational purposes of 400 g/m^3 will be used for target effluent values. In investigating these passive treatment methods, a full-scale passive treatment system can be designed and commissioned in order to treat the discharges from OceanaGold's Globe Progress Mine post-closure to meet compliance limits post closure. By utilising waste products and the reduction in labour/maintenance, the overall cost of this system should be significantly less than the current active treatment. This should also be a useful tool for other mine sites or government bodies to inform decisions or designs for closure plans and, also, for the mitigation of legacy sites.

All water sources that require treatment long-term report to the DCSP catchment area, and although the DCSP will be removed and partially superseded by the Globe Pit spillway, there will be a limited area available in which a passive treatment system could be built post closure. While the DCSP is still in operation there is an area of approximately 50m^2 at the toe of DCWRS, near the combined seepage collection sump in which the passive treatment trial was set up. This area allows for the TSF and PAG seepages to be gravity fed vertically upward about 10m (essentially creating a gooseneck as water sources are approximately 100m vertically higher than the trial site) into a header tank. The Rock Drain water is pumped back approximately 50m and up 10m to the trial area. Because the Pit lake is still forming, it is impractical to pump or transport water from Globe Pit to the trial area. The TSF return water at the end of 2017 had similar concentrations of antimony, arsenic and iron as the forming Globe Pit Lake water and therefore was an appropriate proxy and could be gravity fed to the trial area.

Table 3.2-1: Compliance Limits between upstream compliance point PC01 and downstream compliance point DC01

Parameter	Median	90th Percentile	Maximum
pH	-	-	6.5-9.0 (min-max range)
Total Suspended Solids	6 g/m^3	-	25 g/m^3
Antimony	-	-	1.6 g/m^3
Arsenic	0.1 g/m^3	0.25 g/m^3	3.3 g/m^3
Iron	-	-	5.0 g/m^3

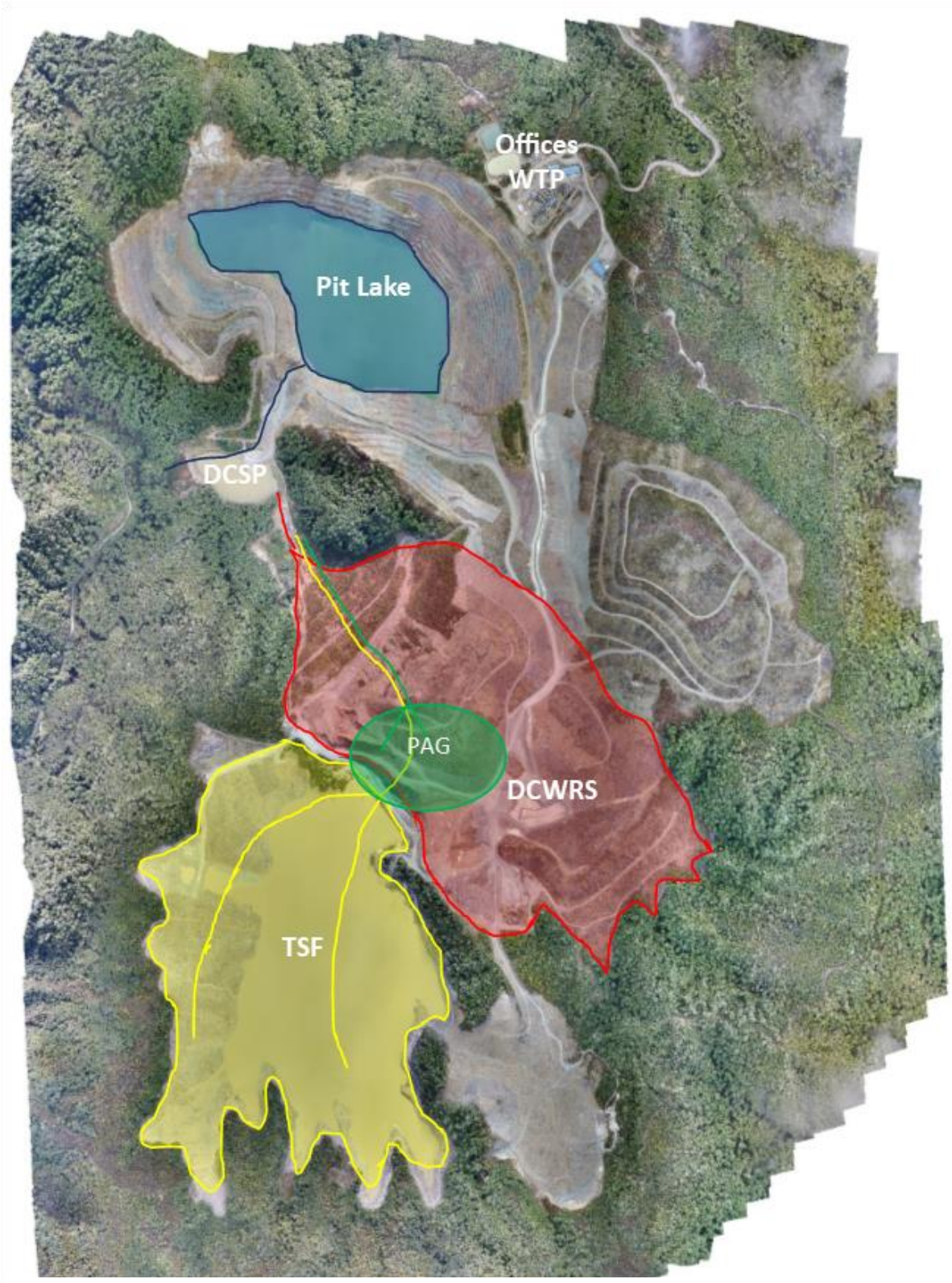

Figure 3.2-1: Site layout of Globe Progress Mine site (2019) and indicative water sources. Coloured lines in the TSF and PAG indicate Underdrains.

4. Chapter Four- Methods

4.1 Introduction

In this chapter the experimental design is explained in detail and the materials used within the system are described. This includes the sampling/testing regimes and the methods involved. Appendix 4. has photos which may provide more detail.

4.2 Site Description

The objectives of this research are to trial bioreactors with different substrate material compositions to treat combined TSF and PAG underdrain flows at Globe Progress Mine site and also to trial a Vertical Flow Reactor to remove iron and arsenic from the WRS Underdrains. This is explained in more detail in Chapter 3.

4.3 Materials and Methods- Bioreactors

4.3.1 Experimental Design

4.3.1.1 Substrates

The three major factors which need to be considered when choosing media for bioreactors are cost, longevity and permeability (McCauley et al. 2008; DiLoreto et al. 2016; Vasquez et al. 2016b; Muhammad et al. 2017; Skousen et al. 2017). The first major factor to be considered is normally driven by cost and availability, as one of the main benefits of passive treatment is the reduction in cost comparative to an active treatment system. The second major factor to be considered is ensuring there is a mixture of materials which have different breakdown rates. This is essential to extend the functional life of these systems as long as possible. The last major factor is ensuring the media mix is permeable enough to prevent the system clogging and/or short circuiting caused by the build-up of precipitates and compaction of media over time (McCauley et al. 2008; Skousen et al. 2017). The pH of the waters requiring treatment in this trial are circum-neutral, and therefore alkalinity sources are not required to increase the pH. Bioreactors, as described by the equation in chapter 2, do not produce acidity through the production of metal sulphide precipitate. However, in an aerobic system such as a Vertical Flow Reactor, H^+ is produced by during the formation of iron precipitates (Sapsford et al. 2006). This was discussed in more detail in chapter 2.

When selecting substrates, we focused on waste products that were only produced incidentally for production of another primary product. To allow the sulphate reducing bacteria to have a carbon source which is readily available, a substrate which broke down rapidly or released carbon as soon as water is added is required. The substrates selected for this trial were Spent Mushroom Compost, Sawdust, Bark, Biosolids and Mussel Shells. In the following paragraphs I will provide further explanation and justification for each substrate choice. See figure 4.3-9 for images of the substrates.

Mushroom Compost

Mushroom Compost, the compost in which mushrooms are grown, is initially produced using wheat straw, poultry and/or horse manure, gypsum, nitrogen supplements, and water (Velusami et al. 2013). After the supplier has grown sufficient mushrooms the compost is replaced with fresh compost, this is referred to as SMC (Spent Mushroom Compost). SMC, while a waste product, is still available for purchase for a low cost and is commonly used in the agricultural sector as a fertiliser.

The closest supplier of this product in bulk was 3 hours from the site but by utilising trucking companies' backloads, transport costs were reasonable.

Sawdust

Sawdust is created through the milling of timber. It is fine dust to small flakes in size (figure 4.3-9). While sawdust is fine grained and has a large surface area it has a higher proportion of lignin than more leafy material which means it has a relatively slow breakdown time. A local mill produces sawdust and sells it for a low cost. The same mill also produces a bark waste product which is created when the logs to be milled are first run through the mill and stripped.

Bark

The bark waste product that is produced is a much coarser material than other possible substrates, such as peat or manure, which may clog the system (figure 4.3-9) and it has also been suggested the higher amounts of polyphenols and lignin contribute to the slow decay of bark (Ganjegunte et al. 2004). Carbon to nitrogen ratios (C/N) have been found to be a limiting aspect of SRB with Okabe et al. (1992) suggesting that ratios outside of a range of 45-120:1 limited sulphate reduction. Bark and woody materials have also been found to contain the highest amounts of carbon and therefore higher carbon to nitrogen ratios (Uster 2015)

The Base Mix

These three materials all have differing breakdown rates and therefore carbon release timeframes. SMC has readily available carbon as it has already been composted, while sawdust requires some time to decompose and release carbon as it has not undergone any composting or breakdown. The bark waste has a lower surface area than sawdust, meaning it will have a much slower breakdown rate. The coarse nature of the bark also adds porosity and permeability to the system which reduces the occurrence of any potential clogging and short circuiting. Due to the breakdown rates, and also the textures of these materials, SMC, sawdust and bark provide all of the necessary attributes to form the base mix for a bioreactor for the site water chemistry.

Biosolids

There are substrate additions which have been trialled to increase the efficiency. This includes the addition of ethanol, manure and chitin (Prasad et al. 1999; Skousen et al. 2017). This is due to the large amounts of readily available carbon for the bacteria to utilise. Biosolids, which is processed human waste, has been shown to be very high in organics and previously been utilised to aid in the re-establishment of grass and native plants in New Zealand (Weber et al. 2012; Waterhouse et al. 2014) and also used to aid growth in reclamation sites in Pennsylvania (Toffey et al. 1998). In Christchurch City (closest city to the site) biosolids are produced by the city council as a useable waste product from the human waste from the city's sewer system. This is done through the wastewater treatment plant (figure 4.3-1). In this process the solids from the waste is collected and digested by bacteria, the methane and carbon dioxide produced is collected and used as biogas and the remaining solids are compressed with much of the water removed. Once the biosolids are concentrated they are then thermally processed to further remove water but also kill any pathogens. The resulting product is a fine-grained organic substance which resembles potting mix, very high in organics and nutrients (Waterhouse et al. 2014). These biosolids therefore have potential for increasing the available carbon within a bioreactor and therefore increase the efficiency in which sulphate and metals are removed.

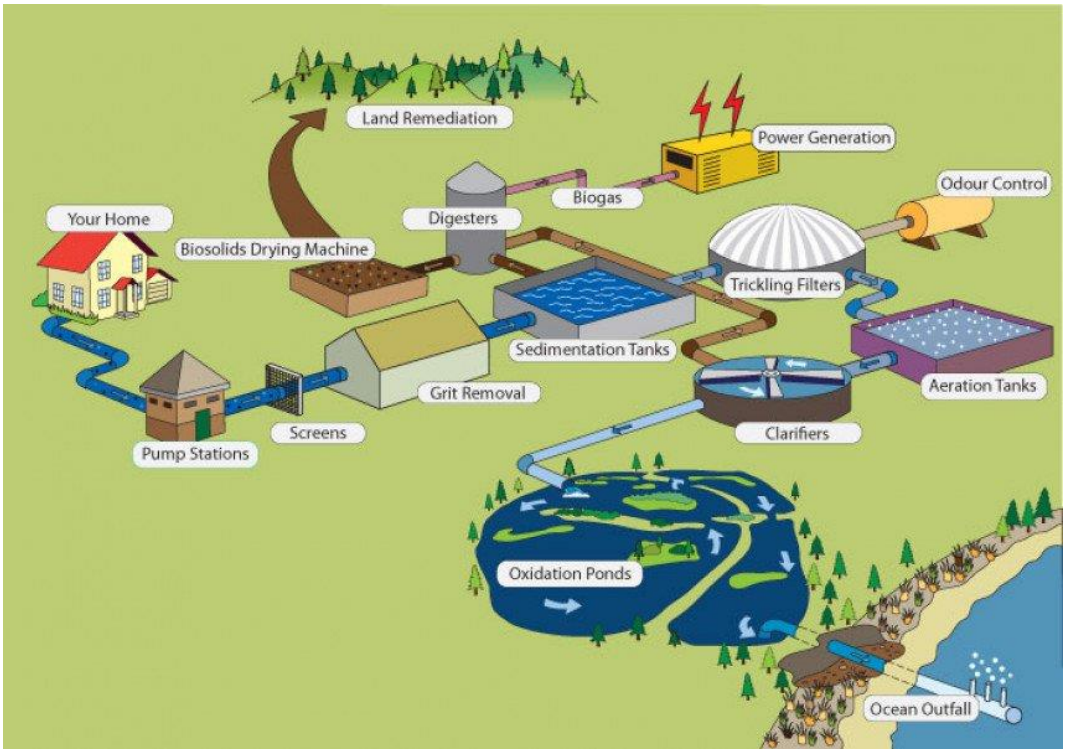

Figure 4.3-1: Diagram of the Christchurch wastewater treatment plant processes. https://ccc.govt.nz/services/water-and-drainage/wastewater/treatment-plants/christchurch-wastewater-treatment-plant

Mussel shells

Mussel shells, produced as a waste product from the shellfish industry, have shown to be effective in Passive Treatment systems (DiLoreto et al. 2016). DiLoreto et al. (2016) suggests that Mussel shells are a favourable substrate for bioreactors as they can contain up to 5-12 wt% of organic material which acts as a readily available source of carbon but also amorphous $CaCO_3$ which is a more recalcitrant source. Another advantage of mussel shells as a substrate for passive treatment of AMD is that they also act as an alkalinity source, however the MAW at the site is circum-neutral and therefore does not require additional alkalinity. Mussel shells do, however, increase the permeability of a system which prevents possible clogging. As a waste product which is available at very low cost, acts as a short- and long-term source of carbon, and also adds alkalinity when needed, mussel shells are becoming an increasingly popular choice for substrate in bioreactors.

4.3.1.2 Tanks

Four identical Devan branded green 15,000L water tanks were used in this trial for the different substrate mixes (refer to table 4.3-1 for dimensions). Two black 7,500L tanks were used for the temperature treatment, both tanks were identical with the exception of one being insulated. The insulation is an approximately 1 cm foam centre between an inner and outer polyethylene skin. The purpose of a foam insulated tank is to achieve more consistent temperatures within the tank, with the air temperature causing less fluctuation to the internal temperature. These tanks had the tops cut out to allow them to be filled with the gravel, piping and mixed substrates; they then had the tops added back on and a tarpaulin added to prevent rainwater getting into the system.

Table 4.3-1: Tank Dimension and Volume

Tank size	Diameter (m)	Height (m)	Gravel volume (m^3)	Organic Substrate volume (m^3)
15,000	2.9	2.1	1.98	9.47
7,500	2.5	1.5	0.62	0.95

4.3.1.3 Substrate Mix

Four different substrate mixes were decided on for this trial. The four mixes were selected for two primary reasons: 1) availability and longevity of carbon and 2) permeability. It has been suggested that a mixture of substrates, especially those which decompose at different rates, provide the best metal removal (Cocos et al. 2002; Zagury et al. 2006; Vasquez et al. 2016b; Muhammad et al. 2017). A paper by Vasquez et al. (2016b) states that a bioreactor *"requires a reactive mixture composed of an organic carbon and nitrogen source, an inoculum with sulphate reducing bacteria, a solid porous medium to support microbial growth, and a naturalising agent to increase alkalinity and pH"* to effectively treat AMD. Various organic substrates have been trialled in bioreactors. It has been suggested that mixed substrates often perform better than single substrates to meet the above requirements (Cocos et al. 2002; Zagury et al. 2006; McCauley et al. 2008; Muhammad et al. 2017). Many studies on the effectiveness of different media mixtures have been undertaken. These are summarised in reviews of passive systems undertaken by McCauley et al. (2008); Skousen et al. (2017). McCauley et al. (2008) used a mix of bark, post peel and compost in all reactive mixes trialled with the addition of mussel shells, limestone and nodulated stack dust in various treatments. This showed that all reactive mixtures worked well to remove metals. Although the treatment with limestone but no mussel shells preformed the poorest, it was also noted that too high a percentage of SMC may lead to poor hydraulic connectivity. (Vasquez et al. 2016b) trialled reactive mixtures comprised of a base of sediment, limestone, gravel and sawdust with the addition of cow manure, poultry manure, compost, SMC, grass silage and paper waste to various treatments. They concluded that the most efficient mixture was 15% cow manure, 10% SMC, 25% sawdust, 15% sediment, 20% gravel and 15% limestone. Whereas Cocos et al. (2002) found the most efficient mixture he trialled had 3% wood chip, 30% leaf compost, 20% poultry manure, and 5% silica sand, combined with a constant 37% bacterial source, 2% limestone and 3% urea added to all treatments. Uster et al. (2014) trialled a mixture of 20% compost, 20% bark mulch and 20% bark with the addition of either 30% mussel shells or 30% limestone and concluded that while all treatments successfully reduced metals that mussel shells were more effective.

Based on these findings, the local availability of the materials, and the pH of the site water sources, the media mixes in table 4.3-2 were selected. Limestone was not considered as the alkalinity source was not required, however mussel shells have been found to be effective at maintaining porosity while adding an organic component and were readily accessible as a waste product. Biosolids have been shown to work in mine site reclamation work (Toffey et al. 1998; Weber et al. 2012) while animal manure has been proven to be an effective additive to several bioreactor trials (Cocos et al. 2002; Vasquez et al. 2016b; Skousen et al. 2017), therefore, biosolids may be as effective a source of readily available carbon as the manure.

Both maintaining porosity and a constant carbon source are needed for bioreactors to work effectively over time (Cocos et al. 2002; McCauley et al. 2008; Vasquez et al. 2016b), therefore I wanted to trial a higher porosity media mix which has slower release carbon sources vs a media which has more readily available carbon but has less porosity (base of treatment 1 and 2 vs 3 and 4).

Once the four treatment mixtures were chosen (table 4.3-2), one was selected to be trialled in two smaller tanks, one of which was insulated whereas the other was not, to trial the effect of ambient air temperature on the bacterial activity, as it has been shown to be reduced in colder temperatures

(Trumm et al. 2015a; Ben Ali et al. 2020). The media chosen for the temperature treatment was selected as it had the highest portion of fine grained, readily available carbon, and therefore was hypothesised to work the most efficient in the early stages of treatment. A total of six treatments were therefore trialled. Substrate mixes were measured using a $1m^3$ digger bucket and then mixed in the back of an A30E Volvo articulated dump truck (figure 4.3-2). Substrates were sampled, prior to being mixed, from the bulk stockpile and sent to Hill Laboratories for analysis for metals (extensive suite at screen level), total sulphur, total nitrogen and total organic carbon. The porosity was measured by placing substrates in a 10L bucket and measuring how much water it took to fill the pore space. All mixes were also sampled. This was done by filling three 10L buckets of substrate for each substrate mix from the back of the articulated dump truck as it was being filled. One of these buckets was subsampled and sent for an extensive suite at screen level of total recoverable metals and the other two were sent for a less broad suite of analysis (averages presented in the results). Each bucket was also filled to the 10L mark with a known volume of water to measure the porosity. Tanks 5 and 6 were filled with the same mix, so therefore, only one set of three replicates was tested.

Figure 4.3-2: Photos of media being loaded and mixed. From left: 1) Bucket with SMC 2) Digger with bucket of sawdust 3) Digger mixing media in back of dump truck.

Table 4.3-2: Tank treatments and the media mixes.

Tank # (15,000L)	% Materials				
	Bark %	Sawdust %	Compost %	Biosolids %	Mussel shells %
1 - B-LC	30	30	20	20	-
2 - M-LC	30	30	20	-	20
3 - B-MC	20	20	40	20	-
4 - M-MC	20	20	40	-	20
Temperature Treatments (7500L)					
5 (control)	20	20	40	20	-
6 (insulated)	20	20	40	20	-

4.3.2 System operation

The bioreactors are all designed as up-flow systems to prevent material compaction, reduce the potential for short-circuiting and reduce the addition of oxygen to maintain a reducing environment. The systems are all operated through gravity flows from a seepage collection sump (figure 4.3-6). Seepage water reports to the seepage collection manhole by four pipes which originate from >100m vertical head, allowing water to be gravity fed by another four pipes (figure 4.3-5) up the Waste Rock Stack approximately 10m where it mixes in an IBC (intermediate bulk container). The water inflows

into the bottom of the IBC to reduce the amount of aeriation that may occur. An overflow pipe then allows any additional flow which is not used, to be discharged back into the seepage collection sump. The IBC has 6 outflow pipes (ball valve discharging through 40mm alkathene pipe) from the bottom of the IBC which then feed into the base of the bioreactors. The bioreactor fed line flows are all controlled by gate valves situated near the outlet from the IBC and each gate valve has a bypass line controlled by a ball valve to allow periodic flushing of the line (figure 4.3-8). The water then enters the base of each tank in which it is evenly distributed through a pipe tree (see figures 4.3-3 and 4.3-4), which is surrounded by a 300mm thick layer of coarse drainage gravel (a rounded river gravel between approximately 10-50mm). The water then passes through the mixed media layer (1470mm in 15,000L tank and 950mm in 7,500L tank) where there is a 100mm free water layer which is then drained evenly by another identical pipe tree drain (Figure 4.3.6).

When the systems were started (on 2nd February 2018) they were filled with MAW and run straight away as the influent was anaerobic so did not need time to become reduced. During the first two weeks of operation there were airlock and flow issues that meant the systems did not operate consistently until after the two-week commissioning period. After this time an HRT of 24 hours was targeted although due to the installed ball valves it was very difficult to adjust. On 20 June 2018, gate valves were fitted (figure 4.3-8), allowing for a much finer adjustment of flows. After the installation of the gate valves, flows were more able to be fine-tuned but tapered off after operation with no adjustment. After a further 5 months of operation a flush line was installed on 5 November 2018, allowing the inlet pipes to be flushed without altering the gate valves thereby keeping the flow much more consistent.

An initial residence time of 24hrs was targeted, but as the trial progressed a longer residence time of 48hrs was targeted to test the effect of a longer HRT on the metal removal. Similarly, a lower HRT of 12hrs was also trialled. These exact HRTs were very difficult to get in the field, even with the addition of gate valves, and therefore the actual HRT of all the treatments for each sampling round was measured instead of recording target HRT.

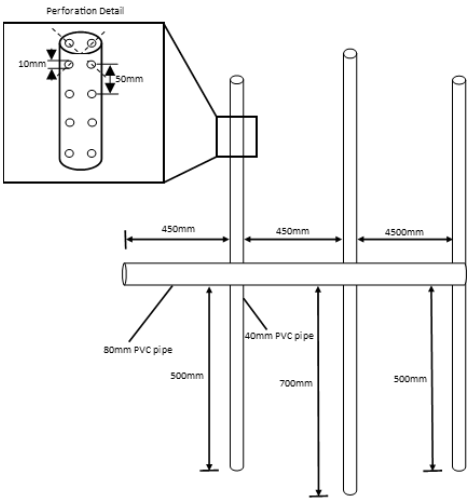

Figure 4.3-3: Detail of piping tree for 15,000L tank (inlet tree and outlet tree identical)

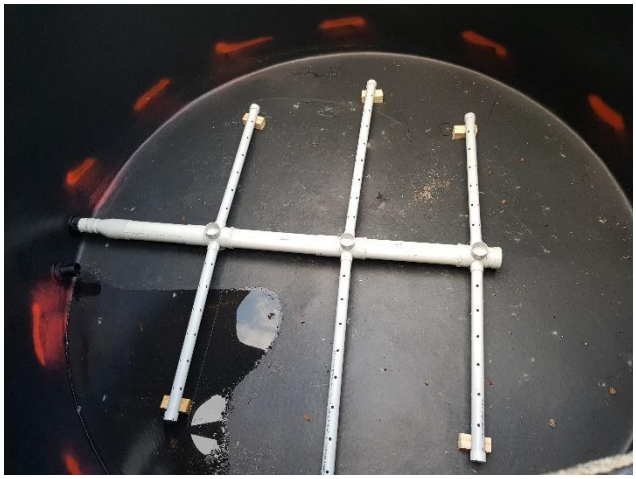

Figure 4.3-4: Photo of inlet tree drain installed in 15,000L tank.

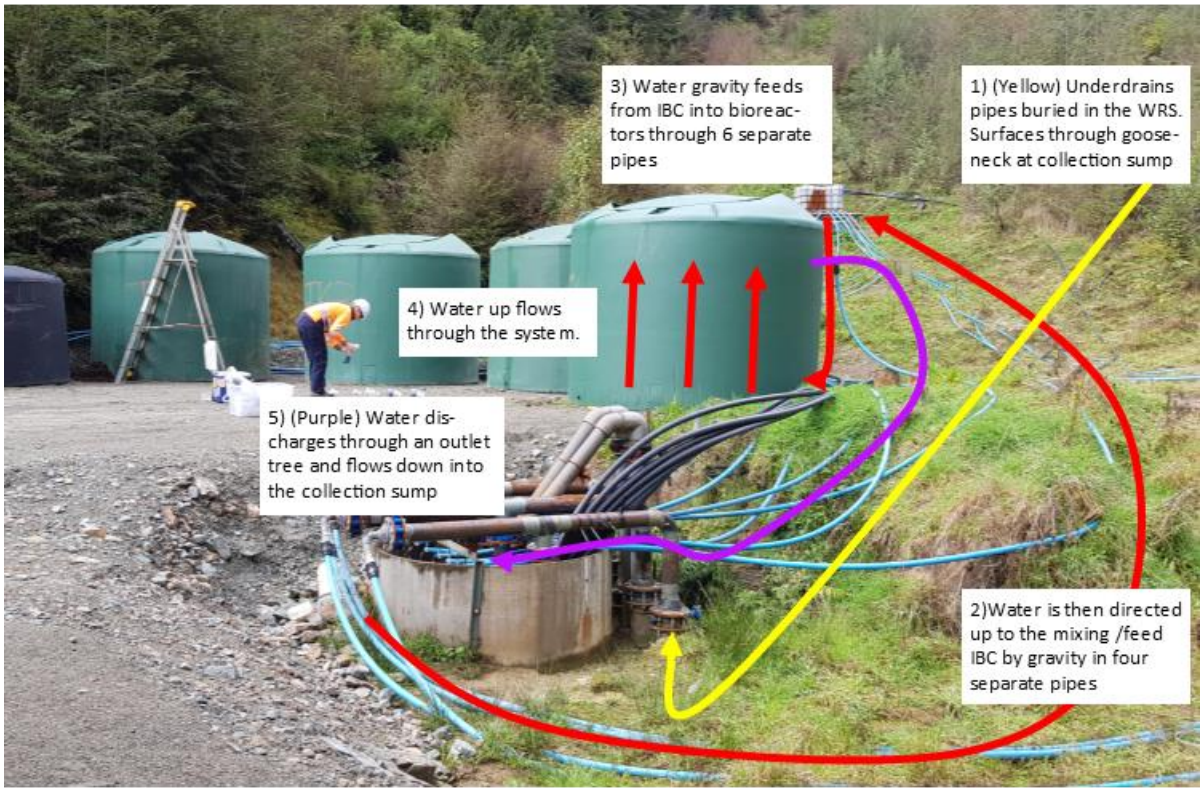

Figure 4.3 5: Piping layout to bioreactor

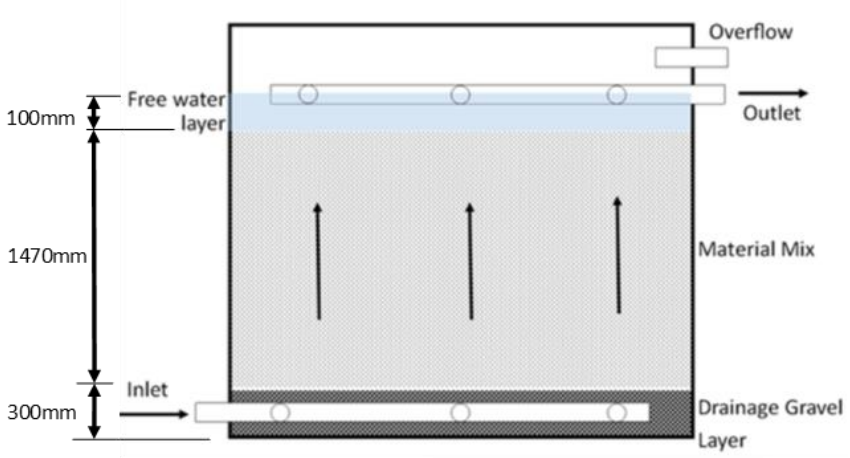

Figure 4.3-6: Schematic of bioreactor, showing measurements

Figure 4.3-7: Photo of the seepage collection sump showing underdrain pipes (large metal pipes) transitioning into 40mm alkathene pipe being fed back up to the WRS to the feed IBC. Also, 40mm bioreactor outlets discharging into the collection sump.

Figure 4.3-8: Evolution of Valves. From Left: ball valve, ball valve with gate valve, and ball valve with gate valve and flushing line.

SMC	Sawdust	Bark	Mussel Shells	Biosolids
				

Figure 4.3-9: Photographs of materials used in bioreactors with a 30cm ruler for scale.

4.3.3 Sampling Methods

Influent and effluent water chemistry were measured in-field once a week for field pH, temperature, specific conductivity and DO (dissolved oxygen). Samples were taken fortnightly and analysed by Hill Laboratories for a range of parameters (refer to table 3.3). Field testing for ferrous iron and sulphide was undertaken approximately every fortnight for the year the trials were operational and periodically after that. Once during operation, samples were taken and analysed using the portable spectrometer to determine arsenic speciation.

Precipitate samples were collected and analysed twice during the operation of these trials.

Field Measurements

Field measurements were taken using a YSI Pro DO handheld meter for DO and a YSI Professional Plus handheld meter for temperature, specific conductivity and pH. The influent was measured by placing the probes in the feed IBC. The treatments were measured by allowing the probes to stabilise in the 100mm of free water in the top of the tanks just prior to the outflow tree. This allowed accurate measurement of the water after it has passed through the system without the introduction of oxygen at the outflow. Flow measurements were taken using a stopwatch and a 1 litre measuring flask at the outflow for all treatments. This data is then then manually entered into an online database system called InViron where it is then stored.

Water Chemistry Samples

Fortnightly samples for the influent were collected from inside the feed IBC, although effluent from the trials is taken from the discharge pipes at the seepage collection sump (Figure 4.3-7). Samples were collected in the approved vessels (refer to table 4.3-3) and sampled using the prescribed methods by Hill Laboratories. A one-time sample of a full suite of metal analyses was also undertaken to ensure all parameters of concern were appropriately selected. Routine sample parameters in table 4.3-6 were selected either because they are the target parameters to meet downstream compliance (e.g. iron, arsenic, antimony and sulphate) or previous research has suggested they may change through operation of the system (e.g. Alkalinity, pH, nitrogen and dissolved organic carbon) (Prasad et al. 1999; McCauley et al. 2008; Skousen et al. 2017). Hills laboratory, which is IANZ accredited (International Accreditation New Zealand), analysed the samples and sends the reported data directly to the InViron database to be stored.

Table 4.3-3: Parameters analysed fortnightly for influent and all effluent.

Parameter	Collection Container
pH	Unpreserved, unfiltered 500ml
Total Alkalinity	Unpreserved, unfiltered 500ml
Carbonate Alkalinity	Unpreserved, unfiltered 500ml
Bicarbonate Alkalinity	Unpreserved, unfiltered 500ml
Dissolved Antimony	Nitric acid preserved, filtered 100ml
Dissolved Arsenic	Nitric acid preserved, filtered 100ml
Dissolved Calcium	Unpreserved, unfiltered 500ml
Dissolved Iron	Nitric acid preserved, filtered 100ml
Total Iron	Nitric acid preserved, unfiltered 100ml
Total Ammoniacal-N	Unpreserved, unfiltered 500ml
Nitrite-N	Unpreserved, unfiltered 500ml
Nitrate-N + Nitrite-N	Unpreserved, unfiltered 500ml
Dissolved Reactive Phosphorus	Unpreserved, unfiltered 500ml
Sulphate	Unpreserved, unfiltered 500ml
Dissolved Organic Carbon (DOC)	Unpreserved, Amber Glass 125ml

Speciation

Regular (approximately fortnightly for the first year of trial) field measurement for ferrous/ferric iron and sulphide was undertaken. This was done using a Hach DR 2800 spectrophotometer. Samples for the influent were collected from inside the feed IBC, although effluent from the trials were taken from the discharge pipes at the seepage collection sump (figure 4.3-7). This was done with care to not introduce any extra oxygen and was done immediately prior to testing. Samples were diluted with deionised water where necessary to give results within the spectrometers measuring range. The methods specified in the instrument's manual for both parameters were followed, and the data were manually entered into the InViron database. Once during the operation of these systems, samples were taken, placed is a freezer until frozen and transported on ice to Christchurch, where As speciation was undertaken using the portable spectrometer using the methods prescribed in Johnson and Pilson (1972). Due to the complexity of the method this was unable to be undertaken in the field.

Precipitate Samples

Sludge sampling was undertaken by two methods in an attempt to prevent oxidation of samples. The first was undertaken by loosening mineral accumulation from the outlet pipes of the treatments in the seepage collection sump, collecting in a 5L bucket and carefully transferring, to minimise addition of oxygen, into soil sample jars and sending via courier to the CRL laboratory in Wellington. Analyses undertaken were moisture content, XRF multi element analysis, XRD scans and analysis of those scans where appropriate. These samples were dried in a nitrogen atmosphere to avoid oxygenation of the sample. All other standard methodology was followed. The second method was undertaken by detaching the system flush line at the bottom of the tanks and collecting precipitate which has accumulated within the tank itself. Once the pipes were disconnected the discharge out of the tanks was controlled by a ball valve. This allowed 5L buckets to be placed at the outlet and the ball valve opened slowly to collect water and material that flowed out. Initial discharge from this was discarded, as the valve and surrounding area within the tank was flushed. Water was then collected and the fine precipitates allow to settle out before the water was then decanted off. This was repeated until enough precipitate sample was present to be tested. This was then transferred to sample jars and carefully topped up with extra water from inside the tank to prevent oxidation in transport, samples were then couriered to the CRL laboratory in Wellington. Analyses undertaken were XRF multi element analysis, XRD scan and scan analysis. These samples were dried in a nitrogen atmosphere to avoid oxygenation of the sample. All other standard methodology was followed.

4.3.4 Temperature Monitoring

To monitor the effect of the insulated tank, Odyssey Extended Temperature Loggers were used measure the internal temperature of each treatment. Temperature loggers were installed in all six of the systems about 8-months after the trials were started. This was done by first draining the bioreactors to just below the surface of the substrate to accurately measure the depth of insertions. The probes were attached to a piece of bamboo using cable ties, which were then gently inserted 500mm deep in the centre of the tanks and 300mm from the side of the tanks. These were set to record a measurement once every 30 minutes. Another probe was installed in the trial area to record ambient air temperature, this probe is located in the shade to prevent sun causing amplified temperature readings.

4.3.5 Statistical Methods

We ran a series one-way analysis of variance (ANOVA) tests with the function *aov* in R to analyse the effect of treatment on iron removal, arsenic removal, sulphate removal and sulphide concentrations. We expected that certain treatments, would be similar to each other whereas others would differ, so we also ran a post hoc tukey test, with a confidence interval of 0.95, with the function *TUKEY*. All data satisfied the assumptions of normalcy and homoscedasticity of variances.

4.4 Materials and Methods – Vertical Flow Reactor

4.4.1 Experimental design

The VFR (Vertical Flow Reactor) is designed to aerate MAW causing precipitation of iron and the co-precipitation or adsorption of other metals onto a non-reactive gravel filter bed (figure 4.4-1). The VFR is operated as a downflow system, with water entering the system from a spray nozzle at the top of a cut open 25,000L tank (see table 4.4-1), into a 1.65m free water layer where oxygenation of Fe^{2+} to Fe^{3+} occurs. The water then passes through a 100mm fine chip layer (Grade 6 chip, ranging from 2.3-<6.7mm), 100mm coarse chip layer (Grade 3 chip, ranging from 7.5 – 10mm) and then finally into the 100mm drainage gravel layer (rounded, ranging from 5-53mm) , through the outlet coil and an outflow gooseneck, which maintains the water level within the tank, and then discharges into a second seepage collection sump. Influent water treated through this system varied through the operation of the trial. The initial influent water was pumped by a small submersible pump from a weir through which the Waste Rock Stack underdrain (referred to from now as Rock Drain) surfaces and flows. This is pumped approximately 80m horizontally and 8m vertically through a 20mm alkathene pipe to the tank, with a T-join allowing a high-pressure pump to flush the line periodically. This removes iron build up in the line which causes reduced flow to the tank. A maintenance schedule was also implemented from August 2018 whereby the pump was swapped out and cleaned as iron build up in the fins caused the pump capacity to be increasingly restricted. This was undertaken monthly to bimonthly depending on the varying flow.

A second influent water source was added to this system shortly after it began to operate (April 2018), this water is referred to as the TSF (Tailings Storage Facility) return water, this water was used as a proxy for the Pit Lake as it had relatively high arsenic concentrations (0.4g/m^3) and below detection iron concentrations. This operated from the beginning of May until mid-June 2018, from when the TSF return water quality improved to no longer being applicable for this trial and was thereby switch off for the remainder of the trial. A 1000L tank was plumbed into the return water line from Fossickers TSF using a T-Join. This tank was therefore fed from the same line which transported the TSF return water to the water treatment plant. The inflow into the tank was controlled by a high-pressure ballcock valve. The tank was located approximately 110m vertically

above the trials and therefore gravity fed into the VFR tank with a constant and consistent flow down a 333m long, 20mm alkathene pipe to the VFR reactor. This influent was treated until June 2018, when the water chemistry changed and was no longer an appropriate proxy for the Pit Lake.

Table 4.4 1: VFR capacity and gravel porosities.

Tank	Diameter (m)	Height (m)	Gooseneck height *1	Water Volume (m^3) *2
25,000	3.5	2.4	1.95	17.21
*1 At the start of operation, this was adjusted as system ran. HRT was calculated using water height inside of tank. *2 Water volume incorporating the different gravel densities				
Fine Gravel Porosity		**Fine Gravel Porosity**		**Fine Gravel Porosity**
47%		50%		42%

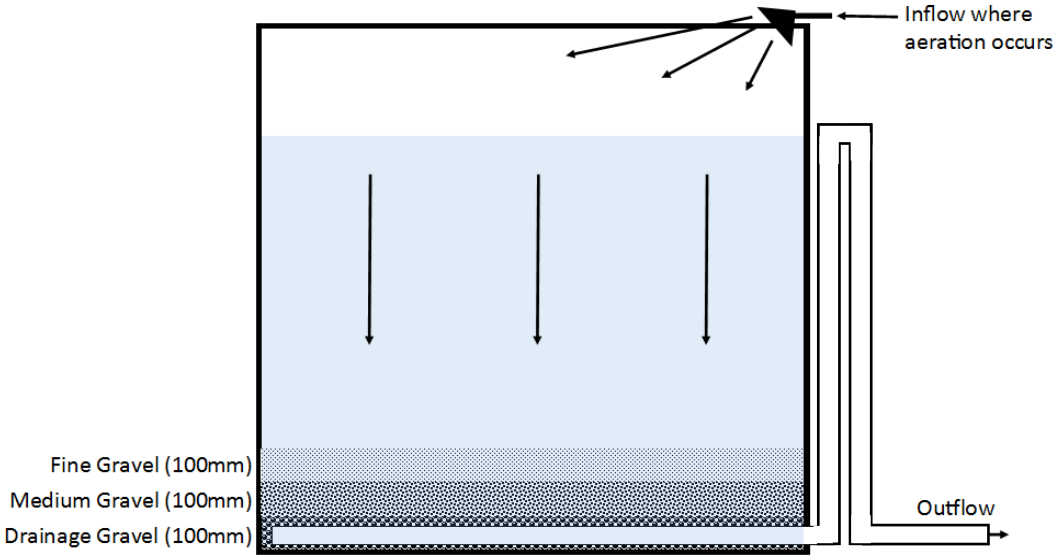

Figure 4.4-1: Schematic of the VFR setup, with water flow direction.

4.4.2 System Operation

The VFR was started on 2 February 2018 After filling, it was found that it was syphoning dry. A breather was then added to the top of the goose neck a few days later to prevent this from occurring. The system targeted a 24h HRT initially, but during the course of the trial lower residence times were targeted. Due to iron build up on the submersible pump and in the inflow piping and nozzles, longer HRTs were often obtained. A flush line was, therefore, installed on pipe which transfers water from the rock drain weir to the VFR. This utilised a high-pressure pump in the area to send pulse of water from a mid-point on the pipeline both towards the VFR and down to the pump at the rock drain weir. Both ends had t-joins installed to allow the iron build up to bypass the VFR and also the weir and pump. This was initially done approximately monthly and then more regularly to try to accomplish lower HRT. After the flush lines were installed, it was noted the small submersible pump flows had also dropped off. At this point, the pump was removed and serviced, and it was noted that the fins had become clogged with iron. A cleaning schedule was implemented immediately, and a second pump was purchased in July to allow for the pumps to be swapped out and cleaned while minimising operational downtime of the VFR. After the system had run for approximately nine months it was noted that the driving head had increased to the point that the

system was overtopping during flushing when lower HRTs were being targeted. To prevent this, the goose neck was lowered (from 1.65m to 1.57m) on the 21st October 2018. Over topping continued to occur so the outlet height was dropped then dropped on the 7th December to 1.29m, this prevented the overtopping issues which were caused by the decrease in permeability as a result of the thickening of the ochre layer. The VFR was switched off and drained on the 30/01/2019 to sample the precipitate sludge. This was sampled day 1, day 2, and day 7 after draining to measure the percent dry matter and monitor how quickly the sludge was drying. The sample from day one was also tested by ICP-MS and XFR for metal concentration. All sludge was then removed, and the system restarted on 14th February 2019.

4.4.3 Sampling Methods

Influent and effluent water chemistry were measured in-field once a week for field pH, temperature, specific conductivity and DO. Samples were taken fortnightly and analysed by Hill Laboratories for a range of parameters (refer to table 4.4-2) to measure the removal of metals and the effect on the alkalinity of the water. Field testing for ferrous iron was undertaken to test how efficiently the iron was being oxidised. This was done approximately every fortnight for the year the trials were operational and periodically after that. Field testing for sulphide was undertaken fortnightly using a portable spectrometer at the beginning of this trial but ceased early into the operation due to below detection results, which were to be expected as this system operated in oxidising conditions. Once during operation, samples were taken and analysed using the portable spectrometer to determine arsenic speciation. This was undertaken to determine in what form the arsenic was reporting to the system and if it became more oxidised as it passed through the system.

Sludge samples were collected and analysed twice during the operation of these trials to understand what the portion of Fe to other metals was accumulating on the gravel bed and to measure the percent of dry matter to measure the drying rate.

Field Measurements

Field measurements were taken using a YSI Pro DO handheld meter for DO and a YSI Professional Plus handheld meter for temperature, specific conductivity and pH. The influent was measured by placing the probes in the Rock Drain weir. The rock drain water was also measured where it enters the tank, as iron began to precipitate in the pipeline. The TSF return water and the Rock drain water were both measured separately as they entered the tank by collecting water in a 5L bucket, which had been rinsed three times. The probes were then allowed to stabilise before readings were recorded. The effluent was measured as it discharges into the collection sump where, as with the influent samples, water is collected in a 5L bucket which had been rinsed three times. The probes were then allowed to stabilise before readings were recorded. Flow measurements were also measured. These were done at the effluent using a measuring flask and a stopwatch but at the influent nozzles this had to be done using a 5L bucket to allow for the water to be captured. The driving head, which is the difference in height of the water level within the tank to the outlet height, differed throughout the operation of this system due to the accumulation of the low permeability hydroxide and oxyhydroxide precipitates. Driving head was measured from 4 months into the trial. This was done by measuring from the lip of the tank to the outflow gooseneck and then from the lip to the water level within the tank and calculating the difference. This data is then then manually entered into an online database system InViron where it is then stored.

Water Chemistry Samples

Fortnightly samples for the influent were collected from the Rock Drain weir, and the two sprayer nozzles at the VFR (figure 4.4-2) The Rock Drain sample and the TSF return water samples were both analysed for a full range of analyses as per table 4.4-2, although the VFRIN sample (Rock Drain influent at the sprayer nozzle) was just analysed for total and dissolved iron and dissolved arsenic. This was done to capture the potential aeration and loss of metals in the pump and pipe. Samples were collected in the approved vessels (refer to table 4.4-2) and sampled using the prescribed methods by Hill Laboratories. Hills laboratory then analyses the samples and sends the reported data directly to the InViron database to be stored.

Table 4.4-2: Parameters analysed fortnightly for all influent and effluent

Parameter	Collection Container
pH	Unpreserved, unfiltered 500ml
Total Alkalinity	Unpreserved, unfiltered 500ml
Carbonate Alkalinity	Unpreserved, unfiltered 500ml
Bicarbonate Alkalinity	Unpreserved, unfiltered 500ml
Dissolved Antimony	Nitric acid preserved, filtered 100ml
Dissolved Arsenic	Nitric acid preserved, filtered 100ml
Dissolved Calcium	Unpreserved, unfiltered 500ml
Dissolved Iron	Nitric acid preserved, filtered 100ml
Total Iron	Nitric acid preserved, unfiltered 100ml
Sulphate	Unpreserved, unfiltered 500ml

Spectrometer

Regular (approximately fortnightly for the first year of trial) field measurement for ferrous/ferric iron were also undertaken. This was done using a Hach DR 2800 spectrophotometer. Samples were collected with the same methodology as the water chemistry samples. Samples were diluted with deionised water where necessary to give results within the spectrophotometers measuring range. The methods specified in the instrument's manual were followed and the data manually entered into the InViron database. Once during the operation of this system, samples were taken, frozen using and transported to Christchurch, where arsenic speciation was undertaken using the portable spectrometer using the method prescribed in Johnson and Pilson (1972) . Due to the complexity of the method this was unable to be undertaken in the field.

Precipitates Samples

The system was drained, exposing the built-up iron ochre sludge, and samples of the sludge were collected from the top of the fine gravel. This was done using a sampling pole and a sterile cut open bottle. The sample was then sent to CRL for XRF Multi element analysis and Hill Laboratories for total recoverable iron, arsenic, antimony and also percent dry matter. The system was left to dry for eleven days with sample repeats taken at days 1, 6 and 11 to measure percent dry matter in order to establish the how quickly the sludge would dry. This effects how long the system will need to dry in order to reduce the density and increase the ease of removing the sludge. The system was then cleared of dry sludge and restarted on 14 February 2019. Sludge was resampled after eleven months of operation and sent for XRF multi element analysis to CRL and total recoverable iron, arsenic and antimony as well as percent dry matter by Hill Laboratories.

Figure 4.4-2: Photograph of the TSF water (right) and the RDRN influent water (left) entering the VFR through the spray nozzles.

5. Chapter Five- Results

5.1 Introduction

The purpose of this study was to evaluate the most effective treatment method for MAW (Mine Affected Water) at OceanaGold's Globe Progress Mine site. This was done by a) trialling four mesoscale bioreactors with different organic substrate mixes to establish the most efficient mix for reduction of metals over a 24-month period, b) testing the effect of air temperature on the efficiency of SRB's (Sulphate Reducing Bioreactor) by comparing removal rates of an insulated tank compared to a standard uninsulated tank and c) trialling a VFR (Vertical Flow Reactor) using a high iron seep with the addition of high arsenic/low iron water as a proxy for the sites pit lake. Experimental design of these systems is explained in chapter 3.

The purpose of this chapter is to present the results of this study. These results will be delivered in two sections. The first section (4.2) will present the results of the bioreactor substrate and temperature treatments, in particular metal and sulphate removal and the effect of temperature and HRT (hydraulic Retention Time). The second section (4.3) will present the results from the VFR treatment trial, in particular the effect of the iron to arsenic ratios, the effect of HRT and the driving head changes due to sludge accumulation. These systems were monitored weekly and tested in field for pH, DO (Dissolved Oxygen), conductivity, temperature and flow rate. Driving head was also monitored for the VFR treatment. Samples were taken fortnightly and sent to Hill Laboratories for testing. Methodology, frequency and testing parameters of the monitoring of this system is explained in detail in the section 4.4. Data was analysed with R-Studio, using ANOVA and Tukey (95% confidence intervals) tests to assess the statistical variance between treatments.

5.2 Bioreactor Substrate Treatments

There are 2 key results from the bioreactor substrate treatment trials performed as part of this thesis. These key results include: 1) biosolids as a substrate had a higher amount of most metals when compared to other substrates (i.e. bark, compost, sawdust, mussel shells); 2) biosolids had a higher amount of nitrogen and phosphorous compared the other substrates; and 3) treatments with biosolids are more effective at removing iron and arsenic than mussel shells irrespective of the substrate's compost content. Full water chemistry results are available in appendix 2.

Samples of all substrate materials were sent to Hill Laboratories and tested for a range of parameters. Below in table 5.2-1, results from this analysis are presented. Results show that biosolids have the highest total nitrogen of all the materials at 3.8 g/100g dry weight, followed by compost. Compost had the highest total sulphur, followed by biosolids. The material with the highest organic carbon is in the sawdust, closely followed by bark. Mussel shells had the most calcium by an order of magnitude, as well as the highest amounts sodium and strontium. In general, biosolids had higher amounts of all metals including antimony, lead, copper, zinc, mercury and silver, and similar amounts of arsenic as compost. Compost had higher amounts of magnesium, potassium and rubidium than the other materials.

Table 5.2-1: Results of Individual Material Analysis

Field ("mg/kg dry wt" unless otherwise stated)	**Bark Load 1 (Tanks 1-4)**	**Bark Load 2 (Tanks 5 and 6)**	**Biosolids**	**Compost Load 1 (Tanks 1-4)**	**Compost Load 2 (Tanks 5 and 6)**	**Mussel-shells**	**Sawdust Load 1 (Tanks 1-4)**	**Sawdust Load 2 (Tanks 5 and 6)**
Total Nitrogen (g/100g dry wt)	0.29	0.14	3.8	2.1	1.88	1.43	<0.13	0.14
Total Sulphur (g/100g dry wt)	0.03	0.05	1.49	3.4	3.9	0.12	0.05	0.04
Total Organic Carbon (g/100g dry wt)	42	44	27	28	28	7.6	45	44
Total Recoverable Aluminium	310	570	9,100	930	1,130	86	35	21
Total Recoverable Antimony	<0.9	<0.6	2.6	<0.4	<0.4	<0.4	<0.9	<0.8
Total Recoverable Arsenic	<5	<4	10	10	13	<2	<5	<4
Total Recoverable Barium	1.5	2	900	92	66	4.3	1.3	<0.8
Total Recoverable Bismuth	<0.9	<0.6	8.2	<0.4	<0.4	<0.4	<0.9	<0.8
Total Recoverable Cadmium	<0.3	<0.2	4.6	0.27	0.18	<0.1	<0.3	<0.2
Total Recoverable Caesium	<0.5	<0.3	0.8	<0.2	<0.2	<0.2	<0.5	<0.4
Total Recoverable Calcium	580	1,370	30,000	91,000	81,000	330,000	450	490
Total Recoverable Chromium	<5	<4	128	9	6	<2	<5	<4
Total Recoverable Cobalt	<0.9	<0.6	4.1	1.2	1.4	<0.4	<0.9	<0.8
Total Recoverable Copper	<5	<4	320	75	63	<2	<5	<4
Total Recoverable Iron	320	790	18,000	1,750	1,840	152	113	105
Total Recoverable Lanthanum	<0.5	<0.3	9.4	1	1.1	<0.2	<0.5	<0.4
Total Recoverable Lead	<0.9	1.1	80	2.2	2	<0.4	<0.9	<0.8
Total Recoverable Lithium	<0.9	0.9	8	1.2	1.6	2.5	<0.9	<0.8
Total Recoverable Magnesium	240	270	4,100	5,500	6,900	490	178	190
Total Recoverable Manganese	14	21	560	430	390	11.7	20	20
Total Recoverable Mercury	<0.3	<0.2	1.44	<0.1	<0.1	<0.1	<0.3	<0.2
Total Recoverable Molybdenum	<0.9	<0.6	7.1	5.5	7.2	0.6	<0.9	<0.8
Total Recoverable Nickel	<5	<4	23	6	5	<2	<5	<4
Total Recoverable Phosphorus	<90	93	16,800	8,300	4,700	560	<90	<80
Total Recoverable Potassium	820	800	1,560	17,900	25,000	<100	550	540
Total Recoverable Rubidium	4.3	3.2	5.1	12.9	21	<0.4	2.8	2.4
Total Recoverable Selenium	<50	<30	<20	<20	<20	<20	<50	<40
Total Recoverable Silver	<0.9	<0.6	4.5	<0.4	<0.4	<0.4	<0.9	<0.8
Total Recoverable Sodium	<90	103	660	1,690	2,200	5,400	<90	<80
Total Recoverable Strontium	3	4.2	165	660	540	1,340	7	3
Total Recoverable Thallium	<0.5	<0.3	<0.2	<0.2	<0.2	<0.2	<0.5	<0.4
Total Recoverable Tin	<3	<1.5	50	<1	<1	<1	<3	<2
Total Recoverable Uranium	<0.3	<0.15	1.76	0.44	0.19	0.15	<0.3	<0.2
Total Recoverable Vanadium	<300	<150	<100	<100	<100	<100	<300	<200
Total Recoverable Zinc	<9	28	1,170	420	290	5	<9	<8

Samples of the mixed substrates were also and sent for analysis. These results are presented below in table 5.2-2. Treatments are referred to by the identifying characteristics of their mixes (more details of the mixtures are in section 4.3.1). These are as follows 1) B-LC (biosolids, with less compost), 2) M-LC (mussel shells, with less compost), 3) B-MC (biosolids, with more compost), 4) M-MC (mussel shells, with more compost), 5) TT (temp control- small non-insulated tank with biosolids, more compost, not insulated), and 6) INS (small insulated tank- with biosolids, more compost). Treatments with biosolids and more compost (B-MC and the two small temperature treatments) had the highest amount of total sulphur. Treatments with biosolids also had the highest nitrogen, and organic carbon. Tank four (M-MC) had the highest total recoverable arsenic and antimony. Calcium was higher in tanks containing mussel shells, with tank two (M-LC) having higher amounts than tank 4 (M-MC). All treatments with biosolids generally had higher metals.

Table 5.2-2: Mixed Material Analysis Results, averages are presented for those parameters with duplicate sampling.

Field ("mg/kg dry wt" unless otherwise stated)	**Tank 1 Materials (B-LC)**	**Tank 2 Materials (M-LC)**	**Tank 3 Materials (B-MC)**	**Tank 4 Materials (M-MC)**	**Tank 5/6* Materials (Temp Treatments)**
Total Nitrogen (g/100g dry wt)	2.04	0.81	1.89	1.17	1.92
Total Sulphur (g/100g dry wt)	1.62	1.19	2.38	1.66	2.16
Total Organic Carbon (g/100g dry wt)	31.00	11.43	25.33	19.90	27.50
Total Recoverable Aluminium	3900	1010	3300	240	3600
Total Recoverable Antimony	2.60	2.50	1.80	7.00	3.30
Total Recoverable Arsenic	26	39	33	154	12
Total Recoverable Barium	330	38	330	37	280
Total Recoverable Bismuth	3.00	<0.4	2.60	<0.4	3.20
Total Recoverable Cadmium	1.34	0.17	1.85	0.14	0.53
Total Recoverable Caesium	0.80	0.30	0.50	0.50	0.40
Total Recoverable Calcium	25000	144000	31000	93000	44000
Total Recoverable Chromium	58.33	4.50	48.33	5.33	44.67
Total Recoverable Cobalt	3.90	1.60	2.30	2.50	2.30
Total Recoverable Copper	142	27	130	37	123
Total Recoverable Iron	11000	2800	8000	5600	8300
Total Recoverable Lanthanum	4.50	1.00	3.40	1.40	4.10
Total Recoverable Lead	32.00	2.67	30.33	6.07	23.30
Total Recoverable Lithium	4.50	2.00	3.20	2.70	4.30
Total Recoverable Magnesium	3000	3000	2900	3300	4200
Total Recoverable Manganese	320	196	310	250	340
Total Recoverable Mercury	0.54	<0.1	0.43	<0.1	0.57
Total Recoverable Molybdenum	3.40	3.10	3.50	2.00	4.50
Total Recoverable Nickel	13.50	5.50	11.33	7.00	10.33
Total Recoverable Phosphorus	7200	2400	7800	3100	-
Total Recoverable Potassium	3300	6900	5500	5200	9100
Total Recoverable Rubidium	5.00	6.60	5.90	4.70	9.10
Total Recoverable Selenium	<20	<20	<20	<20	<20
Total Recoverable Silver	1.60	<0.4	1.50	<0.4	1.60
Total Recoverable Sodium	530	2100	650	1400	1010
Total Recoverable Strontium	151	640	210	480	340
Total Recoverable Thallium	<0.2	<0.2	<0.2	<0.2	<0.2
Total Recoverable Tin	19.40	<1	17.70	<1	17.20
Total Recoverable Uranium	0.80	0.25	0.71	0.28	0.70
Total Recoverable Vanadium	<100	<100	<100	<100	<100
Total Recoverable Zinc	530	129	507	195	480
Porosity (%)	59.5%	60%	59.2%	54.6%	55.5%

*Tank 5 and 6 were filled from a single mix.

5.2.1 Water Chemistry Results

A summary of influent chemistry is presented in table 5.2-3, see appendix 2 for a full data set. This shows that influent concentration of metals over the operation of the system was low for antimony (Sb), stable moderate levels of arsenic (As) and relatively high iron (Fe) which fluctuates over the course of this trial. The influent remains circum-neutral for the duration of this experiment with the lowest pH observed at 6.6 and there were moderate levels of sulphate and extremely low sulphide concentrations.

Table 5.2- 3: Mixed Influent Concentrations (BIOIN) over the operation of the systems.

	Sulphate (g/m3)	Sulphide (µg/L)	Calcium-Total (g/m3)	Antimony-Dissolved (g/m3)	Arsenic-Dissolved (g/m3)	Iron-Dissolved (g/m3)	pH (pH unit)	Dissolved Organic Carbon (DOC) (g/m3)	Nitrogen-Total Ammoniacal (g/m3)	Reactive Phosphorus-Dissolved (g/m3)
Minimum	310	0	96	0.0008	1.19	19.8	6.6	1	0.22	0.004
Maximum	580	110	96	0.0037	2.1	48	7.2	35	0.8	0.1
Median	430	10	96	0.0016	1.69	28	6.8	13	0.35	0.004

Median effluent concentrations from over the operation of these systems is presented below in table 5.2-4, see appendix 2 for a full data set. Results show slightly higher sulphate, iron, arsenic, calcium, dissolved organic carbon and pH from mussel shell tanks, and higher sulphide, and ammonia from biosolid tanks. Median flows are similar for all of the larger tanks (1-4) and half that amount for the smaller tanks (which are half the size).

Table 5.2- 4: Median concentrations of effluent from all tanks over the operation of the systems.

	Sulphate (g/m3)	Sulphide (µg/L)	Calcium-Dissolved (g/m3)	Antimony-Dissolved (g/m3)	Arsenic-Dissolved (g/m3)	Iron-Dissolved (g/m3)	pH (pH unit)	Dissolved Organic Carbon (DOC) (g/m3)	Nitrogen-Total Ammoniacal (g/m3)	Reactive Phosphorus-Dissolved (g/m3)	Flow rate (L/S)
Tank 1/ B-LC	360	251	95	0.0004	0.3	11	6.9	15.9	0.45	0.04	0.043
Tank 2/ M-LC	390	37.5	160	0.0004	0.73	18.1	7.2	19.3	0.33	0.004	0.05
Tank 3/ B-MC	360	539.5	97.5	0.0004	0.34	10.4	7	14.4	0.71	0.0065	0.05
Tank 4/ M-LC	390	70	162	0.0005	0.72	16.3	7.2	17.9	0.41	0.004	0.044
Tank 5/ TT	340	674	97	0.0004	0.365	7	7	16.8	0.5	0.04	0.023
Tank 6/ INS	340	1,950	99	0.0004	0.325	4.1	6.9	15	0.61	0.29	0.021

Results from a one-off extended suite of analyses are presented below in table 5.2-5. Results show that even though some metals are elevated in the materials analysis that they are not elevated in the effluent of these tanks.

Table 5.2- 5: Results from the one-off extended suite of analysis on the influent and all effluent, from the 2nd July 2018.

	BIOIN/ Influent	Tank 1/ B-LC	Tank 2/ M-LC	Tank 3/B-MC	Tank 4/ M-LC	Tank 5/ TT	Tank 6/ INS
Chloride (g/m3)	9.3	9.5	9.6	9.7	9.5	9.2	9.3
Sulphate (g/m3)	430	400	400	330	410	390	290
Alkalinity - Bicarbonate (g/m3 as CaCO3)	380	430	580	480	550	420	520
Carbonate Alkalinity (g/m3 as CaCO3)	<1	<1	<1	<1	<1	<1	<1
Hardness-Total (g/m3 as CaCO3)	610	620	770	630	760	620	640
Alkalinity - Total (g/m3 as CaCO3)	380	430	580	490	550	420	520
Total Suspended Solids (g/m3)	54	66	52	61	53	35	8
Electrical Conductivity (EC) (mS/m)	142.5	143.8	167.6	146.5	166.1	145.5	145.8
pH (pH unit)	6.8	6.9	7.1	6.9	7.1	6.8	6.9
Field Dissolved Oxygen (%)	-0.1	0	0	0.5	-0.1	0.1	0.1
Field Temp (°C)	11.9	9.6	9.6	8	10.2	10.5	7
Dissolved Organic Carbon (DOC) (g/m3)	5.8	7.8	5.8	8.8	4.8	7.8	10.8
Nitrate-N (g/m3)	0.019	<0.02	<0.02	<0.02	<0.02	<0.02	<0.002
Nitrate-N + Nitrite-N (g/m3)	0.047	<0.02	<0.02	<0.02	<0.02	<0.02	<0.002
Nitrite-N (g/m3)	0.028	<0.02	<0.02	<0.02	<0.02	<0.02	<0.002
Nitrogen-Total Ammoniacal (g/m3)	0.4	1.05	0.63	1.09	0.6	0.51	1.06
Reactive Phosphorus-Dissolved (g/m3)	<0.004	<0.004	<0.004	<0.004	<0.004	<0.004	4
Calcium-Dissolved (g/m3)	92	98	161	98	158	97	99
Magnesium-Dissolved (g/m3)	92	90	88	93	89	92	95
Potassium-Dissolved (g/m3)	12.8	12.6	12.3	12.7	13	12.5	12.5
Sodium-Dissolved (g/m3)	65	63	65	64	65	63	62
Aluminium-Dissolved (g/m3)	0.028	0.015	0.008	0.017	0.011	0.019	0.023
Antimony-Dissolved (g/m3)	0.001	0.0007	0.0005	0.0007	0.0005	0.0004	0.0004
Arsenic-Dissolved (g/m3)	1.56	1.37	0.88	0.85	0.84	0.21	0.166
Barium-Dissolved (g/m3)	0.068	0.087	0.058	0.073	0.062	0.117	0.084
Boron-Dissolved (g/m3)	0.097	0.11	0.098	0.093	0.099	0.098	0.086
Cadmium-Dissolved (g/m3)	<0.00005	<0.00005	<0.00005	<0.00005	<0.00005	<0.00005	<0.00005
Chromium-Dissolved (g/m3)	0.0017	0.0015	0.0014	0.0015	0.0013	0.0017	0.0017
Cobalt-Dissolved (g/m3)	0.072	0.0151	0.0182	0.0183	0.0199	0.0091	0.0041
Copper-Dissolved (g/m3)	<0.0005	<0.0005	<0.0005	<0.0005	<0.0005	<0.0005	<0.0005
Dissolved Caesium (g/m3)	0.00182	<0.0001	0.00036	<0.0001	0.0007	<0.0001	<0.0001
Iron- Ferrous (g/m3)	28.6	24.1	22.2	25.9	25.7	19.8	0.58
Iron-Dissolved (g/m3)	33	30	22	24	23	16.5	0.58
Iron-Total (g/m3)	34	30	22	25	22	16.2	1.81
Lanthanum- Dissolved (g/m3)	0.00029	<0.0001	<0.0001	<0.0001	<0.0001	<0.0001	<0.0001
Lead-Dissolved (g/m3)	<0.0001	<0.0001	<0.0001	<0.0001	<0.0001	<0.0001	<0.0001
Lithium-Dissolved (g/m3)	0.037	0.037	0.036	0.035	0.036	0.036	0.036
Manganese-Dissolved (g/m3)	3.8	3.8	3.7	3.7	3.7	4.2	3.3
Molybdenum-Dissolved (g/m3)	0.0006	0.0024	0.0003	0.0017	<0.0002	<0.0002	<0.0002
Nickel-Dissolved (g/m3)	0.2	0.0055	0.007	0.0046	0.0078	0.0022	0.0024
Rubidium-Dissolved (g/m3)	0.016	0.018	0.0166	0.0179	0.0167	0.0157	0.0164
Selenium-Dissolved (g/m3)	<0.001	<0.001	<0.001	<0.001	<0.001	<0.001	0.002
Silver-Dissolved (g/m3)	<0.0001	<0.0001	<0.0001	<0.0001	<0.0001	<0.0001	<0.0001
Strontium-Dissolved (g/m3)	0.52	0.59	0.89	0.63	0.92	0.6	0.63
Thallium-Dissolved (g/m3)	<0.00005	<0.00005	<0.00005	<0.00005	<0.00005	<0.00005	<0.00005
Tin-Dissolved (g/m3)	<0.0005	<0.0005	<0.0005	<0.0005	<0.0005	<0.0005	<0.0005
Uranium-Dissolved (g/m3)	0.0021	0.00036	0.00022	0.00062	0.00031	0.00004	0.00003
Vanadium- Dissolved (g/m3)	<0.001	<0.001	<0.001	<0.001	<0.001	<0.001	<0.001
Zinc-Dissolved (g/m3)	0.005	0.0021	0.003	0.0014	<0.001	0.0022	<0.002

5.2.2 Iron Removal

Dissolved iron removal was higher for both more compost and less compost treatments with biosolids than for mussel shell treatments (figures 5.2-1, 5.2-2, and 5.2-3). A one-way analysis of variance (ANOVA) was undertaken on the effect of treatment on iron removal (summarised in table 5.2-6). A post hoc tukey test (full results in appendix 3) showed B-LC removed 21% more iron than M-LC (±16% at a 95% confidence interval, p-value=0.001) and while B-MC removed more iron than M-MC, this difference was not statistically significant (p-value=0.236). There was little difference for iron removal for more or less compost in either biosolid or mussel shell treatments.

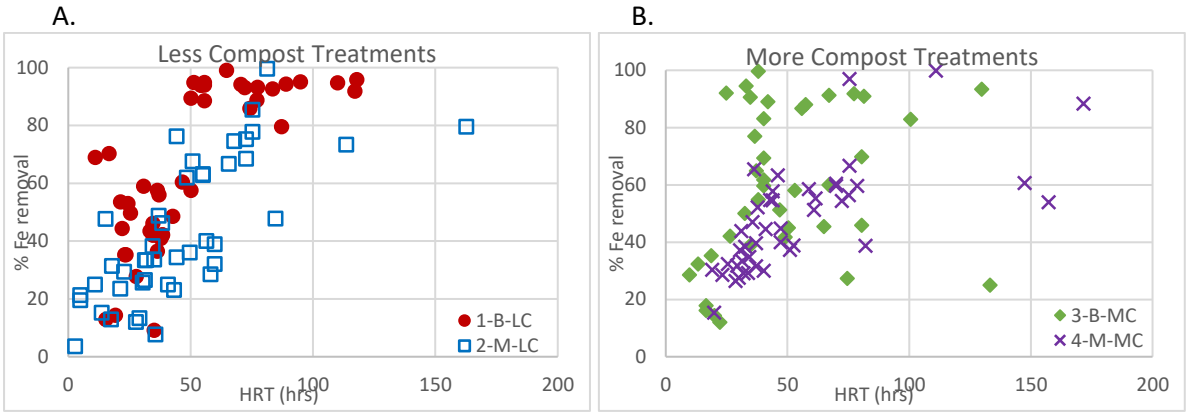

Figure 5.2- 1: Graphs showing dissolved iron removal over HRT(up to 200hrs) between A) The less compost treatments (biosolids (B-LC) and mussel shells (M-LC)), and B) The more compost treatments (biosolids(B-MC) and mussel shells (M-MC)).

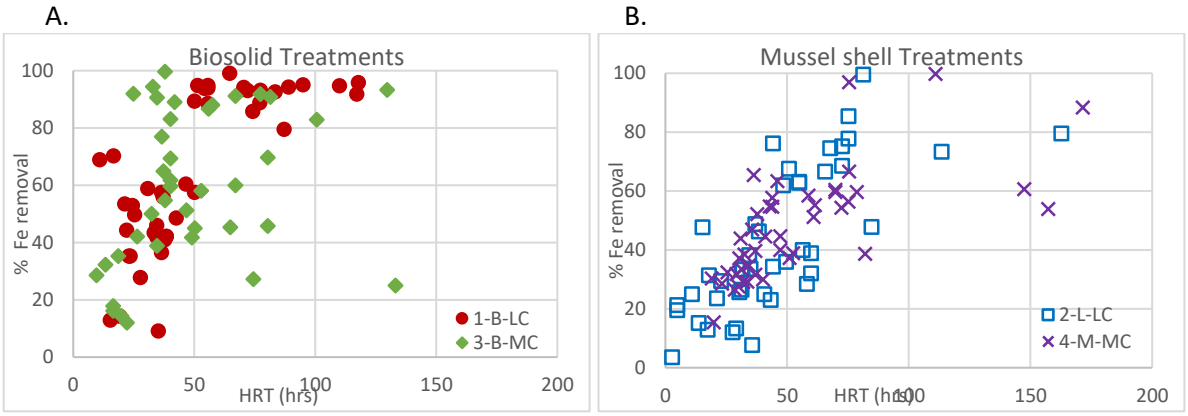

Figure 5.2- 2: Graphs showing dissolved iron removal over HRT (up to 200hrs)between A) The biosolid treatments (less compost (B-LC) and more compost (B-MC)), and B) The mussel shell treatments (less compost (M-LC) and more compost(M-MC)).

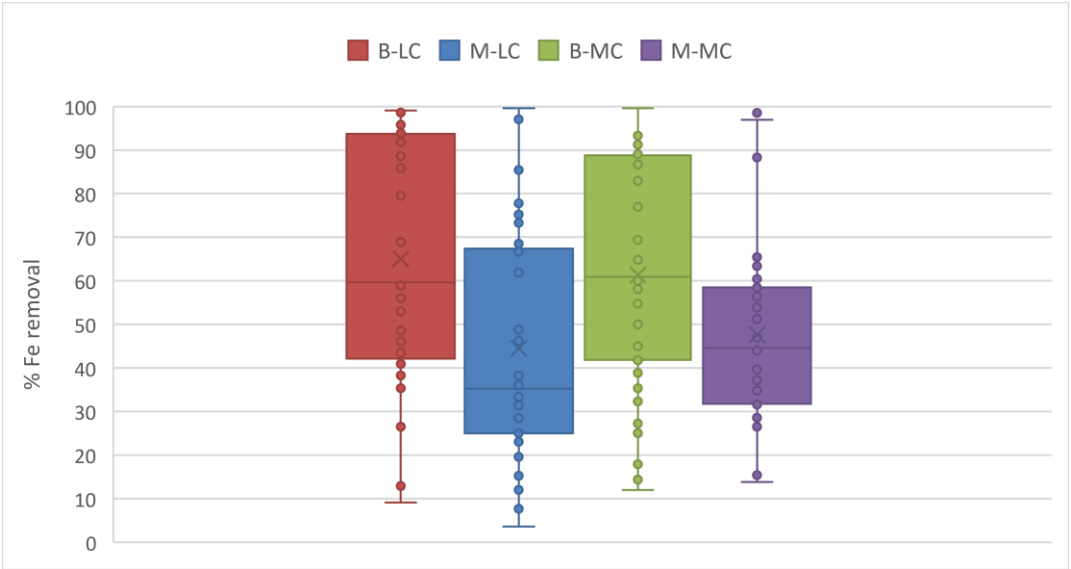

Figure 5.2- 3: Box Plot displaying all treatments with percentage removal for dissolved iron for the duration of the operation of the system. B-LC: Biosolids with less compost, M-LC: mussel shells with less compost, B-MC: biosolids with more compost, & M-MC: mussel shells with more compost.

Table 5.2- 6: Results of ANOVA on the effect of treatment on the removal of iron

Effect of treatment on:	Df	F value	P-value	
Iron removal	5	12.38	<0.001	***

5.2.3 Arsenic Removal

As with iron, dissolved arsenic removal was higher in the biosolid treatments, both with more and less compost, than the mussel shell treatments, although there was little to no variation between more and less compost treatments for both biosolid and mussel shell treatments (figures 5.2-4 - 5.2-6). A one-way analysis of variance (ANOVA) was undertaken on the effect of treatment on arsenic removal (summarised in table 5.2-7). A post hoc tukey test (full results in appendix 3) showed that the less compost treatments, B-LC (tank 1) removed 24% more arsenic than M-LC (tank 2) (±13% at a 95% confidence interval, p-value =<0.001) and for the more compost treatments B-MC (tank 3) removed 23% more arsenic than M-MC (tank 4) (±14% at a 95% confidence interval, p-value=<0.001).

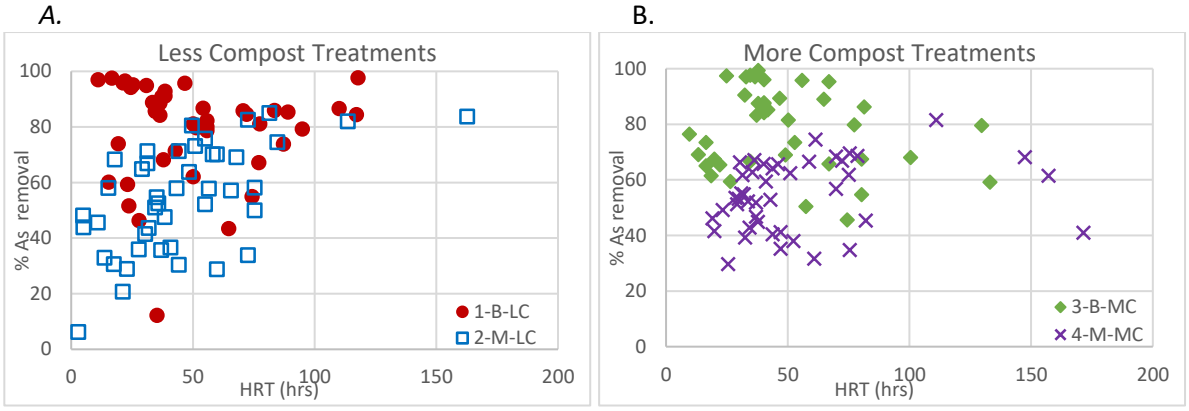

Figure 5.2- 4: Graphs showing dissolved arsenic removal over HRT (up to 200hrs) between A) The less compost treatments (biosolids (B-LC) and mussel shells (M-LC)), and B) The more compost treatments (biosolids(B-MC) and mussel shells (M-MC)).

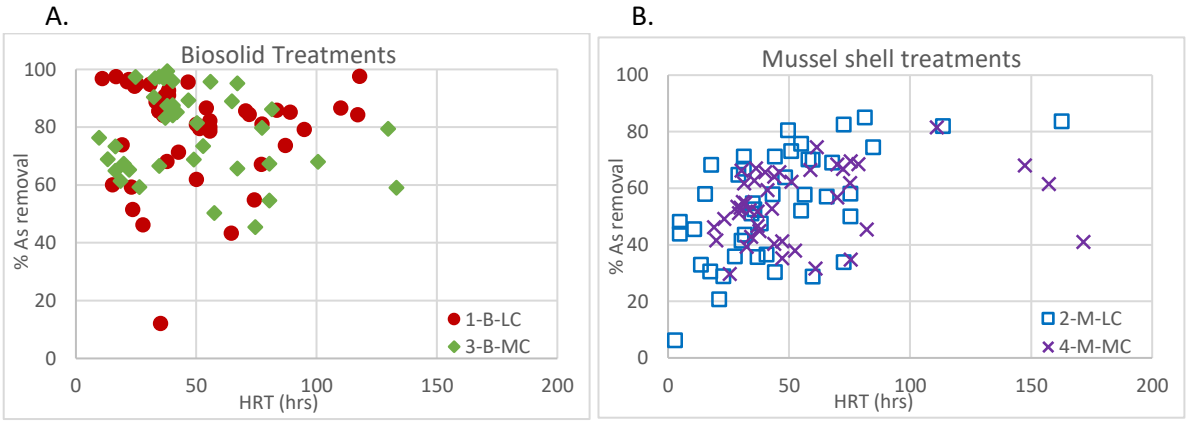

Figure 5.2- 5: Graphs showing dissolved arsenic removal over HRT (up to 200hrs) between A) The biosolid treatments (less compost (B-LC) and more compost (B-MC)), and B) The mussel shell treatments (less compost (M-LC) and more compost(M-MC)).

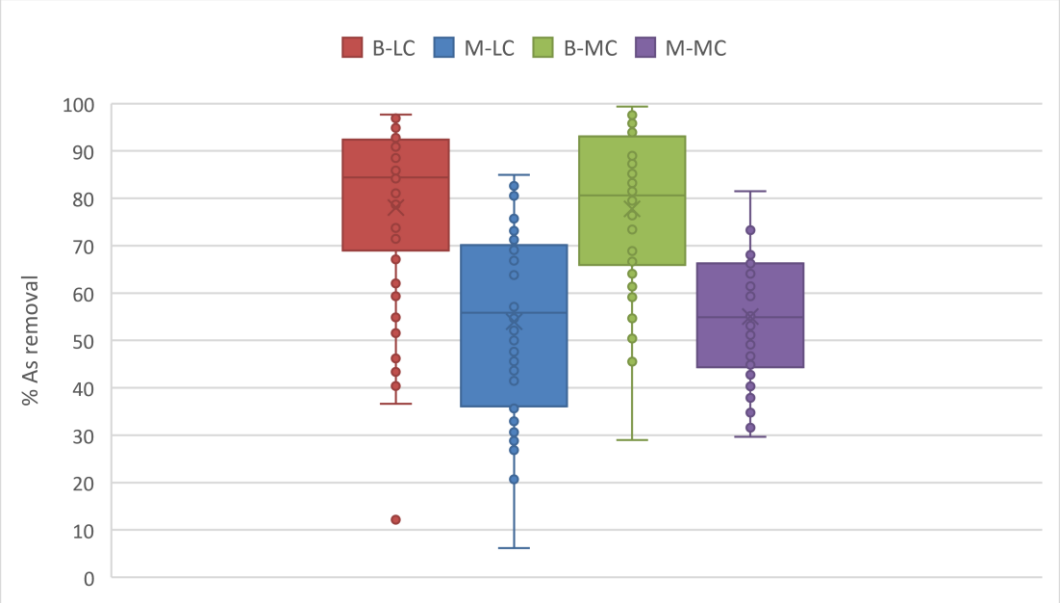

Figure 5.2- 6: Box Plot displaying all treatments with percentage removal for dissolved arsenic. B-LC: Biosolids with less compost, M-LC: mussel shells with less compost, B-MC: biosolids with more compost, & M-MC: mussel shells with more compost.

Table 5.2- 7: Results of ANOVA on the effect of treatment on the removal of arsenic

Effect of treatment on:	Df	F value	Pr(>F)
Arsenic removal	5	14.51	<0.001 ***

5.2.4 Sulphate Removal

A one-way analysis of variance (ANOVA) was undertaken on the effect of treatment on sulphate removal, which resulted in p-value=0.002 (summarised in table 5.2-8). As was the case for iron and arsenic, sulphate removal was also greater in treatments with biosolids compared to treatments with mussel shells, although a post hoc tukey test (full results in appendix 3) showed that there was not a statistically significant difference in the result between less compost treatments and more compost treatments (p-value=0.493 and 0.0.313 respectively). There was no statistical difference in removal between treatments with more or less compost (Biosolid treatments p-value= 1.000 and Mussel shell treatments 0.999 respectively). There was however a significant effect on the sulphate removal when comparing the M-LC treatment with the small temperature control and the M-MC treatment with both the small temperature control and the small insulated tank. Sulphate concentrations are only higher in the effluent than the influent (negative removal), after the commissioning period, in the mussel shell treatments. Result are presented in figures 5.2-7, 5.2-8 and 5.2-9.

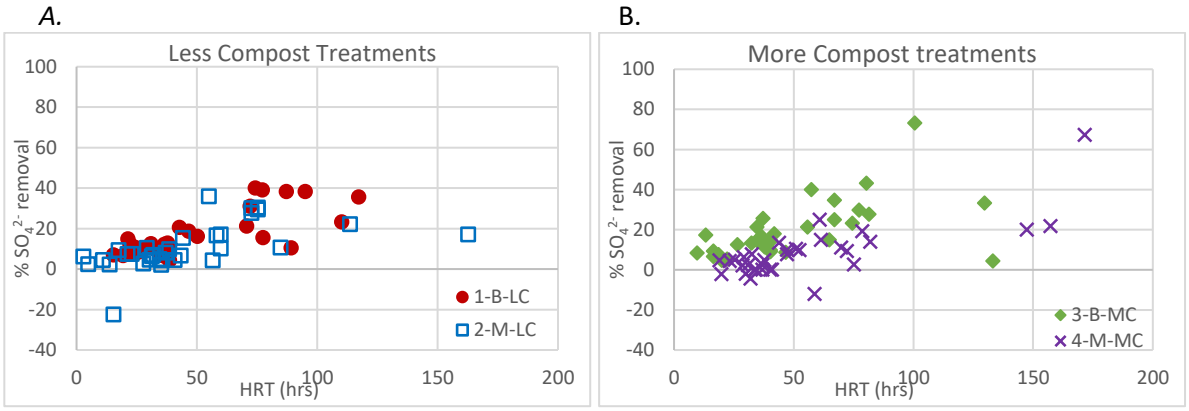

Figure 5.2- 7: Graphs showing sulphate removal over HRT (up to 200hrs) between A) The less compost treatments (biosolids (B-LC) and mussel shells (M-LC)), and B) The more compost treatments (biosolids(B-MC) and mussel shells (M-MC)). Note: first two months of data while systems during comissioning where sulphate removal is negative have not been included.

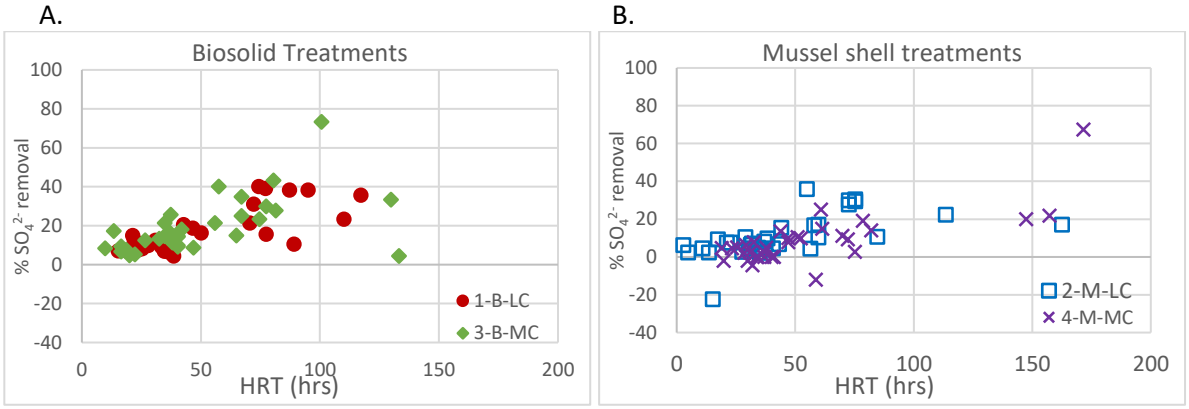

Figure 5.2- 8: Graphs showing sulphate removal over HRT (up to 200hrs) between A) The biosolid treatments (less compost (B-LC) and more compost (B-MC)), and B) The mussel shell treatments (less compost (M-LC) and more compost(M-MC)). Note: first two months of data while systems during comissioning where sulphate removal is negative have not been included.

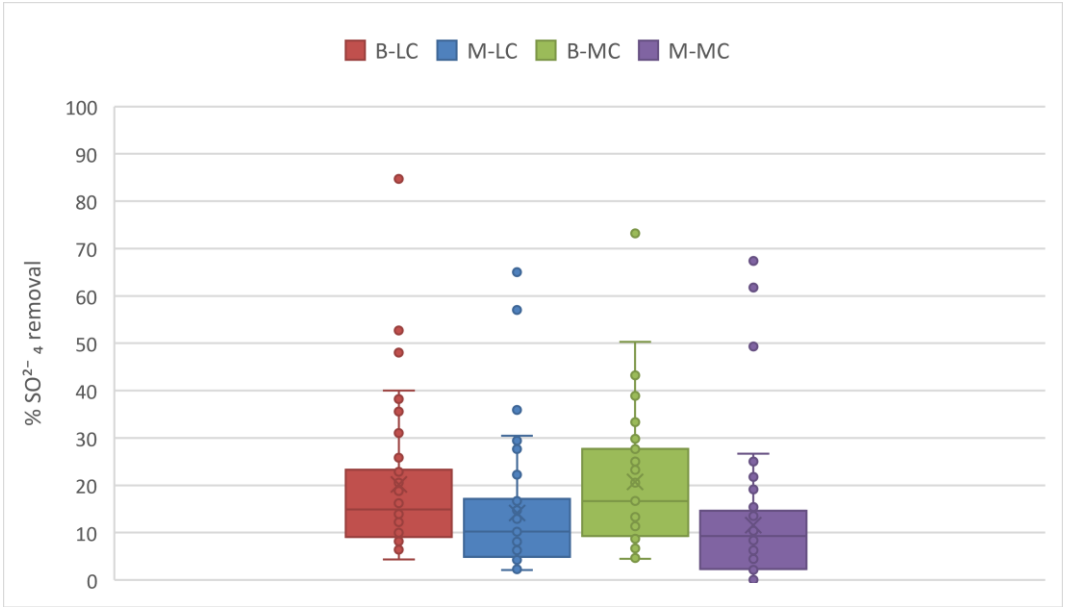

Figure 5.2- 9: Box and Wisker diagram displaying all treatments with percentage removal for sulphate. B-LC: Biosolids with less compost, M-LC: mussel shells with less compost, B-MC: biosolids with more compost, & M-MC: mussel shells with more compost.

Table 5.2- 8: Results of ANOVA on the effect of treatment on the removal of sulphate

Effect of treatment on:	Df	F value	Pr(>F)
Sulphate removal	5	3.994	0.002 **

5.2.5 Speciation Results

Infield speciation of both iron and sulphur were undertaken fortnightly dependent on the availability of the spectrometer, however on several occasions, measurements were not able to be taken for up to 2 months. A one-off arsenic speciation was undertaken by transporting frozen samples to the CRL Lab for speciation (more details in section 4.3.6). Below, in figure 5.2-10, results of the iron speciation are presented for the influent. This shows that in the majority of samples measured, the influent was predominantly made up of ferrous iron (Fe^{2+}) and only on a few occasions did ferric iron (Fe^{3+}) make up a larger portion. In table 5.2-9 the max, min and mean percentages of the ferrous iron portion of total iron for the effluent of all tanks is presented, this shows that the majority of iron present is ferrous iron. The minimums show that there were a few outlying points but in general the portion of reduced is above 90% for tanks 1,2,4, and 5. Tank 3's mean ferrous percentage is still high at 87% and tank 5 is only slightly lower at 73%. Speciation of arsenic showed that all arsenic present, in the influent and effluent, is in the reduced form of arsenite (As^{3+}) (figure 5.2-11). Figure 5.2.12 shows results from field analysis for sulphide concentrations, this showed that sulphide was higher in those treatments with biosolids than in that with mussel shells, and also higher in treatments with more compost compared to less compost (results for sulphide analysis on the temperature treatment tanks are presented in section 5.4). A one-way analysis of variance (ANOVA) was undertaken on the effect of treatment on sulphide concentrations, which resulted in a p-value=0.007 (summarised in table 5.2-10), although a post hoc tukey test (for full results see appendix 3) determined that the only significant differences were between the small insulated tank and the two mussel shell treatments (M-LC and M-MC).

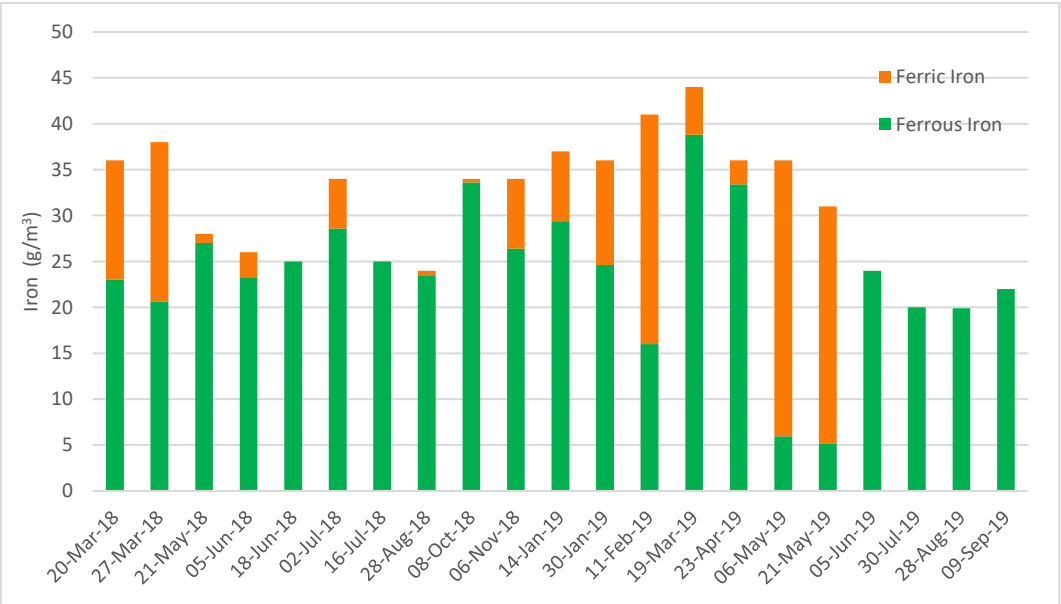

Figure 5.2- 10: Bar graph showing speciation of total iron in the influent of the systems (BioIn), from field measurements taken with a portable spectrometer.

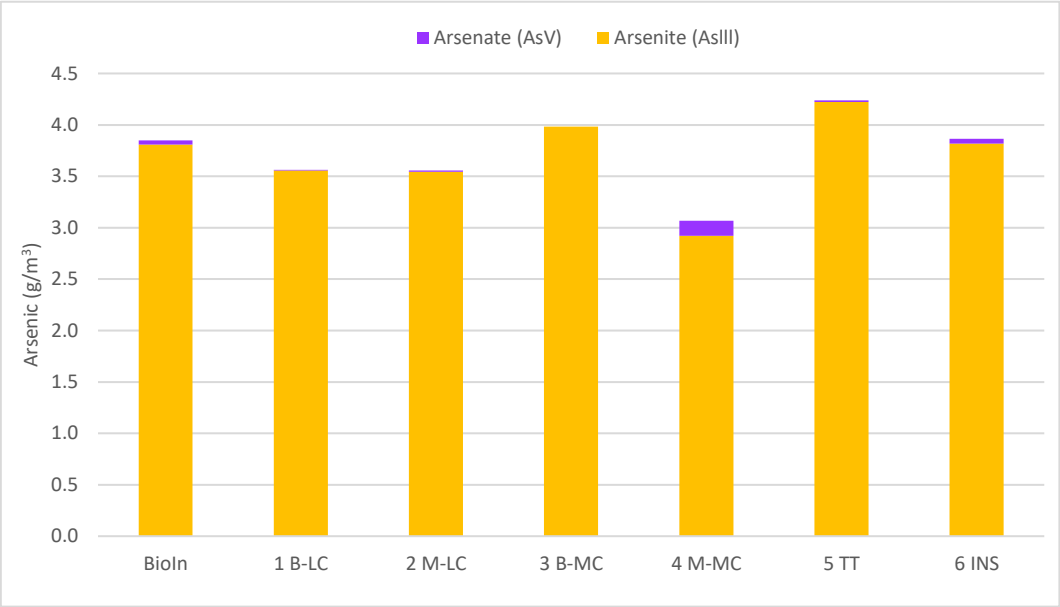

Figure 5.2- 11: Bar graph showing speciation results of total arsenic from influent (BioIn) and all effluent. B-LC: Biosolids with less compost, M-LC: mussel shells with less compost, B-MC: biosolids with more compost, M-MC: mussel shells with more compost, TT: small temperature control treatment, and INS: small insulated tank

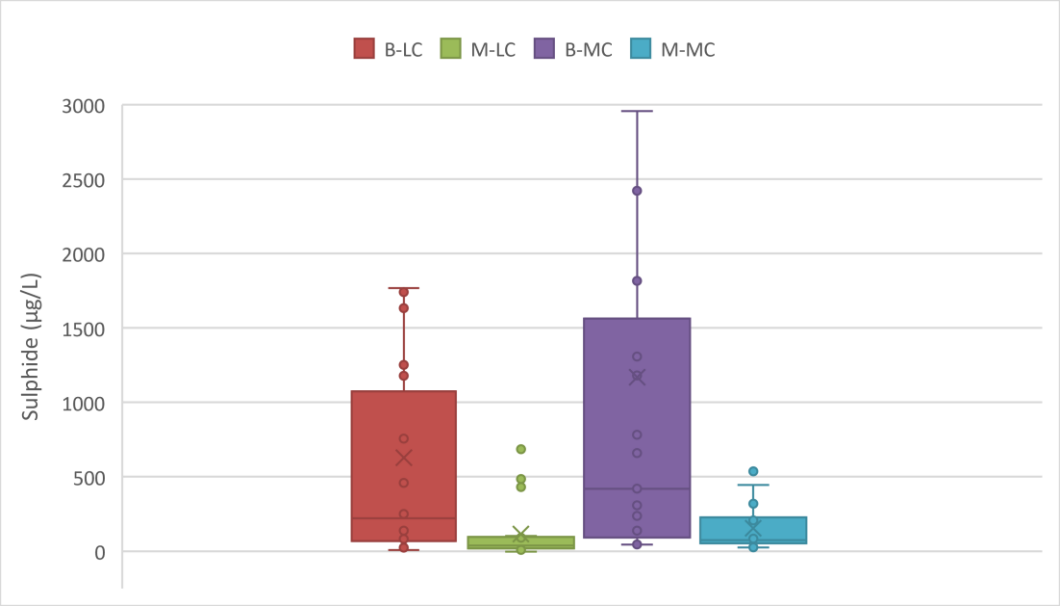

Figure 5.2- 12: Box and Wisker diagram showing concentrations of sulphide in the effluent of the systems. B-LC: Biosolids with less compost, M-LC: mussel shells with less compost, B-MC: biosolids with more compost, and M-MC: mussel shells with more compost.

Table 5.2- 9: Results of ANOVA on the effect of treatment on the sulphide concentrations

Effect of treatment on:	Df	F value	Pr(>F)
Sulphide concentrations	5	3.504	0.007 **

5.3 Hydraulic Residence Time- Bioreactors

Hydraulic residence time (HRT) was compared with iron, arsenic and sulphate removal for the treatments with different substrate mixtures. The key results from the comparisons of HRT include: 1) Iron has a positive response with HRT for all treatments; 2) Arsenic removal has the least positive relationship with HRT; and 3) Sulphate removal, while lower than both iron and arsenic, has the strongest positive relationship with HRT. Full water chemistry results are available in appendix 2.

5.3.1 Iron Removal

All treatments show an increase in percentage removal for dissolved iron with increased HRT (figure 5.3-1). Less compost treatments show that close to 100 percent removal can be achieved at 50 to 100 hours HRT, whereas the more compost treatments show a much wider spread in the data showing much less of a correlation especially for the B-MC treatment. Interestingly, the less compost treatments also show more of a linear relationship while the more compost show a more logarithmic relationship.

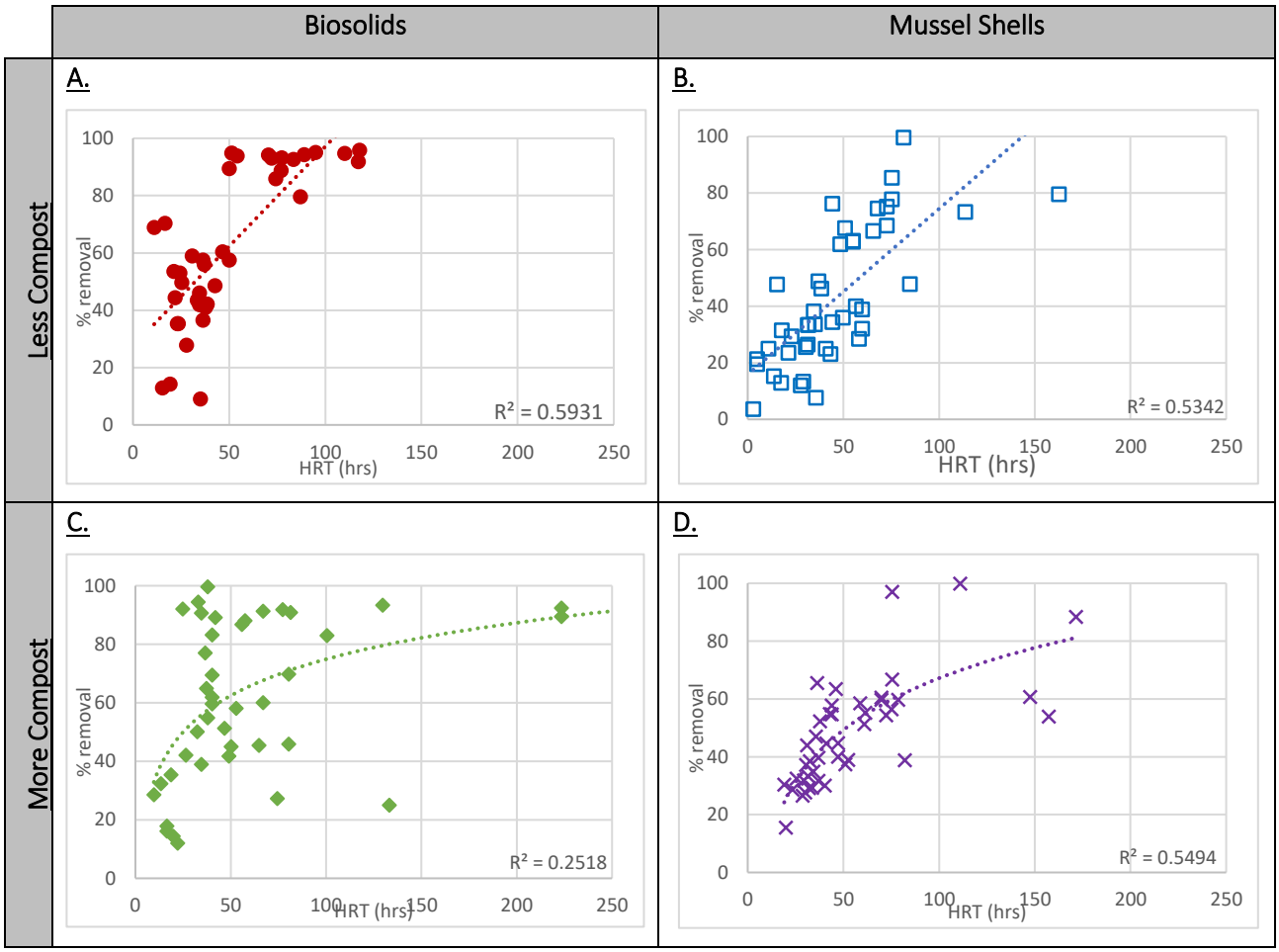

Figure 5.3- 1: Graphs showing dissolved iron removal over HRT for A) B-LC (Biosolids with less compost), B) M-LC (mussel shells with less compost), C) B-MC (biosolids with more compost) and D) M-LC (mussel shells with less compost).

5.3.2 Arsenic Removal

Dissolved arsenic removal data with HRT is presented below in figure 5.3-2. Dissolved arsenic removal shows a positive logarithmic relationship with both mussel shell treatments. The minimum percentage removal for the B-LC treatment shows a strong positive correlation with HRT but that removal of >90% also occurs at all HRTs giving a weak R^2 value. The B-MC treatment showed no correlation with HRT.

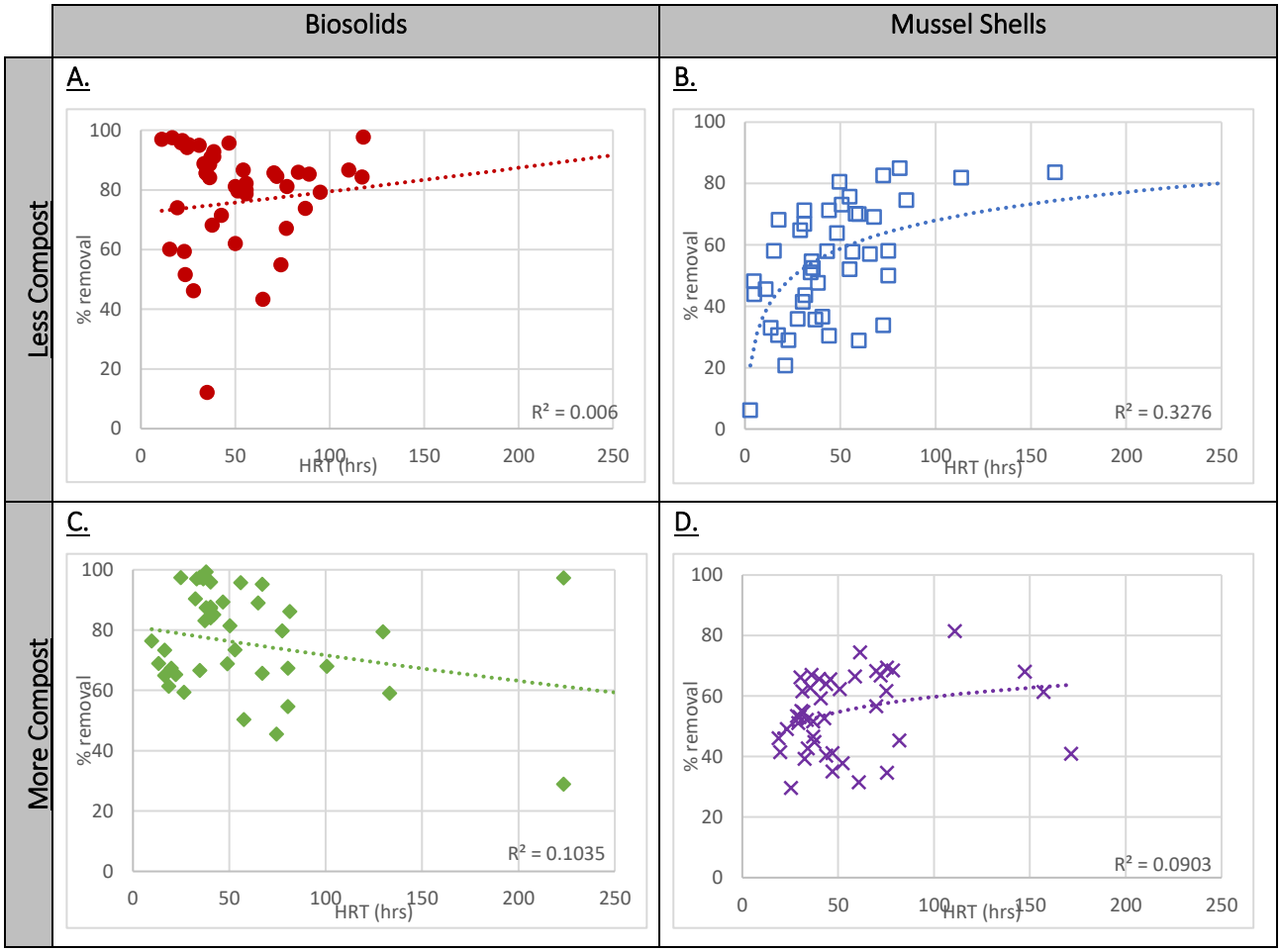

Figure 5.3- 2: Graphs showing dissolved arsenic removal over HRT for A) B-LC (Biosolids with less compost), B) M-LC (mussel shells with less compost), C) B-MC (biosolids with more compost) and D) M-LC (mussel shells with less compost)

5.3.3 Sulphate Removal

Sulphate removal data with HRT is presented below in figure 5.3-3. Sulphate removal for all treatments showed a positive relationship with HRT, with percent removal increasing with the longer HRT. While the removal was less than that of arsenic or iron, sulphate removal has the strongest relationship overall, when looking at all treatments. It also shows that treatments with biosolids have higher sulphate removal than treatments with mussel shells, with up to 40% removal achieved in biosolid treatments at about a 75hour HRT.

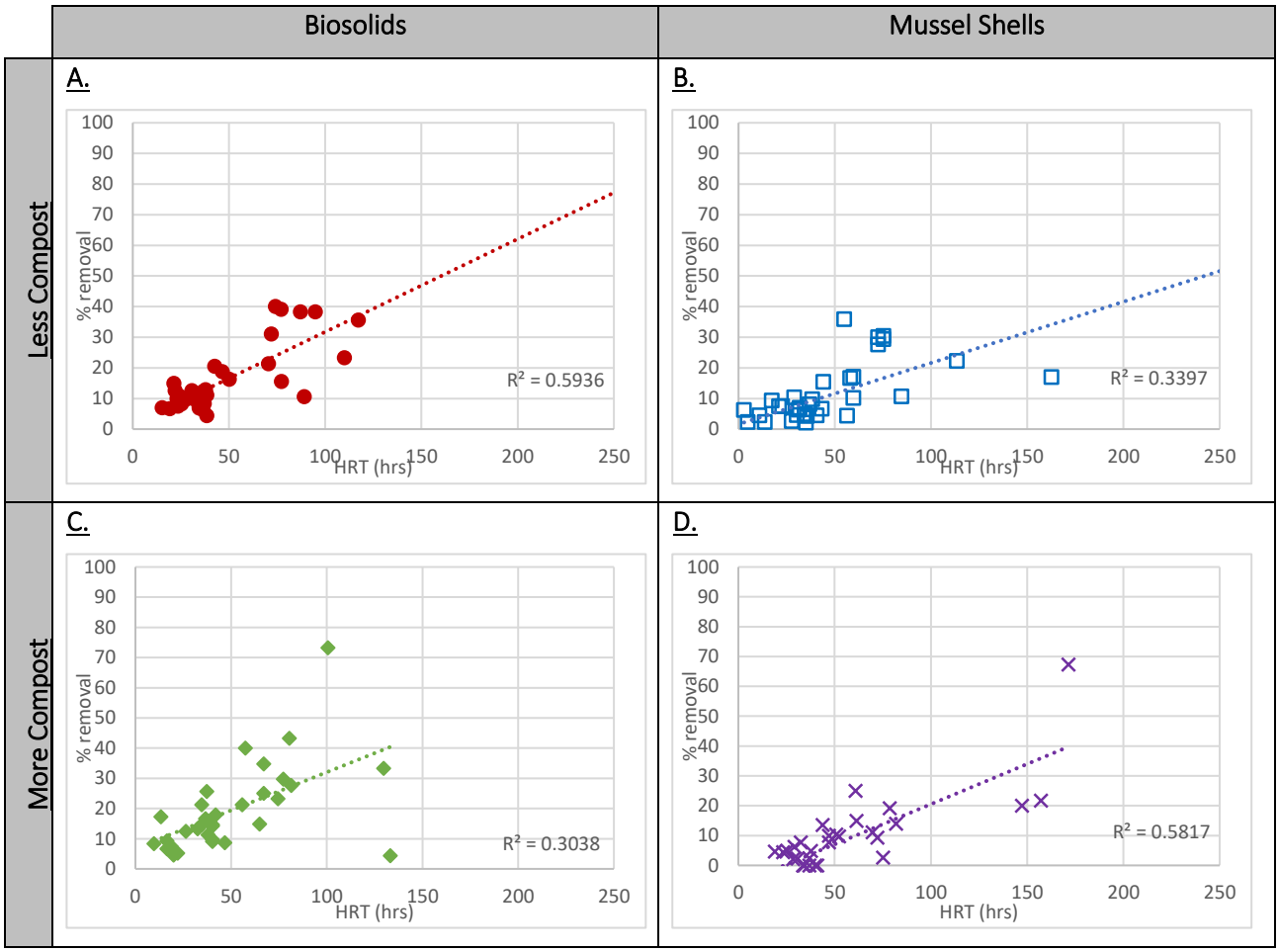

Figure 5.3- 3: Graphs showing sulphate removal over HRT for A) B-LC (Biosolids with less compost), B) M-LC (mussel shells with less compost), C) B-MC (biosolids with more compost) and D) M-LC (mussel shells with less compost)

5.4 Temperature Treatments- Bioreactors

Temperature treatments include iron, arsenic and sulphate removal trials for insulated and variably controlled temperature regimes within bioreactors including different substrate compositions. The key results from the temperature treatments include: 1) Temperatures in the side of the tanks fluctuates diurnally whereas temperature in the middle of the tanks is more stable; 2) Internal temperature is more controlled by influent temperature than by ambient air temperature; 3) Insulated tanks prevent diurnal fluctuations more than standard tanks; and 4) Removal of metals and sulphate is greater in smaller tanks than large tanks. Full water chemistry results are available in appendix 2.

5.4.1 Temperature Probe Results

Temperature probes were located at the sides and middle of all tanks as well as a probe in the influent IBC and one to record the ambient air temperature (figure 5.4-1), with the average temperatures displayed in table 5.4-1. Influent water temperature showed very little variation and was stable at around 12°C. The data from the probes shows that for tanks 2-5 there was more temperature fluctuation in the sides of the tanks than in the middle of the tanks. The side temperature fluctuation followed the same diurnal fluctuation as the ambient air temperature, although to a much less varied extent and delayed by 12 hours. The temperature in the middle of the tanks, while more stable, was also variable between tanks. The average temperature in all tanks, with the exception of tanks 2 and 5, was higher on the side than in the middle, with the mean temperature in the middle being more similar to the influent temperature. Tank 2's average temperature in the middle was similar to all other tanks although the average side temperature was much lower than all other tanks. Tank 5's average temperatures showed a similar trend to tank 2 with the average middle temperature being similar to all other tanks but the average side temperature being much lower. It is worth noting that tank 5 only has a very small amount of available data due to a probe fouling after only a few weeks, which may have skewed the temperature averages. Tank 6 (insulated tank) was trialled with the intention to lessen the effect of cold ambient air temperatures on the internal temperature, which has been shown to reduce the SRB activity and therefore lower the removal efficiency. As seen on figure 5.4-1 (6a) the average temperature on the sides of the tank fluctuated less than all other tanks, and the side temperatures remained very similar to the middle temperatures until mid-April where the probe seems to have fouled. Figure 5.4-2 shows the side and middle data for tank 6 plotting in between the warmer middle temperatures and colder side temperatures of tank 5.

1a.

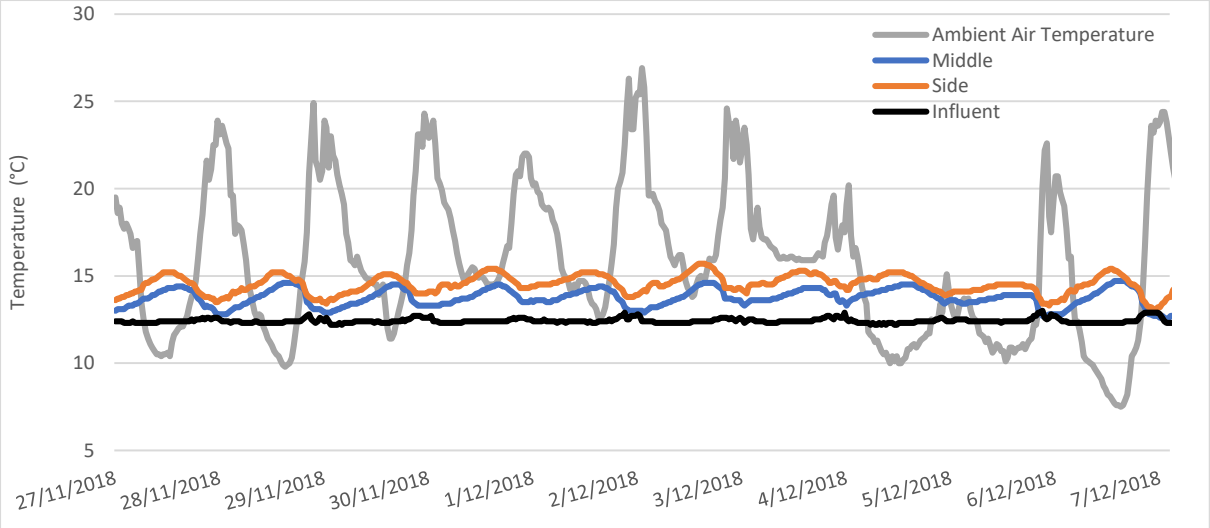

1b.

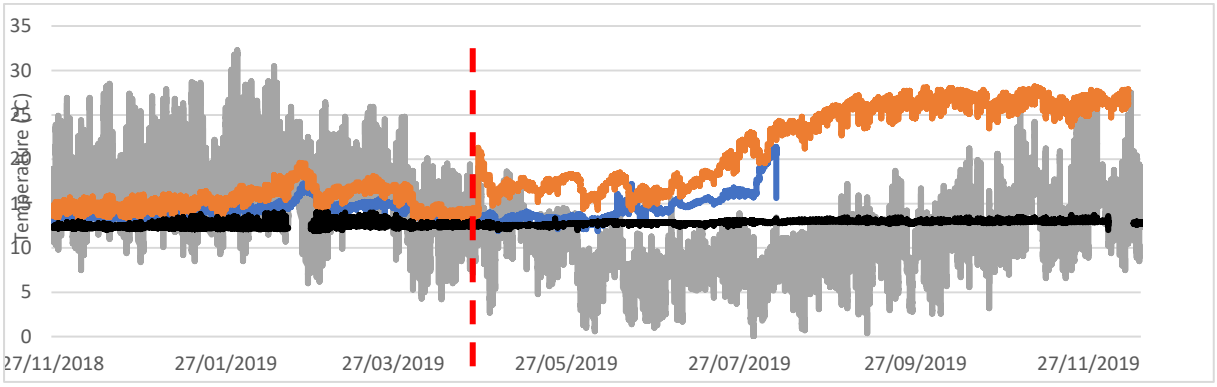
35
30
25
20
15
10
5
0
Temperature (°C)
27/11/2018
27/01/2019
27/03/2019
27/05/2019
27/07/2019
27/09/2019
27/11/2019

2a.

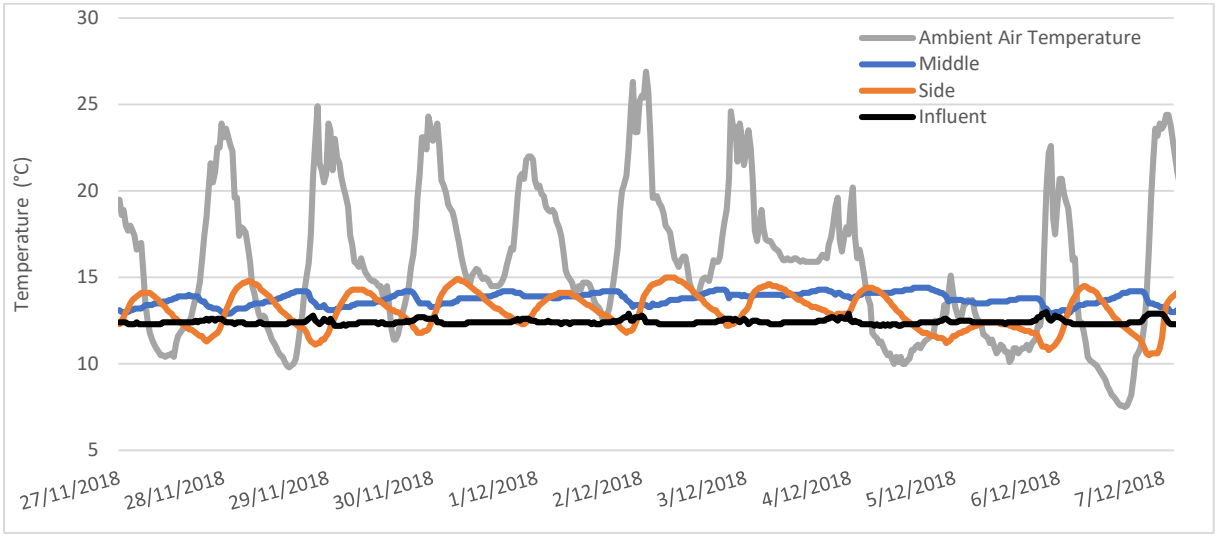
30
25
20
15
10
5
Temperature (°C)
Ambient Air Temperature
Middle
Side
Influent
27/11/2018
28/11/2018
29/11/2018
30/11/2018
1/12/2018
2/12/2018
3/12/2018
4/12/2018
5/12/2018
6/12/2018
7/12/2018

2b.

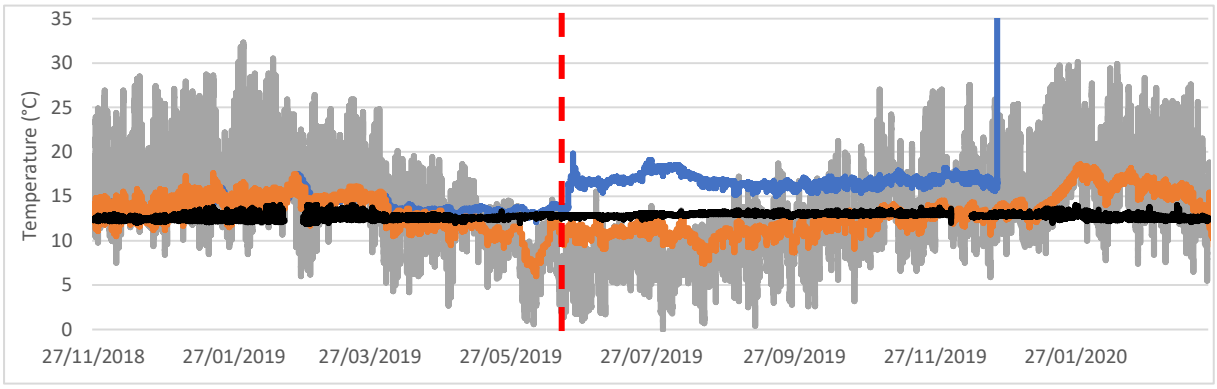
35
30
25
20
15
10
5
0
Temperature (°C)
27/11/2018
27/01/2019
27/03/2019
27/05/2019
27/07/2019
27/09/2019
27/11/2019
27/01/2020

3a.

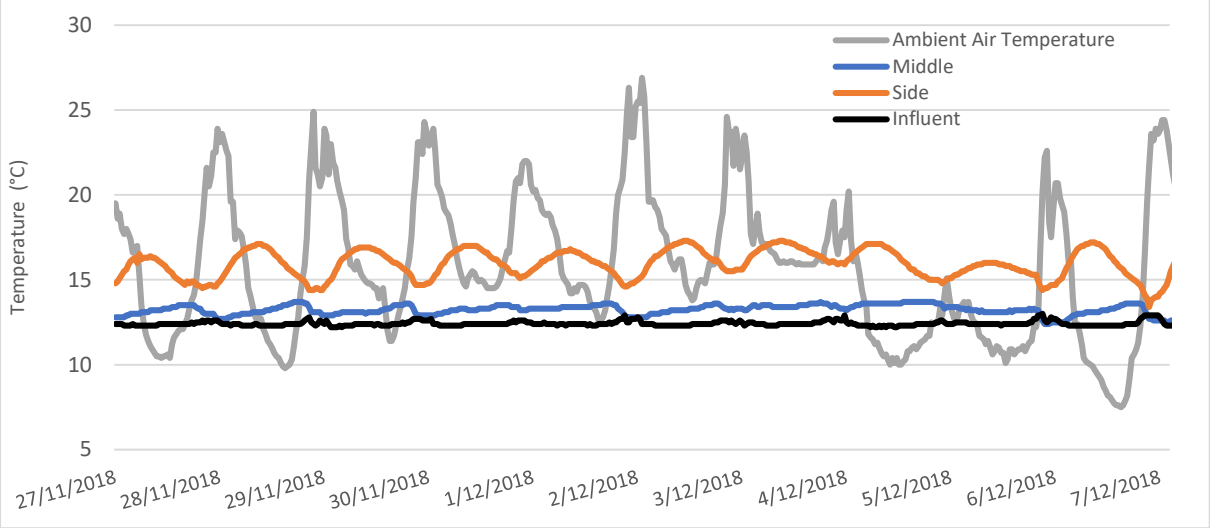
Ambient Air Temperature
Middle
Side
Influent
Temperature (°C)
30
25
20
15
10
5
27/11/2018
28/11/2018
29/11/2018
30/11/2018
1/12/2018
2/12/2018
3/12/2018
4/12/2018
5/12/2018
6/12/2018
7/12/2018

3b.

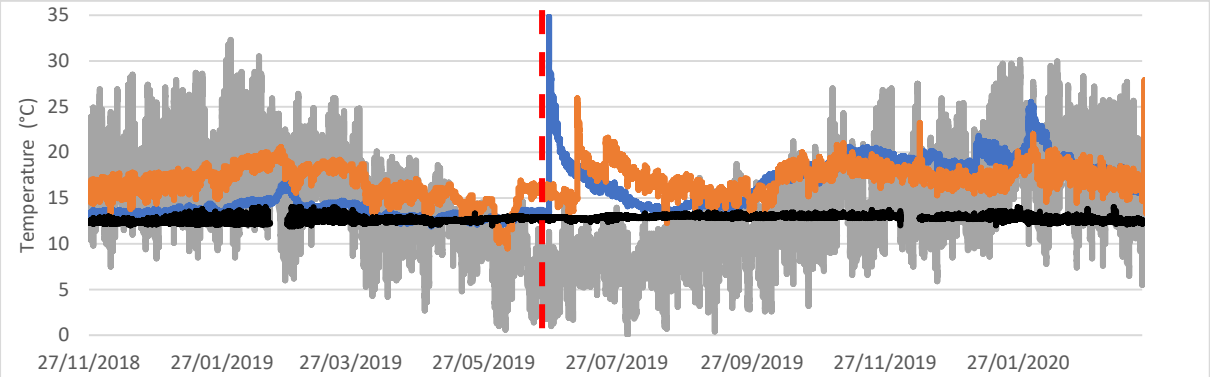
Temperature (°C)
35
30
25
20
15
10
5
0
27/11/2018
27/01/2019
27/03/2019
27/05/2019
27/07/2019
27/09/2019
27/11/2019
27/01/2020

4a.

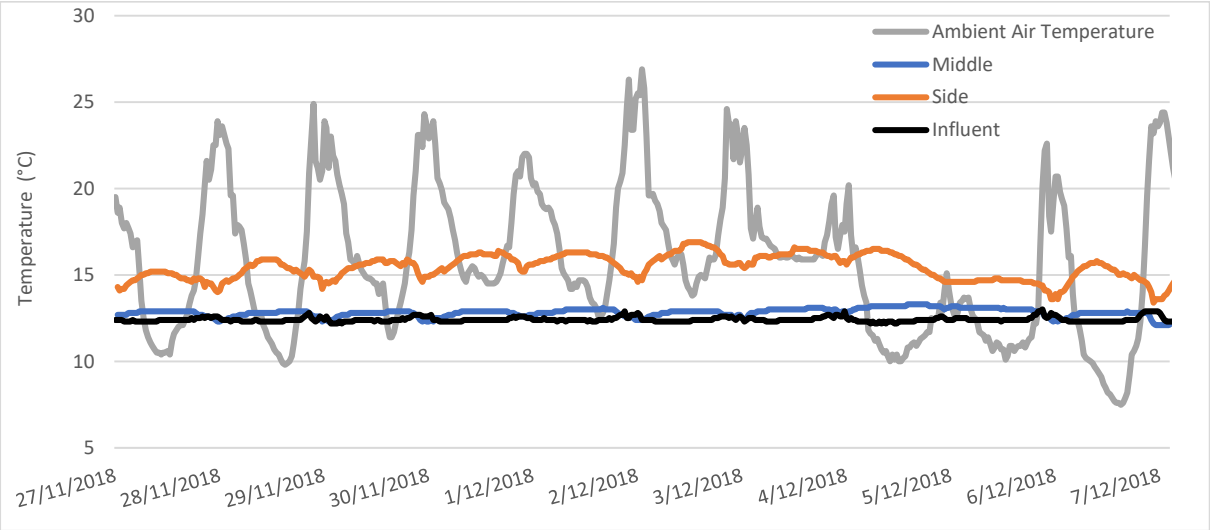
Ambient Air Temperature
Middle
Side
Influent
Temperature (°C)
30
25
20
15
10
5
27/11/2018
28/11/2018
29/11/2018
30/11/2018
1/12/2018
2/12/2018
3/12/2018
4/12/2018
5/12/2018
6/12/2018
7/12/2018

4b.

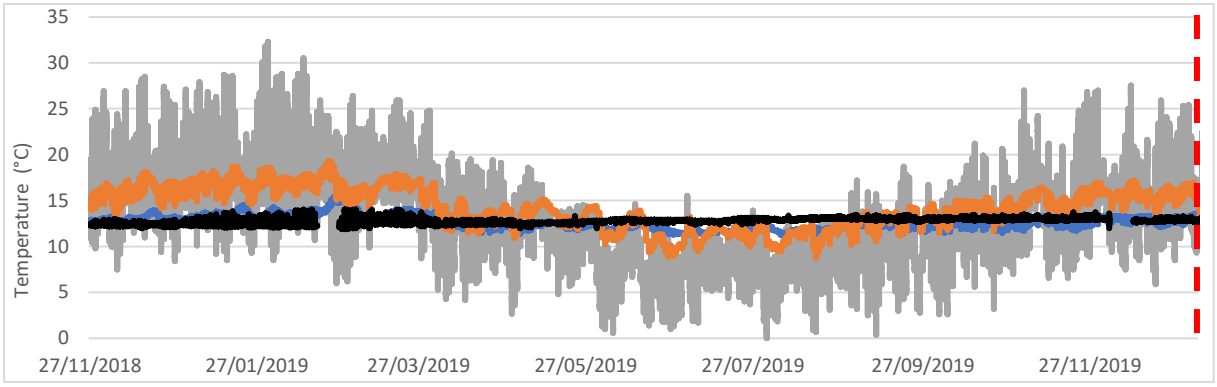
Temperature (°C)
35
30
25
20
15
10
5
0
27/11/2018
27/01/2019
27/03/2019
27/05/2019
27/07/2019
27/09/2019
27/11/2019

5a.

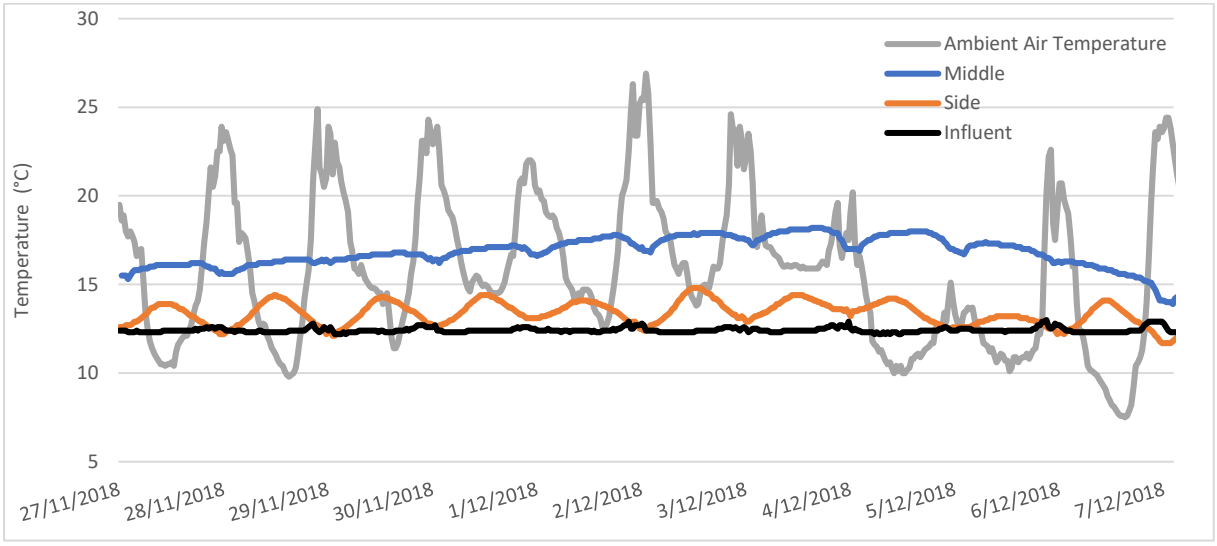
Temperature (°C)
30
25
20
15
10
5
Ambient Air Temperature
Middle
Side
Influent
27/11/2018
28/11/2018
29/11/2018
30/11/2018
1/12/2018
2/12/2018
3/12/2018
4/12/2018
5/12/2018
6/12/2018
7/12/2018

5b.

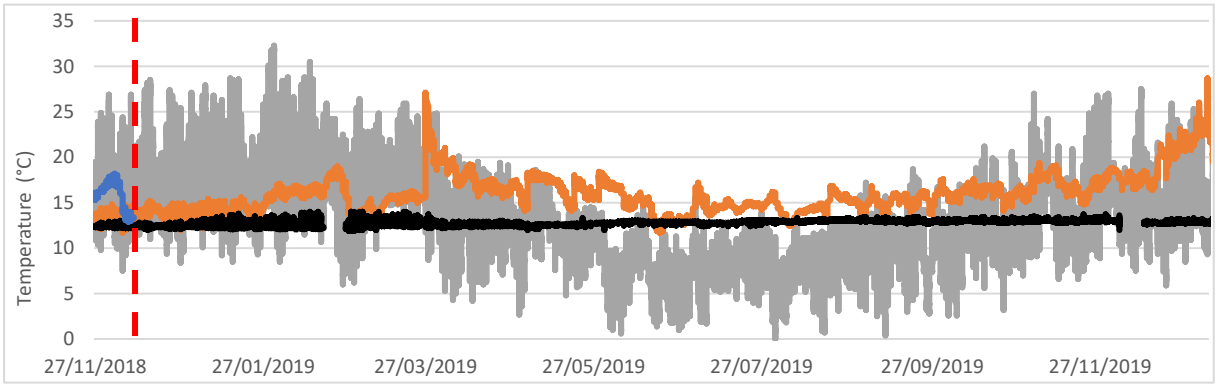
Temperature (°C)
35
30
25
20
15
10
5
0
27/11/2018
27/01/2019
27/03/2019
27/05/2019
27/07/2019
27/09/2019
27/11/2019

6a.

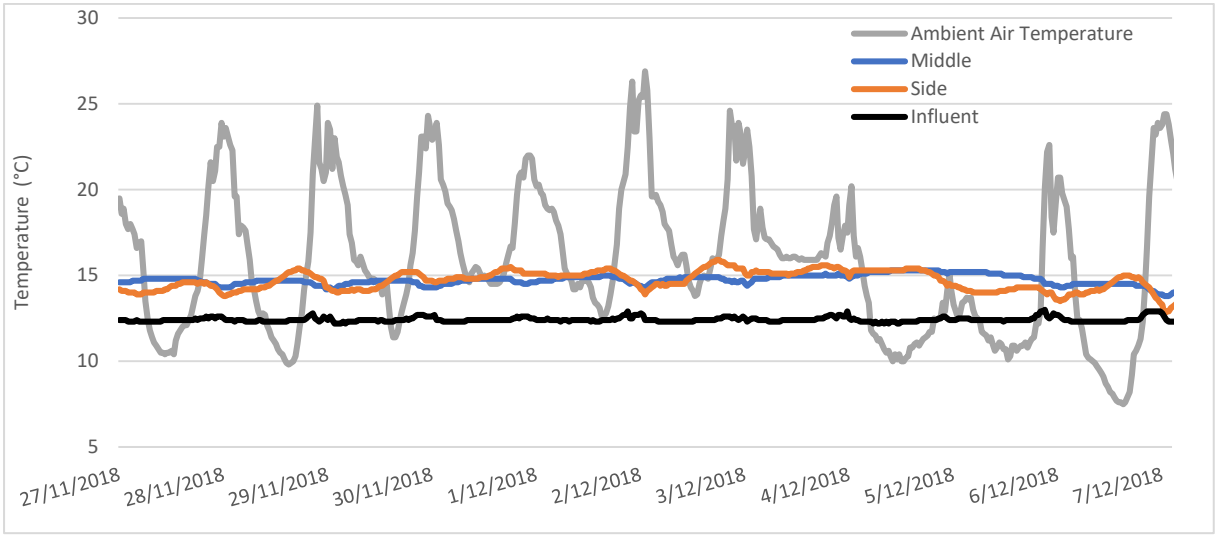

6b.

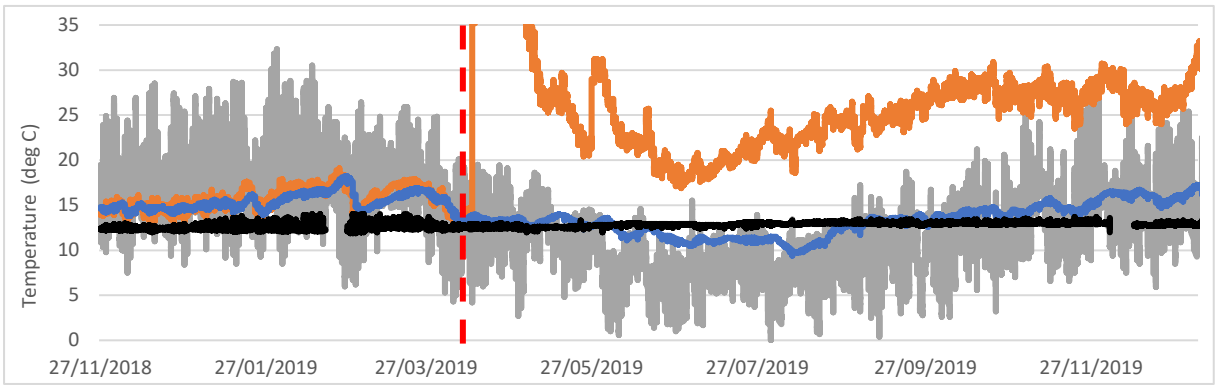

Figure 5.4- 1: (1a., 1b., 2a., 2b., 3a., 3b.,4a., 4b., 5a., 5b., 6a. & 6b.) Temperature probe data from inside Tanks 1-6 plotted with ambient air temperature and influent temperature, A. graphs: depict a close up of 1 month's data and B. graphs: a year's worth of data. Note: Numbers are representative of tank numbers eg. 1a and 1b are Tank 1's temperature data. Note: Several of the probes seem to have fouled after a few months showing erratic data. Data from beyond this point is considered erroneous (depicted as red dashed line).

Table 5.4- 1: Average Temperatures in tanks (in degrees Celsius). Note: Erroneous data excluded, and only where data is available for both middle and side used to calculate

Tank #	Middle (average)	Side (average)
1	14.00	15.75
2	13.80	11.70
3	14.55	15.40
4	13.15	15.00
5	14.35	12.85
6	14.20	14.30

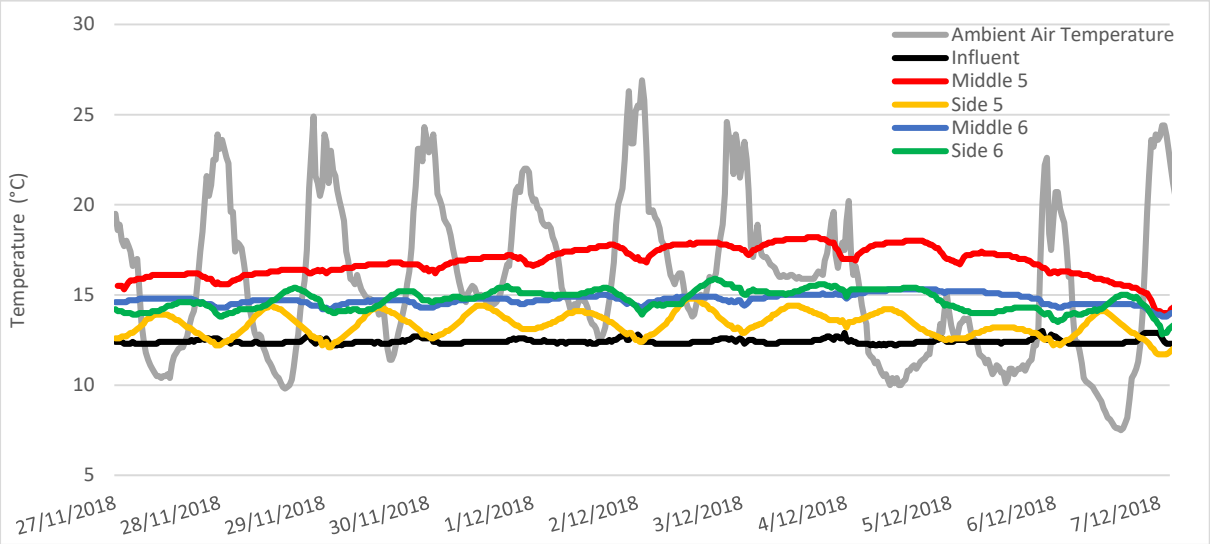

Figure 5.4- 2: Graph showing a snapshot of the internal temperature (side and middle) of Tank 5 (temperature control), plotted with the internal temperature of (side and middle) of Tank 6 (insulated). Ambient air temperature at the site and the influent temperatures are also plotted for comparison.

5.4.2 Iron Removal

Results comparing dissolved iron removal in the temperature treatments are presented below in figure 5.4-3. The insulated tank showed higher mean dissolved iron removal than both the temperature control treatment (TT) and the large tank of the same mix (B-MC), although the small control showed a higher mean removal than the big control treatment (5.4-4). Although mean iron removal is higher in the insulated tank, the scatter of the data according to HRT appears to show little difference between treatments. A one-way analysis of variance (ANOVA) was undertaken on the effect of treatment on iron removal (summarised in table 5.2-6). A post hoc tukey test (full results in appendix 3) showed there was no statistical difference between either the different sized tanks with the same mix (B-MC and TT), or between the small control and the insulted tank (TT and INS) (p-value=0.649 and 0.344 respectively).

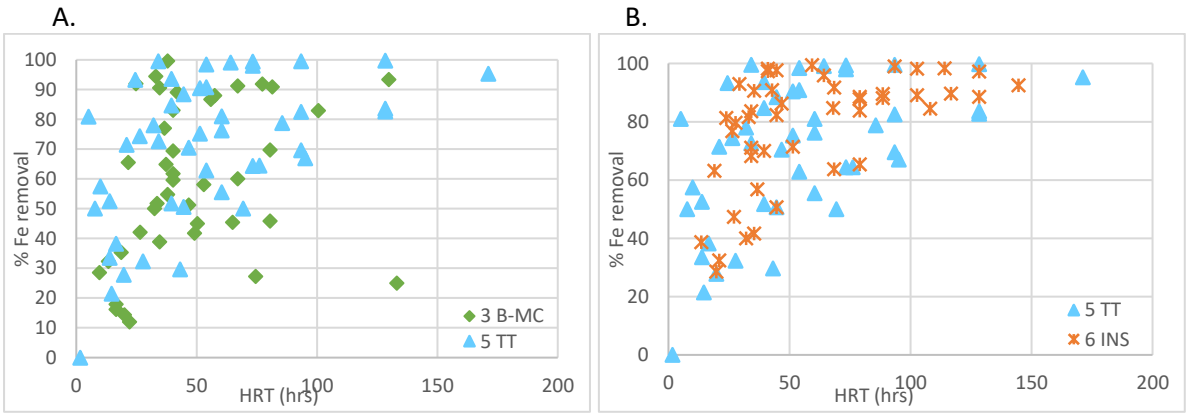

Figure 5.4- 3: Graphs comparing dissolved iron removal between A) the large treatment of biosolids with more compost (B-MC) and the small temperature control tank (TT) of the same mix to show effect of size, and B) small temperature control (TT) and insulated treatment (INS). Note: all tanks have the same substrate mix with biosolids and more compost.

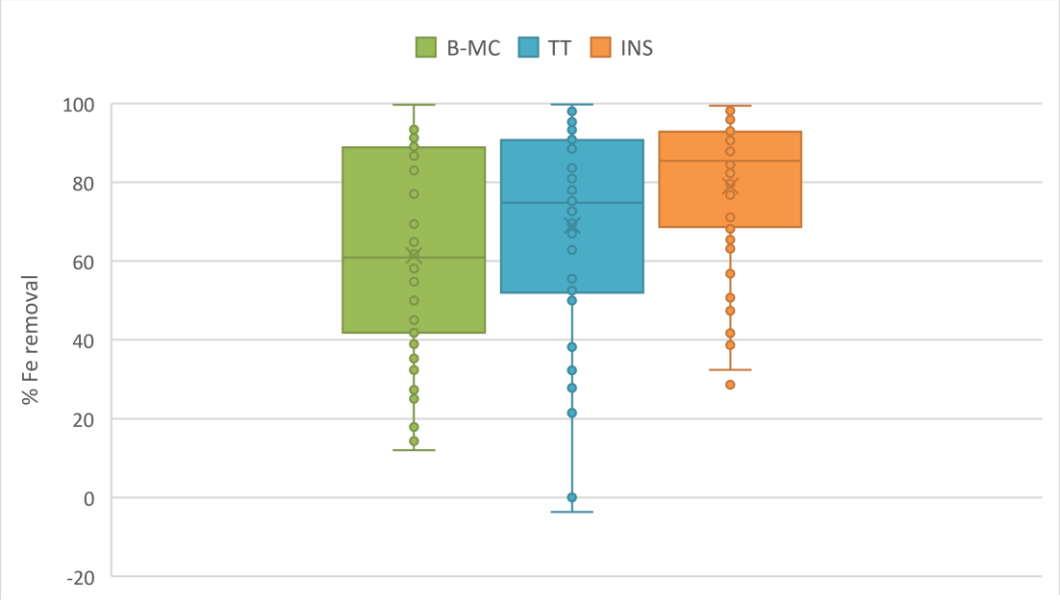

Figure 5.4- 4: Box and Wisker diagram displaying dissolved iron removal for the temperature treatments and the large tank of the same mix (B-MC). B-MC: biosolids more compost (large tank),TT: small temperature control treatment with biosolids more compost mix, and INS: small insulated tank with biosolids more compost.

5.4.3 Arsenic Removal

Results comparing dissolved arsenic removal in the temperature treatments are presented below in figure 5.4-5. Figure 5.4-6 shows that, unlike dissolved iron, mean dissolved arsenic removal was similar between all treatments. A one-way analysis of variance (ANOVA) was undertaken on the effect of treatment on arsenic removal in the insulated tank compared to non-insulated tanks (summarised in table 5.2-7). A post hoc tukey test (full results in appendix 3) determined that there is no significant difference between either the large and small control tanks (B-MC and TT) or the small control tank compared to the insulted tank (TT and INS), with p-values of 0.332 and 0.546 respectively.

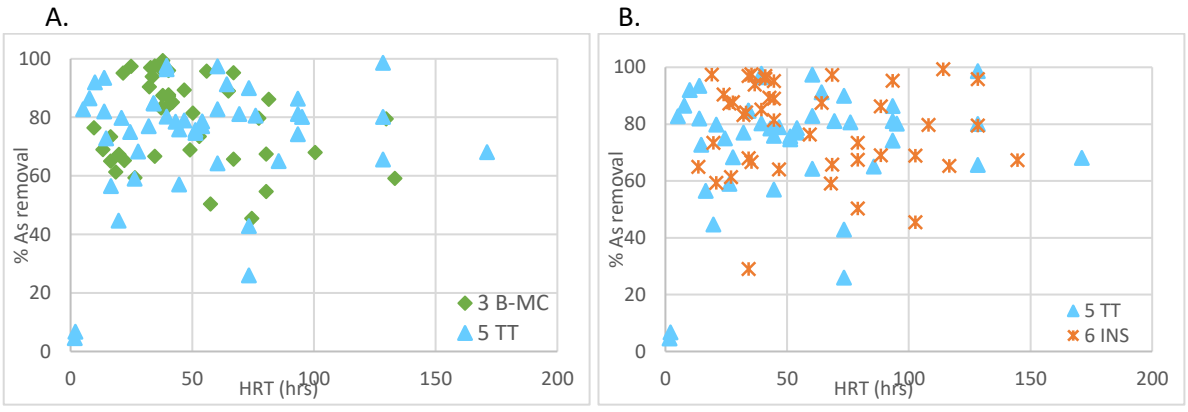

Figure 5.4- 5: Graphs comparing dissolved arsenic removal between A) the large treatment of biosolids with more compost (B-MC) and the small temperature control tank (TT) of the same mix to show effect of size, and B) small temperature control (TT) and insulated treatment (INS). Note: all tanks have the same substrate mix with biosolids and more compost.

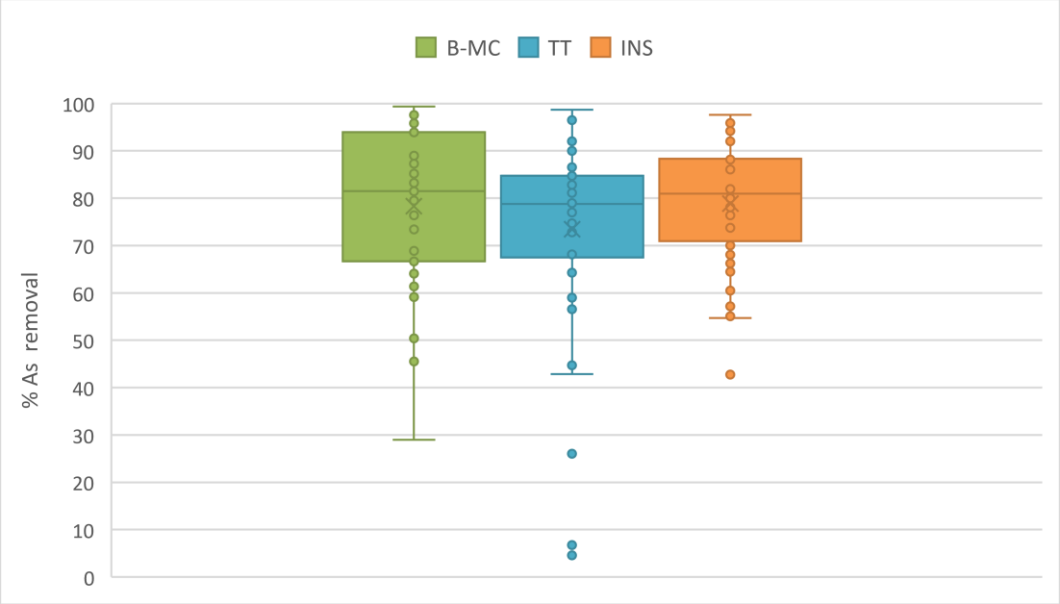

Figure 5.4- 6: Box and Wisker diagram displaying dissolved arsenic removal for the temperature treatments and the large tank of the same mix (B-MC). B-MC: biosolids more compost (large tank),TT: small temperature control treatment with biosolids more compost mix, and INS: small insulated tank with biosolids more compost.

5.4.4 Sulphate Removal

Results comparing sulphate removal in the temperature treatments are presented below in figure 5.4-7. Figure 5.4-8 shows that as with arsenic there is no difference in sulphate removal between temperature treatments. Although arsenic removal showed a slightly higher mean result for the insulated treatment, removal for sulphate is very similar in all treatments. A one-way analysis of variance (ANOVA) was undertaken on the effect of treatment on sulphate removal (summarised in table 5.2-6). A post hoc tukey test (full results in appendix 3) showed that there is no significant difference between either the large and small control tanks (B-MC and TT) or the small control tank compared to the insulted tank (TT and INS), with p-values of 0.999 and 0.999 respectively.

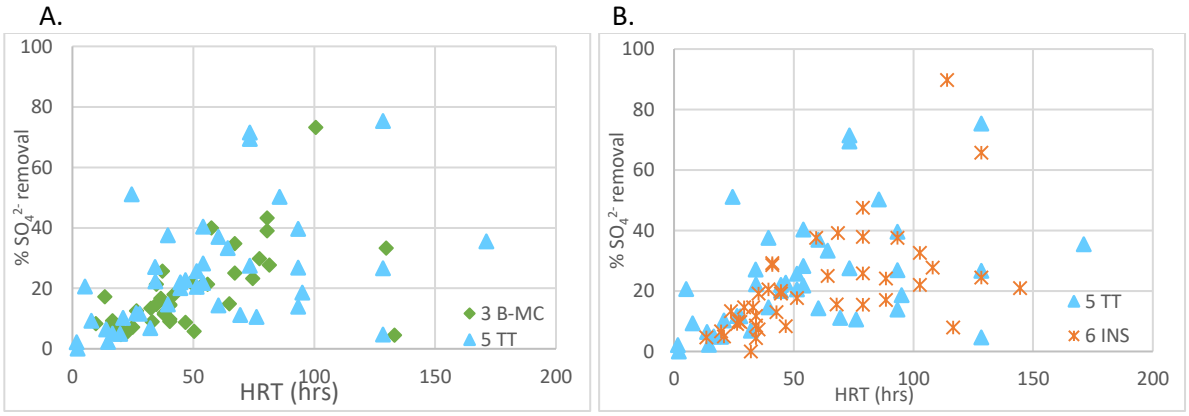

Figure 5.4- 7: Graphs comparing sulphate removal between A) the large treatment of biosolids with more compost (B-MC) and the small temperature control tank (TT) of the same mix to show effect of size, and B) small temperature control (TT) and insulated treatment (INS). Note: all tanks have the same substrate mix with biosolids and more compost.

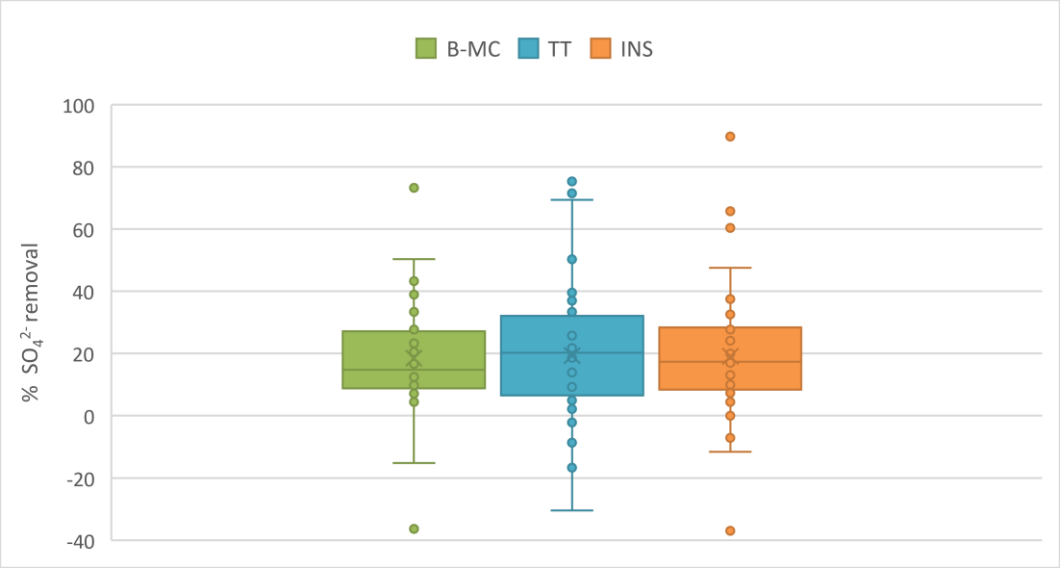

Figure 5.4- 8: Box and Wisker diagram displaying sulphate removal for the temperature treatments and the large tank of the same mix (B-MC). B-MC: biosolids more compost (large tank),TT: small temperature control treatment with biosolids more compost mix, and INS: small insulated tank with biosolids more compost.

5.4.4 Sulphide Results

Sulphide in the effluent was determined in field using a portable spectrometer results of the temperature treatments are presented in figure 5.4-9. Ferrous iron and arsenic speciation were also completed on these treatments but is presented in section 5.2.5. A one-way analysis of variance (ANOVA) was undertaken on the effect of treatment on sulphide concentrations (summarised in table 5.2-10). A post hoc tukey test (full results in appendix 3) shows that while mean sulphide production was higher in the insulated tank (INS), than both controls (B-MC and TT), and the concentrations of sulphide were generally higher in the small control (TT) than the large tank with the same mix (B-MC), there was no statistical difference between these treatments.

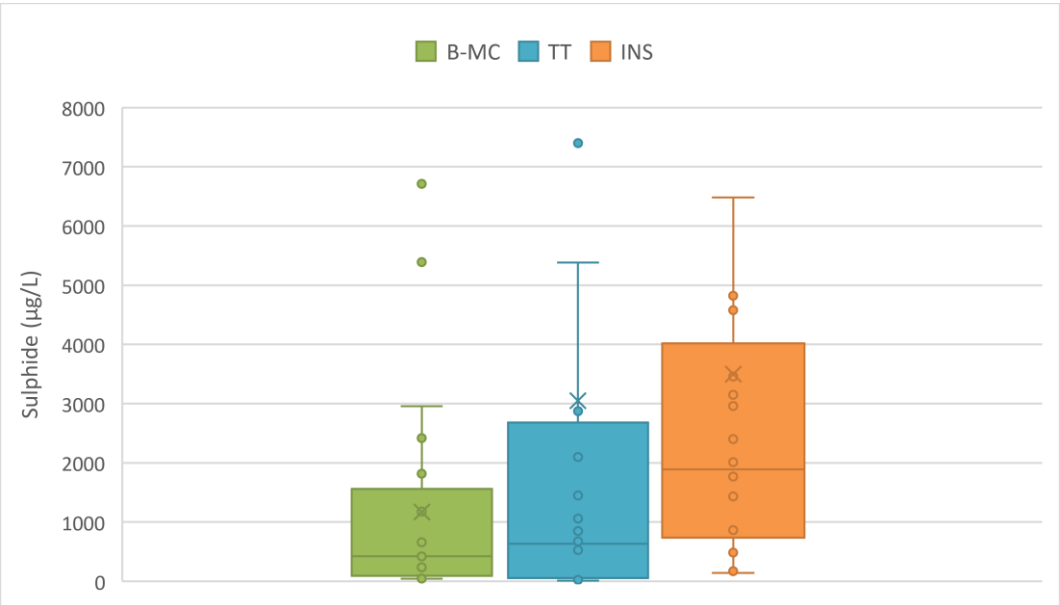

Figure 5.4- 9: Box and Wisker diagram displaying sulphide concentrations in the effluent of the temperature treatments and the large tank of the same mix (B-MC). B-MC: biosolids more compost (large tank), TT: small temperature control treatment with biosolids more compost mix, and INS: small insulated tank with biosolids more compost. Note: Outlying data not displayed on graph.

5.5 Precipitate Analysis Results- Bioreactors

Key findings from the precipitate analysis are: 1) metal concentrations were variable with different sampling methods, 2) Iron oxide appear to be present in the outlets of mussel shell treatments, whereas crystalline sulphur was found in the outlets of the two small tanks, and 3) Iron sulphide was detected by XRD analysis from precipitates from inside tank 2 (M-LC).

Precipitate sludge samples were taken on two occasions during this trial. The first was approximately 6 months after the systems started operating and was taken from the discharge pipes. The second was taken at the end of the trial and was taken from the flush valve at the base of each tank. The different methods were undertaken to attempt to get a sample which had as little oxygen contamination as possible to prevent the oxidation of any potential sulphides (for more details see section 3.3.6). Both methods of sampling made this extremely difficult and therefore results are variable. As seen in figure 5.5-1, precipitates from the outlets of tanks from the first sampling round showed that tanks with biosolids (1, 3, 5 & 6) had precipitates that were dark brown to black (suggesting sulphides), whereas tanks with mussel shells (2 & 4) produced an orange sludge (suggesting oxidised iron). In the second round of sampling, the precipitates were a hard, platy texture and a dark grey/ black colour for all tanks. There was no visible difference in precipitates between tanks in the second round of sampling.

Figure 5.5- 1: Photo of precipitate sludge from the first round of precipitate sampling. From left: Tank 1, Tank 2, Tank 3, Tank 4, Tank 5, Tank 6

5.5.1 X-Ray Fluorescence Multi-element scan

Iron (weight %) was highest in tank 2 (M-LC) on both sampling occasions. On the first round of sampling both mussel shell tanks (2 & 4) had higher iron than the biosolid tanks. All tanks, except for tank 2, contained much less iron for the second round of sampling compared to the first see figure 5.5-2.

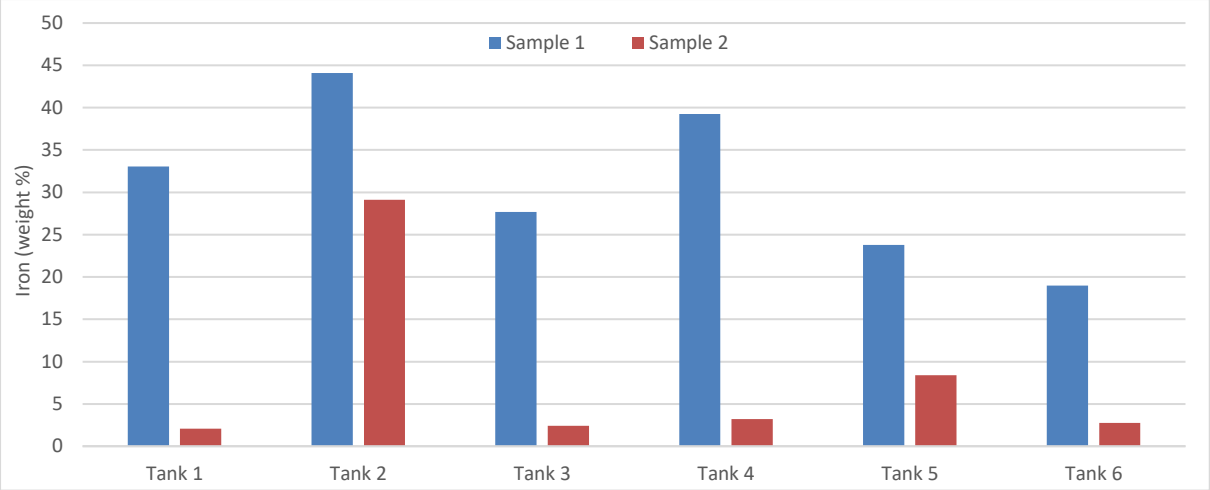

Figure 5.5- 2: Bar graph showing iron (by % weight) from precipitate sludge samples taken on the 1) 28/8/2018 and on the 2)10/3/2020. (Tank mix by number: 1= B-LC, 2=M-LC, 3=B-MC, 4=M-MC, 5=Temp control, 6=Insulated, where B=biosolids, M=mussel shell, LC=less compost and MC=more compost)

Arsenic (weight %) was higher in the mussel shell tanks (2 & 4) on the first round of sampling compared to the biosolid tanks (figure 5.5-3). The second round of sampling showed relatively low arsenic in all tanks except for tank 5 (small temperature control).

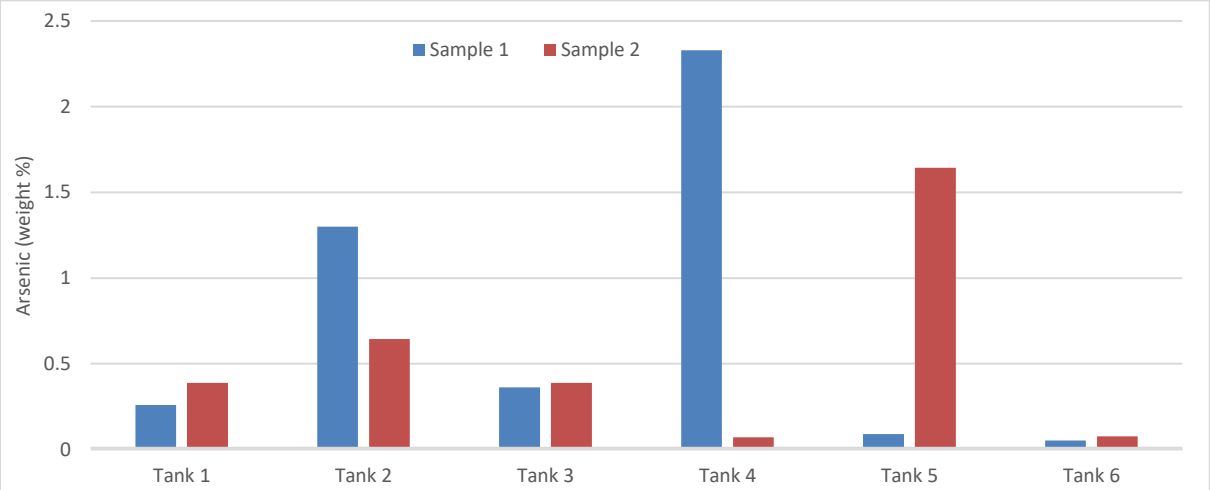

Figure 5.5- 3: Bar graph showing arsenic (by % weight) from precipitate sludge samples taken on the 1) 28/8/2018 and on the 2)10/3/2020. (Tank mix by number: 1= B-LC, 2=M-LC, 3=B-MC, 4=M-MC, 5=Temp control, 6=Insulated, where B=biosolids, M=mussel shell, LC=less compost and MC=more compost)

Sulphur (weight %) on the first sampling round was higher in the tanks containing biosolids (1, 3, 5 & 6) than those with mussel shells, especially when comparing the smaller temperature treatment tanks (5 & 6) (figure 5.5-4). The second round of sampling showed low results for all treatments except for tank 2 (M-LC), which had the lowest weight % in the first round of sampling.

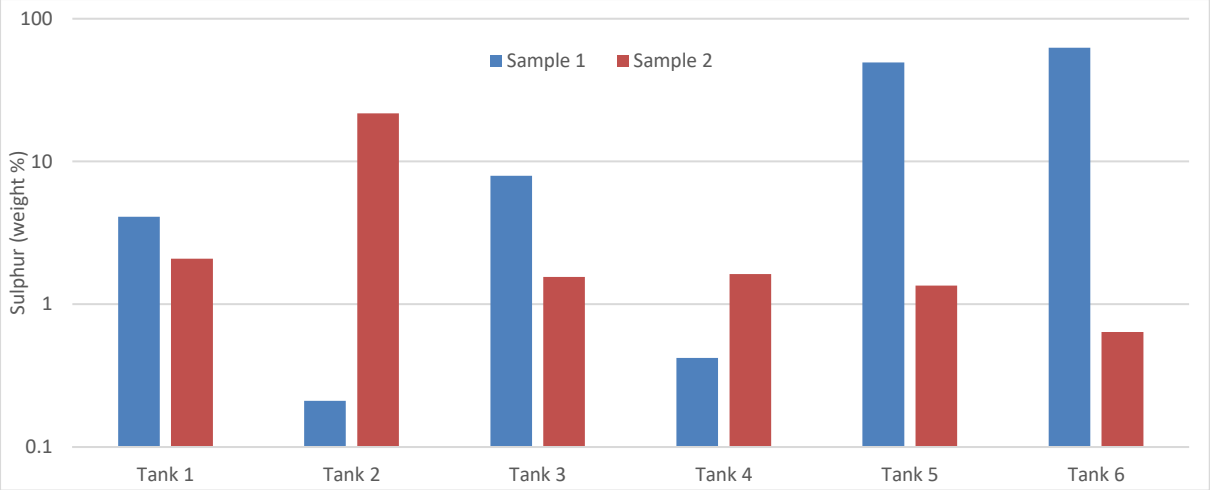

Figure 5.5- 4: Bar graph showing Sulphur (by % weight) from precipitate sludge samples taken on the 1) 28/8/2018 and on the 2)10/3/2020. (Tank mix by number: 1= B-LC, 2=M-LC, 3=B-MC, 4=M-MC, 5=Temp control, 6=Insulated, where B=biosolids, M=mussel shell, LC=less compost and MC=more compost)
Note: displaying logarithmic scale.

5.5.2 X-Ray Diffraction Analysis

XRD on the precipitates collected on the first round of sampling showed no peaks (i.e. 100% amorphous solid, such as iron-oxy-hydroxide) except for tanks 5 and 6 (the small temperature treatments), where the peaks were identified as 100% crystalline sulphur (figure 5.5 -5 and 5.5-6).

The XRD analysis on the second round of sampling showed very different results to the first. It showed for tanks 1, 3, 4, 5, and 6 that the most common minerals present were quartz, muscovite, plagioclase feldspar and potassium feldspar, although all these samples were noted as als having amorphous material present. Tank 2 showed lesser amounts of those minerals, but the most common crystalline mineral in this sample was Greigite, figure 5.5-7.

Phase Name	Phase Formula	Presence (%)
Sulfur	S	100

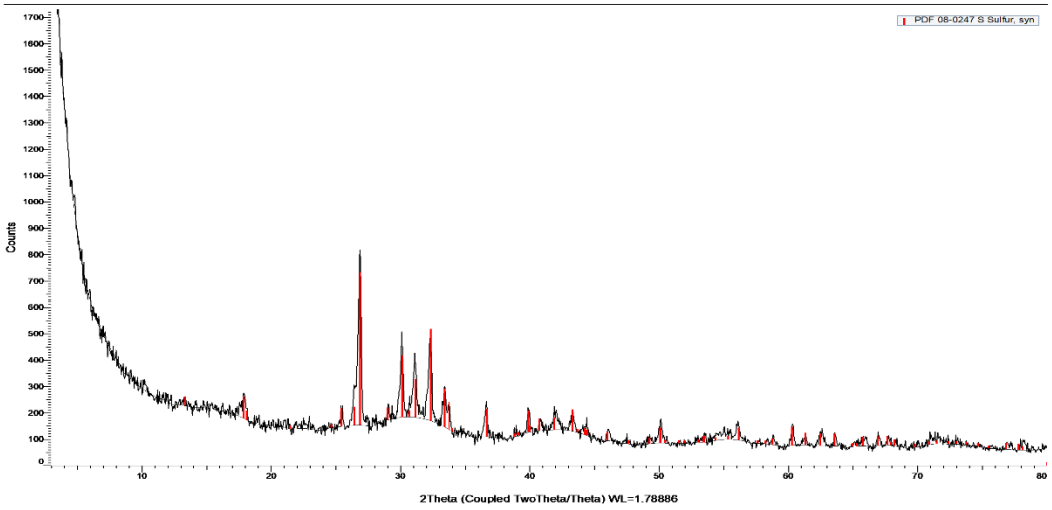

Figure 5.5- 5: XRD analysis of Tank 5 (small temperature control) from the first round of precipitate sampling

Phase Name	Phase Formula	Presence (%)
Sulfur	S	100

SA20511-06

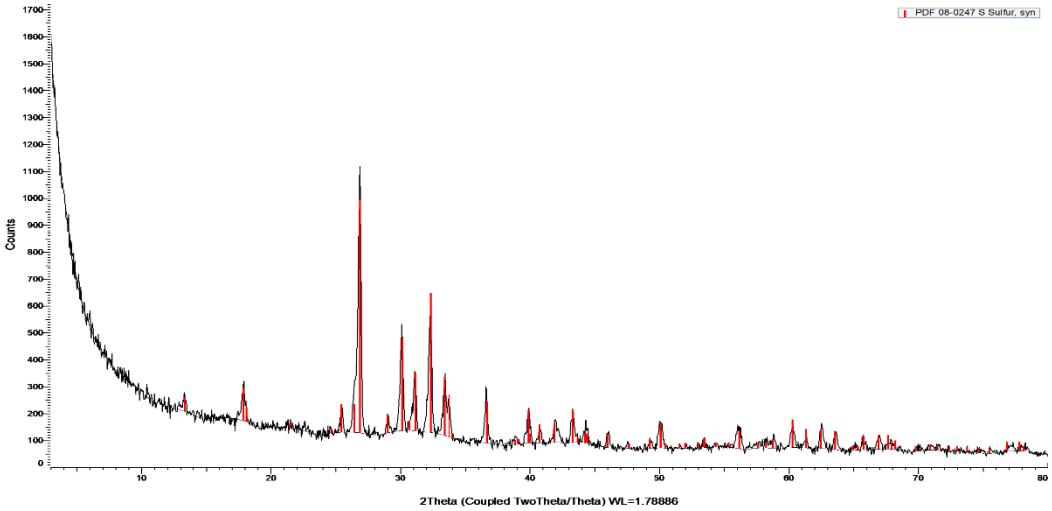

Figure 5.5- 6: XRD analysis of Tank 6 (Insulated tank) from the first round of precipitate sampling.

Phase Name	Phase Formula	Weight %
Quartz	SiO2	18
Muscovite	KAl2(Si3Al)O10(OH,F)2	9
Plagioclase Feldspar	NaAlSi3O8	6
Potassium Felspar	KAlSi3O8	Probable Trace
Chlorite	(Mg,Fe)6(Si,Al)4O10(OH)8	2
Kaolinite	Al2Si2O5(OH)4	Probable Trace
Gregeite	Fe3S4	49
Polyhalite	K2Ca2Mg(SO4)4·2H2O	7
Siderite (Mg, Ca form)	Ca0.1Mg0.33Fe0.57(CO3)	9

SA21716-02

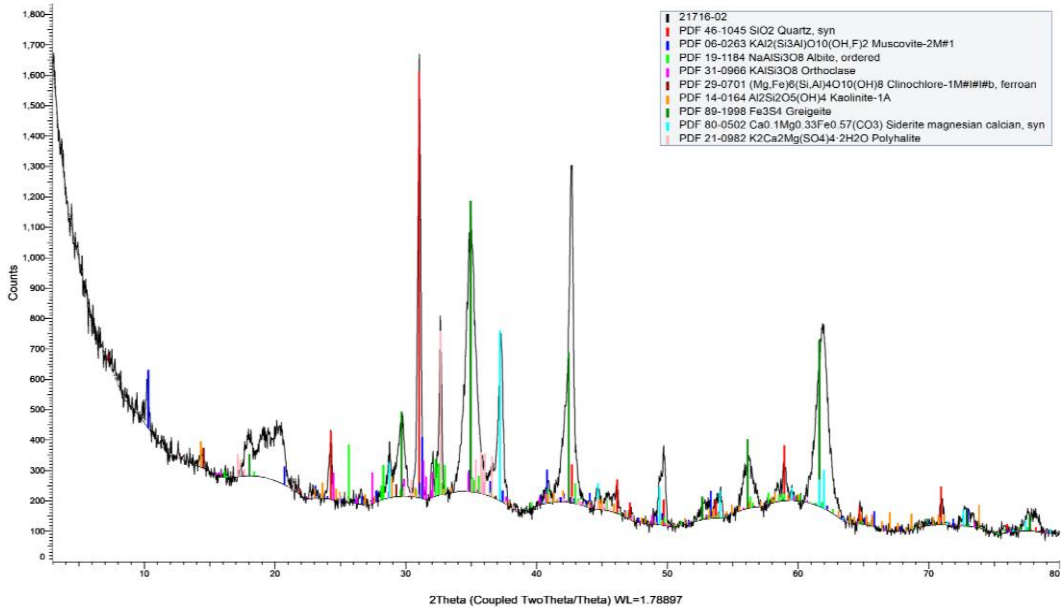

Figure 5.5- 7: XRD analysis of Tank 2 (M-LC) from the second round of precipitate sampling.

5.6 Vertical Flow Reactor

Results from the meso-scale VFR trial are presented in this section. Key findings are as follows: 1) High iron and arsenic removal were recorded even at low HRTs; 2) driving head increased with operation due to the thickening of the ochre layer; and 3) In dry weather iron precipitate sludge inside the VFR can get to as high as 63% solids in just 12 days after being drained.

5.6.1 Metal Removal

Iron loads reporting to the VFR are always higher than iron loads leaving the VFR. Figure 5.6-1 shows that although the load was variable, due to fluctuating iron concentrations in the influent, the VFR was consistently removing a significant portion of the load. This shows that iron is being captured and held within the system.

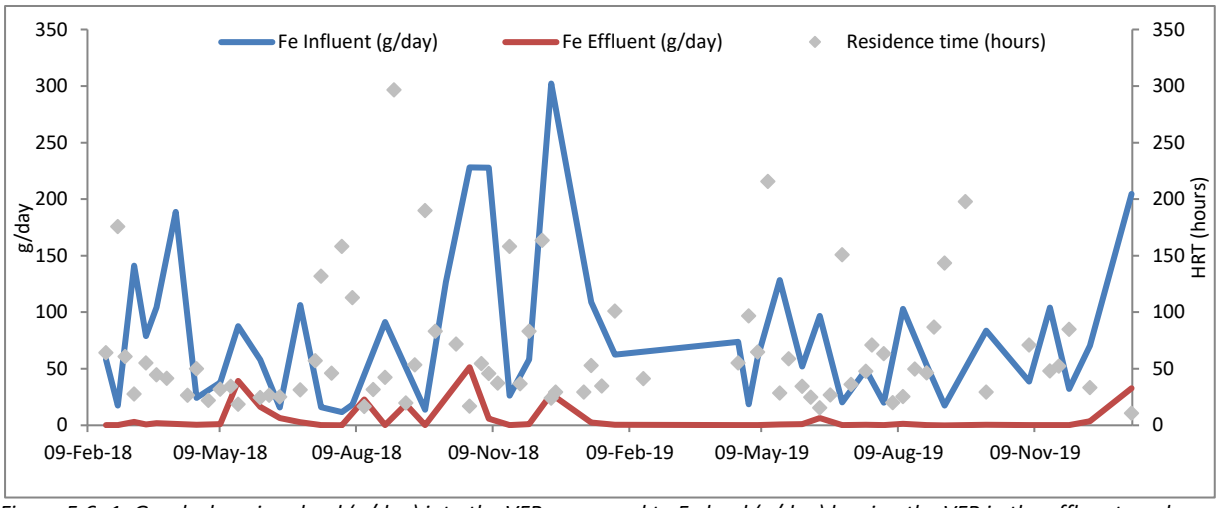

Figure 5.6- 1: Graph show iron load (g/day) into the VFR compared to Fe load (g/day) leaving the VFR in the effluent, and the HRT for each point.

As with iron, arsenic loads reporting to the VFR are also always higher that than leaving the VFR (with the exception of one anomalous data point) (figure 5.6-2). Although arsenic loads vary, they were consistently lower in the effluent compared to the influent. This shows that arsenic is being captured and held within the system.

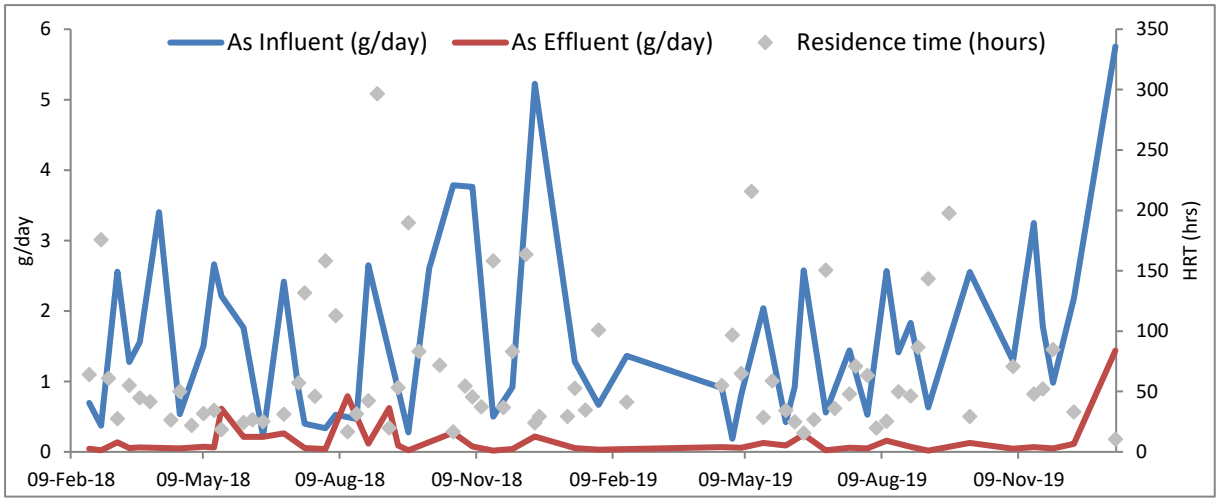

Figure 5.6- 2: Graph show arsenic load (g/day) into the VFR compared to Fe load (g/day) leaving the VFR in the effluent, and the HRT for each point.

Figure 5.6-3 shows that removal of both iron and arsenic was is predominately high (median removal for arsenic was 94.89% and iron was 98.99%), although some anomalous low results bring the mean results much lower (90.31% and 94.61% respectively). The variation in iron of only a few data points is evident with the mean value of iron presenting below the whisker (minimum data point 1.5 times the IQR below the 1st quartile). This can also be seen in arsenic, with the mean value below the 1st quartile of data. Therefore the mean is below 75% of the data.

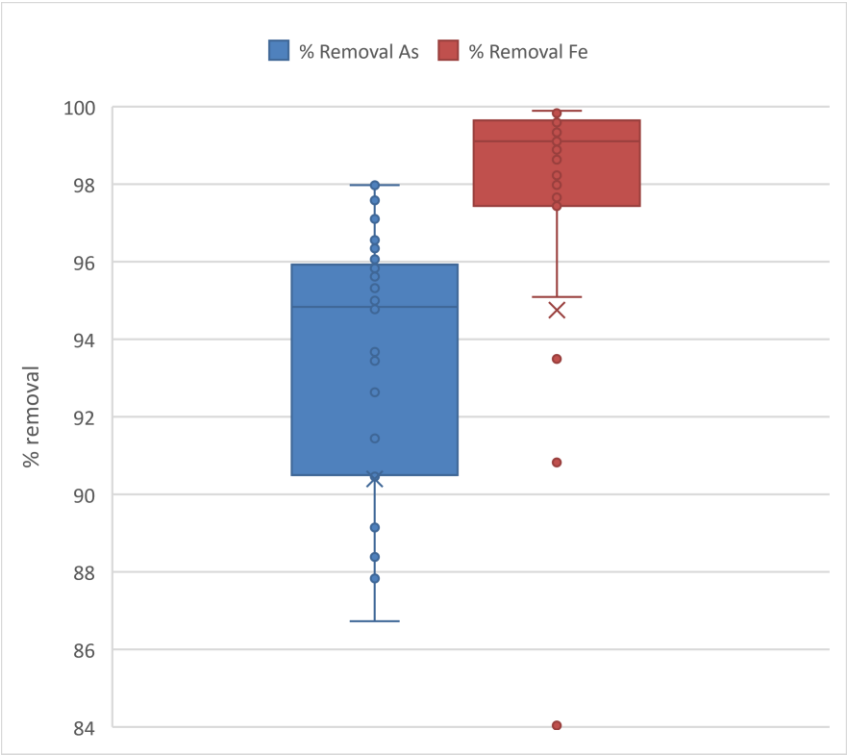

Figure 5.6- 3: Box and whisker diagram showing removal of arsenic and iron in the VFR. Note the axis has been adjusted to exclude outliers (values which exceed 1.5 times the interquartile range below the first quartile or above the third quartile).

5.6.2 Driving Head

Driving head was not originally planned to be measured until its importance became evident part the way through the trial. It was observed that the outlet height from the VFR needed to be adjusted lower several times during the trial to prevent the water level in the VFR from overtopping the tank. Lowering the outlet pipe to maintain a constant water level increased the driving head, and this was necessary as the thickness of the iron precipitate sludge increased. Figure 5.6-4 shows measured driving head from when the iron precipitate sludge was removed in April through until the systems ceased to operate, due to the buried Rock-Drain pipe failing and therefore no water being able to be pumped to the system. Driving head increased with time (figure 5.6-4). The percent increase in driving head for a given change in flow rate is much greater with thicker precipitate than with thinner precipitate, and in order to maintain the same flow rate, driving head must increase as the precipitate layer builds up.

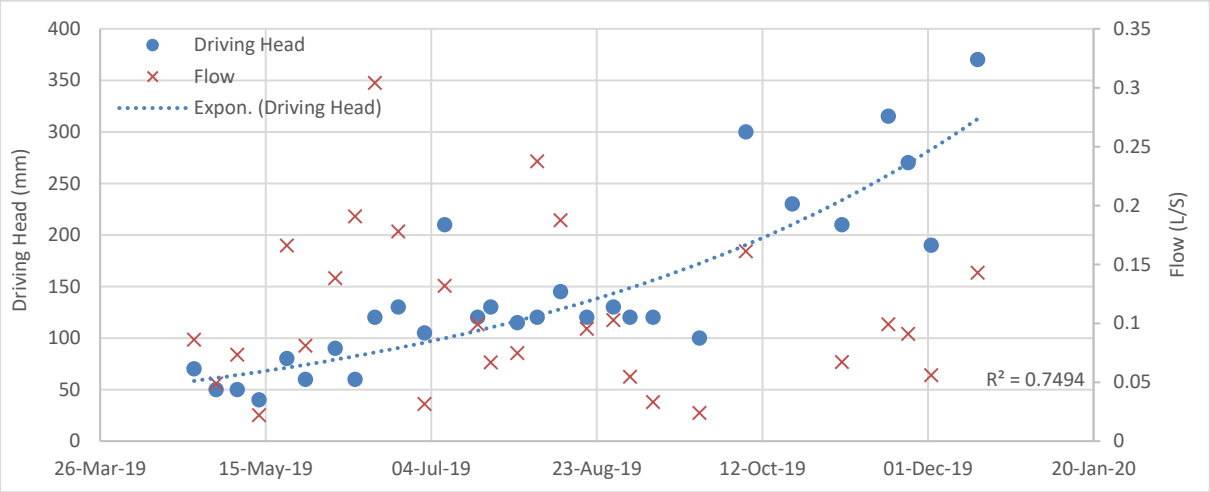

Figure 5.6- 4: Graph showing the driving head and flow measurements from the vertical flow reactor, from when sludge was removed until system could no longer operate due to a rock drain piping failure which prevented pumping of water.

5.6.3 Hydraulic Residence Time

Figure 5.6-5 shows both iron and arsenic removal increases with HRT. While there are a few outlying data points (>50 hours) there is consistent iron removal in the VFR from as low as 10 hours through to 190 hours HRT. Iron had a maximum removal of 99.89% removal at 65 hours residence time and removes over 97.7% at an HRT of 50 hours or more. Arsenic removal shows less variation at low HRT than iron with only 3 data points below 80% removal and all of those points <50 hours HRT. Arsenic showed a maximum removal of 97.97% at a 48 hour residence time and removes over 87% at all residence times over 50 hours.

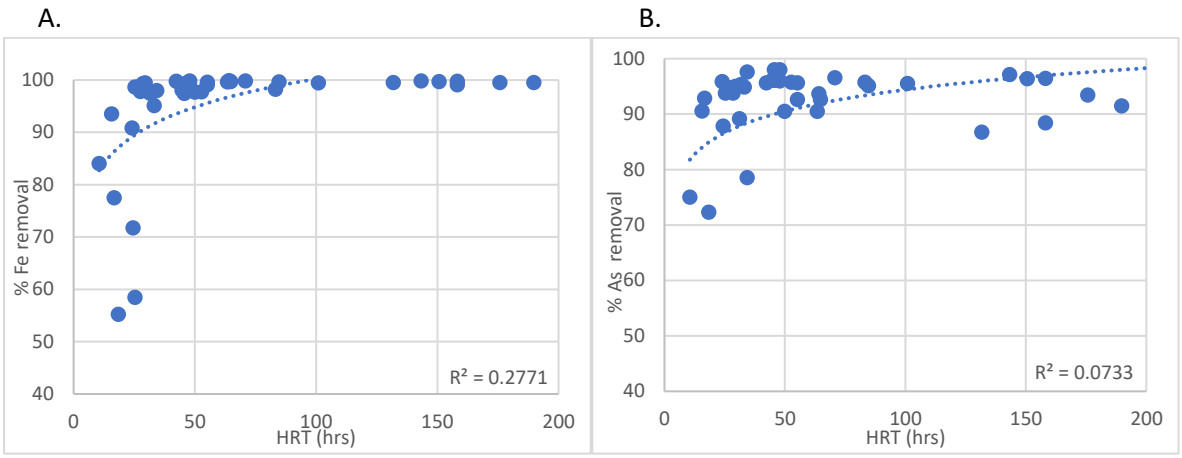

Figure 5.6- 5: Graphs showing A) percentage iron removal over HRT and B) percentage arsenic removal over HRT by treatment through the VFR over the duration of the system operation.

5.6.4 Arsenic and Iron Speciation

Speciation of iron was undertaken on both the Rock Drain (RDRN) water (the influent water for the VFR at its source) and the VFR effluent. Results for this are presented in figures 5.6-6 and 5.6-7. These results show that almost all iron present is in its reduced Fe^{2+} form in the influent and that what iron is still present in the effluent is mostly the oxidized form of Fe^{3+}. Arsenic speciation was only undertaken on the RDRN or influent water. Results from this showed that 100% of arsenic present was in the reduced As^{3+} form of arsenite.

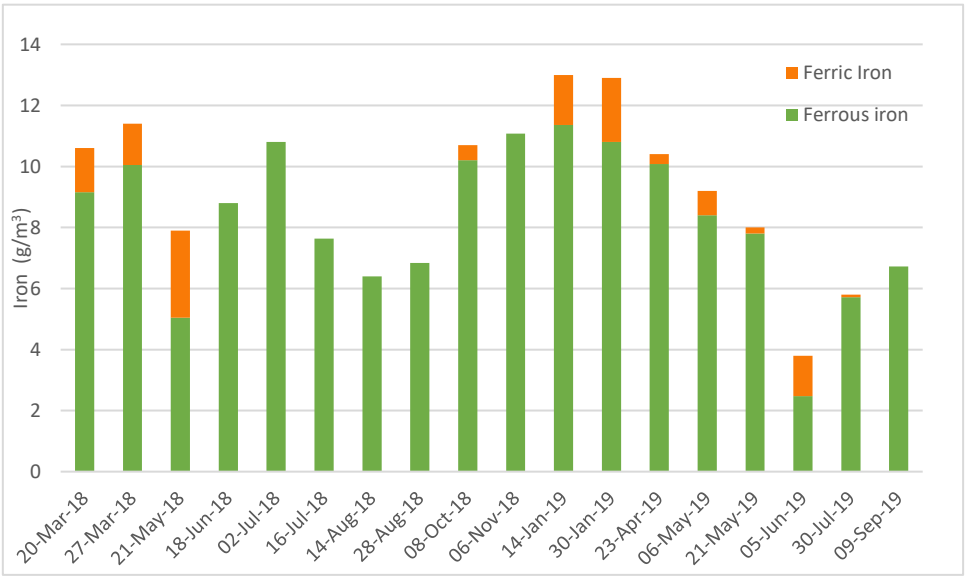

Figure 5.6- 6: Bar graph show the portions of reduced to oxidised iron present in the RDRN water (the VFR influent at its source). Green, is the reduced ferrous portion and the orange is the oxidised ferric portion.

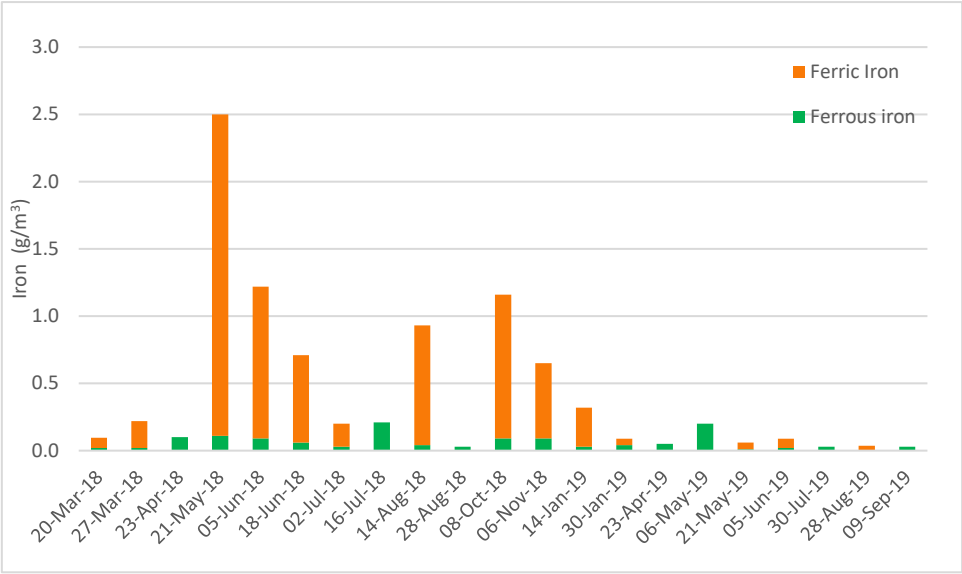

Figure 5.6- 7: Bar graph show the portions of reduced to oxidised iron present in VFR effluent. Green, is the reduced ferrous portion and the orange is the oxidised ferric portion.

5.6.5 Precipitate Analysis Results

The vertical flow reactor was drained on two occasions and the iron sludge precipitate was sampled and analysed by Hill Laboratories using IPC-MS for metals and by XRF analysis by CRL Energy Ltd. The sludge was resampled multiple times in the days following the draining to assess the percent moisture of the sludge as it dried. The first draining event showed laminations of light sediment which is likely due to the addition of sediment from the TSF return water, figure 5.6-8.

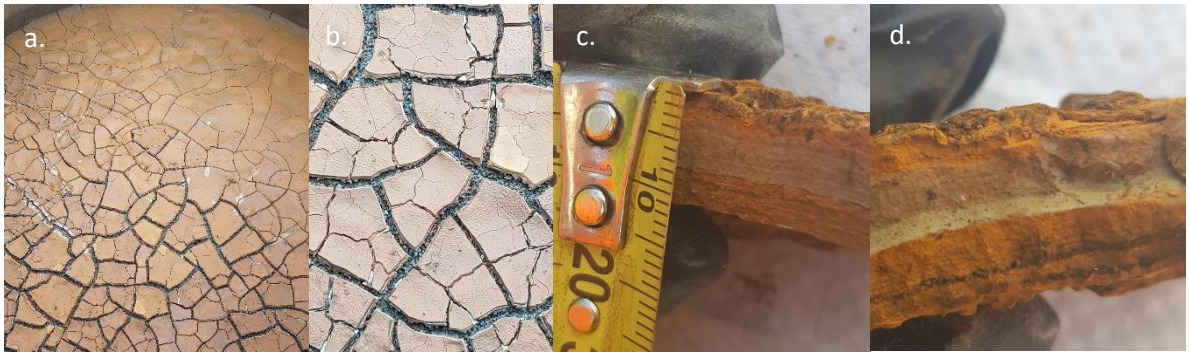

Figure 5.6- 8: Photographs of iron precipitate sludge from first draining event after 12 days of drying. a) Sludge in tank starting to crack as it dries, b) Zoomed in image of cracked sludge in-situ, c) Caked sludge removed from tank showing dried thickness d) Caked sludge removed from tank showing laminations of light sediment.

During the first round of draining, there was dry weather (a total of 11.65mm of rain in the duration of drying) and the sludge dried quickly (figure 5.6-8). Starting at 18% dry matter it then increased to 63% within 12 days. On the second draining event, the sludge started to dry quickly increasing from 21% dry matter on day 1 to 32% on day 2 but then became more saturated due to rain and remained low until day 20 (21%), when sampling ceased (figure 5.6-9).

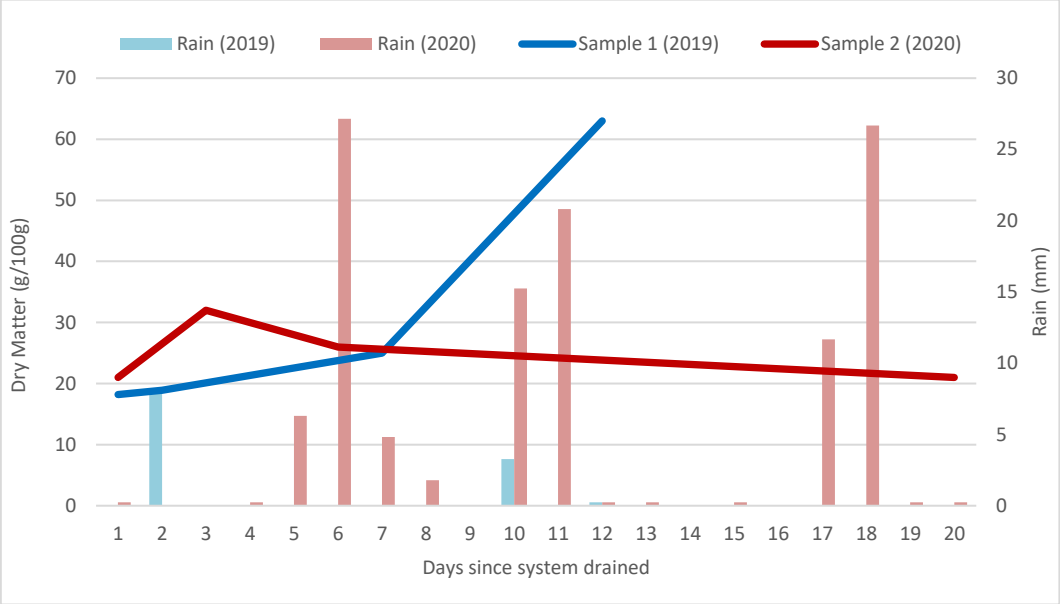

Figure 5.6- 9: Graph showing % dry matter and rain (mm) from the 2 rounds of sludge sampling in days following draining of the VFR. Blue: the first sampling round in 2019 and Red: the second sampling round in 2020.

Results from the ICP-MS and XRF are presented in figure 5.6-10. Both the ICP-MS method used by Hill Laboratories and the XRF analysis undertaken by CRL Energy Ltd showed very similar results for iron. The ICP-MS method reported 32%/29% compared to the 29.5%/34.3% reported through XRF analysis. Similar results can be seen with arsenic, with ICP-MS method reporting 0.56%/0.86% compared to the XRF result of 0.67%/0.89% respectively. Antimony results from the XRF analysis showed nill detected, although low results were recorded through ICP-MS of 0.0043%/0.0065% (percent by weight). Sulphur was much higher in the first round of XRF compared to the second round, whereas iron and arsenic results were similar for the first set of samples compared to the second.

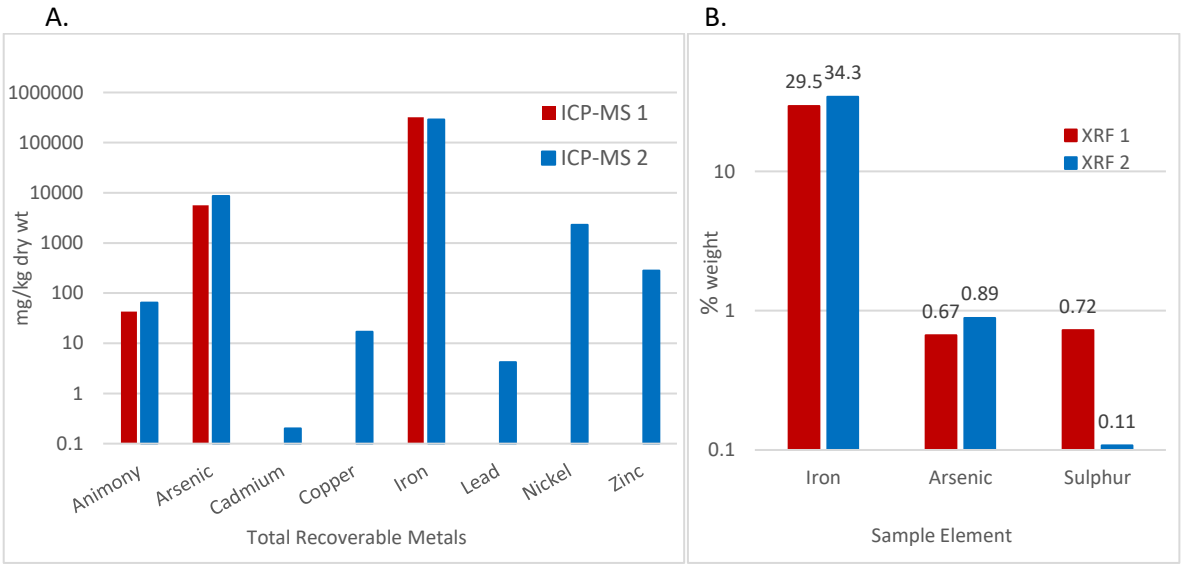

Figure 5.6- 10: Graphs showing the results of iron precipitate sludge sampled from the vertical flow reactor that were analysed for A) total recoverable metal results by Hill Laboratories (only Antimony, Arsenic and Iron were analysed for in round 1) and B) % weight of iron, arsenic and sulphur by XRF analysis undertaken by CRL ltd. Note: Red indicates the first sample and blue indicates the second sample. Both graphs shown in log scale.

5.7 Conclusions

The primary results presented in this chapter provide important insights into how to most effectively remove iron, arsenic and sulphate from mine effluent/wastewater systems. The results presented in this chapter demonstrate that: 1) biosolids are more effective at removing iron, arsenic and sulphate than mussel shells; 2) internal temperature of bioreactors are influenced more by influent temperature than ambient air temperature ; 3) Sulphate removal has a strong positive linear relationship with HRT; and 4) The vertical flow reactor showed extremely high removal rates (median removal for arsenic=94.89% and iron= 98.99%) at relatively low HRTs.

6. Chapter Six- Discussion

6.1 Introduction

The purpose of this chapter is to explain and evaluate the results of this study. This will be undertaken in two sections. The first section, 5.2 Bioreactor, will discuss the results of the bioreactor substrate and temperature treatments, in particular the possible mechanisms which effect metal and sulphate removal, the temperature trends and the effect in which HRT (hydraulic Retention Time) had on the efficiency of the systems. The second section, 5.3 Vertical Flow Reactor, will discuss the results from the VFR treatment trial, in particular the effect of the iron to arsenic ratios, the effect of HRT on removal rates and the driving head/sludge accumulation dynamics.
Data was analysed with R-Studio, using ANOVA and Tukey (95% confidence level) tests to assess the statistical significance of variance between treatments. Experimental design of these systems is explained in chapter 4. Data and results are presented in chapter 5.

6.2 Bioreactor

6.2.1 Metal removal with different substrates

All treatment mixtures trialled, irrespective of composition, proved to be effective at removing iron, arsenic and sulphate. All treatments showed a decrease in these contaminants in the effluent compared to the influent.

Biosolids

Properties of the substrates differed drastically. While the biosolids had less organic carbon than all other substrates other than mussel shells, it did however have the highest nitrogen and phosphorous concentrations, which are necessary for SRB activity (Dev et al. 2015). Wastewaters from urban environments generally have higher heavy metal concentrations, especially zinc, copper and lead, along with high suspended solids and nutrients (Mosley and Peake 2001). As biosolids were sourced from the Christchurch wastewater treatment plant, from the treatment of urban wastewater, they contain the highest levels of anthropogenic contaminants, such as aluminium, barium, cadmium, chromium, cobalt, lanthanum, lead, lithium, mercury, nickel, silver, tin, uranium, and zinc, of all of the substrates. The one-off full suite of analyses on the bioreactor effluent showed that there were not elevated concentrations of these in the biosolid treatments. However, in most cases, such as uranium, zinc and especially nickel, concentrations were actually lower than in the influent, likely due to a range of different metal sulphides being formed (eg. Nickel sulphide). Aluminium was also lower in the effluent than the influent, although when in the presence of water aluminium does not form a stable sulphide mineral, it is therefore most likely that the minor removal was due to formation of a hydroxide (Jong and Parry 2003; Jouini et al. 2020).

Mussel Shells

Mussel shells contained the highest levels of strontium and sodium, most likely due to being from a marine environment, as well as the highest concentrations of calcium. Marine waters have been shown to contain approximately 8 times more strontium than lakes or springs and an average of 22 times higher in other surface waters (International Programme on Chemical and Inter-Organization Programme for the Sound Management of 2010). It has also been found that due to strontium's similarities to calcium it often found to acts as a calcium substitute (International Programme on Chemical and Inter-Organization Programme for the Sound Management of 2010). While strontium was slightly higher in the effluent from tanks with mussel shells, sodium concentrations were similar in all effluents. This is likely due to concentrations also being elevated in the compost and therefore not causing enough of an effect to be noticed in the effluent concentrations. Calcium concentrations

were much higher in the effluent of tanks containing mussel shells, and effluent from these tanks also had higher alkalinity and a slightly higher pH.

For context, mussel shells are generally used in passive treatment of AMD as they act as a source of calcium which in turn adds alkalinity to the water and brings the pH of the previously acidic water to circum-neutral (McCauley et al. 2008; DiLoreto et al. 2016) with the added benefit of organic material acting as a carbon source (mixture of flesh and seaweed) for SRB activity. The other advantage of using mussel shells as a substrate is it can add porosity to a system preventing clogging due to the build-up of the metal precipitate, which has been proven to cause systems to fail (Uster et al. 2014). The MAW water being treated at this site does not require any added alkalinity as it is already circum-neutral. All treatments had higher alkalinities and pH than the influent, although reactors which contained mussel shells were higher, in general, than those reactors with biosolids (see appendix 1 for further detail).

Spent Mushroom Compost

Spent mushroom compost had the highest concentrations of total recoverable sulphur of all of the substrates. This is due to the naturally occurring sulphur found within the organic material (straw and manures) and also the addition of gypsum (calcium sulphate) during production of the compost (Velusami et al. 2013). During the commissioning of the systems the sulphate concentrations were much higher in the effluent of all tanks than in the influent. This is thought to be due to export to finer grained materials in the early stages of operation prior to the SRB communities becoming established. After approximately one month of operation the sulphate levels decreased in the effluent to below that of the influent, indicating the establishment of the SRB communities. Arsenic and iron concentrations did not show the same increased concentrations in the effluent as the sulphate in the commissioning period. In fact, iron and arsenic exhibited lower concentrations in the effluent from the first test results, indicating that there were other removal mechanisms occurring, either during commissioning or also simultaneously through operation. The most likely mechanism for this removal in the commissioning of a bioreactor has been suggested to be absorption of metals onto the organic substrates, although other mechanisms such as filtration, polymerisation on inorganic material , and other sorption methods have been shown to occur during the operation of a bioreactor (Neculita et al. 2007). It is unlikely to be caused by the formation of iron oxides and the adsorption of arsenic onto these oxides as the dissolved oxygen in the influent and effluent of all the systems was generally 0% saturation (see appendix 2 for full data set).

Bark and Sawdust

Bark and sawdust contain the highest amounts of organic carbon present compared to all other materials (see table 5.2-2), containing approximately 35% more than both biosolids and spent mushroom compost and 83% more than mussel shells. The carbon to nitrogen ratio (C/N) is important for the degradation of both organic material and to stimulate SRB growth (Prasad et al. 1999; Uster 2015). Prasad et al. (1999) suggests for the decomposition of biological material a C/N ratio between 6 and 10 is appropriate for organic material, although Okabe et al. (1992) suggests a range of 45 -120. In this trial the C/N ratios for substrate mixes vary from 13.4-17, which falls between the two suggested ranges. Uster (2015) suggests that as this is calculated from total organic carbon, a certain portion will not be biologically available and therefore may not be representative of the true C/N ratios.

Substrate Mixtures

A bioreactor's removal efficiency is determined by the SRB cultures and their reduction ability, which are dependent on the availability of key nutrients (Dev et al. 2015). Nutrients which have been shown to be essential for SRB include: nitrogen, phosphorous, carbon and other trace metals (Patidar and Tare 2006; Dev et al. 2015). Measured dissolved reactive phosphorus, was below detection for all treatments frequently throughout this trial, and in fact below detection limits in most results for both the mussel shell treatments (M-LC and M-MC) and the biosolid treatment with less compost (B-LC), which suggests uptake by the SRB. Interestingly, biosolid treatments with more compost showed higher results of dissolved reactive phosphorus than the influent. This is likely due to biosolids, and a lesser extent compost, containing higher amounts of phosphorus than the other bioreactor ingredients, which suggests a surplus (see appendix 1 for graph). Removal of arsenic, iron and sulphate were higher in all treatments with biosolids, including the small temperature control and the insulated treatments (tanks 5 & 6), when compared to mussel shells. This is most likely due to higher amounts of available nutrients and metals in the biosolids which enabled the SRB to more efficiently carry out their functions ultimately increasing the metal and sulphate removal (Patidar and Tare 2006; Dev et al. 2015). Along with phosphorus, the biosolids also contained higher amounts of other nutrients and metals compared to other substrates, including nitrogen, iron and cobalt, which have been shown to increase SRB activity (Patidar and Tare 2006). Although it also has high levels of an array of other metals (such as nickel) which have been shown to inhibit SRB at high concentrations (Teclu et al. 2009).

Removal of iron was higher in the biosolid treatment with less compost (B-LC) compared to the mussel shell treatment with less compost (M-LC) (with $p = < 0.001$), whereas when comparing the more compost treatments (B-MC and M-MC) although removal was even higher (figure 5.2-1), the *p* value was only 0.236, meaning the difference between the two means in this instance isn't statistically significant. When comparing all treatments (including the temperature treatment control and insulated) there is a statistically significant difference between all treatments with biosolids when compared to mussel shells, with the exception of more compost treatments (B-MC and M-MC). However, there was no significant difference between mussel shell treatments with more or less compost and between bioreactor treatments with more or less compost. While the result for B-MC compared to M-MC isn't statically significant, the data in figure 5.2-3 clearly shows that the biosolid treatment (B-MC) is more effective overall but that it also has a large amount of variability. Table 5.2-4 shows that the difference in the median outlet iron concentrations between the more compost treatments for biosolids (B-MC) (10.4 g/m^3) and mussel shells (M-MC) (16.3 g/m^3) is similar to the difference in median values between the less compost treatments for biosolids (B-LC) (11 g/m^3) and mussel shells (M-LC) (18.1 g/m^3). This suggests that biosolids, in general, outperformed mussel shells for both the more compost and less compost treatments. The black appearance of the biosolid effluent suggests the SRB are most likely producing a variety of iron sulphides (Uster et al. 2014).

Arsenic removal was also higher in all treatments with biosolids when compared to the mussel shell treatments. Statistical analysis showed that the effect of treatment, in this instance between biosolids and mussel shells for both more and less compost treatments, showed a significant effect on arsenic removal, with *p-values* <0.001 in both cases. All treatments, in fact, (including the temperature treatment control and insulated) showed a statistically significant difference when comparing a biosolid to a mussel shell treatment. However, as was the case with iron, there was no apparent difference between less compost and more compost treatments for arsenic removal, for either biosolids or mussel shells (figures 5.2-4 and 5.2-5). Removal of arsenic occurs most probably by the formation of amorphous arsenic sulphide or arsenopyrite (Altun et al. 2014; Le Pape et al. 2017).

Removal of sulphate was also higher in biosolid treatments when compared to mussel shell treatments but did not show any statistically significant difference, with all *p*-values > 0.05. Figures

5.2-7 and 5.2-8 showed that while only marginally, sulphate removal was in fact consistently higher in treatments with biosolids when compared to less compost and more compost treatments. As indicated above, sulphate increased substantially in all effluents during commissioning, but after about a month of operation, concentrations began to decrease, indicating the establishment of the SRB communities. From this point on, given enough HRT, sulphate concentrations were consistently lower in the effluent than the influent. Reductions in sulphate, along with the reduction in various other metal and trace metals suggest the formation of a variety of sulphides, including iron, arsenic, and nickel. This was also supported by the presence of hydrogen sulphide that was noted during most sampling occasions, especially during the field measurements taken from inside the top of the tanks.

6.2.2 HRT and effect on removal

Flow rate field trial issues

Hydraulic residence time (HRT) has often been shown to be one of the major influencing factors of the efficacy of bioreactors with data suggesting that a treatment period of 40 hours up to 4 days is required (Younger et al. 2002; Neculita et al. 2008a; Uster et al. 2014; Vasquez et al. 2018). HRT in this trial was targeted at 24 hours at the beginning of this trial but it was extremely difficult at first to adjust to the correct flow and to maintain effective flow conditions. Initially the systems were fed from the feed IBC with a ball valve to control flow. This gave very little control in that a small adjustment greatly affected flow rate. To allow for a more controlled adjustment, gate valves were installed, which proved successful and meant fine adjustments could be made in order to reach target flows and therefore residence times. Although, what began to happen in response to these changes, was that, without any adjustment, the flows began to decrease over time, suggesting a partial blockage in the feed pipes or reduced permeability throughout the tanks, as the tanks were not overtopping. The absence of overtopping indicated this response was not a block in the outlet line. This meant continual adjustment of the gate valve to maintain the target flow was required, which was not always successful and took several attempts.

In the configuration used, the IBC and feed lines were situated near the bottom of the IBC in order to prevent any oxidation of water prior to the entry of the feed line. This appeared to be successful due to the clear nature of the water indicating there was very little oxidation of the Fe^{2+} (photo in appendix 4). This indicated that the blockage must either be occurring at the entry point to the tank or within the tanks themselves. Flushing of the lines/tanks was trialled by opening the gate valve to full capacity for approximately 10 seconds to create a pulse of water, although this meant adjustment of the gate valves to get the correct flows would take several attempts.

A bypass line around the gate valve was then installed to allow for the flushing of the feed line into the tank without the adjustment of the gate valve (see figure 4.3-8). This meant flows were able to be more closely maintained to the target flows and therefore HRT (see graph in appendix 1 for more detail). Notably, throughout the operation of this trial there were airlock issues in the outlet pipes which reoccurred due to the uneven ground and the amount of pipes which were required to fit into a relatively small area. Airlocks were addressed when sampling was undertaken, but this meant that often the sample or flow from that round was not able to be used. All of these issues combined to mean that it was difficult to get consistent flow data between all 4 treatments and the 2 small temperature treatments.

Iron removal

Seasonal fluctuation of temperature has been shown to effect the communities and efficiency of the SRB removal rates (Nevatalo et al. 2010; Van Den Brand et al. 2014; Nielsen et al. 2018). Therefore, having different flows and also temperature fluctuations meant that several variables were occurring

on the systems at once. In order to analyse the data and control for these effects I plotted data showing only points with effluent temperatures above certain temperatures (figure 6.2-1).

Referring to the plots of all the data across the seasons, iron removal had a positive relationship with HRT, meaning that with increased residence time there was increased iron removal. In both less compost treatments (B-LC and M-LC) the trendline showed a more linear relationship, whereas the more compost treatments (B-MC and M-MC), showed a more logarithmic relationship (figure 5.3-1) The biosolid treatment with more compost had the weakest relationship with HRT and also showed larger variation within the data. The variation in the dataset and the less obvious trend with HRT is likely due to there being high removal at low residence time as well as a trend in increasing removal with HRT. This is most likely caused by a seasonal fluctuation, whereby in colder temperatures the system's performance was impaired. Figure 6.2-1 shows that, if just data points from when the system is operating >10°C are plotted, there is a much stronger relationship.

Arsenic removal

Treatments with mussel shells showed a positive relationship with arsenic removal, whereas the biosolid treatments did not. As with the iron removal, the B-MC treatment showed more scatter in the data than other treatments, especially compared to the treatments with mussel shells, and it seems to have a negative relationship to HRT. This, however, is likely to be due to more data points associated with lower residence times and outlying data points at high residence time causing a skew in the data.

It is unclear why mussel shell treatments have a better relationship of HRT with arsenic removal, although it is evident that biosolid treatments have higher removal at lower HRT. This may be due to extra nutrients provided by the biosolids meaning that the SRB communities have an increased sulphate reduction ability even at low HRT compared to the mussel shell treatments which require a longer contact time to get the same removal. When removing the high HRT times for B-MC (>50 hours) the data then presents a linear relationship with HRT (figure 6.2-2), indicating that removal increases with HRT but over about 50 hours it has no effect. This also shows much higher removal than that of the equivalent mussel shell treatment which at 40 hours has approximately 40-50% removal (figure 5.3-2) as compared to the 85-95% removal shown by the biosolid treatment.

Sulphate removal

Sulphate removal shows a strong positive linear relationship with HRT in all treatments (figure 5.2-9). Biosolid treatments have slightly higher removal for all HRT compared to mussel shells treatments (about 20% removal at 50 hours versus 15%), but all treatments indicate that with longer residence time, removal of sulphate is greater This again, seems to indicate that the bacteria have a higher sulphate reduction capacity in treatments with biosolids, but the removal is also dependent on the HRT. This relationship is much stronger with sulphate removal opposed to iron or arsenic, which suggests that perhaps there are other mechanisms aside from sulphate reduction which are leading to the removal of arsenic and iron such as adsorption and other binding mechanisms to the substrates within the system (Neculita et al. 2008b).

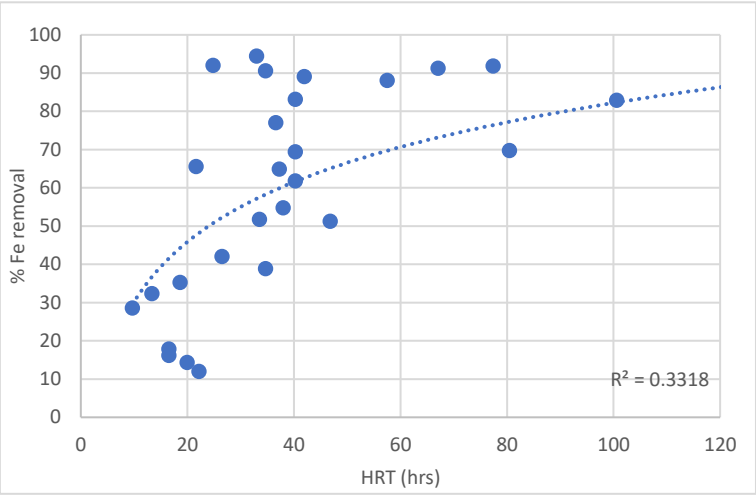

Figure 6.2- 1: Graph showing the % Fe removal for the biosolids more compost treatment (B-MC) for all results over 10°C in the effluent over HRT.

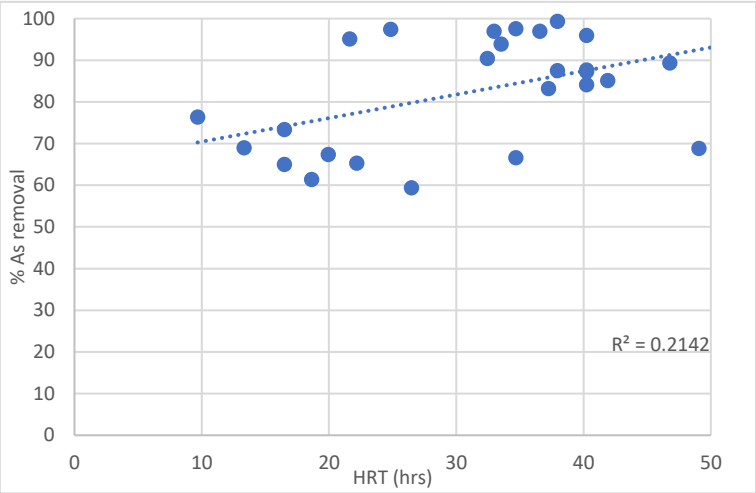

Figure 6.2- 2: Graph showing % arsenic removal for the biosolids with more compost treatment (B-MC) with data points of <50hours HRT.

6.2.3 Temperature treatments

Metal removal

Removal rates of iron in the temperature treatments were not statistically significantly different although the median concentrations for the insulated treatment were lower than that of the small control which was lower again than the large tank with the same mix (B-MC). As the mix is the same for B-MC in the large tank (which is in a 15,000L tank) as for the small temperature control treatment (TT) (7,500L tank), there must be another contributing effect to the difference in removal rates. This may be the shape of the tank as the smaller tanks are shorter compared to the diameter (D=2.5m & height to outlet=1.35m) than the big tanks (D=2.9m & height to outlet=1.87m). The small tanks were also black whereas the larger tanks were green, which may have affected the temperature as black would absorb more sunlight, and therefore hold more heat. This is not evident in the effluent temperature data, however, which is similar to the ambient air temperature and

follows the seasonal fluctuation. This indicates the water temperature equilibrates with the ambient temperature fairly quickly after it exits the substrate.

Temperature Probe Data

The temperature probe data from inside the substrate (figure 5.4-1), suggests that tank 3 (B-MC) has the coldest internal temperature of all of the temperature treatments and that the insulated tank (tank 6) is warmer. The probe data also show that tank 5 (TT) has the warmest internal temperature which was not expected. Unfortunately, an issue with the sensor cable from the probe in the middle of tank 5 meant just less than one month's data was captured, and therefore a completed comparison of the internal temperatures could not be made. The flow rates in the smaller tanks were also more difficult to maintain than the larger tanks even with the gate valves and flushing mechanism. The exact cause of this is not known but it is suspected that higher amount of sulphides, (figure 5.4-9) that were produced in these smaller tanks probably lead to faster and more common blockages than that of the larger tanks.

Issues with probe reliability

Probe data (displayed in section 5.4.1)) proved to be increasingly unreliable as it showed sudden shifts or erroneous results for most tanks. For example, data from tank 1 (B-LC) showed a sudden shift in the temperature from the side probe with an increase of approximately 4°C, which is thought to be caused by a fault in the probe. The middle probe of tank 2 (M-LC) started to suddenly trend upward from the 1st of August 2019 before ceasing to log anymore data days later on the 9th of August. It is possible that this was caused by condensation in the electronics causing a fault.

Probe data - Substrate treatments

However, tank 2 (M-LC) did return a good temperature record until mid-June 2019 when the middle probe had a sudden shift up of around 5°C which continued until the probe ceased to log data on the 24th of December 2019. On removal of this probe a small incision in the cable was located, which possibly caused the issues in the data. The side probe performed well, logging what appears to be an accurate temperature from installation to removal. These data show that temperatures at 300mm from the outside of the tank exhibit some seasonal fluctuation, similar to that of the ambient air temperature, but to a lesser magnitude. Tank 3 (B-MC) middle and side probes both returned good temperature data with the side data being more closely related to ambient air temperatures and the middle being more closely related to the influent temperatures. A diurnal pattern was expressed in the side logger compared to the middle which appeared to not be affected by daily temperature flux at all. From late June 2019 both probes had sudden and separate increases, which seemingly cannot be explained by any physical or chemical changes. Therefore, it is thought to be caused by separate faults in both probes. Tank 4 (M-MC) continued to record for the full year and 4 months that these probes were installed. Data from this treatment shows that middle temperatures were very similar to the influent and that there was only a small amount of fluctuation which occurred with the seasonal flux, whereby in summer the temperature was slightly above the influent but in winter it dropped slightly below the influent temperature. The temperature towards the side of the tank was more highly influenced by the air temperature, whereby it was affected by both diurnal and seasonal fluctuations.

Probe data - Temperature treatments

The small temperature control treatment's middle probe cable was chewed by a rat in the early stages of measure but due to the location was not identified until the probe was removed (figure 6.2-3). The small control tank showed a different trend than any of the other tanks with the middle being warmer than the side in the summer months. It is possible that the cable was damaged nearly immediately after being installed and therefore the data is erroneous, as no other tank has shown this trend. It shows the middle to be much warmer than all the other treatments including the insulated tank, as well as showing the middle to be warmer than the side which is being influenced by the warm summer air temperatures. It is considered that data from the middle of the

temperature control tank is anomalous and therefore not representative of the underlying trend which was occurring (figure 6.2-4).

The temperature probes in the insulated tank showed that the side temperatures were far more similar to the middle of the tank and showed a much lesser diurnal pattern than all of the other treatments. The side temperature showed slightly more fluctuation than the middle which may be attributed to diurnal cycle. These data indicate that the internal temperature of an insulated tank is determined more by the temperature of the influent than the ambient air temperature, although a slight seasonal fluctuation seems to be evident from the middle probe data, as temperatures vary by approximately 1-4°C degrees either side of the influent temperature (above the influent in summer and below it in winter). As all the tanks have slightly differing pipe lengths from the influent to the tank it is also possible that the ambient air temperature has more effect on the temperature of the influent which is not captured by the probes. The large tanks have similar piping lengths, whereas the small tanks are slightly further away, with the insulated tank being the furthest.

The insulated tank showed the highest temperatures in the middle of the tank. However, without being able to compare with the uninsulated tank data, it is difficult to say whether this is caused by an effect of size, insulation or distance from the influent. It is possible that since the influent water had further to travel within the 40mm pipe, it was therefore able to warm up an extra few degrees before it entered the tank. Based on the lack of diurnal fluctuations this seems like the most likely scenario. All other tanks, from the data that is able to be compared, seem to be much closer to the influent temperature. The side probe in the insulated tank increased suddenly and unexpectedly in April 2019 and recorded much higher temperature results from then on, it is likely there was a fault in the sensor at this time and it is considered that data from this point on is erroneous.

Implications of temperature probe data

The temperature data indicates that the ambient air temperature only affects the very outside edges of a bioreactor, and that the influent water temperature has a far greater influence on the inner operational temperatures. This is an important conclusion because this means ambient air temperatures may be less important to the inner core of these systems than influent temperature as data from this trial suggests. Results also indicate that providing insulation can, in fact, prevent fluctuations within the substrate from fluctuating external temperatures (figure 5.4-2).

As SRB activity decreases in colder temperatures it is thought that these systems may not be applicable for colder climates or areas with low winter temperatures (Trumm 2014; Skousen et al. 2017; Nielsen et al. 2018) . However, if, as indicated in this trial, it is the influent temperature which actually controls the internal operating temperature, there may be other approaches to counter this issue. One option, if the influent temperatures are warm enough (>15°C) for mesophiles or even psychrotolerant mesophiles SRB (Nevatalo et al. 2010), is to maintain these temperatures internally from fluctuating ambient temperatures. This would mean short influent pipe lengths, utilisation of insulation where applicable and a system with lower surface area could increase the inner operational temperature and therefore the sulphate reduction capacity of these organisms.

Another option, if the influent temperature was low (<15 °C), would be utilisation of either solar or hydro powered systems. This could include solar water heaters (uses the suns energy to directly heat the water) in areas which have high sun exposure, or even a hydro turbine system which powers a water heater. Other research also suggests that sulphate reducing microbes can be efficient in colder temperatures due to selective enrichment of cold tolerant species, but are not as effective with unstable temperatures with high temperature fluctuations (Nevatalo et al. 2010). Therefore, insulation could prevent significant fluctuations caused by ambient air temperature and potentially increase SRB activity, even at low influent temperatures.

Figure 6.2- 3: Photograph showing damage to the small temperature control middle probe cable due to rat gnawing

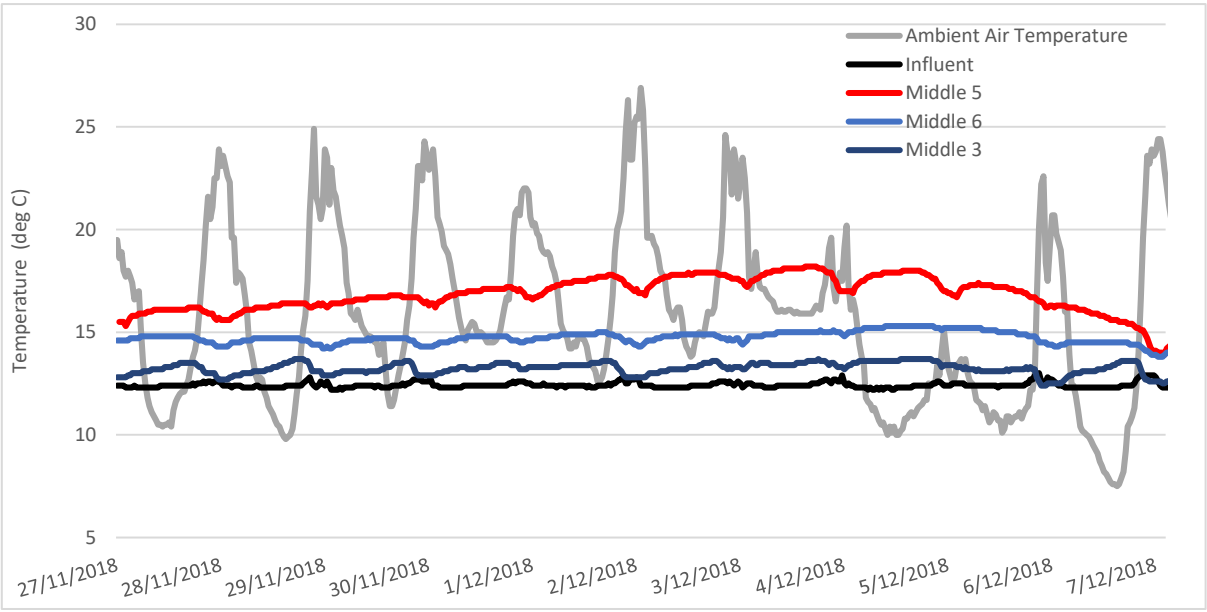

Figure 6.2- 4: Temperatures from the probes in the middle of the tanks, middle 3=middle of tanks 3 (B-MC), middle 5=middle of tank 5 (TT) and middle 6=middle of tank 6 (INS), showing data from a 10-day period. Also showing influent temperature and ambient air temperature.

6.2.4 Precipitate Analysis Results

During the operation of the systems, sampling of the effluent and the precipitates which were forming on the outlets showed there were obvious differences between biosolid and mussel shell treatments. During sampling of biosolid treatments, especially the small temperature treatments, the water was much darker than that of the mussel shell treatments, in fact, in some instances the water was almost black (figure 6.2-5). This is likely to be due to sulphides formed within the systems discharging with the effluent (Omoregie et al. 2013), it also was noted that the darker the effluent,

the higher the measured sulphide concentrations. It was also witnessed in field observations that the faster the effluent flows, the less black that was present in the samples, indicating the higher residence times meant more sulphide present in the effluent.

It was also observed that precipitates were forming on the outlet pipes themselves (figure 6.2-5), which needed to be periodically cleared. The most notable difference between the treatment's precipitates in the outlet pipes was the colour (figure 5.5-1). The precipitates formed in biosolid treatments were black with hints of grey and white, whereas the mussel shell treatments were a reddish-orange, appearing to be iron precipitates.

Precipitates were sampled from the bioreactors by two different methods in an attempt to prevent oxidation of the samples, which proved very difficult for both methods (both are described in more detail in section 4.3.6). The first method was by loosening precipitates from the outlet pipes and capturing with the effluent in small 5L buckets (figure 5.5-1) which settled and had free water decanted off and then the sample was transferred to the sample container with enough water to prevent oxidation.

This method produced a precipitate from the mussel shell treatments which appeared to be an oxidised iron precipitate. Analysis by XRF showed that these samples had higher iron and arsenic and lower sulphur than the biosolid precipitates, which had much lower arsenic, slightly lower iron but much higher sulphur by %-weight.

Figure 6.2- 5: Series of photographs of samples taken on different occasions during the 2-year operation of these systems. Note: top photo shows, from left to right, Influent, tank1, tank 2 ,…., tank 6. Bottom two photos show tank 6, tank5, tank4, … , influent.

Figure 6.2- 6: Photographs of some of the precipitates building up in the effluent pipes. From left to right: 1) black, with white precipitates forming in tank 5's effluent pipe, 2) grey precipitates forming in tank 3's effluent pipe, and 3) reddish brown precipitates forming in tank 4's effluent pipe.

These results indicate that the precipitates forming in the mussel shell treatments were likely to be caused by remnant iron oxidising in the outlet pipe and residual arsenic adsorption as it discharged into the collection sump. Whereas, the higher sulphur concentrations in the biosolid precipitates with the moderate iron and lower arsenic suggests that sulphides that were produced within the system were being captured and accumulating in the outlet pipes.

However, XRD analysis on all of these samples showed little to no peaks meaning there was little to no crystalline material found within the samples, with the exception of the small temperature treatments which showed crystalline sulphur to be present. This may indicate that the samples may have become contaminated with oxygen during the sampling, transportation and sample preparation before testing, or possibly due to biological precipitation causing botryoidal textures within the minerals (Trumm 2014; Uster 2015).

The second round of samples was taken where the influent enters the tank by removing the inlet pipe and allowing water to exit the tank. It was expected that sulphide within the tank would be flushed out as the ball valve was opened and water allowed to exit the system. During this process drainage gravel and organics were also flushed out with the water and precipitate. Pulses of water were captured in 5L buckets and allowed to sit whereby after approximately 5 minutes the water was decanted off. To get enough of the precipitates for a sample this was undertaken multiple times.

The precipitates for all tanks were fine to large grained particles, which was almost platy in texture and black in colour. Organics and drainage gravel were removed as much as possible and samples were carefully decanted with precipitates combined to one bucket for each tank, but due to the amount of decanting and transfer it is possible that some oxygen was introduced.

Results from these samples were significantly different to the first set, in that there was no discernible difference between mussel shell and biosolid treatments. All treatments had relatively low arsenic (figure 5.5-3), with the exception of tank 5 (small temperature control). It is unclear why tank 5 had such an evident increase compared to the other treatments. Tanks with mussel shells (2 and 4) had much less arsenic present compared to the first sampling round, and all other treatments had similar amounts. Iron concentrations were also less in the second round than those in from the first round of sampling for all treatments. It is likely that this is due to higher concentrations of metals being present in the effluent of these treatments, the formation of iron hydroxides occurred in the outlet pipes as the water reacted with oxygen, which allowed for the adsorption of residual arsenic onto these precipitates. Although iron present in M-LC (tank 2) precipitate was much higher than all other treatments (29% compared to a range of 2-8% present in other samples). M-LC also went from having the lowest % sulphur in the first set of samples to the highest in the second set

(21.8% compared to a range of 0.6-2.1%), it is thought that this is due to iron hydroxides making up the majority of the first sample whereas iron sulphide dominated the second sample.

It was also found in the XRD analysis of the mussel shell with less compost treatment (M-LC) that greigite, an iron sulphide mineral, was present (the sampling from the base of the tanks). This explains the higher levels of iron and sulphur identified within this sample. This was the only sulphide mineral identified by XRD for both sets of sampling, although for all other samples amorphous material was identified and therefore it is likely that there may have been sulphide minerals present but the minerals were not crystalline. This would suggest that minerals were present in the outlets of the small temperature treatments (tank 5 & 6), due to the presence of crystalline sulphur, whereas the only sulphide minerals captured from sampling precipitates within the tanks were in the M-LC treatment. Based on the concentrations of sulphide within all biosolid treatments effluent it seems likely that the biosolid treatments will also contain sulphide minerals, considering that tank 2 (M-LC) contain far less sulphides in the effluent but iron sulphide was found to be present in the tank itself. It is therefore concluded that even though tanks 1 (B-LC) and 3 (B-MC) did not show any form of crystalline sulphur in the XRD analysis, this is most likely due to contamination of oxygen or a sampling effect.

It also seems likely that if the less compost mussel shell treatment contained sulphide minerals that more compost mussel shell treatment would also likely contain iron sulphide minerals, as all precipitate samples appeared similar in the second sampling set. Samples taken in the first set for the mussel shell treatments appear to not be representative of what is occurring within the system but perhaps the remaining dissolved metals precipitating and adsorbing as they exit the system as it is evident from the second sample of the M-LC treatment that sulphides are in fact forming within the system.

Effluent concentrations support this theory, as not only are iron, arsenic and sulphate concentrations all higher in the effluent for these treatments than for the biosolid treatments, but DO (dissolved oxygen) measured at the outlets is much higher (~20%) than in the top of the tank (~0%) before it enters the discharge pipe. XRD analysis on the second round of sampling also showed quartz, muscovite, plagioclase feldspar and potassium feldspar for all tanks. This is thought to be due to trace amounts of these minerals from the host rock being present in the Underdrains which has then been filtered out in the bioreactor substrates as it enters the system. It is likely that the substrates act as a fine filter which explains why this was not found in the first set of samples, as it would have been filtered out in the bottom of the tanks, where the second sample was taken.

6.3 Vertical Flow Reactor

6.3.1 Metal Removal and oxidation

Iron removal through oxidation and removal is a common method of passively or semi passively treating MAW with elevated iron, although sedimentation of iron particulates requires a long HRT and therefore a large footprint (Sapsford et al. 2007; Hedin 2008; Trumm 2010; Trumm and Pope 2015; Florence et al. 2016). VFR reactors have been suggested to be able to result in the same removal rates with potentially less than half the footprint of an aerobic wetland or settling pond (Sapsford et al. 2006; Blanco et al. 2018). The VFR trialled in this study found iron and arsenic removal were consistently high through the VFR, with median removals of 99% and 95% respectively. Data showed a slight increase in removal efficiency over time but removal rates of 84% for iron and 75% for arsenic at as low as 10.5 hours and 93% for iron and 91% for arsenic at 15.6 hours were recorded.

This indicates that at this site aeration and precipitation can occur despite very low residence time. Due to the high pH of the influent water at this site (median of 7.45), iron oxidation from Fe^{2+} to Fe^{3+}

occurs rapidly, whereby at a pH of 6.5 Fe^{2+} can become fully oxygenated to Fe^{3+} between 5 to10 hours, and at a pH of 6 the same saturation takes closer to 48 hours (Trumm and Pope 2015). Furthermore, an increase in a single pH unit can result in an increase of Fe oxidation rate by 100 times (Sapsford 2013). Although the precipitation of iron produces H+, the VFR effluent shows that the alkalinity remains fairly well unchanged from the RDRN (or influent) water. Moreover, the aeration of the anaerobic water and the subsequent CO_2 degassing actually causes an increase in pH, which further increases the iron oxidation rate (Sapsford 2013; Trumm and Pope 2015). Based on the increase in pH through the stages of aeration (figure 6.3.1 and 6.3-2) it is likely that this degassing effect is occurring during the aeration and oxidation of the RDRN water. Sapsford (2013) also suggested that iron removal is dependent on setting rates in a traditional settling pond rather than aeration, when the pH of the water is over 7. Therefore, by removing the settling rate constraint by utilisation of a gravel bed filter and ultimately nano particulate filter of the iron ochre layer, it has allowed this system to produce very high removal rates at a very low HRT (figure 5.6-5). As well as high iron and arsenic removal, figure 6.3-3 shows high manganese (Mn) removal has occurred in the system. Manganese has been documented as one of the more difficult metals to remove from solution (Sapsford et al. 2006; Trumm et al. 2017). Sapsford et al. (2006) showed that manganese removal is possible in a VFR system, likely either by the iron hydroxide floc scavenging manganese from solution or co-precipitation. Results from this study support those findings. In their trial, Sapsford et al. (2006) found that they could achieve 50% of removal of manganese in a 24hr HRT, whereas in this trial a 99% removal in a 34hr residence time and 86% in a 53hr residence time was achieved.

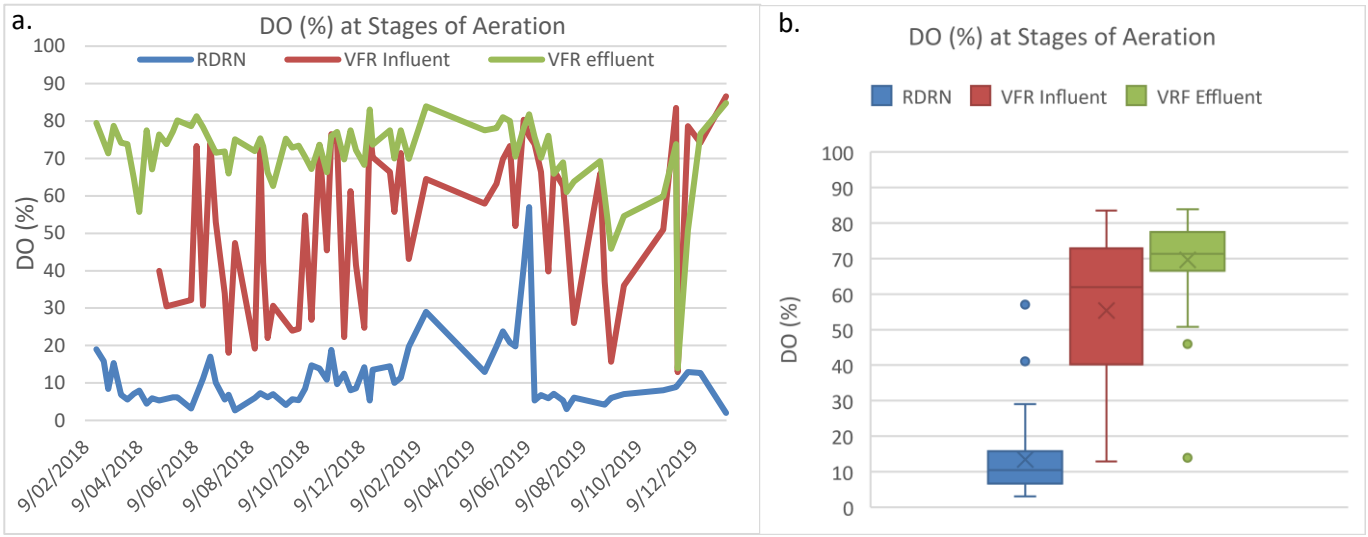

Figure 6.3- 1: Graphs showing the DO (%) at different stages of aeration a) over time and b) a Box Wisker graph. RDRN show the unaltered influent, VFR Influent is the influent entering the system from the spray nozzle and VFR effluent represents the water as it leaves the system.

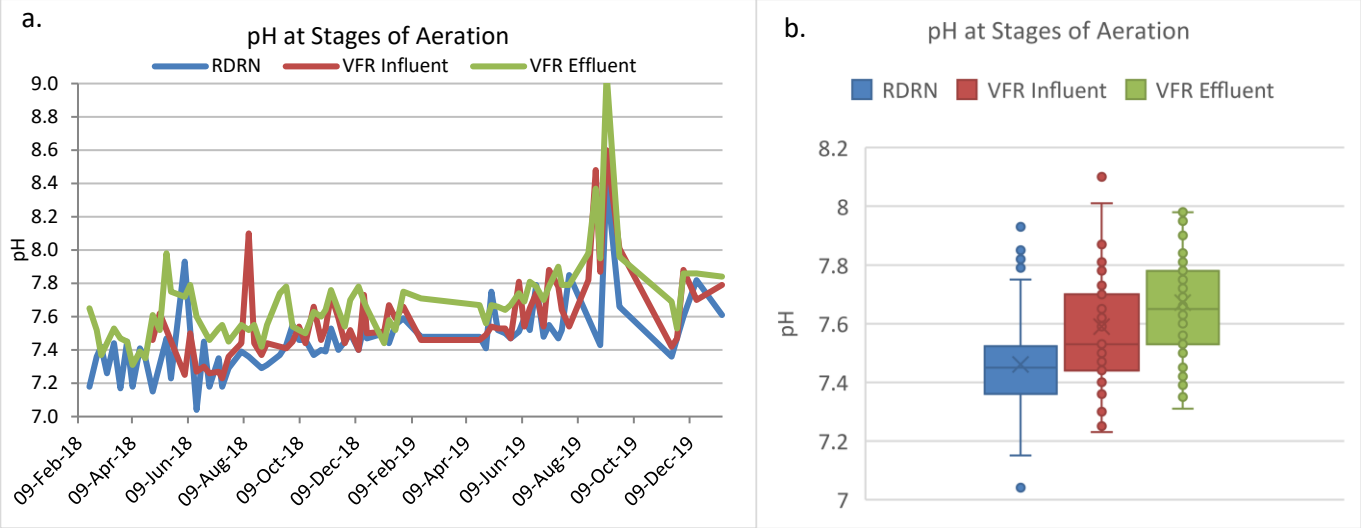

Figure 6.3- 2: Graphs showing the pH at different stages of aeration a) over time and b) a Box and Wisker graph. RDRN show the unaltered influent, VFR Influent is the influent entering the system from the spray nozzle and VFR effluent represents the water as it leaves the system

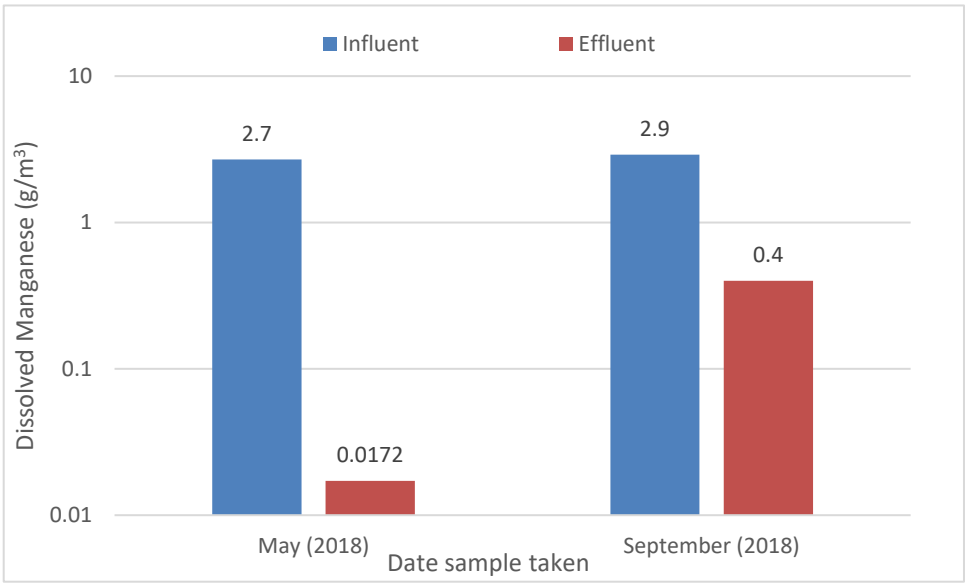

Figure 6.3- 3: Graph showing the two measured manganese concentration in the influent and effluent (note axis in log scale).

6.3.2 Addition of Globe Pit Lake Proxy

The VFR was initially set up to have high arsenic TSF return water to act as a proxy for Globe Pit Lake water. The TSF return water quality, however, improved significantly during the early operation of the system and was therefore switched off on the 18th June. This caused there to be poor removal rates due to low concentration on contaminants in the incoming water, which acted as dilution rather than an arsenic source. As seen in figure 6.3-4, arsenic removal is affected by a higher TSF/RDRN ratio more than it is impacted by an Fe/As ratio. McCauley (2011) suggested that an Fe/As ratio of 3:1 was necessary for efficient removal and long-term stability, which would suggest the Fe/As ratios being treated in this system far exceed that requirement, even with the initial addition of arsenic from the TSF return water line.

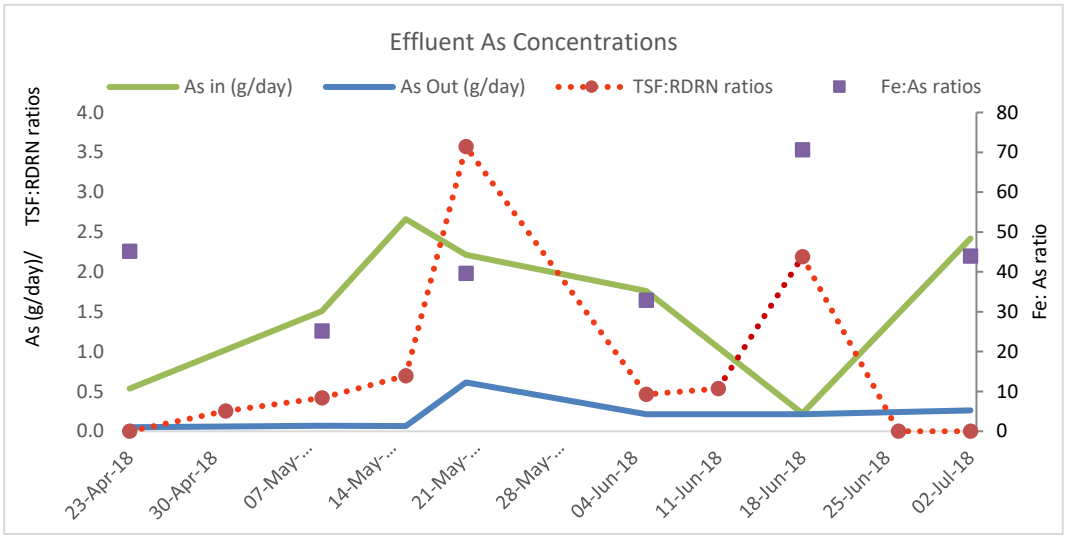

Figure 6.3- 4: Graph showing the dissolved arsenic reporting to the system daily and leaving the system, plotted with the TSF/RDRN ratios and the Fe/As.

6.3.3 Arsenic/Iron Speciation.

Speciation of iron was regularly undertaken on the VFR influent (RDRN) and effluent. This showed that almost all iron present in the influent was ferrous iron (Fe^{2+}) and almost all iron present in the effluent, which was significantly less, was ferric iron (Fe^{3+}) (figure 5.6-6 and 5.6-7)). This shows that the majority of iron entering the system was in the reduced form but by the time it exited the system it was oxidised, which is what was expected.

Arsenic speciation was undertaken on one occasion during the operation of the VFR trial on the influent water, but not on the effluent water. As arsenic has relatively slow redox reactions it is common to find them together in both redox states (Raven et al. 1998). It has also been shown that arsenate (As^{5+}) reacts much faster with iron oxide precipitates than arsenite (As^{3+}) and therefore the speciation and required time for the oxidation reaction to occur can be one of the limiting factors of arsenic removal through adsorption onto iron precipitates (Raven et al. 1998; Rait et al. 2010).

Data from the arsenic speciation completed on the VFR influent water concluded that 100% of the arsenic in the sample was in the reduced form or As^{3+}. As arsenic speciation was not undertaken on the effluent it is impossible to say in which redox state arsenic present in the effluent was in, but it is likely that it was in the oxidised state based on oxidising conditions in the VFR. Although, Raven et al. (1998), found that with high (approximately >7.5) pH adsorption of arsenite could actually surpass that of arsenate especially at high arsenic concentrations. Data shows that the pH going into this system frequently gets to >7.5 and effluent is generally at or above this and therefore redox state

may not be a limiting factor at all in this system. Research also suggests that arsenite and arsenate are regularly found together in AMD or MAW suggesting that slow oxidation process often mean the presence of both species, although microbial oxidation of As^{3+} to As^{5+} can accelerate this process (Paikaray 2015), however it is unclear whether this process is occurring withing the VFR.

6.3.4 Driving head, flow and scour potential.

During the early stages of operation of the system, it became evident that removal rates were extremely high, even when the pump was pushed to full capacity. Clogging of the pipeline and the fins within the pump meant that the flow rate reduced through operation. The flush lines that were installed part way through the trial meant that the piping could regularly (fortnightly-monthly, depending on the decrease in flow) be cleared out. This meant the flows were able to be maintained at higher rate in order to push the system to operate in lower HRTs which were at this stage limited by the piping and the pump capacity. After several months of flushing the pipes with little difference noted on the flow reporting to the system, the pump was removed and serviced. During this service it was identified that the fins within the pump had become clogged with iron floc, which was preventing the pump working to full capacity. A cleaning regime was implemented, and a second pump purchased, which allowed the pumps to be switched out, to minimise operation time in which the system was running on restricted flows.

While the system was operating at higher flows it began to overtop through the overflow. This was caused by the formation of the ochre layer which develops on the fine filter gravel. This ochre layer has a decreasing permeability as it becomes thicker through the system's operation. The decrease in permeability means that the water level rises within the tank until there is enough head pressure to force the water through. This is referred to as the driving head. Driving head was not anticipated in the design of this system and therefore the height of the outlet gooseneck was too close to the height of the overflow and therefore had to be adjusted down throughout the operation of the system (heights shown in table 6.3-1), to allow for sufficient driving head without overflow of the tank. As driving head wasn't considered when the system was first commissioned and monitoring began, it was not measured for several months (see section 4.4.2 for more detail). Adjustments were made to the outlet height during operation of the system which meant comparisons if the driving head were very difficult, as there were several factors, including the sludge layer thickness, which were affecting it.

The changing driving head was exacerbated by the fact the TSF return water has a high suspended solid concentration consisting of fine Greywacke particles which contributed to the ochre layer and therefore further decreased the permeability. The VFR was drained, and the built-up sludge was removed in February 2019. The system was then restarted and run with only the RDRN water fed into it and no further adjustments made to the outlet height. Without the TSF return water, this reduced the effect of suspended solids on the accumulating sludge and allowed a more accurate measurement of driving head over time.

This provided nine months of operation data which showed an increase in driving head with time (figure 5.6-4), showing the driving head is influenced by the amount of iron precipitate contained within the system. The driving head was also affected by flow, by which an increased effect was observed over time. The flow had a much greater impact on the driving head the longer the system operated after the sludge was removed in February 2019. When the ochre layer is thin the flow had less effect on the driving head whereas when the ochre layer was thicker a small change in flow drastically increased the driving head (figure 6.3-5).

Table 6.3- 1: Outlet heights of VFR from dates adjusted and the difference in height from outlet to overflow pipe.

Date	VFR Outlet height (m)	Height to overflow (m)
02/02/2018	1.95	0.17
21/08/2018	1.85	0.27
21/10/2018	1.70	0.42
07/12/2018	1.42	0.70
18/02/2019	1.20	0.92

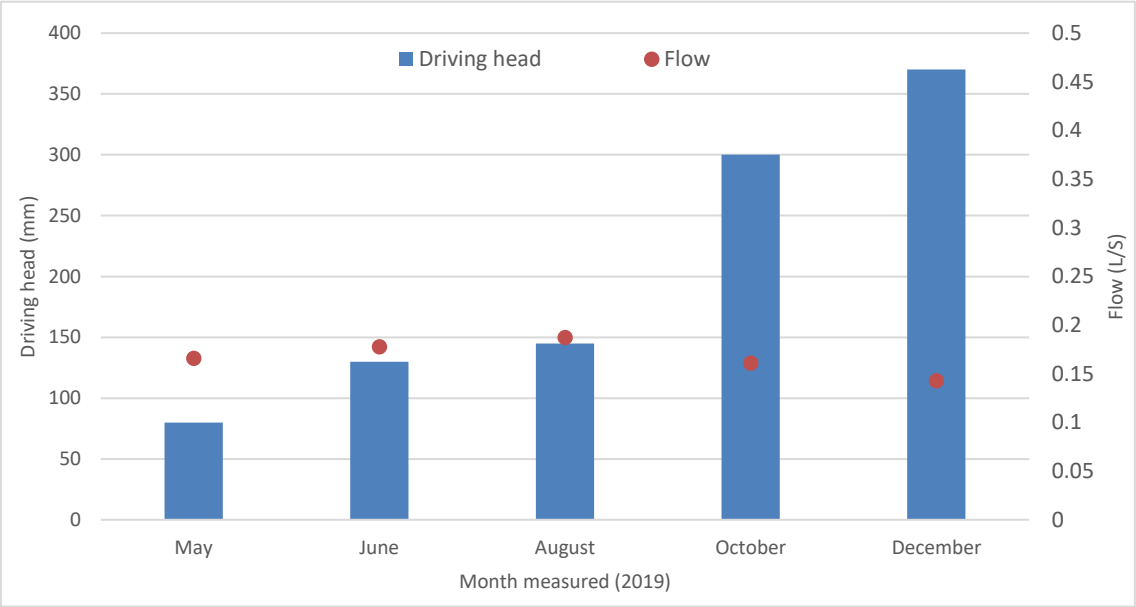

Figure 6.3- 5: Graph showing the increase of driving head within the VFR with similar flows over the operation of the system, from when the sludge was removed and the system restarted, with no adjustments to outlet height.

Barnes (2008) hypothesised that transport of precipitate iron through the filter bed was possible in the form of a sludge scour effect under too high vertical velocity flows and too high driving head. He concluded that at low driving head higher vertical velocities were possible and that at lower vertical velocities it was possible to operate with higher driving head, without sludge scour occurring. He estimated that, without further field trials the "maximum sustainable flow condition" was a vertical velocity of 2 m/day and a change in height (or driving head) of 1m. The VFR trialled onsite had a maximum driving head measurement of 710mm, which is below the known limits of the VFR as tested by Barnes (2008), and the maximum possible driving head at the lowest outlet height of 1.2m, would have only given a maximum of 900mm driving head. Figure 6.3-6 shows the trial data from this study overlaid on the data from Barnes (2008) which shows the vertical velocities and driving head were within his trialled data and that this fell within the zone of which he concluded sludge scour would not occur.

To test the potential of scour on this system it would require higher flow rates to increase the vertical velocity (closer to the maximum indicated by Barnes (2008) of approximately 4.5 m/day (figure 6.3-6)). In the last month of operation, data showed that an increase in flow of 0.39 L/s increased the driving head by 520mm, therefore an increase of 0.2 L/s on the highest flow measurement (0.45 L/s with a driving head of 710mm) may have pushed the system over the 1m theoretical driving head maximum. The other possible method to measure potential scouring would be to decrease the outlet height and therefore increase the distance between the overflow and outlet. Although the depth of the water column may impact allowable driving head due to effects of head pressure on the sludge, this is not considered in the Barnes (2008) sizing assessment.

The maximum sizing of a VFR is partially important for the Globe Progress site as the major limiting factor is available area. Therefore, the maximum height, velocity and driving head need to be well understood and taken into consideration. A maximum water column height to ensure water remains in an oxygenated state needs to be maintained within the entire system, as well as maximum driving head and vertical velocities to prevent potential sludge scour. A second system trialled at this site, which was not part of this research project showed sludge scour throughout its operation with Fe^{3+} precipitates continually being present in the effluent. This system was trialled at very high flow rates and regularly operated at <10hour residence times. The data from this system confirms the sludge scour boundary curve suggested by Barnes (2008), further showing the importance of the balance of velocities, driving head and water column height. Another important aspect that must be considered is HRT. Although the system trialled at this site showed high removal at relatively low HRT, it is important to note that removal did increase with HRT to a degree, and as flows are variable at this site, it is important to maximise the system as much as possible. It, therefore, would be most effective in the design of a system like this to ensure the entire area is being utilised by adjusting the outlet height as flows change and sludge builds.

There are several options for controlling pond heights. Companies such as Agri Drain have developed “Inline Water Level Control Structures™” which use panels, which can be removed or added, to lower or increase pond levels, which require no power but would need to be manually checked and adjusted as needed. Hedin Environmental (2008) uses an Argi Drain Smart Drainage System, which is an automated level control powered by a solar system, that has been especially programmed to flush Limestone Leach Beds with chemical or flow triggers. As these drains use panels to control pond height it is possible to alter the programming of such a drain to, instead of flushing, automatically remove or add panels as pond height increases/decreases, triggered by information fed from a level sensor. Another option to maximise HRT is potentially to use a proportional valve, commonly used with level sensors in water treatment plants to control levels within tanks, which could be powered by a solar or hydro system to open and close in order to control flow and therefore the level within the system.

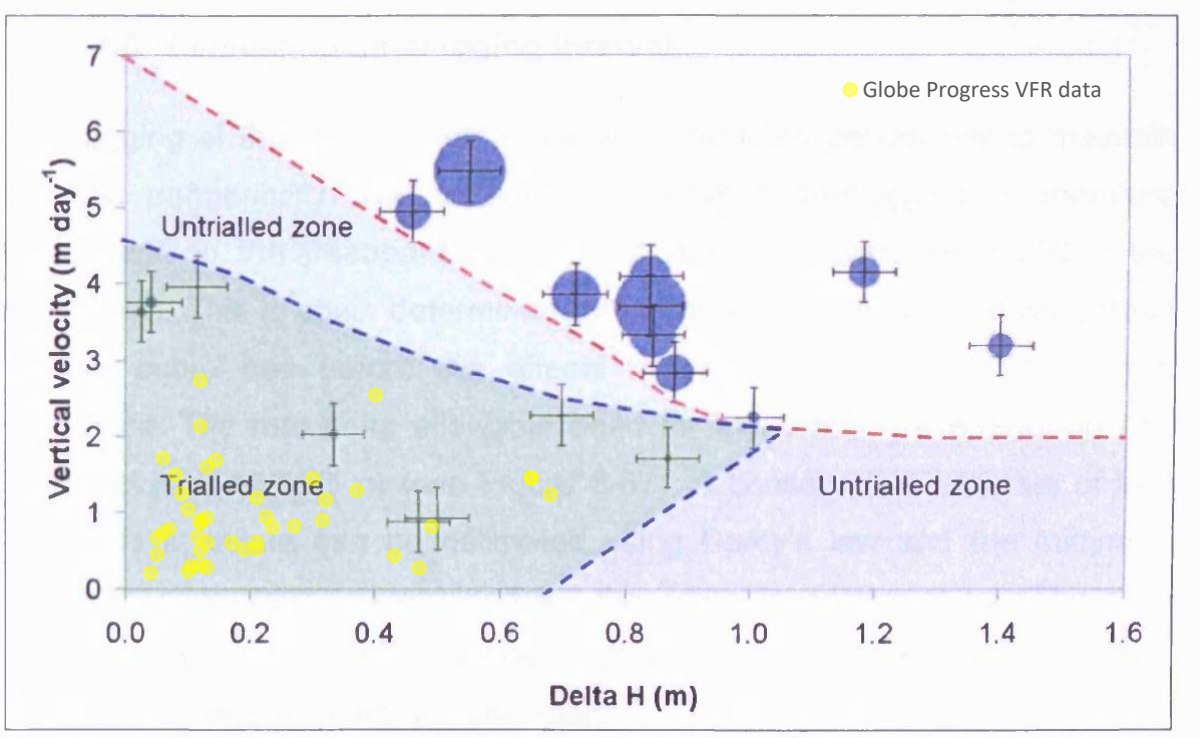

Figure 6.3- 6: Vertical velocity vs driving head and the hypnotised sludge scour boundary (red dashed line) (from Barnes 2008) with the VFR trial data overlayed for comparison (in yellow).

6.3.5 Precipitate Analysis and Drying capacity

The VFR was drained and precipitate sludge from the ochre layer was sampled on both occasions (refer to section 5.6-5 for the full results). During the first operating round TSF water was fed through the system for 64 days (from 24th April to the 26th June) and therefore the high suspended solids concentration in this water contributed to the precipitate sludge that was collected in the system, as shown in photograph on figure 5.6-8. Analysis of total recoverable metals was completed on both sets of samples, although more parameters were measured on the second instance, as well as XRF and XRD analysis. Analysis of total recoverable metals and XRF analysis showed similar results for both sampling occasions and for both methods. This concluded the precipitate was made up of approximately 30% iron (29-34.5%), and 0.75% arsenic (0.56-0.89%), therefore giving an iron to arsenic ratio of approximately 40:1 which is far higher than what was suggested to be the limit by Barnes (2008). This system could therefore potentially remove significantly more arsenic if it was present. Sulphur by percent weight was only measured by XRF, and the first sample was much higher than the second (0.72% compared to 0.11%). This may be due to the formation of schwertmannite, an iron-oxyhydroxysulfate mineral, being higher is the first operation opposed to the second, potentially due to the addition of the TSF water. Manganese showed an opposite trend with the first XRF showing low results (0.82%) and the second much higher (6.77%). This is thought to be due to much lower concentrations in the TSF water (approximately 0.2 g/m^3 during the addition to the VFR) than compared to the RDRN (an average of 2.7g/m^3), meaning that it was potentially diluted in the first sample. XRD analysis identified Quartz and Muscovite in the first sample, and Quartz, Muscovite, Plagioclase Feldspar and Potassium Feldspar, with amorphous material present in the second sample. In the first sample this was thought to be due to sediment from the TSF return water, as the results are consistent of the site host rock (Greywacke) mineralogy. It is also likely that minerals of the host rock are present in the RDRN water and therefore would be present in the second sample, although in low concentrations. It is likely that the amorphous material was Ferric Hydroxide (Hedin 2003).

Samples were sent and tested for TCLP (Toxicity Characteristic Leaching Procedure) and SPLP (Synthetic Precipitation Leaching Procedure) by Hills Laboratories. Both tests are leach tests. The first (TCLP) is used to derive if a material is to be classed as hazardous for the basis of disposal at general landfill sites, and the second (SPLP) is to evaluate the leachability under acidic rain conditions. Test results showed that leachate results were below detection in both circumstances with the exception of manganese, nickel and zinc, which were all low and below the limits for class A and B landfills in New Zealand (Ministry for the Environment 2004). Although it is important to note that it passes all required leach test requirements, the sludge fails the Class A and B landfill screening criteria for an arsenic limit of 100 mg/kg by over an order of magnitude, therefore it would be classed as a hazardous waste and be require to be disposed of as such.

Sludge drying rates were also measured to establish the required time for drying before it was efficient to clear and transport for dispose. Hedin (2003) found that iron sludge at his sample site was 25-35% solids in place and a filter press increased this to an average of 50%. The precipitates within the VFR in this trial were recorded at 18.7% solids at day one of drying, 25% at day 7 and 63% at day 12. The second drying round was far less effective, with the moisture actually increasing after day 3, due to wet weather. This shows that sludge drying rates within the VFR were more effective in dry weather conditions, but under wet weather conditions, it is unlikely to dry over 20% solids. Thus, in dry conditions this system would have a minimum downtime period needed for clearing, compared to that of a tradition sludge pond, which often needs to be dewatered through some sort of filter system such as a filter press (Hedin 2003)

6.4 Options for Full-scale

This research was undertaken to investigate methods of passive treatment that could be upscaled to a full-scale system for the long-term closure of the site. Based on the results from the trials, it seems the most appropriate option for this site is a VFR. The VFR allowed high removal of the target metals, iron and arsenic, with relatively low HRT and therefore footprint, while the bioreactors have less consistent removal over longer HRT.

The VFR performance was also not dependent on temperature and produced a very stable waste product, with analysis showing that metals did not readily leach from the sludge even in slightly acidic conditions. VFRs have also been shown to be more effective at sites with circum-neutral MAW opposed to AMD where they would likely need to be paired with another system, which neutralises the water prior to aeration, to be an effective treatment method (Sapsford 2013; Blanco et al. 2018). The achieved sludge drying rates from the first round of drying also indicate that this would make maintenance to a full-scale system achievable during dry weather and low flows if there were two systems run in parallel.

Another consideration which should be made when considering a VFR, is the VFR did produce a sludge that would within relatively short timeframes need to be cleaned out to ensure the system would remain functional. If left unmaintained, the driving head would increase until the system, full-scale or trial sized, would eventually overtop and therefore lose treatment/removal efficiency as a portion of flow would be bypassing the system.

Results from the bioreactor treatments demonstrate that these would be a viable option for treatment for a site that had a greater area to utilise. Biosolids proved to be an extremely effective substate additive and could provide treatment for metals and sulphate at a site where longer (>48hr) HRT could be achieved. It should be noted that at this site there was no release of metals from the biosolids seen the effluent. This may not be the case at a site with acidic MAW, as it could potentially cause a release of these metals at low pH.

Results from the bioreactor also show a reduction in sulphate. While sulphate was not at high levels at this site, many sites with MAW do have elevated sulphate which requires treatment which could

make bioreactors, especially with the addition of biosolids, a viable treatment option. As this is the first use of biosolids within a passive treatment system, to the authors knowledge, it seems further research should be undertaken on the addition of biosolids as a substrate in a bioreactor considering the success it has shown in this research. The temperature treatments in this trial show that in sites with variable ambient air temperatures, use of an insulated tank can reduce the fluctuation and therefore could allow for greater removal due more stable temperatures within the tank.

7. Chapter Seven-Conclusions

Two different methods of passive treatment were trialled, primarily for the removal of arsenic and iron, at the former Globe Progress mine site in preparation for long term treatment of MAW after closure. These consisted of a) a sulphate reducing bioreactor and 2) a meso-scale vertical flow reactor.

The bioreactor trial consisted of four different substrate treatments, and two temperature treatments. The four substrate mixes consisted of a combination of varying amounts of spent mushroom compost, sawdust, bark and either biosolids or mussel shells. These were referred to as Tank 1- biosolids, less compost; Tank 2- mussel shells, less compost; Tank 3- biosolids, more compost; and Tank 4- mussel shells, more compost. These treatments showed that biosolids is more effective for the removal of iron, arsenic and sulphate than mussel shells, but having more or less compost does not have an effect. Iron removal was just over 60% at 50 hours HRT for biosolid treatments, but only at about 45% at the same HRT for mussel shell treatments. Arsenic removal in biosolids treatments was about 75% at a 50 hours HRT, whereas mussel shell treatments only showed about 55/60% removal at the same HRT. Sulphate removal also showed a similar trend at 50 hours HRT with biosolids treatments showing about 20% removal and mussel shell treatments showing only 10% removal. The higher removal rates of metal and sulphate in all biosolid treatments is likely due to biosolids having higher levels of nitrogen and phosphorus than other substrates used in this trial, which are essential nutrients for SRB activity. The presence of both, crystalline sulphur from the effluent of two systems and the iron sulphide mineral greigite from within another, along with the presence of hydrogen sulphide, indicates in-situ sulphate reduction is occurring.

All treatments showed a positive correlation with percent iron removal and HRT. The less compost treatments showed a positive linear relationship whereas the more compost treatments showed a positive logarithmic relationship. Arsenic removal showed less of a correlation with HRT. Both mussel shell treatments showed a positive logarithmic relationship with removal but the biosolid treatments were more variable. The biosolids less compost treatment showed a positive linear relationship but also showed high removal rates at all HRT, whereas the biosolids more compost treatment showed no relationship. Interestingly, sulphate removal showed a strong linear relationship with HRT for all treatments, with higher removal at longer HRTs. This work indicates that the longer contact time the water has with the substrates and the SRB, the higher the metal and sulphate removal, with about 40% sulphate removal shown in biosolid treatments at 75 hour HRT compared to 20% at 50 hours.

Temperature treatments have shown that the internal temperature of these systems is influenced more by influent temperature than by ambient air temperature and that diurnal temperature fluctuations are evident in the edges of the systems, but not in the middle of the substrate. It was also found that using an insulated tank can minimise the diurnal fluctuations and therefore maintain a more stable temperature within the system. This indicates that the use of insulated tanks or materials may be appropriate in areas with highly fluctuating day or even seasonal temperatures, and that increasing the influent temperature will likely mean a higher internal temperature even in areas with cold ambient air temperatures.

The vertical flow reactor performed better than expected with a median iron removal at 98.99% and median arsenic removal at 94.89%. This system had high removal even at low residence time with iron removal at 84% and arsenic removal at 75% at as low as 10 hours HRT. Speciation of the iron showed that the water was predominantly ferrous iron, the reduced form, in the influent, but the minor concentrations that were detected in the effluent were mostly ferric, the oxidised form. This demonstrates that the system is effectively aerating the water and the removal is in fact due to precipitation of ferric hydroxides, which are being captured within the system. Driving head turned out to be one of the most interesting findings in operating this system. It showed that during

operation and the thickening of the ochre layer, due to the build-up of iron hydroxides, that driving head had to increase to allow for the same flow rates. This meant that when the ochre layer was at the thickest small increases in the flow rate resulted in a much higher driving head, whereas when the system was first started and the ochre layer was thin changes in flow rate was only a small effect on the driving head. Furthermore, this trial also showed that the sludge from the ochre layer could dry very quickly, getting to 63% solids in just 12 days, thus the system would be able to be cleaned out with relative ease and within a short timeframe.

Further work

Further investigation into the potential of biosolids should be undertaken based of how well they performed in this trial. More work should be done to investigate how biosolids would perform as a sole source substrate and also, how they perform with acid MAW or AMD. The potential for biosolids to be used in mine reclamation work is starting to be recognised but the use in passive treatment systems needs further investigation.

Further work also needs to be undertaken to establish the maximum water column depth of a vertical flow reactor in order to prevent sludge scour and reducing conditions, to better establish the maximum depth and therefore required footprint. More investigation should also be undertaken to better quantify the limits of Barnes (2008) sludge scour diagram to establish the true maximum limits in terms of vertical velocity and driving head.

References

Acharya BS, Kharel G. 2020. Acid mine drainage from coal mining in the united states – an overview. Journal of Hydrology. 588:125061.

Altun M, Sahinkaya E, Durukan I, Bektas S, Komnitsas K. 2014. Arsenic removal in a sulfidogenic fixed-bed column bioreactor. Journal of Hazardous Materials. 269:31-37.

Aoyagi T, Hamai T, Hori T, Sato Y, Kobayashi M, Sato Y, Inaba T, Ogata A, Habe H, Sakata T. 2017. Hydraulic retention time and ph affect the performance and microbial communities of passive bioreactors for treatment of acid mine drainage. AMB Express. 7(1).

Australian and new zealand guidelines for fresh and marine water quality. Volume 1, the guidelines / australian and new zealand environment and conservation council, agriculture and resource management council of australia and new zealand. 2000. Canberra: Australian and New Zealand Environment and Conservation Council and Agriculture and Resource Management Council of Australia and New Zealand.

Barnes A. 2008. Rates and mechanisms of fe(ii) oxidation in a passive vertical flow reactor for the treatment of ferruginous mine water. Engineering, Cardiff University.

Ben Ali HE, Neculita CM, Molson JW, Maqsoud A, Zagury GJ. 2020. Salinity and low temperature effects on the performance of column biochemical reactors for the treatment of acidic and neutral mine drainage. Chemosphere. 243.

Blanco I, Sapsford DJ, Trumm D, Pope J, Kruse N, Cheong YW, McLauchlan H, Sinclair E, Weber P, Olds W. 2018. International trials of vertical flow reactors for coal mine water treatment. Mine Water and the Environment. 37(1):4-17.

Cadmus P, Clements WH, Williamson JL, Ranville JF, Meyer JS, Gutiérrez Ginés MJ. 2016. The use of field and mesocosm experiments to quantify effects of physical and chemical stressors in mining-contaminated streams. Environmental Science and Technology. 50(14):7825-7833.

. Environmental effects and importance of the risk assessments for mining wastewater. Proceedings of the 24th International Mining Congress of Turkey, IMCET 2015; 2015.

Champeau O, Cavanagh JAE, Sheehan TJ, Tremblay LA, Harding JS. 2017. Acute toxicity of arsenic to larvae of four new zealand freshwater insect taxa. New Zealand Journal of Marine and Freshwater Research. 51(3):443-454.

Cocos IA, Zagury GJ, Clément B, Samson R. 2002. Multiple factor design for reactive mixture selection for use in reactive walls in mine drainage treatment. Water Research. 36(1):167-177.

Dev S, Patra AK, Mukherjee A, Bhattacharya J. 2015. Suitability of different growth substrates as source of nitrogen for sulfate reducing bacteria. Biodegradation. 26(6):415-430.

DiLoreto ZA, Weber PA, Olds W, Pope J, Trumm D, Chaganti SR, Heath DD, Weisener CG. 2016. Novel cost effective full scale mussel shell bioreactors for metal removal and acid neutralization. Journal of Environmental Management. 183:601-612.

Florence K, Sapsford DJ, Johnson DB, Kay CM, Wolkersdorfer C. 2016. Iron-mineral accretion from acid mine drainage and its application in passive treatment. Environmental Technology (United Kingdom). 37(11):1428-1440.

Ganjegunte GK, Condron LM, Clinton PW, Davis MR, Mahieu N. 2004. Decomposition and nutrient release from radiata pine (pinus radiata) coarse woody debris. Forest Ecology and Management. 187(2-3):197-211.

Gibert O, De Pablo J, Luis Cortina J, Ayora C. 2004. Chemical characterisation of natural organic substrates for biological mitigation of acid mine drainage. Water Research. 38(19):4186-4196.

Golder. 2015. Reefton gold project closure. Mine water management assessment. Prepared for OceanaGold (New Zealand) Limited by Golder Associates (NZ) Limited. No. Reference no. 1478210088-016-R-Rev0.

Gray DP, Harding JS. 2012. Acid mine drainage index (amdi): A benthic invertebrate biotic index for assessing coal mining impacts in new zealand streams. New Zealand Journal of Marine and Freshwater Research. 46(3):335-352.
Gray DP, Harding JS, Lindsay P. 2016. Remediation of a major acid mine drainage point source discharge restores headwater connectivity for a diadromous native fish. New Zealand Journal of Marine and Freshwater Research. 50(4):566-580.
Hassanpour B, Giri S, Pluer WT, Steenhuis TS, Geohring LD. 2017. Seasonal performance of denitrifying bioreactors in the northeastern united states: Field trials. Journal of Environmental Management. 202:242-253.
Hedin RS. 2003. Recovery of marketable iron oxide from mine drainage in the USA. Land Contamination and Reclamation. 11(2):93-98.
Hedin RS. 2008. Iron removal by a passive system treating alkaline coal mine drainage. Mine Water and the Environment. 27(4):200-209.
Hering JG, Chen PY, Wilkie JA, Elimelech M, Liang S. 1996. Arsenic removal by ferric chloride. Journal / American Water Works Association. 88(4):155-167.
Hogsden KL, Harding JS. 2012a. Anthropogenic and natural sources of acidity and metals and their influence on the structure of stream food webs. Environmental Pollution. 162:466-474.
Hogsden KL, Harding JS. 2012b. Consequences of acid mine drainage for the structure and function of benthic stream communities: A review. Freshwater Science. 31(1):108-120.
Hogsden KL, Winterbourn MJ, Harding JS. 2013. Do food quantity and quality affect food webs in streams polluted by acid mine drainage? Marine and Freshwater Research. 64(12):1112-1122.
International Programme on Chemical S, Inter-Organization Programme for the Sound Management of C. 2010. Strontium and strontium compounds. Geneva: World Health Organization.
Isosaari P, Sillanpää M. 2017. Use of sulfate-reducing and bioelectrochemical reactors for metal recovery from mine water. Separation and Purification Reviews. 46(1):1-20.
Jellyman PG, Harding JS. 2014. Variable survival across low ph gradients in freshwater fish species. Journal of Fish Biology. 85(5):1746-1752.
Johnson DL, Pilson MEQ. 1972. Spectrophotometric determination of arsenite, arsenate, and phosphate in natural waters. Analytica Chimica Acta. 58(2):289-299.
Jong T, Parry DL. 2003. Removal of sulfate and heavy metals by sulfate reducing bacteria in short-term bench scale upflow anaerobic packed bed reactor runs. Water Research. 37(14):3379-3389.
Jouini M, Neculita CM, Genty T, Benzaazoua M. 2020. Environmental behavior of metal-rich residues from the passive treatment of acid mine drainage. Science of the Total Environment. 712.
Le Pape P, Battaglia-Brunet F, Parmentier M, Joulian C, Gassaud C, Fernandez-Rojo L, Guigner JM, Ikogou M, Stetten L, Olivi L et al. 2017. Complete removal of arsenic and zinc from a heavily contaminated acid mine drainage via an indigenous srb consortium. Journal of Hazardous Materials. 321:764-772.
Luong VT, Cañas Kurz EE, Hellriegel U, Luu TL, Hoinkis J, Bundschuh J. 2018. Iron-based subsurface arsenic removal technologies by aeration: A review of the current state and future prospects. Water Research. 133:110-122.
Macara GR. 2016. The climate and weather of west coast. NIWA Science and Technology Series (72):40 pp.
Madambik K, Moore J. 2013. Technical report for the reefton project. OceanaGold. Report.
McCauley CA. 2011. Assessment of passive treatment and biogeochemical reactors for ameliorating acid mine drainage at stockton coal mine. [Unpublished Thesis]: Department of Civil and Natural Resources Engineering, University of Canterbury, New Zealand.
. Performance of mesocosm-scale sulfate-reducing bioreactors for treating acid mine drainage in new zealand. 25th Annual Meetings of the American Society of Mining and Reclamation and 10th Meeting of IALR 2008; 2008.

Milham L, Craw D. 2009. Two-stage structural development of a paleozoic auriferous shear zone at the globe-progress deposit, reefton, new zealand. New Zealand Journal of Geology and Geophysics. 52(3):247-259.
Ministry for the Environment. 2004. Module 2: Hazardous waste guidelines landfill waste acceptance criteria and landfill classification Ministry for the Environment, Wellington, New Zealand.
Mosley LM, Peake BM. 2001. Partitioning of metals (fe, pb, cu, zn) in urban run-off from the kaikorai valley, dunedin, new zealand. New Zealand Journal of Marine and Freshwater Research. 35(3):615-624.
Muhammad SN, Kusin FM, Md Zahar MS, Mohamat Yusuff F, Halimoon N. 2017. Passive bioremediation technology incorporating lignocellulosic spent mushroom compost and limestone for metal- and sulfate-rich acid mine drainage. Environmental Technology (United Kingdom). 38(16):2003-2012.
Neculita CM, Zagury GJ. 2008. Biological treatment of highly contaminated acid mine drainage in batch reactors: Long-term treatment and reactive mixture characterization. Journal of Hazardous Materials. 157(2-3):358-366.
Neculita CM, Zagury GJ, Bussière B. 2007. Passive treatment of acid mine drainage in bioreactors using sulfate-reducing bacteria: Critical review and research needs. Journal of Environmental Quality. 36(1):1-16.
Neculita CM, Zagury GJ, Bussière B. 2008a. Effectiveness of sulfate-reducing passive bioreactors for treating highly contaminated acid mine drainage: I. Effect of hydraulic retention time. Applied Geochemistry. 23(12):3442-3451.
Neculita CM, Zagury GJ, Bussière B. 2008b. Effectiveness of sulfate-reducing passive bioreactors for treating highly contaminated acid mine drainage: Ii. Metal removal mechanisms and potential mobility. Applied Geochemistry. 23(12):3545-3560.
Nevatalo LM, Bijmans MFM, Lens PNL, Kaksonen AH, Puhakka JA. 2010. The effect of sub-optimal temperature on specific sulfidogenic activity of mesophilic srb in an h2-fed membrane bioreactor. Process Biochemistry. 45(3):363-368.
Nielsen G, Hatam I, Abuan KA, Janin A, Coudert L, Blais JF, Mercier G, Baldwin SA. 2018. Semi-passive in-situ pilot scale bioreactor successfully removed sulfate and metals from mine impacted water under subarctic climatic conditions. Water Research. 140:268-279.
Okabe S, Nielsen PH, Characklis WG. 1992. Factors affecting microbial sulfate reduction by desulfovibrio desulfuricans in continuous culture: Limiting nutrients and sulfide concentration. Biotechnology and Bioengineering. 40(6):725-734.
Omoregie EO, Couture R-M, Van Cappellen P, Corkhill CL, Charnock JM, Polya DA, Vaughan D, Vanbroekhoven K, Lloyd JR. 2013. Arsenic bioremediation by biogenic iron oxides and sulfides. Applied and Environmental Microbiology. 79(14):4325.
Paikaray S. 2015. Arsenic geochemistry of acid mine drainage. Mine Water and the Environment. 34(2):181-196.
Patidar SK, Tare V. 2006. Effect of nutrients on biomass activity in degradation of sulfate laden organics. Process Biochemistry. 41(2):489-495.
Porter MD, Andrus JM, Bartolerio NA, Rodriguez LF, Zhang Y, Zilles JL, Kent AD. 2015. Seasonal patterns in microbial community composition in denitrifying bioreactors treating subsurface agricultural drainage. Microbial Ecology. 70(3):710-723.
Prasad D, Wai M, Bérubé P, Henry JG. 1999. Evaluating substrates in the biological treatment of acid mine drainage. Environmental Technology (United Kingdom). 20(5):449-458.
Rait R, Trumm D, Pope J, Craw D, Newman N, MacKenzie H. 2010. Adsorption of arsenic by iron rich precipitates from two coal mine drainage sites on the west coast of new zealand. New Zealand Journal of Geology and Geophysics. 53(2-3):177-193.
Raven KP, Jain A, Loeppert RH. 1998. Arsenite and arsenate adsorption on ferrihydrite: Kinetics, equilibrium, and adsorption envelopes. Environmental Science and Technology. 32(3):344-349.

Sapsford D, Barnes A, Dey M, Williams K, Jarvis A, Younger P. 2007. Low footprint passive mine water treatment: Field demonstration and application. Mine Water and the Environment. 26(4):243-250.
Sapsford DJ. 2013. New perspectives on the passive treatment of ferruginous circumneutral mine waters in the uk. Environmental Science and Pollution Research. 20(11):7827-7836.
. Iron and manganese removal in a vertical flow reactor for passive treatment of mine water. 7th International Conference on Acid Rock Drainage 2006, ICARD - Also Serves as the 23rd Annual Meetings of the American Society of Mining and Reclamation; 2006.
Sekula P, Hiller E, Šottník P, Jurkovič Ľ, Klimko T, Vozár J. 2018. Removal of antimony and arsenic from circum-neutral mine drainage in poproč, slovakia: A field treatment system using low-cost iron-based material. Environmental Earth Sciences. 77(13).
Skousen J. 2014. Overview of acid mine drainage treatment with chemicals. Acid mine drainage, rock drainage, and acid sulfate soils: Causes, assessment, prediction, prevention, and remediation. p. 325-337.
Skousen J, Zipper CE, Rose A, Ziemkiewicz PF, Nairn R, McDonald LM, Kleinmann RL. 2017. Review of passive systems for acid mine drainage treatment. Mine Water and the Environment. 36(1):133-153.
Skousen JG, Ziemkiewicz PF, McDonald LM. 2019. Acid mine drainage formation, control and treatment: Approaches and strategies. Extractive Industries and Society. 6(1):241-249.
Teclu D, Tivchev G, Laing M, Wallis M. 2009. Determination of the elemental composition of molasses and its suitability as carbon source for growth of sulphate-reducing bacteria. Journal of Hazardous Materials. 161(2-3):1157-1165.
Toffey W, Miller C, Saylor L. 1998. Two decades of mine reclamation: Lessons learned from one of the nation's largest biosolids beneficial use programs http://www.dep.state.pa.us/dep/subject/advcoun/minrec/Reclamtn.pdf. Accessed 20 February 2020.
Trumm D. 2010. Selection of active and passive treatment systems for amd - flow charts for new zealand conditions. New Zealand Journal of Geology and Geophysics. 53(2-3):195-210.
Trumm D. 2014. Antimony passive treatment trials- results and potential large-scale application, globe progress. Report produced for OceanaGold (New Zealand) Ltd by CRL Energy Ltd. CRL Ref: 13-41007-Sb.
Trumm D, Ball J, Pope J, Weisener C. 2015a. Antimony passive treatment by two methods: Sulfate reduction and adsorption onto amd precipitate. Paper presented at: 10th International Conference on Acid Rock Drainage & IMWA Annual Conference. Santiago, Chile.
Trumm D, Christenson H, Pope J, Watson K, Mason K, Squire R, McDonald G, Mazzetti A. 2017. Passive treatment of fe and mn using vertical flow reactors, limestone leaching beds, and slag leaching beds, waihi gold. Paper presented at: AusIMM New Zealand Branch Annual Conference: Christchurch, pp 334-343.
Trumm D, Pope J. 2015. Passive treatment of neutral mine drainage at a metal mine in new zealand using an oxidizing system and slag leaching bed. Mine Water and the Environment. 34(4):430-441.
Trumm D, Sapsford DJ, Rubio I, Pope J. 2015b. Application of vertical flow reactors in new zealand for removal of iron from amd. Paper presented at: AusIMM New Zealand Branch Annual Conference. Dunedin.
Uster B. 2015. The use of mussel shell in sulphate-reducing bioreactors treating mine-influenced waters. [Unpublished Thesis]: Department of Civil and Natural Resources Engineering, University of Canterbury, New Zealand.
Uster B, O'Sullivan AD, Ko SY, Evans A, Pope J, Trumm D, Caruso B. 2014. The use of mussel shells in upward-flow sulfate-reducing bioreactors treating acid mine drainage. Mine Water and the Environment. 34(4):442-454.

Van Den Brand TPH, Roest K, Brdjanovic D, Chen GH, Van Loosdrecht MCM. 2014. Temperature effect on acetate and propionate consumption by sulfate-reducing bacteria in saline wastewater. Applied Microbiology and Biotechnology. 98(9):4245-4255.

Vasquez Y, Escobar MC, Neculita CM, Arbeli Z, Roldan F. 2016a. Biochemical passive reactors for treatment of acid mine drainage: Effect of hydraulic retention time on changes in efficiency, composition of reactive mixture, and microbial activity. Chemosphere. 153:244-253.

Vasquez Y, Escobar MC, Neculita CM, Arbeli Z, Roldan F. 2016b. Selection of reactive mixture for biochemical passive treatment of acid mine drainage. Environmental Earth Sciences. 75(7).

Vasquez Y, Escobar MC, Saenz JS, Quiceno-Vallejo MF, Neculita CM, Arbeli Z, Roldan F. 2018. Effect of hydraulic retention time on microbial community in biochemical passive reactors during treatment of acid mine drainage. Bioresource Technology. 247:624-632.

Velusami B, Curran TP, Grogan HM. 2013. Hydrogen sulfide gas emissions during disturbance and removal of stored spent mushroom compost. J Agric Saf Health. 19(4):261-275.

Waterhouse BR, Boyer S, Adair KL, Wratten SD. 2014. Using municipal biosolids in ecological restoration: What is good for plants and soil may not be good for endemic earthworms. Ecological Engineering. 70:414-421.

Weber P, Wildy J, Crombie F, Olds W, Rossiter P, Pizey M, Thompson N, Comeskey P, Stone D, Simcock S et al. 2012. Waste or resource: Solid energy's beneficial use of waste streams. Paper presented at: WasteMINZ Annual Conference. Hamilton, New Zealand.

Younger P, Banwart S, Hedin R. 2002. Mine water: Hydrology, pollution, remediation. Dordrecht, The Netherlands: Kluwer Academic Publishers.

Zagury GJ, Kulnieks VI, Neculita CM. 2006. Characterization and reactivity assessment of organic substrates for sulphate-reducing bacteria in acid mine drainage treatment. Chemosphere. 64(6):944-954.

Zagury GJ, Neculita CM, Bussière B. 2005. Passive biological treatment of acid mine drainage:: Challenges of the 21st century. Paper presented at: Paper presented at the 2nd Symposium on the Mining and Environment, Rouyn-Noranda (Canada), 15-18 Mai 2005.

Appendix 1. Additional Graphs

This appendix includes graphs of additional parameters that provide additional insight into the results other various parameters. For all graphs below: Tank 1: Biosolids, less compost; Tank 2: Mussel shells, less compost; Tank 3: Biosolids, more compost; Tank 4: Mussel shells, more compost; Tank 5: small temperature control (biosolids more compost); and Tank 6: small insulated (biosolids, more compost).

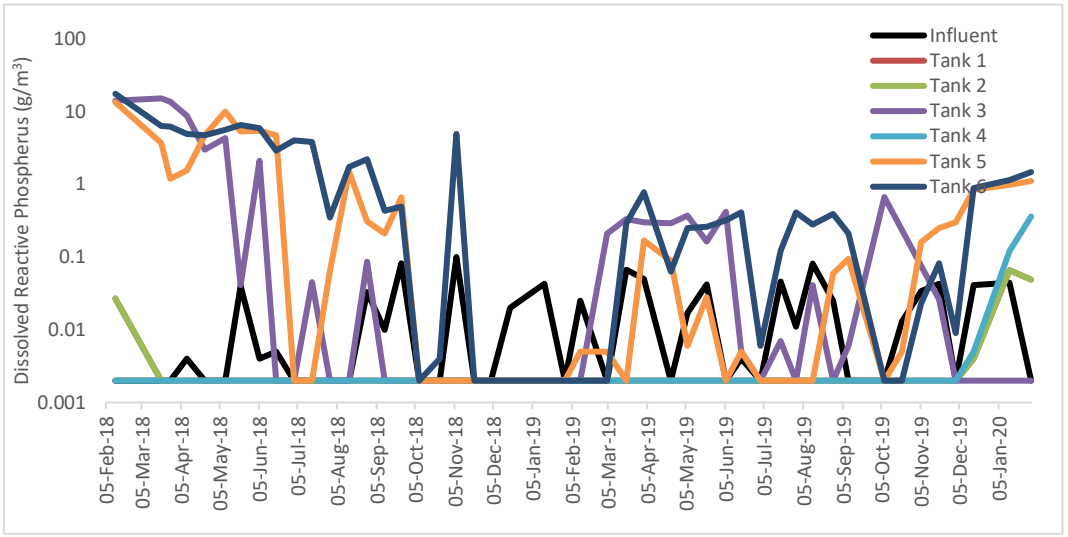

Figure 2: Graph showing dissolved reactive phosphorus concentrations from the influent and the effluent of all tanks during the operation of the systems. Note: log scale axis.

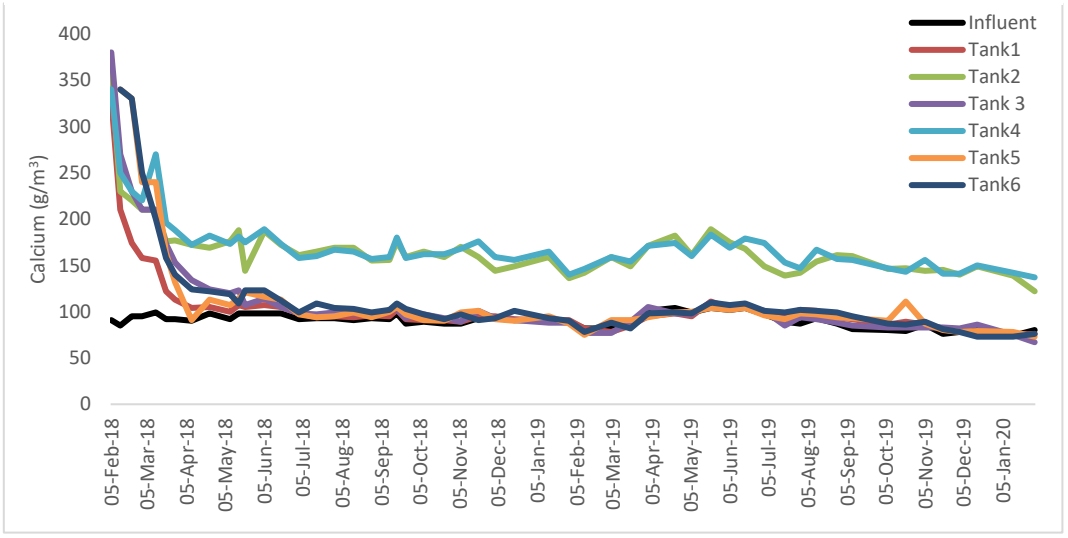

Figure 1: Graph showing dissolved calcium concentrations from the influent and the effluent of all tanks during the operation of the systems.

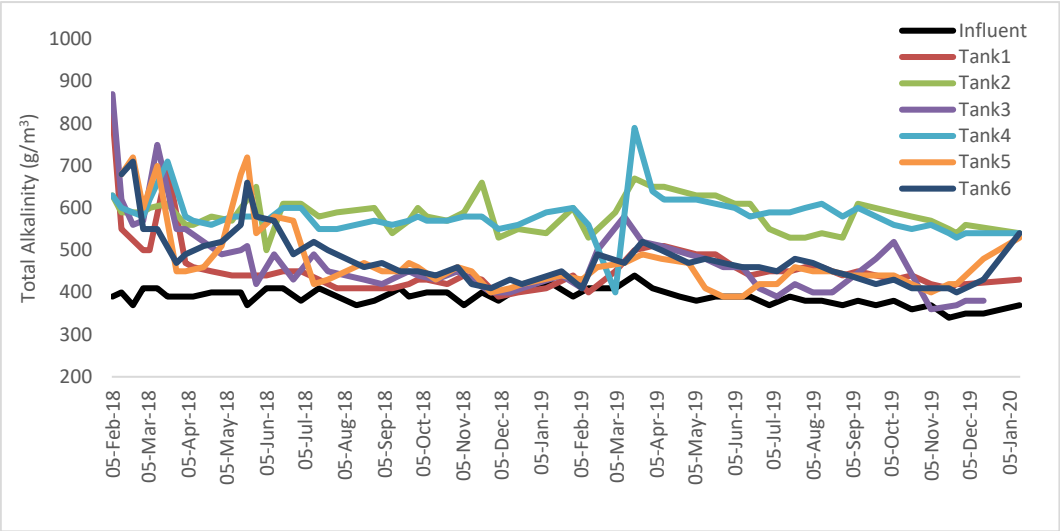

Figure 3: Graph showing total alkalinity concentrations from the influent and the effluent of all tanks during the operation of the systems.

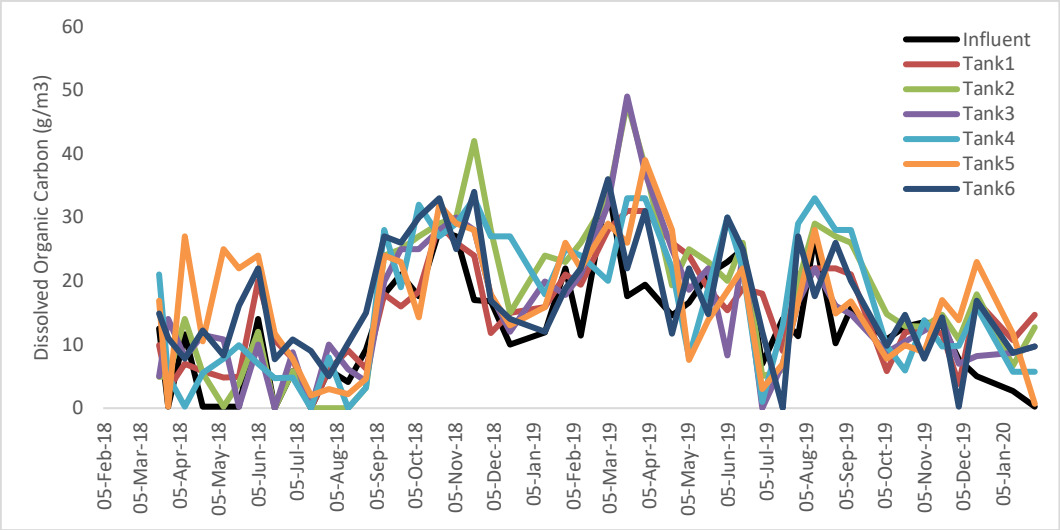

Figure 3: Graph showing dissolved organic carbon concentrations from the influent and the effluent of all tanks during the operation of the systems.

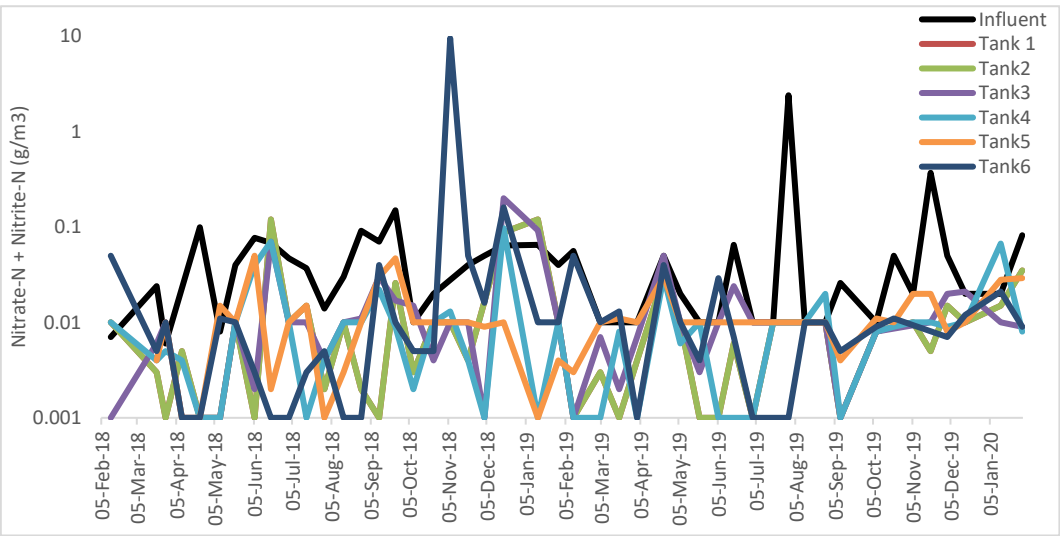

Figure 5: Graph showing nitrate + nitrite concentrations from the influent and the effluent of all tanks during the operation of the systems.

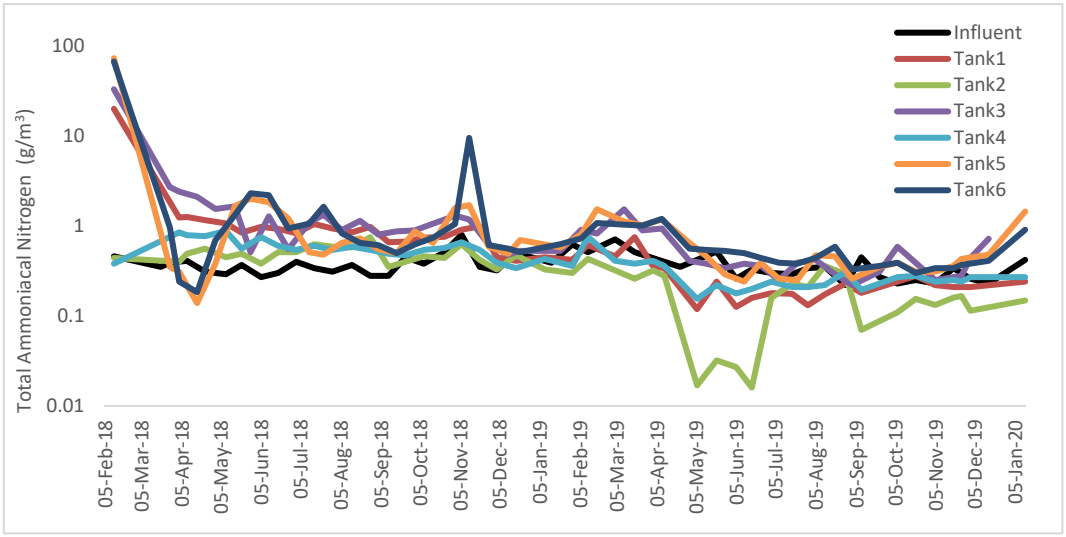

Figure 6: Graph showing total ammoniacal nitrogen concentrations from the influent and the effluent of all tanks during the operation of the systems.

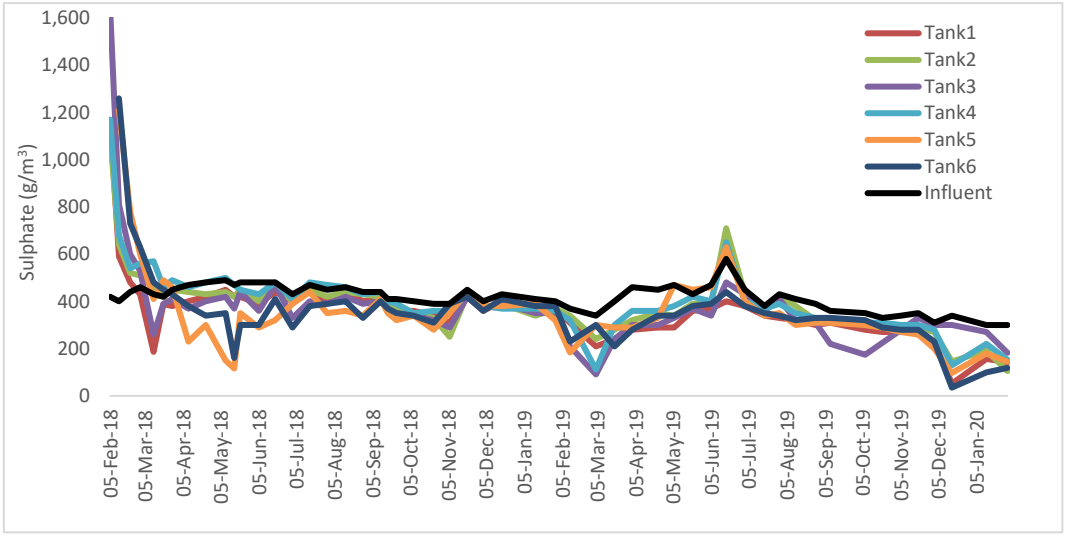

Figure 7: Graph showing sulphate concentrations from the influent and the effluent of all tanks during the operation of the systems.

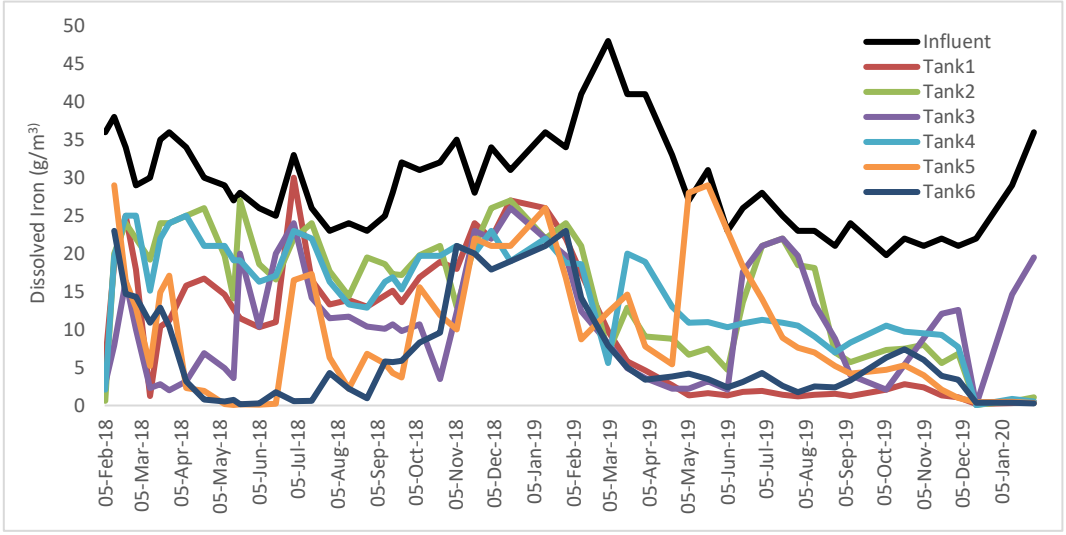

Figure 8: Graph showing dissolved iron concentrations from the influent and the effluent of all tanks during the operation of the systems.

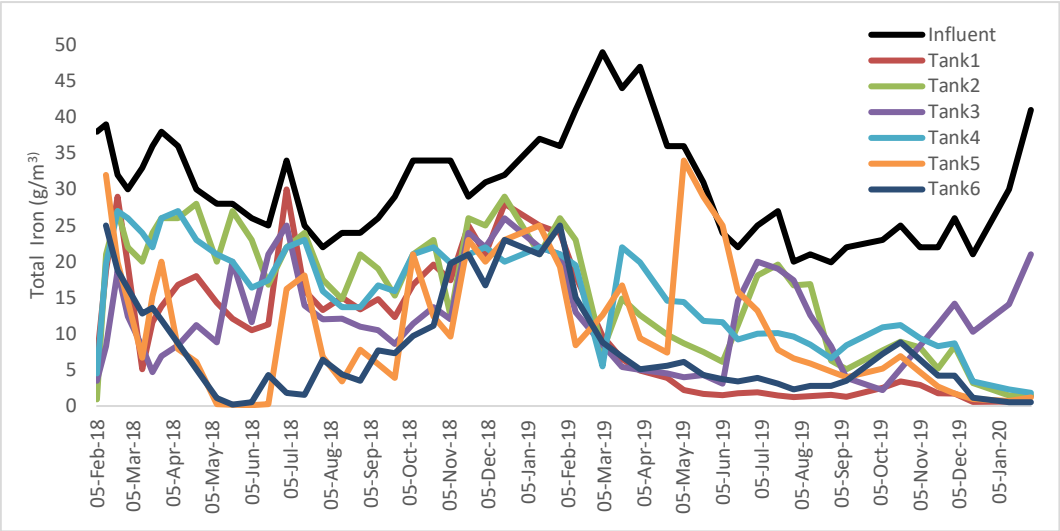

Figure 9: Graph showing total iron concentrations from the influent and the effluent of all tanks during the operation of the systems.

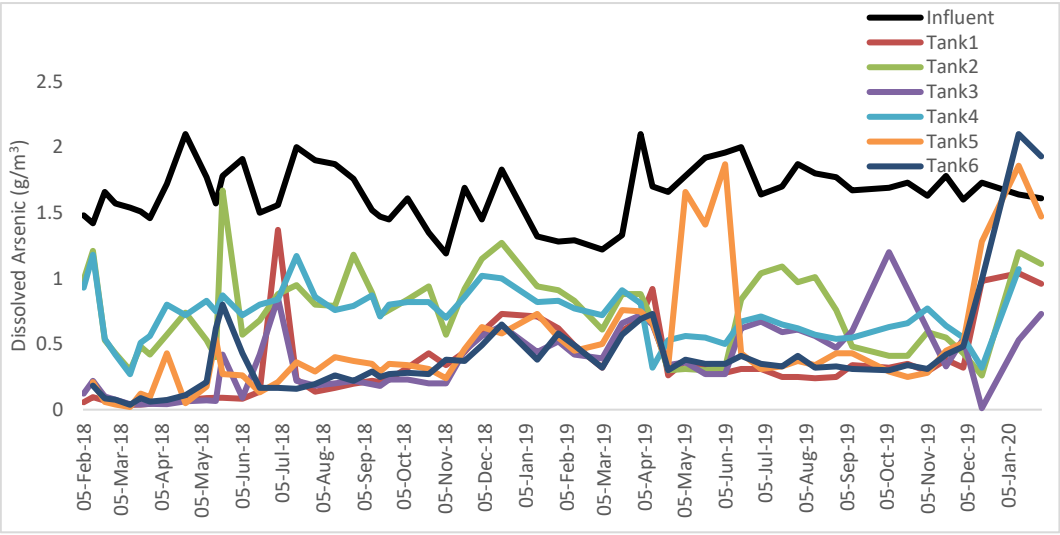

Figure 10: Graph showing dissolved arsenic concentrations from the influent and the effluent of all tanks during the operation of the systems.

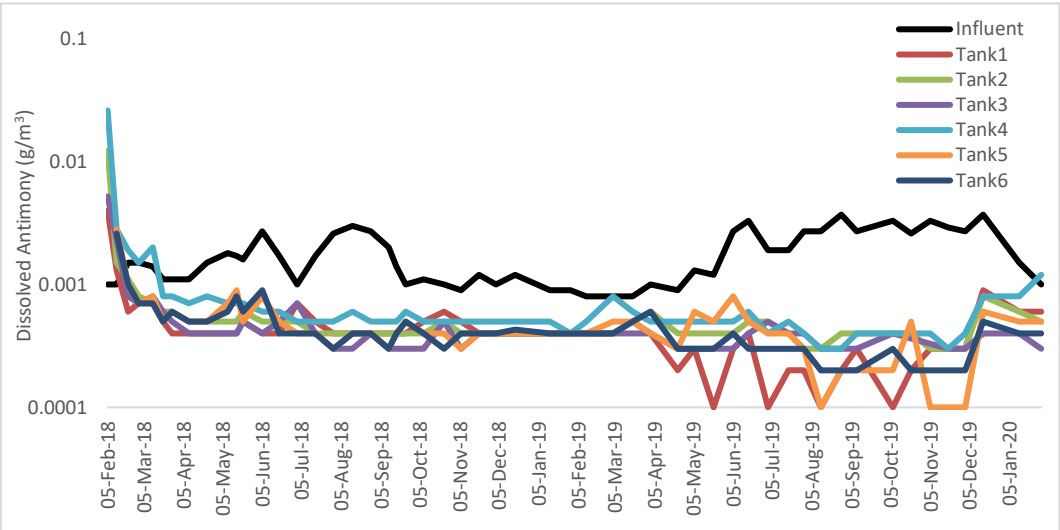

Figure 11: Graph showing dissolved Antimony concentrations from the influent and the effluent of all tanks during the operation of the systems. Note: A lot of values were below detection, therefore the detection values were halved for displaying data on this graph and is has a log scale axis.

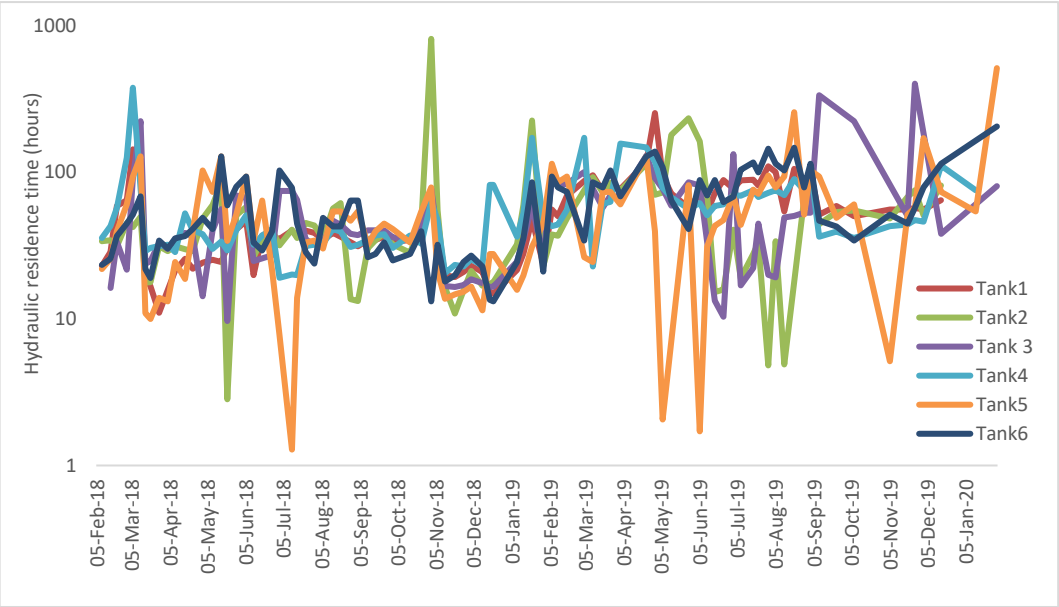

Figure 12: Graph showing hydraulic residence time of all treatments during the operation of the systems. Note: Displayed on a log scale axis

Appendix 2. Raw Data

Data Point	Date	Sulphate (g/m3)	Calcium-Dissolved (g/m3)	Antimony-Dissolved (g/m3)	Arsenic-Dissolved (g/m3)	Iron-Dissolved (g/m3)	Alkalinity - Bicarbonate (g/m3 as CaCO3)	Carbonate Alkalinity (g/m3 as CaCO3)	pH (pH unit)	Alkalinity - Total (g/m3 as CaCO3)	Dissolved Organic Carbon (DOC) (g/m3)	Ferrous Iron (g/m3)	FLS DO (%)	FLS EC (µS/cm)	FLS pH	FLS Temp (°C)	Iron-Total (g/m3)	Nitrate-N (g/m3)	Nitrate-N + Nitrite-N (g/m3)	Nitrite-N (g/m3)	Nitrogen-Total Ammoniacal (g/m3)	Sulphide (µg/L)
REE-BIOIN (Bioreactor Influent)	05-Feb-18	420	91	0.001	1.48	36				390			3.3	1,427	7.2	13.3	38					
	12-Feb-18																	<0.002	0.007	0.005	0.46	
	12-Feb-18	400	85	0.001	1.42	38				400			3.9	1,432	7.16	12.6	39					
	21-Feb-18	440	95	0.0015	1.66	34	370	<1	7	370			3.1	1,440	7.32	12.2	32					
	01-Mar-18	460	95	0.0015	1.57	29				410			2.3	1,438	7.71	12.4	30					
	06-Mar-18												1.7	1,448	7.28	12.2						
	12-Mar-18	430	99	0.0014	1.54	30				410			7.9	1,447	7.28	12.4	33					
	20-Mar-18	420	92	0.0011	1.51	35				390	12.5	23	-0.4	1,432	7.07	12.2	36	0.019	0.024	0.005	0.35	110
	27-Mar-18	450	92	0.0011	1.46	36	390	<1	6.7	390	<0.5	20.6	-0.1	1,424	7.31	12.3	38	<0.002	0.006	0.005	0.39	19
	03-Apr-18												0.8	1,406	7.67	12.8						
	09-Apr-18	470	90	0.0011	1.72	34	390	<1	7	390	11.6		0	1,430	7.67	12.1	36	<0.02	<0.02	<0.02	0.41	
	17-Apr-18												0.3	1,455	7.22	12.3						
	23-Apr-18	480	98	0.0015	2.1	30		<1	6.9	400	<0.5		0.6	1,455	7.12	12.1	30	0.089	0.099	0.01	0.31	
	01-May-18												0.3	1,488	7.05	12.4						
	09-May-18	490	92	0.0018	1.77	29	400	<1	6.9	400	<0.5	26.6	-0.2	1,486	7.03	12.5	28	0.004	0.008	0.004	0.29	7
	16-May-18	470	98	0.0017	1.57	27	400	<1	7	400			2.6	1,483	7.84	12.2						
	21-May-18	480	98	0.0016	1.78	28	370	<1	6.8	370	<0.5	27	0.5	1,460	7.11	12.2	28	0.04	0.04	<0.02	0.37	4
	28-May-18												-0.1	1,464	7.21	12.3						
	05-Jun-18	480	98	0.0027	1.91	26	410	<1	6.9	410	14	23.3	1.4	1,488	7.3	12	26	0.051	0.077	0.027	0.27	9
	11-Jun-18												0.6	1,489	7.13	12.2						
	18-Jun-18	480	98	0.0017	1.5	25	410	<1	6.9	410	<0.5	27.5	0.4	1,473	6.94	12.1	25	0.056	0.068	0.011	0.3	10
	26-Jun-18												0	1,462	7.16	12.1						
	02-Jul-18	430	92	0.001	1.56	33	380	<1	6.8	380	5.8	28.6	-0.1	1,425	7.15	11.9	34	0.019	0.047	0.028	0.4	
	12-Jul-18												0	1,432	7.16	12.2						
	16-Jul-18	470	93	0.0017	2	26	410	<1	6.7	410	<0.5	28.4	-1.2	1,456	7.13	12.1	25	0.028	0.037	0.009	0.34	2
	23-Jul-18												-1.4	1,465	7.15	12.2						
	30-Jul-18	450	93	0.0026	1.9	23					6						22	0.014	0.014	<0.002	0.31	
	06-Aug-18												-0.5	1,444	7.33	12.2						
	14-Aug-18	460	91	0.003	1.87	24	370	<1	7	370	4.1		0	1,432	7.32	12.2	24	0.03	0.03	<0.02	0.37	8
	20-Aug-18												-0.9	1,412	7.4	12.2						
	28-Aug-18	440	93	0.0027	1.76	23	380	<1	6.9	380	9.2	23.5	-0.8	1,392	7.3	12.2	24	0.029	0.091	0.062	0.28	13
	03-Sep-18												-0.6	1,401	7.31	12.2						
	11-Sep-18	440	92	0.002	1.52	25	400	<1	6.9	400	17.9		-0.3	1,396	7.28	12.2	26	0.032	0.07	0.038	0.28	
	17-Sep-18	410	98	0.0014	1.47	28	410	<1	6.9	410			-2.1	1,384	7.39	12.2						10
	24-Sep-18	410	87	0.001	1.45	32	390	<1	6.7	390	21		-0.2	1,369	7.53	12.4	29	0.089	0.15	0.061	0.45	
	01-Oct-18												0	1,356	7.4	12.2						
	08-Oct-18	400	89	0.0011	1.61	31	400	<1	6.7	400	17.6	33.6	-1.9	1,374	7.92	12.2	34	<0.02	<0.02	<0.02	0.38	14
	15-Oct-18												-0.9	1,395	7.5	13.4						
	24-Oct-18	390	87	0.001	1.35	32	400	<1	6.9	400	28		-1.1	1,388	7.36	12.3	34	<0.02	0.02	<0.02	0.51	
	01-Nov-18												-0.5	1,489	7.39	13.1						
	06-Nov-18	390	87	0.0009	1.19	35	370	<1	6.8	370	27	26.4	0	1,440	7.37	12.3	34	<0.1	<0.1	<0.1	0.8	13
	12-Nov-18												-0.6	1,364	7.43	11.8						
	20-Nov-18	450	93	0.0012	1.69	28	400	<1	6.8	400	17		0	1,441	7.45	12.1	29	0.04	0.04	<0.02	0.35	63
	27-Nov-18												-0.4	1,422	7.57	12.3						
	03-Dec-18	400	93	0.001	1.45	34	380	<1	6.6	380	16.8		-0.2	1,442	7.38	12.4	31	0.039	0.05	0.012	0.32	
	12-Dec-18												-0.8	1,407	7.46	12.7						
	18-Dec-18	430	91	0.0012	1.83	31	410	<1	6.8	410	10		-1.8	1,415	8.17	12.4	32	0.025	0.064	0.039	0.5	
	21-Dec-18												0	1,408	7.55	12.3						
	09-Jan-19												-0.5	1,400	7.35	12.4						
	14-Jan-19	410	91	0.0009	1.32	36	420	<1	6.8	420	11.9	29.4	0	1,504	7.53	12.3	37	0.037	0.065	0.028	0.39	14
	21-Jan-19												-1.3	1,485	8.2	12.3						
	30-Jan-19	400	89	0.0009	1.28	34	390	<1	6.6	390	22	24.6	-2.3	1,447	7.36	12.4	36	0.03	0.04	<0.02	0.62	17
	06-Feb-19												-0.6	1,425	7.38	12.4						
	11-Feb-19	370	82	0.0008	1.29	41	410	<1	6.8	410	11.4	16	-1.5	1,394	7.7	12.2	41	0.017	0.056	0.04	0.51	
	18-Feb-19												0	1,381	7.42	12.3						
	04-Mar-19	340	82	0.0008	1.22	48	410	<1	6.8	410	35		-0.9	1,385	7.46	12.2	49	<0.02	<0.02	<0.02	0.71	32
	11-Mar-19												0	1,370	7.5	13.2						
	19-Mar-19	400	88	0.0008	1.33	41	440	<1	6.8	440	17.6	38.8	0	1,452	7.52	12.3	44	<0.02	<0.02	<0.02	0.51	13
	25-Mar-19												-0.5	1,451	7.4	12.4						
	02-Apr-19	460	101	0.001	2.1	41	410	<1	6.8	410	19.4		-0.6	1,463	7.48	11.9	47	<0.02	<0.02	<0.02	<0.5	
	09-Apr-19												-1.4		7.51	12						
	11-Apr-19				1.7																	
	23-Apr-19	450	104	0.0009	1.66	33	390	<1	6.8	390	14.6	33.4	0	1,450	7.38	12.8	36	0.04	0.05	<0.02	0.35	15
	30-Apr-19													1,462	7.42	11.8						
	06-May-19	470	99	0.0013	1.78	27	380	<1	6.6	380	16.6	5.94	-1.8	1,476	7.41	12.1	36	<0.02	0.02	<0.02	0.42	-3
	13-May-19												0	1,501	7.56	12						
	21-May-19	430	104	0.0012	1.92	31	390	<1	6.9	390	21	5.2	-0.7	1,454	7.35	12.1	31	<0.02	<0.02	<0.02	0.52	-1
	27-May-19												-0.3	1,481	7.44	12.3						
	05-Jun-19	470	102	0.0027	1.96	23	390	<1	6.7	390	23	26.4	-1.8	1,482	7.3	12.2	24	<0.02	<0.02	<0.02	0.26	3
	11-Jun-19												0	1,515	7.62	12.4						
	17-Jun-19	580	104	0.0033	2	26	390	<1	6.8	390	25		-0.5	1,468	7.52	12.2	22	0.036	0.065	0.029	0.33	
	24-Jun-19												-0.2	1,423	7.86	12.4						17
	02-Jul-19	450	97	0.0019	1.64	28	370	<1	6.8	370	7		0	1,458	7.6	12.1	25	<0.02	<0.02	<0.02	0.3	
	08-Jul-19												0.5	1,407	7.66	12						
	18-Jul-19	380	89	0.0019	1.7	25	390	<1	6.7	390	14		-0.4	1,333	7.6	12.2	27	<0.02	<0.02	<0.02	0.29	
	22-Jul-19												0	1,360	7.57	12.2						
	30-Jul-19	430	87	0.0027	1.87	23	380	<1	7.2	380	11.3	25.3	0	1,401	7.69	12.3	20	2.4	2.4	<0.02	0.34	-3
	05-Aug-19												-1.3	1,341	7.52	12.3						
	12-Aug-19	410	93	0.0027	1.8	23	380	<1	6.7	380	27		0	1,334	7.77	12.1	21	<0.02	<0.02	<0.02	0.35	
	20-Aug-19													1,299	7.66	12.1						
	28-Aug-19	390	87	0.0037	1.77	21	370	<1	7	370	10.2	20.1	-0.1	1,296	7.51	12.3	19.9	<0.02	<0.02	<0.02	0.22	1
	02-Sep-19												-0.8	1,285	7.75	12.5						
	09-Sep-19	360	81	0.0027	1.67	24	380	<1	6.9	380	15.7	26.5	0	1,285	7.72		22	0.024	0.026	<0.002	0.45	8
	23-Sep-19	330	83	0.0023	1.85	23	370	<1	6.8	370	6.8		0	1,252	7.79	12.2	25	<0.02	<0.02	<0.02	0.27	
	07-Oct-19	350	80	0.0033	1.69	19.8	380	<1	6.9	380	10.8						23	<0.02	<0.02	<0.02	0.23	
	21-Oct-19	330	79	0.0026	1.73	22	360	<1	6.9	360	12.8						25	<0.1	<0.1	<0.1	0.25	
	05-Nov-19	340	86	0.0033	1.63	21	370	<1	6.7	370	13.5		2.4			12.5	22	0.02	0.02	<0.02	0.23	
	19-Nov-19	350	76	0.0029	1.78	22	340	<1	6.9	340	13		2.8	1,196	7.25	12.2	22	0.34	0.37	0.033	0.34	
	25-Nov-19												2.8	1,207	7.38	12.2						
	02-Dec-19	310	78	0.0027	1.6	21	350	<1	7	350	7.7		4.8	1,202	7.55	12.4	26	0.026	0.05	0.024	0.26	
	16-Dec-19	340	81	0.0037	1.73	22	350	<1	6.9	350	5		1.8	1,211	7.61	12.3	21	<0.02	0.02	<0.02	0.23	
	13-Jan-20	300	74	0.0015	1.64	29	370	<1	7	370	2.7		2.2	1,194	7.61	12.2	30	<0.02	0.02	<0.02	0.42	

Data Point	Date	Sulphate (g/m3)	Calcium-Dissolved (g/m3)	Antimony-Dissolved (g/m3)	Arsenic-Dissolved (g/m3)	Iron-Dissolved (g/m3)	Alkalinity - Bicarbonate (g/m3 as CaCO3)	Carbonate Alkalinity (g/m3 as CaCO3)	pH (pH unit)	Alkalinity - Total (g/m3 as CaCO3)	Dissolved Organic Carbon (DOC) (g/m3)	Ferrous Iron (g/m3)	FLS DO (%)	FLS EC (µS/cm)	FLS Flow rate (L/S)	FLS pH	FLS Temp (°C)	Iron-Total (g/m3)	Nitrate-N (g/m3)	Nitrate-N + Nitrite-N (g/m3)	Nitrite-N (g/m3)	Nitrogen-Total Ammoniacal (g/m3)	Sulphide (µg/L)
REE-TANK1 (Bioreactor 1)	05-Feb-18	1,160	330	0.004	0.056	5.8				820			21.7	3,248		7.31	16.9	6.6					
	09-Feb-18														0.087								
	12-Feb-18	590	210	0.0013	0.096	18.7				550			21.7	1,962		7.1	14.8	18.8	<0.002	<0.002	<0.002	20	
	16-Feb-18														0.07								
	21-Feb-18	480	174	0.0006	0.069	25	500	<1	7	500			28.2	1,738	0.034	7.32	13	29					
	01-Mar-18	430	158	0.0007	0.057	17.9				500			16.8	1,592	0.031	7.22	13.8	19.5					
	06-Mar-18												14	1,598	0.014	7.53	16.5						
	12-Mar-18	187	155	0.0007	0.036	1.25				700			13.5	1,536	0.017	7.42	14.1	5.1					
	16-Mar-18														0.103								
	20-Mar-18	390	122	0.0005	0.038	10.4				470	9.9	11	0.4	1,466	0.12	7.16	12.5	11.6	<0.002	0.003	<0.002	1.24	3,250
	27-Mar-18	380	113	0.0004	0.045	11.2	460	<1	6.8	460	3	10.8	-0.6	1,429	0.182	7.41	12.5	13.8	<0.002	0.01	0.01	1.26	1,740
	03-Apr-18												0.9	1,414		7.37	12.8						
	09-Apr-18	400	104	0.0004	0.072	15.8	450	<1	7	450	7		1	1,409	0.094	7.33	11.5	16.8	<0.02	<0.02	<0.02	1.16	
	17-Apr-18												-0.1	1,411	0.078	7.19	12.4						
	23-Apr-18	420	105	0.0004	0.073	16.7	440	<1	6.9	440	5.8	18.4	0	1,434	0.091	7.13	11.1	18	<0.02	<0.02	<0.02	1.07	6.8
	01-May-18												0	1,482	0.083	7.24	12						
	09-May-18	450	100	0.0004	0.087	14.6	440	<1	6.9	440	4.8	14.5	0	1,478	0.079	7.35	12	14.3	<0.002	<0.002	<0.002	0.84	515
	16-May-18	420	107	0.0004	0.091	12.7	440	<1	7	440			0.5	1,472	0.082	7.5	11.5						
	21-May-18	420	105	0.0005	0.091	11.5	440	<1	6.8	440	4.9	13.5	-0.1	1,452	0.065	7.22	10.6	12.1	<0.02	<0.02	<0.02	0.98	507
	28-May-18												1	1,425	0.049	7.32	9.2						
	05-Jun-18	390	107	0.0004	0.083	10.3	450	<1	7	450	20	10.6	0.8	1,487	0.043	7.35	8.7	10.5	<0.02	<0.02	<0.02	0.93	460
	11-Jun-18												0.1	1,466	0.101	7.23	10.7						
	18-Jun-18	440	105	0.0004	0.137	11	450	<1	7	450	10.7	14.5	0.5	1,455	0.054	7.03	9.6	11.3	0.08	0.08	<0.02	0.83	152
	26-Jun-18												0	1,418	0.055	7.2	8.9						
	02-Jul-18	400	98	0.0007	1.37	30	430	<1	6.9	430	7.8	24.1	0	1,454	0.057	7.18	9.6	30	<0.02	<0.02	<0.02	1.05	
	12-Jul-18												-0.7	1,395	0.05	7.28	9.5						
	16-Jul-18	440	94	0.0005	0.23	16.5	410	<1	6.8	410	<0.5	19.7	-0.9	1,414	0.055	7.25	9.8	16	<0.002	<0.002	<0.002	0.94	251
	23-Jul-18												-0.2	1,425	0.05	7.16	9.3						
	30-Jul-18	400	95	0.0004	0.137	13.3					6				0.052			13.3	0.002	0.003	<0.002	0.85	
	06-Aug-18												0	1,434	0.058	7.42	9.5						
	14-Aug-18	440	94	0.0004	0.167	13.9	410	<1	7.1	410	9.1		0	1,424	0.052	7.65	10.1	15	<0.02	<0.02	<0.02	0.98	139
	20-Aug-18												-0.3	1,400	0.055	7.35	9.6						
	28-Aug-18	400	96	0.0004	0.197	13	410	<1	7.1	410	6.2	14.6	-1.2	1,370	0.06	7.38	10.4	13.4	<0.02	<0.02	<0.02	0.66	83
	03-Sep-18												-0.7	1,379	0.064	7.41	10.6						
	11-Sep-18	410	95	0.0004	0.22	14.5	420	<1	7	420	17.9		-1.3	1,381	0.058	7.36	11.2	14.8	0.003	0.014	0.011	0.67	
	17-Sep-18	380	102	0.0004	0.21	15.1	430	<1	6.9	430			-0.4	1,381	0.058	7.36	11.3						191
	24-Sep-18	360	92	0.0004	0.23	13.6	430	<1	6.8	430	16		-0.9	1,331	0.055	7.35	11.2	12.3	0.004	0.036	0.032	0.74	
	01-Oct-18												-0.8	1,340	0.06	7.45	11.3						
	08-Oct-18	360	91	0.0005	0.32	16.9	420	<1	6.7	420	18.3	17.9	-2.1	1,334		7.32	11.5	16.8	0.03	0.03	<0.02	0.76	85
	15-Oct-18												-0.9	1,342	0.058	7.57	11						
	24-Oct-18	340	91	0.0006	0.43	18.9	440	<1	6.9	440	29		0	1,338	0.053	7.37	13.1	19.6	<0.002	0.003	<0.002	0.91	
	01-Nov-18												-2.2	1,326	0.031	7.31	11.6						
	06-Nov-18	310	89	0.0005	0.34	18	430	<1	7	430	26	20.5	0	1,583	0.047	7.44	11.7	17.4	<0.1	<0.1	<0.1	0.99	28
	12-Nov-18												0	1,371	0.101	7.47	11.3						
	20-Nov-18	420	95	0.0004	0.44	24	390	<1	6.9	390	24		-0.2	1,407	0.104	7.5	10.6	25	<0.02	<0.02	<0.02	0.45	42
	27-Nov-18												0	1,405	0.096	7.46	12.6						
	03-Dec-18	360	95	0.0004	0.59	22	400	<1	6.7	400	11.8		-0.9	1,382	0.087	7.28	13.1	21	<0.002	<0.002	<0.002	0.41	
	12-Dec-18												-0.6	1,370	0.096	7.46	13.2						
	18-Dec-18	400	92	0.0004	0.73	27	410	<1	6.8	410	15		0	1,384	0.131	7.38	12.8	28	0.13	0.13	<0.1	0.45	
	21-Dec-18												0	1,392	0.135	7.5	12.5						
	09-Jan-19												0	1,389	0.093	7.36	13						
	14-Jan-19	370	90	0.0004	0.71	26	440	<1	6.8	440	15.9	27.1	-2.8	1,382	0.072	7.76	12.9	25	0.012	0.071	0.058	0.42	24
	21-Jan-19												-0.2	1,338	0.042	7.72	13.8						
	30-Jan-19	370	91	0.0004	0.62	22	400	<1	6.6	400	21	22.3	0	1,348	0.085	7.33	13.9	24	<0.02	<0.02	<0.02	0.61	56
	06-Feb-19												0	1,344	0.036	7.38	14.6						
	11-Feb-19	310	82	0.0004	0.49	17.4	450	<1	6.8	450	19.4	30	0	1,321	0.04	7.38	14.4	18	0.004	0.005	<0.002	0.46	
	18-Feb-19												0	1,263	0.029	7.42	14.7						
	04-Mar-19	210	78	0.0004	0.32	9.8	500	<1	7	500	28		0	1,236	0.023	7.4	13.4	9.7	<0.002	<0.002	<0.002	0.75	63
	11-Mar-19												0	1,233	0.021	7.58	15.3						
	19-Mar-19	240	85	0.0005	0.6	5.8	510	<1	6.8	510	31	6.5	-0.2	1,283	0.027	7.49	15.7	6.5	<0.002	0.003	<0.002	0.36	135
	25-Mar-19												-1.1	1,319	0.025	7.84	15.4						
	02-Apr-19	280	95	0.0004	0.69	4.6	510	<1	7.1	510	31		-0.2	1,330	0.026	7.53	12.5	4.9	<0.002	<0.002	<0.002	0.34	
	09-Apr-19												-0.89			7.74	10.3						
	11-Apr-19				0.92																		
	23-Apr-19	290	98	0.0002	0.26	2.7	490	<1	7	490	26	3.8	-2.3	1,335	0.0171	7.3	12.1	3.9	<0.002	<0.002	<0.002	0.119	760
	30-Apr-19													1,287	0.0079	7.45	9.4						
	06-May-19	290	95	0.0003	0.37	1.34	490	<1	6.8	490	24	0.1	-0.2	1,343	0.0211	7.6	10.6	2.2	<0.002	<0.002	<0.002	0.24	756
	13-May-19												0	1,396	0.028	7.43	10.9						
	21-May-19	360	111	<0.0002	0.32	1.64	460	<1	7.1	460	18.8	1.68	-2	1,399		7.4	9.6	1.68	<0.002	<0.002	<0.002	0.126	
	27-May-19												0	1,394	0.0348	7.55	10.4						
	05-Jun-19	370	104	0.0003	0.28	1.33	440	<1	6.9	440	15.4	1.44	-0.3	1,390	0.0284	7.6	7.3	1.52	<0.002	<0.002	<0.002	0.158	1,768
	11-Jun-19												0	1,415	0.0377	7.71	9.3						
	17-Jun-19	400	108	0.0004	0.31	1.81	450	<1	6.9	450	18.8		0.5	1,411	0.0278	7.63	9.3	1.78	0.037	0.039	0.002	0.18	
	24-Jun-19												-0.7	1,390	0.0226	8.24	7						492
	02-Jul-19	380	99	<0.0002	0.31	1.92	450	2	7.7	450	18		0	1,391	0.0259	7.9	7.4	1.9	<0.002	<0.002	<0.002	0.177	
	08-Jul-19												0	1,389	0.0227	7.71	7.8						
	18-Jul-19	340	96	0.0002	0.25	1.43	460	<1	6.9	460	9		-0.1	1,347	0.0225	7.78	8.1	1.45	<0.002	<0.002	<0.002	0.131	
	22-Jul-19												0.7	1,312	0.0246	7.73	7.9						
	30-Jul-19	330	102	0.0002	0.25	1.22	460	<1	7.3	460	21	2.48	-0.3	1,326	0.0182	7.4	9.2	1.24	<0.002	<0.002	<0.002	0.173	1,252
	05-Aug-19												0	1,339	0.02	7.79	6.4						
	12-Aug-19	320	101	<0.0002	0.24	1.41	430	<1	6.9	440	22		0	1,288	0.037	8.16	8.9	1.38	<0.002	<0.002	<0.002	0.23	
	20-Aug-19													1,257	0.019	7.76	8.3						
	28-Aug-19	300	94	0.0002	0.25	1.55	450	<1	7	450	22	1.44	-0.6	1,251	0.024	7.67	9.3	1.55	<0.002	<0.002	<0.002	0.181	1,632
	02-Sep-19												-0.8	1,245	0.02	8.09	10.1						
	09-Sep-19	310	92	0.0003	0.34	1.23	430	<1	7	430	21	1.66	0	1,242	0.039	8.01		1.27	<0.002	0.002	<0.002	0.24	1,178
	23-Sep-19	260	88	0.0004	0.41	1.61	440	<1	6.9	440	12.8		0	1,216	0.034	7.71	10.8	2.1	<0.002	0.003	<0.002	0.28	
	07-Oct-19	280	86	<0.0002	0.32	2.1	420	<1	7	420	5.8				0.04			2.5	0.008	0.009	<0.002	0.22	
	21-Oct-19	270	89	0.0002	0.35	2.8	410	<1	7.1	410	11.9				0.029			3.4	0.011	0.012	<0.002	0.21	
	05-Nov-19	270	86	0.0003	0.29	2.4	420	<1	7	420	12.6		1.8		0.036		13	2.9	<0.002	0.007	0.007	0.21	
	19-Nov-19	270	82	0.0003	0.38	1.32	420	<1	7	420	11.7		4.6	1,144	0.036	7.34	10.7	1.77	0.003	0.004	<0.002	0.21	
	25-Nov-19												2.6	1,162	0.035	7.39	12.9						
	02-Dec-19	230	80	0.0003	0.32	1.08	430	<1	7	430	3.8		3	1,141	0.036	7.54	13.8	1.74	0.003	0.024	0.02	0.24	
	16-Dec-19	52	74	0.0009	0.98	0.2	540	<1	7.1	540	16.9		2.8	1,042	0.031	7.62	13.5	0.57	0.005	0.01	0.004	0.3	
	13-Jan-20	156	75	0.0006	1.04	0.33	460	<1	7.3	460	10.7		2.8	1,111	0.023	7.42	13.2	0.61	0.012	0.015	0.003	0.45	

Data Point	Date	Sulphate (g/m3)	Calcium-Dissolved (g/m3)	Antimony-Dissolved (g/m3)	Arsenic-Dissolved (g/m3)	Iron-Dissolved (g/m3)	Alkalinity - Bicarbonate (g/m3 as CaCO3)	Carbonate Alkalinity (g/m3 as CaCO3)	pH (pH unit)	Alkalinity - Total (g/m3 as CaCO3)	Dissolved Organic Carbon (DOC) (g/m3)	Ferrous Iron (g/m3)	FLS DO (%)	FLS EC (µS/cm)	FLS Flow rate (L/S)	FLS pH	FLS Temp (°C)	Iron-Total (g/m3)	Nitrate-N (g/m3)	Nitrate-N + Nitrite-N (g/m3)	Nitrite-N (g/m3)	Nitrogen-Total Ammoniacal (g/m3)	Sulphide (µg/L)
REE-TANK2 (Biorecator 2)	05-Feb-18	1,100	360	0.0122	0.99	0.61				630			39.4	2,977		7.49	19	0.92					
	09-Feb-18														0.06								
	12-Feb-18	640	230	0.0015	1.21	20				590			13	2,049		7.19	14.6	21	<0.02	<0.02	<0.02	0.44	
	16-Feb-18														0.059								
	21-Feb-18	520	220	0.0011	0.53	24	580	<1	7.2	590			18.1	1,868	0.065	7.29	12.7	27					
	01-Mar-18	510	210	0.0008	0.43	22				600			15.8	1,788	0.045	7.3	13.9	22					
	06-Mar-18												8	1,800	0.048	7.22	15						
	12-Mar-18	460	210	0.0007	0.3	19.2				610			11.6	1,765	0.041	7.35	13	20					
	16-Mar-18														0.115								
	20-Mar-18	420	176	0.0006	0.48	24				560	4.9	19.5	0.3	1,665	0.114	7.23	12.5	24	0.002	0.003	<0.002	0.4	470
	27-Mar-18	450	177	0.0006	0.42	24	560	<1	6.9	560	5	21.7	-0.4	1,656	0.065	7.32	12.6	26	<0.002	<0.002	<0.002	0.49	102
	03-Apr-18												0.9	1,635	0.07	7.3	12.5						
	09-Apr-18	440	172	0.0005	0.57	25	570	<1	7.2	580	14		0.4	1,644	0.065	7.29	11.5	26	0.005	0.005	<0.002	0.56	
	17-Apr-18												0.2	1,674	0.068	7.27	12.3						
	23-Apr-18	430	169	0.0005	0.74	26	560	1.6	7.5	570	5.5	26	0	1,687	0.07	7.12	11.2	28	<0.002	<0.002	<0.002	0.45	28
	01-May-18												0	1,730	0.042	7.22	11.7						
	09-May-18	440	176	0.0005	0.53	19.7	610	<1	7.2	620	<0.5	18.2	0	1,753	0.034	7.23	11.4	20	<0.002	<0.002	<0.002	0.49	18
	16-May-18	420	188	0.0005	0.4	14.1	650	1.3	7.3	650			0	1,752	0.024	7.45	10.9						
	21-May-18	450	144	0.0006	1.67	27	500	<1	7.1	500	3.9	26.3	-0.2	1,611	0.719	7.27	11.8	27	<0.02	<0.02	<0.02	0.38	37
	28-May-18												-0.9	1,709	0.04	7.32	9.2						
	05-Jun-18	400	187	0.0005	0.57	18.6	610	<1	7.2	610	12	17.4	0	1,748	0.035	7.39	8.9	23	<0.002	<0.002	<0.002	0.51	8
	11-Jun-18												0.4	1,715	0.077	7.25	10.7						
	18-Jun-18	470	172	0.0005	0.68	16.6	610	1	7.2	610	<0.5	19.6	0.8	1,726	0.058	7.13	10	16.8	0.12	0.12	<0.02	0.51	17
	26-Jun-18												-0.1	1,696	0.05	7.22	8.9						
	02-Jul-18	400	161	0.0005	0.88	22	580	<1	7.1	580	5.8	22.2	0	1,662	0.064	7.22	9.6	22	<0.02	<0.02	<0.02	0.63	
	12-Jul-18												0	1,658	0.05	7.22	9.5						
	16-Jul-18	450	165	0.0004	0.95	24	590	<1	6.9	590	<0.5	26.5	-0.2	1,686	0.057	7.25	9.9	24	0.015	0.015	<0.002	0.59	-2
	23-Jul-18												0	1,689	0.045	7.16	9.2						
	30-Jul-18	420	169	0.0004	0.8	17.7					<0.5				0.047			17.5	0.002	0.002	<0.002	0.58	
	06-Aug-18												0	1,691	0.058	7.44	9.6						
	14-Aug-18	440	169	0.0004	0.79	14.4	600	1.5	7.4	600	<0.5		0	1,686	0.036	7.5	10.1	14.8	<0.02	<0.02	<0.02	0.75	14
	20-Aug-18												0	1,682	0.033	7.36	9.6						
	28-Aug-18	430	155	0.0004	1.18	19.5	540	1.1	7.3	540	3.2	21	-1.1	1,607	0.149	7.31	11.2	21	0.002	0.002	<0.002	0.35	57
	03-Sep-18												0	1,615	0.154	7.39	11.3						
	11-Sep-18	420	156	0.0004	0.89	18.6	570	<1	7.2	570	24		0	1,632	0.067	7.38	11.3	19	<0.002	<0.002	<0.002	0.4	
	17-Sep-18	390	176	0.0004	0.72	17.3	600	<1	7.2	600			-1.4	1,613	0.059	7.44	11.2						50
	24-Sep-18	370	159	0.0004	0.76	17.2	580	<1	7	580	25		-0.9	1,581	0.053	7.48	11.2	15.3	0.024	0.026	<0.002	0.46	
	01-Oct-18												0	1,577	0.063	7.45	11.3						
	08-Oct-18	350	165	0.0004	0.84	19.8	570	<1	6.9	570	27	21.9	-1.3	1,573		7.43	11.5	21	0.002	0.003	<0.002	0.44	29
	15-Oct-18												-0.3	1,582	0.072	7.52	11.4						
	24-Oct-18	330	159	0.0005	0.94	21	590	<1	7.2	590	29		0	1,593	0.046	7.43	13.1	23	<0.02	<0.02	<0.02	0.63	
	01-Nov-18												-1.5	1,593	0.0025	7.35	12.1						
	06-Nov-18	250	170	0.0004	0.57	13	660	1.4	7.4	660	30	16	0	1,583	0.037	7.52	11.7	12.5	<0.02	<0.02	<0.02	0.42	21
	12-Nov-18												0	1,572	0.124	7.48	11.5						
	20-Nov-18	430	159	0.0004	0.92	21	530	<1	7.1	530	42		0	1,611	0.187	7.48	10.8	26	<0.002	0.004	0.005	0.33	47
	27-Nov-18												0	1,607	0.13	7.44	12.3						
	03-Dec-18	370	144	0.0004	1.15	26	550	<1	6.9	550	28		-0.4	1,593	0.096	7.34	13.1	25	<0.1	<0.1	<0.1	0.47	
	12-Dec-18												0	1,568	0.121	7.68	13.2						
	18-Dec-18	390	149	0.0004	1.27	27	540	<1	7	540	15		0	1,587	0.117	7.37	13.2	29	0.087	0.088	<0.002	0.33	
	21-Dec-18												0	1,586	0.114	7.5	12.5						
	09-Jan-19												0	1,586	0.063	7.35	13.5						
	14-Jan-19	340	159	0.0004	0.94	22	600	<1	7.1	600	24	22.1	0	1,577	0.034	7.38	13.6	21	0.12	0.12	<0.002	0.3	10
	21-Jan-19												-2.1	1,599	0.009	7.49	16.1						
	30-Jan-19	370	136	0.0004	0.91	24	530	<1	6.8	530	23	26.2	0	1,597	0.089	7.35	14.2	26	<0.02	<0.02	<0.02	0.43	44
	06-Feb-19												-1.8	1,599	0.054	7.38	14.5						
	11-Feb-19	340	142	0.0004	0.83	21	580	<1	7.1	590	26	65	0	1,591	0.055	7.4	14.2	23	<0.002	<0.002	<0.002	0.32	
	18-Feb-19												0	1,565	0.042	7.46	14.6						
	04-Mar-19	240	159	0.0004	0.61	7	670	1.2	7.3	670	33		0	1,544	0.027	7.52	13.6	7.6	<0.002	0.003	0.004	0.26	484
	11-Mar-19												0	1,512	0.022	7.63	15						
	19-Mar-19	280	149	0.0005	0.88	12.9	650	<1	7.1	650	48	14.9	0	1,543	0.028	7.52	16.2	14.9	<0.002	<0.002	<0.002	0.32	686
	25-Mar-19												-2.4	1,574	0.024	7.52	14.8						
	02-Apr-19	320	171	0.0006	0.88	9.1	650	1.2	7.3	650	38		-1	1,584	0.027	7.59	13	12.6	<0.002	0.004	0.004	0.28	
	09-Apr-19												-1.5			7.84	10.4						
	11-Apr-19				0.68																		
	23-Apr-19	350	182	0.0004	0.3	8.8	630	<1	7.2	630	19.3	7.6	-0.5	1,224	0.0179	7.42	11.7	9.9	0.03	0.03	<0.02	0.017	91
	30-Apr-19													1,640	0.029	7.49	9.7						
	06-May-19	340	161	0.0004	0.31	6.7	630	<1	7.1	630	25	6.76	-0.6	1,614	0.028	7.44	10.7	8.7	<0.02	<0.02	<0.02	0.032	430
	13-May-19												-0.2	1,679	0.0113	7.56	11.2						
	21-May-19	390	189	0.0004	0.3	7.5	610	1.3	7.3	610	23	6.96	-0.4	1,632		7.5	9.8	7.5	<0.002	<0.002	<0.002	0.027	18
	27-May-19												0	1,652	0.0087	7.58	10.2						
	05-Jun-19	390	175	0.0004	0.32	4.7	610	<1	7.2	610	20	6.6	-0.2	1,642	0.0125	7.57	7.6	6.1	<0.002	<0.002	<0.002	0.016	38
	11-Jun-19												0	1,706	0.0298	7.7	9.1						
	17-Jun-19	710	168	0.0005	0.84	13.6	550	<1	7	550	26		-0.1	1,645	0.1333	7.68	10.7	11.2	0.002	0.006	0.004	0.158	
	24-Jun-19												0	1,586	0.1285	7.93	10						56
	02-Jul-19	430	149	0.0005	1.04	21	530	2	7.6	530	5		0	1,619	0.05	7.76	10.3	18.1	<0.002	<0.002	<0.002	0.23	
	08-Jul-19												-0.1	1,560	0.1071	7.76	10.3						
	18-Jul-19	370	139	0.0004	1.09	22	530	<1	6.9	530	6		0	1,511	0.0735	7.73	10.4	19.6	<0.02	<0.02	<0.02	0.21	
	22-Jul-19												0	1,515	0.0614	7.66	10.6						
	30-Jul-19	420	142	0.0003	0.97	18.5	540	1.4	7.4	540	19.7	16.5	0	1,566	0.4219	7.65	11.2	16.7	<0.02	<0.02	<0.02	0.36	30
	05-Aug-19												0	1,539	0.06	7.9	9.9						
	12-Aug-19	380	154	0.0003	1.01	18.1	530	<1	7	530	29		0	1,502	0.415	7.95	10.5	16.9	<0.02	<0.02	<0.02	0.29	
	20-Aug-19													1,497		7.76	7.6						
	28-Aug-19	320	161	0.0004	0.76	7	610	1.3	7.4	610	27	7.2	0.4	1,506	0.031	7.76	9.9	6.3	<0.02	<0.02	<0.02	0.07	20
	02-Sep-19												0	1,607	0.023	7.95	10.5						
	09-Sep-19	320	160	0.0004	0.48	5.7	590	<1	7.2	590	26	5.48	0	1,605	0.046	7.78		5.1	<0.002	<0.002	<0.002	0.11	100
	23-Sep-19	290	153	0.0004	0.52	6.4	580	<1	7.2	580	19.8		0.4	1,466	0.038	7.9	11.1	7.7	<0.002	<0.002	<0.002	0.155	
	07-Oct-19	300	146	0.0004	0.41	7.3	570	<1	7.2	570	14.8				0.037			7.7	0.008	0.008	<0.002	0.132	
	21-Oct-19	290	147	0.0004	0.41	7.5	550	1.1	7.3	550	12.9				0.041			8.9	0.009	0.009	<0.002	0.16	
	05-Nov-19	290	144	0.0003	0.59	8	540	<1	7.1	540	12.8		1		0.042		13	8.1	<0.02	<0.02	<0.02	0.167	
	19-Nov-19	290	145	0.0003	0.55	5.6	560	1.2	7.3	560	14.7		6	1,376	0.03	7.32	10.7	5.2	<0.002	0.005	0.005	0.114	
	25-Nov-19												5.7	1,374	0.027	7.36	13.2						
	02-Dec-19	270	140	0.0003	0.43	6.8	540	1.6	7.5	540	10.8		2.3	1,399	0.04	7.56	13.9	8.3	0.015	0.015	<0.002	0.149	
	16-Dec-19	146	149	0.0008	0.26	0.09	660	1.4	7.3	670	17.9		2.1	1,340	0.025	7.59	12.9	3.2	0.008	0.01	<0.002	0.22	
	13-Jan-20	192	139	0.0006	1.2	0.53	600	1.3	7.4	600	6.7		2.9	1,345	0.016	7.66	13.6	1.46	0.008	0.015	0.006	0.5	

Data Point	Date	Sulphate (g/m3)	Calcium-Dissolved (g/m3)	Antimony-Dissolved (g/m3)	Arsenic-Dissolved (g/m3)	Iron-Dissolved (g/m3)	Alkalinity - Bicarbonate (g/m3 as CaCO3)	Carbonate Alkalinity (g/m3 as CaCO3)	pH (pH unit)	Alkalinity - Total (g/m3 as CaCO3)	Dissolved Organic Carbon (DOC) (g/m3)	Ferrous Iron (g/m3)	FLS DO (%)	FLS EC (µS/cm)	FLS Flow rate (L/S)	FLS pH	FLS Temp (°C)	Iron-Total (g/m3)	Nitrate-N (g/m3)	Nitrate-N + Nitrite-N (g/m3)	Nitrite-N (g/m3)	Nitrogen-Total Ammoniacal (g/m3)	Sulphide (µg/L)
	05-Feb-18	1,630	380	0.0052	0.123	2.9				870			23.4	4,597		7.4	16.2	3.5					
	12-Feb-18	810	270	0.0023	0.22	7.9				620			32.7	2,373		7.21	14.8	8.3	<0.002	<0.002	<0.002	33	
	16-Feb-18														0.124								
	21-Feb-18	600	230	0.0008	0.101	16.4	560	<1	7	560			24.5	1,928	0.06	7.19	12.9	18.7					
	01-Mar-18	530	210	0.0007	0.076	10				570			10.7	1,766	0.093	7.25	14.2	12.4					
	06-Mar-18												24	1,701	0.022	7.26	16.1						
	12-Mar-18	260	210	0.0008	0.041	2.3				750			25.5	1,698	0.009	7.35	13.5	8.2					
	16-Mar-18														0.085								
	20-Mar-18	390	173	0.0006	0.039	2.8				550	5	2.7	0.2	1,588	0.081	7.2	12.6	4.7	<0.002	0.006	0.004	2.7	6,710
	27-Mar-18	410	153	0.0005	0.044	2	550	<1	7	550	14	2	-0.2	1,532	0.061	7.28	12.5	6.9	<0.02	<0.02	<0.02	2.4	2,420
	03-Apr-18												0.8	1,517	0.067	7.29	12.6						
	09-Apr-18	370	134	0.0004	0.042	3.2	520	<1	7.1	520	8		0.8	1,470	0.058	7.23	11.5	8.4	<0.002	<0.002	<0.002	2.1	
	17-Apr-18												0.3	1,478	0.052	7.23	12.2						
	23-Apr-18	400	124	0.0004	0.063	6.9	480	<1	7.1	490	11.5	7.4	0	1,497	0.055	7.18	11.2	11.2	<0.002	<0.002	<0.002	1.55	5,390
	01-May-18												0	1,506	0.141	7.29	11.7						
	09-May-18	420	120	0.0004	0.071	4.9	500	<1	6.9	500	10.8	5.2	0	1,517	0.05	7.23	11.5	8.8	<0.002	<0.002	<0.002	1.65	5,330
	16-May-18	370	123	0.0004	0.066	3.6	510	<1	7	510			0.2	1,505	0.036	7.45	11						
	21-May-18	440	107	0.0005	0.42	20	420	<1	6.8	420	<0.5	21.9	0.4	1,477	0.208	7.33	11.6	20	<0.02	<0.02	<0.02	0.51	420
	28-May-18												1	1,448	0.029	7.39	8.7						
	05-Jun-18	360	114	0.0004	0.091	10.4	490	<1	7	490	10	10.5	0.8	1,464	0.03	7.4	8.4	11.6	<0.002	0.002	<0.002	1.28	1,210
	11-Jun-18												0.4	1,481	0.081	7.2	10.6						
	18-Jun-18	470	105	0.0005	0.42	20	430	<1	6.9	430	<0.5	22.6	0.5	1,477		7.15	11	21	0.07	0.07	<0.02	0.55	138
	26-Jun-18												-0.4	1,430	0.074	7.16	9.1						
	02-Jul-18	330	98	0.0007	0.85	24	480	<1	6.9	490	8.8	25.9	0.5	1,466	0.027	7.2	8	25	<0.02	<0.02	<0.02	1.09	
	12-Jul-18												-0.8	1,393	0.027	7.14	8.6						
	16-Jul-18	400	97	0.0004	0.22	14.2	450	<1	6.7	450	<0.5	17	-1.1	1,410	0.031	7.24	9	13.9	0.004	0.01	0.007	1.33	238
	23-Jul-18												-0.9	1,449	0.058	7.13	9.7						
	30-Jul-18	390	99	0.0003	0.182	11.5					10				0.062			12	0.004	0.004	<0.002	0.9	
	06-Aug-18												0	1,441	0.061	7.42	9.7						
	14-Aug-18	420	98	0.0003	0.199	11.7	430	<1	7.2	430	6.1		-0.8	1,423	0.043	7.45	10.1	12.1	<0.02	<0.02	<0.02	1.14	684
	20-Aug-18												0	1,405	0.046	7.38	9.6						
	28-Aug-18	390	97	0.0004	0.22	10.4	420	<1	7.2	420	4.2	11.7	-0.8	1,372	0.053	7.3	10.2	11	0.01	0.011	<0.002	0.8	362
	03-Sep-18												0	1,386	0.054	7.44	10.4						
	11-Sep-18	400	101	0.0003	0.193	10.1	440	<1	7	440	19.9		0	1,388	0.05	7.47	10.8	10.5	0.03	0.03	<0.02	0.87	
	17-Sep-18	370	103	0.0003	0.181	10.7	450	<1	6.9	450			-2	1,386	0.05	7.43	11.2						659
	24-Sep-18	350	93	0.0003	0.23	9.8	440	<1	6.8	440	25		-0.3	1,346	0.05	7.5	11.2	8.6	0.007	0.017	0.01	0.89	
	01-Oct-18												0	1,343	0.056	7.5	11.1						
	08-Oct-18	340	97	0.0003	0.23	10.7	430	<1	6.7	430	25	13.3	-0.6	1,340		7.33	11.4	11.4	0.01	0.015	0.005	1.06	321
	15-Oct-18												-0.5	1,344	0.057	7.46	11.1						
	24-Oct-18	320	93	0.0005	0.2	3.5	450	<1	7	450	28		0	1,340	0.048	7.47	13.2	13.7	0.004	0.004	<0.002	1.3	
	01-Nov-18												-1.7	1,323	0.026	7.3	11.6						
	06-Nov-18	290	89	0.0003	0.2	12.3	430	<1	7.1	430	30	15.8	0	1,335	0.054	7.45	11.7	12	<0.02	<0.02	<0.02	1.18	309
	12-Nov-18												-0.4	1,369	0.12	7.57	11.6						
	20-Nov-18	420	101	0.0004	0.45	23	400	<1	6.8	400	28		0	1,409	0.122	7.45	10.8	24	<0.02	<0.02	<0.02	0.62	98
REE-TANK3 (Bioreactor 3)	27-Nov-18												0	1,410	0.118	7.5	12.5						
	03-Dec-18	370	93	0.0004	0.56	22	400	<1	6.6	400	17.8		-0.1	1,390	0.108	7.31	13.1	22	<0.002	<0.002	<0.002	0.48	
	12-Dec-18												0	1,372	0.115	7.47	13.3						
	18-Dec-18	390	91	0.0004	0.64	26	410	<1	6.9	410	12		-1.8	1,388	0.122	7.33	13.2	26	0.18	0.2	<0.1	0.53	
	21-Dec-18												0	1,390	0.121	7.55	12.7						
	09-Jan-19												0	1,385	0.082	7.34	13.3						
	14-Jan-19	350	88	0.0004	0.44	22	440	<1	6.9	440	19.9	21.4	-1	1,360	0.058	7.37	13	22	0.059	0.092	0.032	0.53	57
	21-Jan-19												-1.3	1,323	0.034	7.36	14.2						
	30-Jan-19	350	88	0.0004	0.52	19.7	410	<1	6.6	410	17.8	21.1	0	1,387	0.076	7.3	14.1	21	<0.02	<0.02	<0.02	0.91	82
	06-Feb-19												-0.6	1,311	0.022	7.26	15.5						
	11-Feb-19	210	77	0.0004	0.42	12.4	500	<1	7	500	21	104	0	1,283	0.025	7.39	15.5	13	<0.002	<0.002	<0.002	0.82	
	18-Feb-19												0	1,272	0.024	7.45	15.1						
	04-Mar-19	91	77	0.0004	0.39	8.2	580	<1	7	580	32		0	1,198	0.02	7.47	13.9	8.5	0.004	0.007	0.002	1.53	783
	11-Mar-19												0	1,268	0.026	7.49	14.5						
	19-Mar-19	240	89	0.0004	0.66	4.9	520	<1	6.9	520	49	5.8	0	1,332	0.035	7.5	15.2	5.4	<0.002	0.002	<0.002	0.89	1,180
	25-Mar-19												-2.2	1,358	0.029	7.42	14.4						
	02-Apr-19	300	105	0.0004	0.72	3.6	510	<1	7	510	37		-1.2	1,346	0.03	7.58	12.8	5	0.004	0.007	0.003	0.94	
	09-Apr-19												-1.6			7.54	10.4						
	11-Apr-19				0.65																		
	23-Apr-19	300	98	0.0003	0.34	2.2	490	<1	7	490	25	3.3	0	1,373	0.0155	7.4	11.7	4.5	0.04	0.05	<0.02	0.41	1,824
	30-Apr-19													1,348	0.022	7.57	9						
	06-May-19	330	97	0.0003	0.36	2.2	480	<1	6.9	480	18.6	2	-0.2	1,364	0.026	7.36	10.3	4	<0.02	<0.02	<0.02	0.38	2,956
	13-May-19												-1.5	1,410	0.034	7.44	11						
	21-May-19	370	110	0.0003	0.27	3.2	460	<1	7.1	460	22	2.72	-2.2	1,409		7.47	9.7	4.3	<0.002	0.003	0.005	0.34	1,308
	27-May-19												0	1,378	0.0235	7.59	10						
	05-Jun-19	340	104	0.0003	0.27	2.1	460	<1	6.8	460	8.3	2.6	-0.5	1,390	0.0247	7.52	7.2	3.1	<0.02	<0.02	<0.02	0.38	1,816
	11-Jun-19												0.7	1,442		7.46	9.3						
	17-Jun-19	480	106	0.0004	0.62	17.6	410	<1	6.7	410	24		-0.7	1,461	0.1511	7.67	11.2	14.6	<0.002	0.024	0.024	0.36	
	24-Jun-19												0	1,414	0.195	7.75	10.8						45
	02-Jul-19	430	101	0.0005	0.67	21	390	<1	7.2	390	<0.5		-1	1,438	0.0151	7.74	10.6	20	<0.02	<0.02	<0.02	0.25	
	08-Jul-19												0	1,382	0.1189	7.8	10.3						
	18-Jul-19	360	85	0.0004	0.59	22	420	<1	6.7	420	7		0	1,329	0.0907	7.85	10.3	19	<0.02	<0.02	<0.02	0.39	
	22-Jul-19												-0.1	1,324	0.0451	7.64	10.5						
	30-Jul-19	410	94	0.0004	0.61	19.7	400	<1	7.1	400	16.7	19.8	-0.3	1,384	0.1009	7.6	11.2	17.4	<0.02	<0.02	<0.02	0.42	84
	05-Aug-19												0	1,369	0.105	7.9	9.7						
	12-Aug-19	320	92	0.0003	0.56	13.4	400	<1	6.7	400	22		-1	1,284	0.041	7.93	9.5	12.6	<0.02	<0.02	<0.02	0.29	
	20-Aug-19													1,262	0.04	7.77	8.7						
	28-Aug-19	310	88	0.0003	0.47	8.8	430	<1	7	430	16.1	9.5	0.3	1,254	0.038	7.63	9.7	8.3	<0.02	<0.02	<0.02	0.22	76
	02-Sep-19												0	1,243	0.038	7.86	10.4						
	09-Sep-19	220	85	0.0003	0.6	4	480	<1	7	480	14.8	4.16	-0.1	1,246	0.006	7.96		3.9	<0.002	<0.002	<0.002	0.31	45
	07-Oct-19	174	83	0.0004	1.2	2.1	520	<1	7.1	520	8.8				0.009			2.2	0.007	0.008	<0.002	0.59	
	21-Oct-19																						
	19-Nov-19	330	83	0.0003	0.33	12.1	360	<1	7.1	360	13.8		4.3	1,191	0.04	7.24	11.4	11.3	<0.02	<0.02	<0.02	0.25	
	25-Nov-19												3.9	1,202	0.005	7.4	12.2						
	02-Dec-19	300	82	0.0003	0.54	12.6	370	2.2	7.8	370	7		3.2	1,190	29.19	7.54	12.6	14.2	0.02	0.02	<0.002	0.28	
	16-Dec-19	300	86	0.0004	0.0108	0.08	380	<1	6.9	380	8.2		2.2	1,184	0.053	7.61	12.6	10.3	0.019	0.021	<0.002	0.44	
	13-Jan-20	270	75	0.0004	0.53	14.6	380	<1	7	380	8.7		3.2	1,179		7.62	12.2	14.1	<0.02	<0.02	<0.02	0.72	

Data Point	Date	Sulphate (g/m3)	Calcium-Dissolved (g/m3)	Antimony-Dissolved (g/m3)	Arsenic-Dissolved (g/m3)	Iron-Dissolved (g/m3)	Alkalinity - Bicarbonate (g/m3 as CaCO3)	Carbonate Alkalinity (g/m3 as CaCO3)	pH (pH unit)	Alkalinity - Total (g/m3 as CaCO3)	Dissolved Organic Carbon (DOC) (g/m3)	Ferrous Iron (g/m3)	FLS DO (%)	FLS EC (µS/cm)	FLS Flow rate (L/S)	FLS pH	FLS Temp (°C)	Iron-Total (g/m3)	Nitrate-N (g/m3)	Nitrate-N + Nitrite-N (g/m3)	Nitrite-N (g/m3)	Nitrogen-Total Ammoniacal (g/m3)	Sulphide (µg/L)
REE-TANK4 (Bioreactor 4)	05-Feb-18	1,170	340	0.026	0.93	2.1				630			43.9	3,216		7.56	18.2	4.5					
	09-Feb-18														0.053								
	12-Feb-18	680	250	0.0028	1.18	19.6				600			27.1	2,085		7.28	15	19.7	<0.02	<0.02	<0.02	0.38	
	16-Feb-18														0.044								
	21-Feb-18	540	230	0.0019	0.54	25	580	<1	7.2	580			29.6	1,938	0.033	7.29	13	27					
	01-Mar-18	560	220	0.0015	0.42	25				620			24.2	1,917	0.015	7.29	14.9	26					
	06-Mar-18												28.1	1,943	0.005	7.47	15.4						
	12-Mar-18	570	270	0.002	0.27	15.1				710			47.7	2,077		7.55	13	24					
	16-Mar-18														0.065								
	20-Mar-18	460	196	0.0008	0.51	22				580	21	16.3	0.2	1,758	0.062	7.29	12.6	22	<0.002	0.004	<0.002	0.85	120
	27-Mar-18	490	188	0.0008	0.56	24	570	<1	6.9	570	5	20.2	-0.3	1,702	0.06	7.28	12.4	26	0.003	0.005	<0.002	0.79	130
	03-Apr-18												1.1	1,680	0.059	7.34	12.4						
	09-Apr-18	460	172	0.0007	0.8	25	560	<1	7.2	560	<0.5		0.4	1,677	0.066	7.27	11.5	27	0.003	0.004	<0.002	0.77	
	17-Apr-18												0.1	1,699	0.036	7.16	11.9						
	23-Apr-18	480	182	0.0008	0.72	21	580	1.1	7.3	580	5.5	21.1	0	1,735	0.047	7.18	10.8	23	<0.002	<0.002	<0.002	0.88	30
	01-May-18												0	1,743	0.05	7.27	11.5						
	09-May-18	500	173	0.0007	0.83	21	580	<1	7.2	580	7.8	21.1	0	1,743	0.063	7.22	11.5	21	<0.002	<0.002	<0.002	0.56	52
	16-May-18	470	181	0.0007	0.75	19.1	580	<1	7.2	580			0.5	1,740	0.056	7.46	11.2						
	21-May-18	450	175	0.0007	0.87	19.1	570	<1	7.1	570	9.9	21.7	0.8	1,708	0.0645	7.39	10.5	20	<0.02	<0.02	<0.02	0.75	53
	28-May-18												1	1,706	0.047	7.46	8.9						
	05-Jun-18	430	189	0.0006	0.72	16.3	590	<1	7.2	600	7	17.2	0.5	1,756	0.037	7.38	8.5	16.4	0.04	0.04	<0.02	0.6	25
	11-Jun-18												0.2	1,725	0.059	7.23	10.4						
	18-Jun-18	480	173	0.0006	0.8	17.1	590	<1	7.2	600	4.7	20.4	0.3	1,725	0.051	7.17	9.7	17.4	0.07	0.07	<0.02	0.54	26
	26-Jun-18												-0.1	1,690	0.046	7.2	8.1						
	02-Jul-18	410	158	0.0005	0.84	23	550	<1	7.1	550	4.8	25.7	-0.1	1,643	0.099	7.19	10.2	22	<0.02	<0.02	<0.02	0.6	
	12-Jul-18												-1.7	1,649	0.094	7.22	10.1						
	16-Jul-18	480	160	0.0005	1.17	22	550	<1	6.9	550	<0.5	23.9	-1.2	1,670	0.095	7.36	10.6	23	<0.002	<0.002	<0.002	0.54	52
	23-Jul-18												-0.3	1,702	0.06	7.12	9.5						
	30-Jul-18	470	167	0.0005	0.86	16.3					8				0.059			15.9	0.004	0.004	<0.002	0.59	
	06-Aug-18												0	1,691	0.058	7.4	9.5						
	14-Aug-18	460	165	0.0006	0.76	13.3	570	1.4	7.4	570	<0.5		0	1,680	0.046	7.4	9.9	13.7	<0.02	<0.02	<0.02	0.54	28
	20-Aug-18												0	1,644	0.048	7.35	9.2						
	28-Aug-18	430	157	0.0005	0.79	12.9	560	1.4	7.4	560	3.2	14.3	-1	1,630	0.061	7.37	10.1	13.7	<0.02	<0.02	<0.02	0.49	65
	03-Sep-18												-2.2	1,632	0.059	7.42	10.5						
	11-Sep-18	440	159	0.0005	0.87	16.3	570	<1	7.2	570	28		-1.5	1,637	0.055	7.46	10.9	16.7	0.02	0.022	<0.002	0.47	
	17-Sep-18	400	180	0.0005	0.71	16.9	580	<1	7.2	580			-1.9	1,622	0.051	7.49	11						60
	24-Sep-18	390	158	0.0006	0.8	15.3	570	<1	7.1	570	19		-1.5	1,585	0.05	7.56	11.1	15.9	0.006	0.009	0.004	0.54	
	01-Oct-18												-1.8	1,580	0.062	7.51	11						
	08-Oct-18	350	162	0.0005	0.82	19.7	570	<1	6.9	570	32	21	-1.8	1,570		7.38	11.3	21	<0.002	0.002	<0.002	0.57	66
	15-Oct-18												0	1,582	0.051	7.45	10.8						
	24-Oct-18	360	162	0.0005	0.82	19.7	580	<1	7.2	580	27		-0.5	1,585	0.058	7.52	12.9	22	<0.02	<0.02	<0.02	0.66	
	01-Nov-18												-2.1	1,602	0.03	7.39	11.3						
	06-Nov-18	360	168	0.0005	0.7	21	580	<1	7.1	580	29	23	-0.8	1,619	0.04	7.54	11.5	19.8	0.012	0.013	<0.002	0.54	65
	12-Nov-18												0	1,578	0.092	7.58	11.5						
	20-Nov-18	430	176	0.0005	0.86	20	550	<1	7.1	550	33		0	1,615	0.081	7.47	10.4	21	0.002	0.004	<0.002	0.39	53
	27-Nov-18												0	1,625	0.083	7.5	12.5						
	03-Dec-18	380	159	0.0005	1.02	23	550	<1	6.9	560	27		-1.6	1,605	0.074	7.39	13.5	22	<0.002	<0.002	<0.002	0.34	
	12-Dec-18												0	1,592	0.082	7.49	13.4						
	18-Dec-18	370	156	0.0005	1	19	590	<1	7.2	590	27		-0.3	1,610	0.023	7.38	14.7	20	0.096	0.097	<0.002	0.43	
	21-Dec-18												0	1,607	0.023	7.55	13.9						
	09-Jan-19												0	1,610	0.052	7.33	13.6						
	14-Jan-19	370	165	0.0005	0.82	22	600	<1	7.1	600	17.9	20.9	-1.1	1,602	0.036	7.55	12.3	22	<0.002	<0.002	<0.002	0.36	63
	21-Jan-19												-1.9	1,609	0.011	7.42	14.9						
	30-Jan-19	360	140	0.0004	0.83	18.8	560	<1	6.8	560	25	21.2	0	1,611	0.04	7.31	15	21	<0.02	<0.02	<0.02	0.76	87
	06-Feb-19												-0.6	1,604	0.044	7.38	14.2						
	11-Feb-19	320	146	0.0005	0.77	18.6	400	<1	6.8	400	24	85	0	1,576	0.043	7.46	14.1	19.5	<0.002	<0.002	<0.002	0.41	
	18-Feb-19												-0.3	1,662	0.034	7.46	14.4						
	04-Mar-19	111	159	0.0008	0.72	5.6	780	1.7	7.4	790	20		0	1,498	0.011	7.47	13.3	5.5	<0.002	<0.002	<0.002	0.38	246
	11-Mar-19												0	1,517	0.083	7.5	14.4						
	19-Mar-19	300	154	0.0006	0.91	20	640	<1	7	640	33	20.5	0	1,561	0.031	7.6	14.7	22	0.007	0.008	<0.002	0.41	74
	25-Mar-19												-1.4	1,608	0.03	7.5	14.4						
	02-Apr-19	360	171	0.0005	0.81	18.9	610	<1	7.2	620	33		-1.9	1,621	0.012	7.58	12.3	19.9	<0.002	<0.002	<0.002	0.36	
	09-Apr-19												-1.2			7.63	10						
	11-Apr-19				0.32																		
	23-Apr-19	360	174	0.0005	0.53	13	620	<1	7.1	620	22	11.2	0	1,646	0.0128	7.41	10.7	14.6	0.02	0.03	<0.02	0.155	85
	30-Apr-19													1,640	0.016	7.67	9.1						
	06-May-19	380	160	0.0005	0.56	10.9	610	<1	6.9	610	8	10.12	-2.3	1,628	0.024	7.36	10.7	14.4	0.005	0.006	<0.002	0.22	570
	13-May-19												0	1,667	0.028	7.44	10.8						
	21-May-19	420	183	0.0005	0.55	11	600	1.2	7.3	600	18.8	10.8	-2.2	1,650		7.49	9.8	11.8	<0.02	<0.02	<0.02	0.178	536
	27-May-19												0	1,663	0.0335	7.63	10.3						
	05-Jun-19	400	169	0.0005	0.5	10.3	580	<1	7.2	580	30	11.4	-0.2	1,642	0.0307	7.61	7.7	11.6	<0.002	<0.002	<0.002	0.2	340
	11-Jun-19												-1.1	1,688	0.037	7.48	9.3						
	17-Jun-19	650	179	0.0006	0.67	10.8	590	<1	7.1	590	22		-2.3	1,668	0.0321	7.73	9.3	9.2	<0.002	<0.002	<0.002	0.24	
	24-Jun-19												-1.1	1,625	0.0312	7.68	7.4						122
	02-Jul-19	400	174	0.0004	0.71	11.3	590	1.5	7.4	590	1		0	1,642	0.027	7.69	7.8	10	<0.002	<0.002	<0.002	0.21	
	08-Jul-19												-0.9	1,622	0.0273	7.8	7.7						
	18-Jul-19	370	153	0.0005	0.65	10.9	600	<1	7.1	600	13		-0.2	1,568	0.0251	7.94	8	10.1	<0.02	<0.02	<0.02	0.21	
	22-Jul-19												0	1,546	0.0278	7.76	8.5						
	30-Jul-19	390	147	0.0004	0.62	10.5	600	1.8	7.5	610	29	9.08	-2.7	1,603	0.0261	7.78	9.4	9.6	<0.02	<0.02	<0.02	0.22	208
	05-Aug-19												0	1,584	0.025	7.86	6.8						
	12-Aug-19	350	167	0.0003	0.57	9.1	580	<1	7	580	33		0	1,521	0.027	7.83	8.4	8.5	<0.02	<0.02	<0.02	0.31	
	20-Aug-19													1,505	0.021	7.84	7.7						
	28-Aug-19	330	157	0.0003	0.54	7	600	1	7.3	600	28	16.6	-1.4	1,506	0.025	7.68	9.2	6.6	<0.02	0.02	<0.02	0.195	444
	02-Sep-19												-0.1	1,604	0.018	7.81	9.6						
	09-Sep-19	330	156	0.0004	0.55	8.3	560	<1	7.2	560	28	8.92	0	1,608	0.052	7.81		8.4	<0.002	<0.002	<0.002	0.27	320
	23-Sep-19	300	147	0.0004	0.71	10	550	<1	7.1	550	10.8		-2.5	1,439	0.048	8.14	10.7	11.8	<0.002	<0.002	<0.002	0.28	
	07-Oct-19	310	147	0.0004	0.63	10.5	560	<1	7	560	9.8				0.053			10.9	0.008	0.008	<0.002	0.24	
	21-Oct-19	310	143	0.0004	0.66	9.7	540	<1	7.2	540	5.9				0.045			11.2	0.009	0.009	<0.002	0.25	
	05-Nov-19	300	156	0.0004	0.77	9.5	530	<1	7	530	13.8		0.8		0.044		12.5	9.4	<0.02	<0.02	<0.02	0.24	
	19-Nov-19	300	141	0.0003	0.64	9.3	540	1.4	7.4	540	9.7		4.9	1,396	0.043	7.22	11	8.3	<0.02	<0.02	<0.02	0.27	
	25-Nov-19												3.9	1,411	0.04	7.4	12.8						
	02-Dec-19	280	141	0.0004	0.55	7.7	540	1	7.3	540	9.8		1.7	1,397	0.041	7.49	13.7	8.7	0.008	0.009	<0.002	0.27	
	16-Dec-19	130	150	0.0008	0.32	0.04	690	1.2	7.3	690	15.9		2.7	1,362	0.017	7.6	13.2	3.4	0.009	0.01	<0.002	0.41	
	13-Jan-20	220	142	0.0008	1.07	0.88	580	1.4	7.4	590	5.7		3.6	1,379	0.025	7.61	12.9	2.3	0.058	0.067	0.009	0.48	

Data Point	Date	Sulphate (g/m3)	Calcium-Dissolved (g/m3)	Antimony-Dissolved (g/m3)	Arsenic-Dissolved (g/m3)	Iron-Dissolved (g/m3)	Alkalinity - Bicarbonate (g/m3 as CaCO3)	Carbonate Alkalinity (g/m3 as CaCO3)	pH (pH unit)	Alkalinity - Total (g/m3 as CaCO3)	Dissolved Organic Carbon (DOC) (g/m3)	Ferrous Iron (g/m3)	FLS DO (%)	FLS EC (µS/cm)	FLS Flow rate (L/S)	FLS pH	FLS Temp (°C)	Iron-Total (g/m3)	Nitrate-N (g/m3)	Nitrate-N + Nitrite-N (g/m3)	Nitrite-N (g/m3)	Nitrogen-Total Ammoniacal (g/m3)	Sulphide (µg/L)
REE-TANK5 (Bioreactor 5)	09-Feb-18														0.047								
	12-Feb-18	1,210	340	0.0028	0.21	29				680			21.1	3,540		7.06	15.3	32	<0.1	<0.1	<0.1	73	
	16-Feb-18														0.04								
	21-Feb-18	780	330	0.001	0.058	16.4	720	<1	7	720			24.7	2,461	0.026	7.16	12.9	19.9					
	01-Mar-18	600	240	0.0007	0.04	12.9				600			27.9	1,928	0.017	7.21	14.9	14.5					
	06-Mar-18												18.6	1,749	0.011	7.24	15.2						
	12-Mar-18	410	240	0.0008	0.02	5.2				700			17	1,883	0.008	7.22	13.2	6.7					
	16-Mar-18														0.094								
	20-Mar-18	490	163	0.0005	0.121	14.9				450	16.9	13	0.9	1,514	0.103	7.14	12.4	15.2	<0.002	0.004	0.004	0.35	2,110
	27-Mar-18	460	132	0.0006	0.095	17.1	450	<1	6.8	450	<0.5	18.1	-0.2	1,828	0.074	7.18	12.6	20	<0.02	<0.02	<0.02	0.31	1,450
	03-Apr-18												0.7	1,431	0.078	7.2	14.5						
	09-Apr-18	230	91	0.0005	0.43	2.3	460	2	7.7	460	27		4.3	1,204	0.042	7.25	11.3	7.9	<0.002	<0.002	<0.002	0.139	
	17-Apr-18												-0.1	1,451	0.055	7.12	12.6						
	23-Apr-18	300	113	0.0005	0.048	1.93	510	<1	7	510	10.5	4.4	0	1,365	0.026	7.07	10.4	6.1	<0.002	<0.002	<0.002	0.38	7,400
	01-May-18												0	1,324	0.01	7.15	10.9						
	09-May-18	150	107	0.0007	0.177	0.19	680	<1	7	680	25	0.17	0	1,409	0.014	7.14	10.7	0.24	<0.002	0.015	0.017	1.66	15,180
	16-May-18	116	114	0.0009	0.54	0.07	720	<1	7.1	720			0	1,417	0.008	7.29	10.3						
	21-May-18	350	121	0.0005	0.27	0.14	530	<1	7.1	540	22	0.19	-0.2	1,463	0.0301	7.24	10	0.155	<0.02	<0.02	<0.02	2	15,520
	28-May-18												-1.2	1,430	0.02	7.14	7.7						
	05-Jun-18	290	116	0.0008	0.26	0.12	580	<1	7	580	24	0.21	0	1,444	0.011	7.34	5.9	0.118	0.04	0.05	<0.02	1.84	16,720
	11-Jun-18												0	1,463	0.03	7.28	9.2						
	18-Jun-18	320	113	0.0005	0.131	0.24	570	<1	7	570	11.7	0.23	0.8	1,422	0.016	7.25	8	0.28	<0.002	0.002	0.003	1.21	15,320
	26-Jun-18												-0.1	1,416	0.048	7.11	7.9						
	02-Jul-18	390	97	0.0004	0.21	16.5	420	<1	6.8	420	7.8	19.8	0.1	1,413	0.132	7.18	10.5	16.2	<0.02	<0.02	<0.02	0.51	
	12-Jul-18												-0.3	1,389	0.8	7.17	9.7						
	16-Jul-18	440	94	0.0004	0.36	17.3	430	<1	6.7	430	2	22.9	66	1,429	0.074	7.18	8.6	18.1	0.014	0.015	<0.002	0.48	590
	23-Jul-18												-0.1	1,405	0.031	7.07	8.9						
	30-Jul-18	350	95	0.0003	0.29	6.3					3				0.03			6.8	<0.002	<0.002	<0.002	0.65	
	06-Aug-18												-0.5	1,421	0.034	7.5	8.1						
	14-Aug-18	360	99	0.0004	0.4	2.2	470	<1	7.1	470	2.2		0	1,404	0.019	7.34	9	3.4	<0.002	0.003	<0.002	0.73	5,380
	20-Aug-18												0	1,390	0.019	7.34	7.9						
	28-Aug-18	340	94	0.0004	0.37	6.8	450	<1	7.3	450	4.6	7.3	-2.5	1,330	0.022	7.43	9	7.8	<0.02	<0.02	<0.02	0.55	2,100
	03-Sep-18												-3	1,338	0.019	7.47	9.1						
	11-Sep-18	410	100	0.0003	0.35	5.5	450	<1	7	450	24		-2.5	1,378	0.032	7.34	10.6	5.8	0.02	0.03	<0.02	0.5	
	17-Sep-18	350	105	0.0004	0.29	4.3	470	<1	7	470			-2.5	1,365	0.026	7.59	10.8						2,870
	24-Sep-18	320	97	0.0005	0.35	3.7	460	<1	6.9	460	23		-2.6	1,341	0.023	7.61	10.8	3.9	0.045	0.047	<0.002	0.87	
	01-Oct-18												-0.5	1,352	0.025	7.55	10.6						
	08-Oct-18	340	91	0.0004	0.34	15.6	430	<1	6.7	430	14.3	21.5	-2.2	1,340		7.4	11.2	21	<0.02	<0.02	<0.02	0.65	54
	15-Oct-18												-1.3	1,359	0.031	7.67	11						
	24-Oct-18	280	90	0.0004	0.31	11.9	460	<1	7	460	32		-2.5	1,313	0.019	7.45	13.3	12.4	<0.02	<0.02	<0.02	1.58	
	01-Nov-18												0	1,338	0.013	7.44	12.5						
	06-Nov-18	350	99	0.0003	0.24	10	450	<1	7	450	29	12.1	0	1,376	0.049	7.45	11.4	9.6	<0.02	<0.02	<0.02	1.7	850
	12-Nov-18												0	1,383	0.075	7.63	11.4						
	20-Nov-18	440	101	0.0004	0.46	22	400	<1	6.8	400	28		-0.2	1,424	0.07	7.55	10.2	23	<0.02	<0.02	<0.02	0.59	122
	27-Nov-18												0	1,407	0.067	7.37	12.5						
	03-Dec-18	380	92	0.0004	0.63	21	410	<1	6.6	410	17.9		-2.1	1,400	0.062	7.36	13.4	20	<0.002	0.009	0.008	0.49	
	12-Dec-18												-0.9	1,377	0.09	7.56	13.4						
	18-Dec-18	380	90	0.0004	0.58	21	420	<1	6.9	420	13		-0.8	1,370	0.037	7.37	13.7	23	<0.002	0.01	0.01	0.7	
	21-Dec-18												0	1,382	0.037	7.59	13.1						
	09-Jan-19												0	1,416	0.065	7.45	13.2						
	14-Jan-19	390	95	0.0004	0.73	26	440	<1	6.9	440	15.9	23	0	1,418	0.052	7.35	12.6	25	<0.002	<0.002	<0.002	0.58	36
	21-Jan-19												-0.7	1,409	0.033	7.38	13.9						
	30-Jan-19	320	87	0.0004	0.55	16.8	430	<1	6.6	430	26	21.6	0	1,351	0.023	7.26	15.3	19.3	0.003	0.004	<0.002	0.81	40
	06-Feb-19												-1.9	1,246	0.009	7.3	16.3						
	11-Feb-19	184	75	0.0004	0.45	8.7	460	<1	6.7	460	22	55	0	1,258	0.012	7.38	15.5	8.4	<0.002	0.003	0.003	1.53	
	18-Feb-19												-1.2	1,229	0.011	7.54	15.4						
	04-Mar-19	300	91	0.0005	0.5	12.3	470	<1	7	470	29		0	1,351	0.039	7.4	12	12.6	<0.02	<0.02	<0.02	1.12	55
	11-Mar-19												0	1,348	0.042	7.7	14.4						
	19-Mar-19	290	91	0.0005	0.76	14.6	490	<1	6.8	490	26	16.6	0.6	1,335	0.014	7.51	14.9	16.7	0.003	0.011	0.008	1.02	84
	25-Mar-19												0	1,348	0.014	7.47	15						
	02-Apr-19	290	94	0.0004	0.75	7.8	480	<1	7	480	39		-0.9	1,328	0.017	7.63	11.8	9.4	<0.02	<0.02	<0.02	1.18	
	09-Apr-19												-0.3			8.28	9.3						
	11-Apr-19				0.66																		
	23-Apr-19	330	99	0.0003	0.33	5.4	470	<1	6.9	470	28	5.6	-2.8	1,361	0.008	7.33	10.2	7.4	0.03	0.03	<0.02	0.65	674
	30-Apr-19													1,323	0.026	7.41	7.8						
	06-May-19	470	100	0.0006	1.66	28	410	<1	6.7	410	7.6	25.9	-2.3	1,467	0.5	7.21	11.9	34	<0.02	<0.02	<0.02	0.46	10
	13-May-19												2.7	1,474		7.48	10.5						
	21-May-19	450	104	0.0005	1.41	29	390	<1	6.9	390	13.8	26.5	-0.7	1,450		7.5	11.8	29	<0.02	<0.02	<0.02	0.29	
	27-May-19												2.2	1,398	0.0126	7.46	9.8						
	05-Jun-19	460	102	0.0008	1.87	23	390	<1	6.7	390	18.4	26.3	-1.1	1,482	0.6024	7.42	11.6	25	<0.02	<0.02	<0.02	0.24	42
	11-Jun-19												0.5	1,472	0.0331	7.75	9.8						
	17-Jun-19	630	104	0.0005	0.43	18.3	420	<1	6.9	420	22		2	1,432	0.0238	7.95	8.8	15.8	<0.02	<0.02	<0.02	0.39	
	24-Jun-19												0	1,415	0.0218	7.68	5.7						68
	02-Jul-19	400	96	0.0004	0.31	14	420	1.7	7.6	420	3		-1.1	1,397	0.0148	8.14	6.8	13.2	<0.02	<0.02	<0.02	0.26	
	08-Jul-19												3.9	1,377	0.0235	7.95	7.3						
	18-Jul-19	340	92	0.0004	0.33	8.9	460	<1	6.9	460	7		-0.6	1,349	0.0135	8.12	7.4	7.8	<0.02	<0.02	<0.02	0.25	
	22-Jul-19												0.3	1,295	0.0144	7.83	6.6						
	30-Jul-19	350	98	0.0003	0.37	7.6	450	<1	7.3	450	16.7	7.7	-2.2	1,305	0.0108	8.13	8.2	6.6	<0.02	<0.02	<0.02	0.47	23
	05-Aug-19												-1	1,344	0.013	8.1	6.3						
	12-Aug-19	300	97	<0.0002	0.34	7	440	<1	6.9	450	28		-1	1,273	0.011	8.5	6.5	5.9	<0.02	<0.02	<0.02	0.46	
	20-Aug-19													1,267	0.004	7.8	6.3						
	28-Aug-19	310	94	0.0002	0.43	5.2	440	<1	7	440	14.9	5.9	0.8	1,260	0.02	7.77	8.3	4.8	<0.02	<0.02	<0.02	0.26	1,060
	02-Sep-19												0	1,248	0.01	8.33	8.8						
	09-Sep-19	310	93	0.0002	0.43	4.2	440	<1	7	440	16.8	3.92	0	1,248	0.011	7.99		4	<0.002	0.004	0.002	0.35	526
	23-Sep-19	280	88	0.0003	0.49	3.8	440	<1	6.9	440	0.8		-2.7	1,221	0.021	8.46	9.8	4.8	0.003	0.003	<0.002	0.39	
	07-Oct-19	300	90	0.0002	0.29	4.7	420	<1	7	420	7.8				0.017			5.2	0.009	0.011	<0.002	0.31	
	21-Oct-19	290	111	0.0005	0.25	5.3	400	<1	7	400	9.9				0.022			6.9	0.004	0.01	0.006	0.31	
	05-Nov-19	270	87	<0.0002	0.28	4	420	<1	6.8	420	8.8		0.6		0.2		12.3	4.7	0.02	0.02	<0.02	0.36	
	19-Nov-19	260	80	<0.0002	0.45	2.1	420	<1	7	420	17		4.7	1,117	0.02	7.05	10.5	2.7	<0.02	0.02	<0.02	0.43	
	25-Nov-19												2.5	1,162	0.018	7.33	12.7						
	02-Dec-19	200	78	<0.0002	0.51	0.99	480	<1	7.2	480	13.8		3	1,113	0.006	7.76	14.6	1.74	0.005	0.008	0.003	0.48	
	16-Dec-19	97	79	0.0006	1.28	0.44	530	<1	6.9	530	23		2.3	1,104	0.014	7.67	13.2	0.97	0.006	0.01	0.004	1.45	
	13-Jan-20	179	78	0.0005	1.86	0.47	490	<1	7.2	490	11.7		3	1,157	0.019	7.57	13	0.69	0.007	0.028	0.022	2.5	

Data Point	Date	Sulphate (g/m3)	Calcium-Dissolved (g/m3)	Antimony-Dissolved (g/m3)	Arsenic-Dissolved (g/m3)	Iron-Dissolved (g/m3)	Alkalinity - Bicarbonate (g/m3 as CaCO3)	Carbonate Alkalinity (g/m3 as CaCO3)	pH (pH unit)	Alkalinity - Total (g/m3 as CaCO3)	Dissolved Organic Carbon (DOC) (g/m3)	Ferrous Iron (g/m3)	FLS DO (%)	FLS EC (µS/cm)	FLS Flow rate (L/S)	FLS pH	FLS Temp (°C)	Iron-Total (g/m3)	Nitrate-N (g/m3)	Nitrate-N + Nitrite-N (g/m3)	Nitrite-N (g/m3)	Nitrogen-Total Ammoniacal (g/m3)	Sulphide (µg/L)
	09-Feb-18														0.044								
	12-Feb-18	1,260	340	0.0026	0.182	23				680			4.8	3,542		7.01	15.4	25	<0.1	<0.1	<0.1	67	
	16-Feb-18														0.04								
	21-Feb-18	730	330	0.001	0.085	14.7	710	<1	7.1	710			15.8	2,399	0.028	7.19	12.9	18.8					
	01-Mar-18	630	250	0.0007	0.077	14.3				550			22.1	1,141	0.023	7.11	15	16.3					
	06-Mar-18												12.9	1,811	0.02	7.12	14.8						
	12-Mar-18	480	200	0.0007	0.037	10.9				550			18.2	1,708	0.015	7.19	13.4	12.8					
	16-Mar-18														0.047								
	20-Mar-18	450	158	0.0005	0.088	12.9				470	14.9	11	0.3	1,795	0.054	7.04	13	13.6	0.003	0.005	0.002	0.96	980
	27-Mar-18	430	140	0.0006	0.06	10.4	490	<1	6.7	490	11	11.5	-0.4	1,620	0.03	7.09	12.9	11.9	<0.02	<0.02	<0.02	0.24	2,960
	03-Apr-18												0.6	1,479	0.034	7.18	13						
	09-Apr-18	380	124	0.0005	0.074	3.2	510	<1	7.1	510	7.8		0.2	1,490	0.029	7.15	11.5	8.7	<0.002	<0.002	0.002	0.184	
	17-Apr-18												0.8	1,432	0.028	7.13	12						
	23-Apr-18	340	122	0.0005	0.109	0.79	520	<1	7.1	520	12.2	1.4	0	1,428	0.025	7.01	11	5.1	<0.002	<0.002	<0.002	0.69	6,480
	01-May-18												-0.4	1,759	0.021	7.3	11.9						
	09-May-18	350	119	0.0006	0.21	0.53	560	<1	7.1	560	8.3	0.23	0	1,489	0.025	7.14	11.5	1.1	0.004	0.011	0.007	1.32	12,300
	16-May-18	161	109	0.0008	0.62	0.75	660	<1	7.2	660			0.6	1,399	0.008	7.34	10.6						
	21-May-18	300	123	0.0006	0.8	0.17	580	<1	7	580	16.1	0.19	0.2	1,506	0.0173	7.15	10.2	0.196	<0.02	<0.02	<0.02	2.3	16,960
	28-May-18												-0.5	1,477	0.0129	7.13	7.5						
	05-Jun-18	300	123	0.0009	0.43	0.27	570	<1	7	570	22	0.19	0	1,500	0.011	7.21	6.9	0.53	<0.002	0.003	0.004	2.2	11,040
	11-Jun-18												0.1	1,539	0.031	7.19	10.4						
	18-Jun-18	410	112	0.0004	0.167	1.76	490	<1	7	490	7.7	1.78	0	1,451	0.035	7.22	10.2	4.3	<0.002	<0.002	<0.002	0.94	4,820
	26-Jun-18												0	1,398	0.026	7.09	8.7						
	02-Jul-18	290	99	0.0004	0.166	0.58	520	<1	6.9	520	10.8	0.58	0.1	1,423	0.01	7.21	7	1.81	<0.002	<0.002	<0.002	1.06	
	12-Jul-18												-0.3	1,403	0.0131	7.17	8						
	16-Jul-18	380	109	0.0004	0.159	0.6	500	<1	6.9	500	9	0.44	-1.6	1,440	0.023	7.14	9.2	1.54	<0.002	0.003	0.005	1.64	15,080
	23-Jul-18												-1.4	1,457	0.036	7.13	10.3						
	30-Jul-18	390	104	0.0003	0.196	4.3					5				0.043			6.4	0.005	0.005	<0.002	0.83	
	06-Aug-18												-1.2	1,736	0.021	7.55	8.7						
	14-Aug-18	400	103	0.0004	0.26	2.2	460	<1	7.2	460	10.2		0	1,413	0.024	7.2	9.8	4.4	<0.002	<0.002	<0.002	0.65	3,150
	20-Aug-18												-0.9	1,388	0.024	7.37	9						
	28-Aug-18	330	99	0.0004	0.22	0.95	470	<1	7.1	470	15	3.3	-2	1,352	0.016	7.52	9	3.5	<0.002	<0.002	<0.002	0.61	4,580
	03-Sep-18												-2.2	1,354	0.016	7.59	9.8						
	11-Sep-18	400	102	0.0003	0.29	5.8	450	<1	7	450	27		-2.2	1,365	0.039	7.49	11.1	7.7	0.03	0.04	<0.02	0.5	
	17-Sep-18	370	109	0.0004	0.25	5.7	450	<1	7	450			-0.2	1,381	0.037	8.05	11.3						2,400
	24-Sep-18	350	103	0.0005	0.27	5.9	450	<1	6.8	450	26		-3.2	1,337	0.031	7.75	11.5	7.3	<0.02	<0.02	<0.02	0.62	
	01-Oct-18												-2.2	1,348	0.041	7.68	11.5						
	08-Oct-18	340	97	0.0004	0.28	8.3	440	<1	6.7	440	30	11.6	-1.9	1,318		7.47	11.6	9.7	<0.002	0.005	0.004	0.74	2,010
	15-Oct-18												-1.5	1,362	0.037	7.87	11.5						
	24-Oct-18	310	92	0.0003	0.27	9.6	460	<1	6.9	460	33		-2.5	1,339	0.026	7.6	13.1	11.1	0.004	0.005	<0.002	1.05	
	01-Nov-18												-2.2	1,421	0.078	7.47	11.7						
	06-Nov-18	390	97	0.0004	0.38	21	420	<1	6.9	420	25	12.1	-0.4	1,401	0.032	7.6	12.1	19.7	9.5	9.5	<0.02	9.5	172
	12-Nov-18												-1.8	1,382	0.057	7.77	11.7						
	20-Nov-18	420	91	0.0004	0.37	20	410	<1	6.9	410	34		-2.2	1,418	0.052	7.66	10.6	21	<0.1	<0.1	<0.1	0.61	484
	27-Nov-18												-0.7	1,415	0.042	7.4	12.6						
REE-TANK6 (Bioreactor 6)	03-Dec-18	360	93	0.0004	0.49	17.9	430	<1	6.6	430	16.9		-2.9	1,386	0.038	7.45	13.4	16.7	<0.002	0.016	0.016	0.56	
	12-Dec-18												-0.7	1,377	0.045	7.74	13.7						
	18-Dec-18	410	101	0.00043	0.65	19	420	<1	6.8	420	14		-0.8	1,399	0.076	7.48	13.2	23	0.14	0.16	<0.1	0.51	
	21-Dec-18												-0.2	1,402	0.078	7.74	12.7						
	09-Jan-19												-0.8	1,407	0.042	7.66	13.6						
	14-Jan-19	380	93	0.0004	0.38	21	450	<1	6.9	450	12	22	-0.7	1,415	0.029	7.42	13.2	21	<0.02	<0.02	<0.02	0.63	142
	21-Jan-19												-0.5	1,335	0.012	7.39	14.7						
	30-Jan-19	380	90	0.0004	0.58	23	410	<1	6.6	410	18.8	24.3	0	1,408	0.049	7.3	13.9	25	<0.02	<0.02	<0.02	0.73	292
	06-Feb-19												0	1,309	0.011	7.41	15.5						
	11-Feb-19	230	78	0.0004	0.49	14.2	490	<1	6.7	490	22	51	0	1,284	0.013	7.4	15	15	<0.1	<0.1	<0.1	1.08	
	18-Feb-19												-1.3	1,274	0.014	7.33	15.2						
	04-Mar-19	300	88	0.0004	0.32	7.9	470	<1	7.1	470	36		0	1,329	0.03	7.47	12.3	8.8	<0.02	<0.02	<0.02	1.03	547
	11-Mar-19												-1.3	1,254	0.012	7.73	15.1						
	19-Mar-19	210	82	0.0005	0.57	5	520	<1	6.9	520	22	5.5	-0.1	1,289	0.013	7.72	15.7	6.8	0.009	0.013	0.004	1.01	926
	25-Mar-19												0	1,309	0.01	7.4	15.4						
	02-Apr-19	280	98	0.0006	0.69	3.4	500	<1	7	500	31		-2.8	1,357	0.015	7.77	12.2	5.1	<0.002	<0.002	0.002	1.2	
	09-Apr-19												-0.2			8.8	9.9						
	11-Apr-19				0.73																		
	23-Apr-19	340	99	0.0003	0.3	3.8	470	<1	6.9	470	11.7	3.6	-1.3	1,378	0.008	7.34	10.7	5.6	0.03	0.04	<0.02	0.56	864
	30-Apr-19													1,347	0.0074	7.49	8.7						
	06-May-19	340	98	0.0003	0.38	4.2	480	<1	6.8	480	22	1.24	-2.1	1,360	0.0095	7.32	10	6.1	<0.02	<0.02	<0.02	0.54	3,460
	13-May-19												-2.2	1,392	0.016	7.93	10.6						
	21-May-19	380	110	0.0003	0.35	3.5	470	<1	7.1	470	14.8	3.68	-0.9	1,405		7.82	8.8	4.3	<0.002	0.004	0.004	0.53	1,460
	27-May-19												-2.6	1,389	0.0251	7.62	9.6						
	05-Jun-19	390	107	0.0004	0.35	2.4	460	<1	6.8	460	30	2.86	-0.1	1,392	0.0116	7.8	6.3	3.7	0.018	0.029	0.011	0.5	2,960
	11-Jun-19												1.2	1,466	0.0148	8.3	8						
	17-Jun-19	440	109	0.0003	0.41	3.1	460	<1	6.8	460	25		0.8	1,433	0.0116	8.2	8.2	3.4	<0.002	0.007	0.009	0.44	
	24-Jun-19												0	1,382	0.0164	7.58	6.4						1,430
	02-Jul-19	380	101	0.0003	0.35	4.3	450	<1	7.3	450	12		0	1,414	0.0151	8.6	6	3.9	<0.002	<0.002	<0.002	0.39	
	08-Jul-19												-0.2	1,417	0.0099	8.43	6.6						
	18-Jul-19	350	99	0.0003	0.33	2.6	480	<1	6.9	480	<0.5		-0.6	1,367	0.0088	8.7	7.2	3.1	<0.002	<0.002	<0.002	0.38	
	22-Jul-19												0.5	1,332	0.0103	8.15	6.6						
	30-Jul-19	340	102	0.0003	0.41	1.74	470	1.2	7.4	470	27	2.2	-2.5	1,354	0.0071	8.59	6.72	2.3	<0.002	<0.002	<0.002	0.44	1,770
	05-Aug-19												-1.5	1,358	0.009	8.72	6.2						
	12-Aug-19	320	101	0.0002	0.32	2.5	440	<1	6.9	450	17.6		-2.4	1,317	0.01	8.77	6	2.8	<0.02	<0.02	<0.02	0.59	
	20-Aug-19													1,280	0.007	8.24	6.3						
	28-Aug-19	330	99	0.0002	0.33	2.4	440	<1	7.1	440	26	2.9	0.6	1,304	0.013	7.95	8.7	2.8	<0.02	<0.02	<0.02	0.33	1,890
	02-Sep-19												-0.5	1,285	0.009	8.78	9.1						
	09-Sep-19	330	95	0.0002	0.31	3.3	420	<1	6.9	420	20	3.48	0	1,289	0.022	8.03		3.5	0.003	0.005	0.002	0.36	612
	23-Sep-19	300	90	0.0003	0.32	4.1	430	<1	6.9	430	6.8		-2.2	1,242	0.024	9.13	10.1	5.5	0.005	0.005	<0.002	0.39	
	07-Oct-19	320	87	0.0003	0.3	6.3	410	<1	6.9	410	9.8				0.03			7.2	0.008	0.009	<0.002	0.3	
	21-Oct-19	290	86	0.0002	0.34	7.4	410	<1	7.1	410	14.7				0.02			8.8	0.004	0.011	0.007	0.34	
	05-Nov-19	280	89	<0.0002	0.31	6	410	<1	6.8	410	7.8		0.8		0.02		12.2	6.4	<0.02	<0.02	<0.02	0.34	
	19-Nov-19	280	81	0.0002	0.42	3.9	400	<1	6.9	400	14.3		11.6	1,199	0.023	6.95	10.7	4.2	<0.02	<0.02	<0.02	0.37	
	25-Nov-19												12.6	1,175	0.018	7.27	12.6						
	02-Dec-19	230	78	<0.0002	0.48	3.4	430	<1	7.3	430	<0.5		3.8	1,141	0.013	7.9	14.4	4.2	0.006	0.007	<0.002	0.41	
	16-Dec-19	35	73	0.0005	0.99	0.37	540	<1	7	540	16.9		1.8	1,013	0.009	7.7	13.6	1.16	0.009	0.012	0.003	0.91	
	13-Jan-20	99	73	0.0004	2.1	0.37	520	<1	7.3	520	8.7		1.6	1,098	0.008	7.73	13.3	0.52	0.009	0.021	0.012	2.1	

Data Point	Date	Sulphate (g/m3)	Calcium-Dissolved (g/m3)	Antimony-Dissolved (g/m3)	Arsenic-Dissolved (g/m3)	Iron-Dissolved (g/m3)	Alkalinity - Bicarbonate (g/m3 as CaCO3)	Carbonate Alkalinity (g/m3 as CaCO3)	pH (pH unit)	Alkalinity - Total (g/m3 as CaCO3)	Ferrous Iron (g/m3)	FLS DO (%)	FLS EC (µS/cm)	FLS Flow rate (L/S)	FLS pH	FLS Temp	Iron-Total (g/m3)
REE-RDRN (Rock Drain - also known as Tree Drain)	05-Feb-18	550	95	0.0021	0.129	10.5				500		29.7	1,697		7.93	12.5	11.9
	09-Feb-18													6			
	12-Feb-18	480	87	0.0165	0.053	6.3				440		11	1,508		7.27	12.4	6.8
	21-Feb-18	570	99	0.006	0.109	9	500	<1	7.3	500		19	1,727	9	7.18	12.2	9.1
	01-Mar-18	630	102	0.0032	0.16	8.7				520		15.8	1,772	10	7.36	12.3	7.5
	06-Mar-18											8.4	1,764	10	7.42	12.1	
	12-Mar-18	580	106	0.0022	0.172	9.2				510		15.3	1,760	9	7.26	12.6	9.5
	15-Mar-18	600	99	0.0024	0.158	9.1	500	2.7	7.8	510							
	16-Mar-18													0.142			
	20-Mar-18	560	100	0.002	0.172	10.1				490	9.16	6.9	1,729	6	7.44	12	10.6
	27-Mar-18	640	97	0.0016	0.17	10.7	500	<1	6.9	500	10.05	5.6	1,721	6	7.17	12	11.4
	03-Apr-18											7.1	1,752	6	7.45	12	
	09-Apr-18	640	99	0.0016	0.22	11.8	510	<1	7.1	510		8	1,757	7	7.18	11.9	12.2
	17-Apr-18											4.5	1,629	10	7.41	12.1	
	18-Apr-18	580	100	0.0051	0.141	8.3	500	<1	7.1	500							
	23-Apr-18	670	111	0.0042	0.144	7.5		<1	6.9	550		5.9	1,865	10	7.35	12.1	6.5
	01-May-18											5.3	1,882	16	7.15	12.2	
	09-May-18	640	102	0.0024	0.175	7.6	540	<1	7.1	540							7.7
	16-May-18	610	108	0.0024	0.181	8.1	520	1	7.3	520		6.2	1,803		7.47	12.1	
	21-May-18	560	100	0.0024	0.189	8	510	<1	6.9	510	5.04	6.2	1,752	15	7.23	12.1	7.9
	28-May-18											7.9	1,925	25	7.48	12.1	
	05-Jun-18	660	109	0.0022	0.151	6.5	550	<1	7	550		3.2	1,886		7.93	12.3	6.3
	12-Jun-18	630	106	0.0021	0.189	7.6	530	1.1	7.3	530							
	18-Jun-18	620	100	0.0018	0.185	7.4	520	1.4	7.4	520	8.8	11.1	1,771	14	7.04	11.8	7.4
	26-Jun-18											17	1,664	6	7.45	11.7	
	02-Jul-18	700	93	0.0018	0.2	8.8	490	<1	6.9	490	10.8	10.1	1,694	6	7.18	11.8	8.8
	11-Jul-18	560	98	0.0031	0.177	7.4	490	1.3	7.4	500				14			
	12-Jul-18											5.6	1,778	14	7.35	12.1	
	16-Jul-18	660	103	0.0029	0.159	6.4	550	<1	7	550	7.64	6.9	1,867	20	7.18	11.9	6.4
	23-Jul-18											2.7	1,722	23	7.29	12.2	
	30-Jul-18	580	98	0.0024	0.149	5.4											5.2
	14-Aug-18	600	93	0.0024	0.165	6	500	<1	7	500	6.4	6	1,737	20	7.39	12.1	5.7
	20-Aug-18											7.3	1,694	14	7.36	11.9	
	23-Aug-18	540	97	0.0026	0.18	6.6	470	<1	7.2	470							
	28-Aug-18	580	95	0.0027	0.194	6.7	490	<1	7.3	490	6.84	6.2	1,688	14	7.29	12	6.7
	03-Sep-18											7	1,640	12	7.31	12	
	11-Sep-18	550	86	0.0025	0.2	7.2	490	<1	7.2	490		8.6	1,626	10	7.3	12.1	7.3
	17-Sep-18	500	97	0.002	0.18	8.6	490	<1	7.1	490		4.1	1,602		7.37	12.2	
	24-Sep-18	500	88	0.0017	0.169	8.8	470	<1	6.9	470		5.7	1,583	6	7.43	12.1	8.4
	01-Oct-18											5.4	1,578	4	7.55	12.2	
	08-Oct-18	490	83	0.0015	0.22	10.7	480	<1	6.8	480	10.2	8.5	1,590		7.46	12.1	10.7
	15-Oct-18											14.7	1,598	3	7.46	12.6	
	17-Oct-18	500	82	0.0015	0.22	10.7	490	<1	6.8	490				3			
	24-Oct-18	500	90	0.0014	0.161	8.8	490	<1	7	490		13.9	1,620	1.75	7.37	12.2	9.7
	01-Nov-18											10.9	1,636	1.5	7.4	21.1	
	06-Nov-18	520	89	0.0015	0.18	11.4	480	<1	7	490	11.08	18.8	1,625	1	7.39	12	10.9
	12-Nov-18											9.7	1,640	4	7.53	12.1	
	20-Nov-18	580	95	0.0026	0.2	9.9	500	<1	7	500		12.5	1,725	6	7.4	11.9	10.5
	21-Nov-18	580	91	0.0025	0.22	10.6	520	<1	6.9	520							
	27-Nov-18											8.1	1,697	3	7.45	12.1	
	03-Dec-18	520	92	0.0014	0.186	11.6	500	<1	6.8	500		8.6	1,692	2.5	7.5	12.1	11.8
	12-Dec-18											14.2	1,690	3	7.4	12.8	
	13-Dec-18	590	100	0.002	0.22	11.8	500	<1	7.2	500				3			
	18-Dec-18	560	98	0.0017	0.23	10.5	510	<1	7	510		5.3	1,711	3	7.54	12.1	13.3
	21-Dec-18											13.5	1,719	3	7.47	12.2	
	09-Jan-19											14.5	1,685	2	7.5	12.3	
	14-Jan-19	570	89	0.0013	0.153	11.3	510	<1	7	510	11.36	10	1,733	1.5	7.44	12	13
	21-Jan-19											11.4	1,735	1	7.55	12	
	22-Jan-19	560	95	0.0013	0.165	12	510	<1	6.9	510				1			
	30-Jan-19	570	98	0.0013	0.138	11.5	520	<1	7	520	10.8	19.7	1,753	1	7.59	12.7	12.9
	06-Feb-19											12.6	1,752	0.001	7.39	12.1	
	11-Feb-19	540	109	0.0012	0.156	12.5	520	<1	6.7	520		20	1,743	0.0001	7.33	12.3	13
	18-Feb-19											29	1,755	0.001	7.48	12.1	
	18-Feb-19	530	98	0.0013	0.136	11.3	520	<1	7.2	520				0.001			
	12-Mar-19	580	95	0.0025	0.055	8.3	520	<1	7.3	520				0.0001			
	03-Apr-19	580	108	0.0185	0.054	5.6	510	<1	7	510							5.7
	10-Apr-19	640	116	0.0085	0.083	7.7	530	<1	7.3	530							
	11-Apr-19				0.0033												
	23-Apr-19	610	105	0.003	0.128	9.7	510	<1	6.8	510	10.08	12.9	1,809		7.48	12.2	10.4
	30-Apr-19	560		0.0083	0.079	7.6							1,593		7.41	10.3	7.9
	06-May-19	660	109	0.0026	0.125	7.2	520	<1	6.8	520	8.4	19.8	1,872		7.75	12	9.2
	13-May-19											23.8	1,799		7.52	11.9	
	16-May-19	660	110	0.0041	0.161	9.6	520	<1	6.9	520							
	21-May-19	610	118	0.0027	0.127	7.6	510	<1	7.1	510	7.8	20.8	1,821		7.5	12	8
	27-May-19											19.8	1,914		7.47	12.1	
	05-Jun-19	800	123	0.0119	0.031	3	570	<1	7.1	570	2.48	41.1	2,054		7.51	11.8	3.8
	11-Jun-19	1,010	131	0.008	0.074	4.7	580	<1	6.8	580		57	1,960		7.59	12.2	
	17-Jun-19	920	119	0.0048	0.133	6.3	540	<1	6.8	540		5.3	1,967		7.52	12.5	5
	24-Jun-19											6.8	1,899	5	7.79	12.4	
	02-Jul-19	630	104	0.0026	0.19	8.1	520	<1	6.8	520		5.9	1,865		7.48	12.3	6.9
	08-Jul-19											7.1	1,851		7.55	12.3	
	18-Jul-19	590	101	0.0027	0.167	5.8	520	<1	6.8	520		5.3	1,765		7.47	12.2	5.7
	22-Jul-19											3	1,904		7.52	12.3	
	23-Jul-19	660	104	0.003	0.13	5.6	580	<1	6.8	580							
	30-Jul-19	660	109	0.0026	0.154	5.8	550	1.4	7.4	550	5.72	6.1	1,874		7.85	12.5	5.8
	05-Aug-19											7.8	1,762		7.55	12.4	
	12-Aug-19	580	102	0.0024	0.152	6.3	510	<1	6.9	510		8.5	1,740		7.58	11.7	6.1
	20-Aug-19	620	102	0.0023	0.162	5.4	530	<1	7.1	530			1,788		7.49	12.5	
	28-Aug-19	570	94	0.0021	0.189	5.9	510	<1	7.1	520	5.84	2.4	1,717		7.64	12.5	5.5
	02-Sep-19											4.2	1,708		7.43	12.5	
	09-Sep-19	540	91	0.002	0.22	6.7	510	<1	7	510	6.72	6	1,671		8.42		6.1
	11-Sep-19	500	97	0.0026	0.23	7.3	510	<1	7	510							
	23-Sep-19	520	91	0.0021	0.22	6	510	<1	6.8	510		7	1,664		7.66	12.3	8.1
	07-Oct-19	550	96	0.0023	0.174	5	540	<1	7	540							5.7
	16-Oct-19	530	91	0.0022	0.196	5.6	510	<1	7	510							
	21-Oct-19	510	91	0.0019	0.21	6.4	500	<1	7.3	500							7.1
	05-Nov-19	510	95	0.0022	0.22	6.6	490	<1	6.8	490		8.1				12.4	6.6
	19-Nov-19	520	85	0.0022	0.2	6.5	490	<1	6.9	490		8.9	1,603		7.36	12.3	6.4
	21-Nov-19	530	90	0.0024	0.2	6.3	500	1.1	7.4	510							
	02-Dec-19	500	88	0.0024	0.21	6.5	490	<1	6.7	500		12.9	1,597		7.6	12.5	6.9
	16-Dec-19	530	94	0.0022	0.167	5.5	520	<1	7	520		12.7	1,680		7.82	12.4	5.4
	08-Jan-20	470	87	0.0022	0.22	7	480	<1	7.1	480							
	13-Jan-20	440	80	0.002	0.18	6.4	470	2.1	7.7	470		2	1,515		7.61	12.2	6.4

Data Point	Date	Sulphate (g/m3)	Calcium-Dissolved (g/m3)	Antimony-Dissolved (g/m3)	Arsenic-Dissolved (g/m3)	Iron-Dissolved (g/m3)	Alkalinity - Bicarbonate (g/m3 as CaCO3)	Carbonate Alkalinity (g/m3 as CaCO3)	pH (pH unit)	Alkalinity - Total (g/m3 as CaCO3)	Driving Head (mm)	Ferrous Iron (g/m3)	FLS DO (%)	FLS EC (µS/cm)	FLS Flow rate (L/S)	FLS pH	FLS Temp (°C)	Iron-Total (g/m3)
	09-Feb-18														0.347			
	12-Feb-18	490	87	0.0142	0.0063	<0.02				460			81.5	1,576		7.66	15.1	0.063
	16-Feb-18														0.124			
	21-Feb-18	590	101	0.0148	0.0069	<0.02	490	2.4	7.7	500			79.5	1,724	0.074	7.65	14.3	<0.021
	01-Mar-18	620	104	0.02	0.0105	<0.02				500			74.4	1,733	0.027	7.52	15.7	0.037
	06-Mar-18												71.4	1,734	0.078	7.37	17.4	
	12-Mar-18	610	105	0.0035	0.009	<0.02				500			78.7	1,728	0.172	7.44	13.7	0.21
	16-Mar-18														8			
	20-Mar-18	560	100	0.0058	0.0075	<0.02				500		0.02	74.2	1,708	0.86	7.53	14.2	0.095
	27-Mar-18	610	98	0.0043	0.0067	<0.02	490	1.3	7.5	490		0.02	73.8	1,685	0.106	7.47	13.8	0.22
	03-Apr-18												64.7	1,688	0.114	7.45	13.8	
	09-Apr-18	640	97	0.0044	0.0058	<0.02	490	4.5	8	490			55.7	1,724		7.31	12.3	0.45
	13-Apr-18																	
	17-Apr-18												77.5	1,574	0.179	7.39	12.8	
	23-Apr-18	640	109	0.0046	0.0062	<0.02	510	5.1	8	520		0.1	67.1	1,821	0.095	7.35	11.4	0.069
	01-May-18												76.4	1,759	0.204	7.61	12.6	
	09-May-18	490	77	0.053	0.0068	<0.02	400	2.1	7.7	400		4.5	73.8	1,473	0.12	7.52	12.6	0.094
	16-May-18	410	72	0.072	0.0069	<0.02	350	1.9	7.8	350			77.2	1,296	0.108	7.98	11	
	21-May-18	175	30	0.24	0.039	0.04	153	<1	7.7	154		0.11	80.2	597.2	0.182	7.75	8.9	2.5
	05-Jun-18	270	51	0.146	0.016	0.04	250	<1	7.6	250		0.09	78.6	1,012	0.155	7.72	6.8	1.22
	11-Jun-18												81.3	980	0.133	7.79	8.1	
	18-Jun-18	240	41	0.21	0.023	<0.02	210	1.2	7.8	210		0.06	78.4	856	0.107	7.6	7.5	0.71
	02-Jul-18	620	94	0.034	0.02	<0.02	490	2.5	7.7	490		0.03	71.5	1,646	0.152	7.46	9.5	0.2
	12-Jul-18												71.9	1,604	0.083	7.53	9.4	
	16-Jul-18	620	95	0.036	0.017	<0.02	500	1.7	7.6	500		0.21	66	1,429	0.036	7.55	8.6	0.025
	23-Jul-18												75.1	1,748	0.103	7.45	9	
	30-Jul-18	570	96	0.025	0.015	<0.02									0.03			<0.021
	06-Aug-18												72	1,736	0.042	7.55	7.4	
	14-Aug-18	590	94	0.0084	0.032	<0.02	500	4.7	8	510		0.04	75.4	1,707	0.286	7.52	10.7	0.93
	20-Aug-18												73.2	1,666	0.15	7.55	9.5	
	28-Aug-18	550	95	0.0122	0.012	<0.02	480	1.9	7.6	490		0.03	66.2	1,639	0.112	7.42	9.5	0.023
	03-Sep-18												62.6	1,651	0.016	7.55	9	
	11-Sep-18	550	88	0.0068	0.03	0.04	480	3.6	7.9	480			74.7	1,598	0.24	7.54	11.5	0.9
	17-Sep-18	500	95	0.0103	0.0116	<0.02	470	2.1	7.7	470	235		75.3	1,580	0.089	7.74	12	
	24-Sep-18	500	87	0.0148	0.011	<0.02	470	2.4	7.7	470			72.9	1,565	0.025	7.78	11.9	0.032
	01-Oct-18										210		73.4	1,541	0.057	7.54	11.2	
	08-Oct-18	500	92	0.0072	0.0099	<0.02	460	1.3	7.5	470	320	0.09	70.4	1,551		7.52	11.9	1.16
	15-Oct-18										170		67.2	1,555	0.066	7.5	12.5	
	24-Oct-18	520	88	0.0049	0.0111	0.03	480	3.5	7.9	490	400		73.7	1,585	0.283	7.63	13.3	2.1
	01-Nov-18												66.3	1,589	0.087	7.6	13.3	
	06-Nov-18	510	87	0.0082	0.0085	0.05	460	3.3	7.9	470	225	0.09	76	1,576	0.104	7.64	12.4	0.65
	12-Nov-18												77.1	1,523	0.127	7.76	11.7	
REE-VFR (Vertical Flow Reactor)	20-Nov-18	570	95	0.0076	0.0069	<0.02	490	2.7	7.8	490	130		69.7	1,683	0.03	7.64	11.3	0.091
	27-Nov-18										320		77.5	1,675	0.129	7.54	13.6	
	03-Dec-18	520	95	0.0077	0.0079	<0.02	490	2.3	7.7	490			72.2	1,661	0.057	7.7	15.9	0.21
	12-Dec-18										470		68.3	1,630	0.029	7.78	17.5	
	18-Dec-18	570	93	0.0052	0.0128	<0.02	500	2.9	7.8	500			83.1	1,676	0.197	7.69	14.6	1.63
	21-Dec-18										650		73.7	1,666	0.161	7.65	13.6	
	09-Jan-19										650		77.5	1,699	0.162	7.44	14.9	
	14-Jan-19	570	98	0.0067	0.007	<0.02	500	2.2	7.7	500	490	0.03	70	1,707	0.09	7.58	14.6	0.32
	21-Jan-19										680		77.5	1,686	0.137	7.52	14.1	
	30-Jan-19	570	96	0.0085	0.0074	<0.02	500	2.5	7.7	500	430	0.04	69.9	1,717	0.047	7.75	17.8	0.088
	31-Jan-19																	
	01-Feb-19																	
	06-Feb-19																	
	11-Feb-19																	
	18-Feb-19										100		83.9	1,723	0.115	7.71	14	
	02-Apr-19																	<0.42
	23-Apr-19	600	106	0.0099	0.009	<0.02	500	2.3	7.7	500	70	0.05	77.5	1,776	0.086	7.67	12.3	0.041
	30-Apr-19										50			1,673	0.049	7.56	9.6	
	06-May-19	650	106	0.0093	0.0095	<0.02	510	2.1	7.6	510	50	0.2	78.1	1,814	0.0732	7.67	11.5	0.03
	13-May-19										40		81	1,788	0.022	7.66	10.8	
	21-May-19	600	110	0.0062	0.0089	<0.02	500	4.2	8	500	80	0.01	80	1,760	0.166	7.64	10.2	0.06
	27-May-19										60		70.5	1,881	0.0808	7.67	11.2	
	05-Jun-19	760	119	0.0061	0.0076	<0.02	550	2.3	7.7	550	90	0.02	78.1	1,987	0.1382	7.74	8.6	0.088
	11-Jun-19										60		81.83	1,996	0.1907	7.69	10.4	
	17-Jun-19	830	119	0.0062	0.0093	<0.02	540	2	7.6	540	120		75.7	1,961	0.3041	7.81	9.4	0.24
	24-Jun-19										130		70.2	1,896	0.1779	7.78	8.6	
	02-Jul-19	650	110	0.0066	0.0075	<0.02	510	3.5	7.9	520	105		76.1	1,861	0.0315	7.7	7.5	0.023
	08-Jul-19										210		65.9	1,805	0.1317	7.78	8.7	
	18-Jul-19	590	93	0.0048	0.0068	<0.02	490	1.6	7.5	490	120		69	1,690	0.0991	7.9	9	0.064
	22-Jul-19										130		61	1,796	0.0669	7.79	9	
	30-Jul-19	670	109	0.0057	0.0078	<0.02	550	4.5	7.9	560	115	0.03	63.8	1,885	0.0748	7.79	9.6	<0.021
	05-Aug-19										120		73.7	1,736	0.2374	7.9	7.9	
	12-Aug-19	580	102	0.0039	0.0099	<0.02	500	2.1	7.6	500	145		52.9	1,710	0.1873	8.28	8.9	0.087
	20-Aug-19										120			1,771	0.0952	7.98	8.6	
	28-Aug-19	570	95	0.0038	0.0081	<0.02	500	2.7	7.7	510	130	-0.01	69.3	1,706	0.1026	8.37	10.2	0.037
	02-Sep-19										120		59.9	1,703	0.0547	7.95	11.9	
	09-Sep-19	560	94	0.0043	0.0064	<0.02	500	2	7.6	500	120	0.03	45.9	1,670	0.0331	9.06		<0.021
	23-Sep-19	510	90	0.0068	0.0073	<0.02	470	1.7	7.6	480	100		54.6	1,584	0.024	7.96	10.5	0.025
	07-Oct-19	560	95	0.0037	0.0092	<0.02	520	2.4	7.7	530	300				0.161			0.034
	21-Oct-19	500	91	0.0052	0.0078	<0.02	490	2.7	7.8	490	230				0.083			<0.021
	05-Nov-19	510	95	0.0058	0.0077	<0.02	470	1.7	7.6	480	210		59.9		0.067		14.8	<0.021
	19-Nov-19	490	85	0.0036	0.0077	<0.02	480	4.1	8	480	315		73.8	1,556	0.099	7.69	11.1	0.026
	25-Nov-19										270		13.9	1,607	0.091	7.53	13.9	
	02-Dec-19	510	86	0.0053	0.0099	<0.02	480	9.4	8.3	490	190		50.8	1,577	0.056	7.86	15.6	0.023
	16-Dec-19	530	95	0.0033	0.009	<0.02	510	3	7.8	510	370		76.6	1,649	0.143	7.86	13.5	0.28
	13-Jan-20	410	82	0.0022	0.037	0.09	470	2.7	7.8	470	710		84.8	1,510	0.45	7.84	12.4	0.84

Data Point	Date	Arsenic-Dissolved (g/m3)	Iron-Dissolved (g/m3)	Ferrous Iron (g/m3)	FLS DO (%)	FLS EC (µS/cm)	FLS Flow rate (L/S)	FLS pH	FLS Temp (°C)	Iron-Total (g/m3)
REE-VFRIN (VFR In from RDRN)	09-Feb-18						0.347			
	16-Feb-18						0.124			
	21-Feb-18						0.73			
	01-Mar-18						0.027			
	06-Mar-18						0.078			
	12-Mar-18						0.172			
	16-Mar-18						0.142			
	20-Mar-18						0.086			
	26-Mar-18						0.106			
	03-Apr-18						0.114			
	17-Apr-18						0.179			
	23-Apr-18						0.095			
	01-May-18						0.043			
	09-May-18	0.067	3.9	8.6	40	1,808	0.069	7.46	16.1	10
	16-May-18				30.5	1,754	0.043	7.62	12	
	21-May-18						0.021			
	28-May-18						0.084			
	05-Jun-18		4.3	4.48	32.2	1,896	0.084	7.25	9.7	5.2
	11-Jun-18				73.3	1,795	0.037	7.5	11.7	
	18-Jun-18	0.051	5.9	6.52	30.7	1,721	0.014	7.27	10.3	5.9
	26-Jun-18				74	1,683	0.278	7.3	11.4	
	02-Jul-18	0.127	5.4	5.8	53	1,683	0.14	7.26	11.9	5.7
	12-Jul-18				33.9	1,766	0.057	7.27	13.2	
	16-Jul-18	0.07	4.1	4.46	18.1	1,867	0.029	7.23	11.3	4.9
	23-Jul-18				47.4	1,713	0.02	7.36	12.2	
	30-Jul-18	0.049	3.3				0.026			3.7
	06-Aug-18				19.2	1,769	0.037	7.44	12	
	14-Aug-18	0.134	4.1	4.1	73.6	1,737	0.064	8.1	12.4	4
	20-Aug-18				42.2	1,684	0.03	7.44	11.7	
	28-Aug-18	0.089	3.7		22	1,684	0.158	7.37	12.7	4.5
	03-Sep-18				30.6	1,634	0.015	7.44	12.1	
	11-Sep-18	0.147	4.7		62.8	1,620	0.271	7.53	12.5	5.4
	24-Sep-18	0.053	4.2		24	1,575	0.019	7.41	14.5	5.7
	01-Oct-18				24.5	1,550	0.081	7.45	13.2	
	08-Oct-18	0.114	5.5		54.8	1,577	0.137	7.54	12.8	6.3
	15-Oct-18				26.9	1,606	0.39	7.44	21.5	
	24-Oct-18	0.105	5.5		73.6	1,612	0.272	7.66	13.1	6.5
	01-Nov-18				45.4	1,619	0.048	7.46	19.6	
	06-Nov-18	0.132	8.5		76.5	1,615	0.242	7.53	12.9	8.6
	12-Nov-18				74.3	1,629	0.162	7.73	11.8	
	20-Nov-18	0.086	4.2		22.3	1,709	0.029	7.59	11.8	5.8
	27-Nov-18				61.3	1,685	0.127	7.44	13.3	
	03-Dec-18	0.069	4.4		41.5	1,683	0.057	7.52	15.5	5.3
	12-Dec-18				24.7	1,691	0.025	7.4	20.6	
	18-Dec-18	0.168	6.9		77.9	1,702	0.263	7.73	13.4	12.3
	21-Dec-18				70.3	1,697	0.157	7.5	13.7	
	09-Jan-19				66.4	1,726	0.167	7.51	13.9	
	14-Jan-19	0.09	6.5		55.7	1,727	0.097	7.67	13.3	7
	21-Jan-19				71.45	1,716	0.162	7.59	13	
	30-Jan-19	0.048	4.1		43.1	1,746	0.056	7.66	16.7	5.2
	18-Feb-19				64.5	1,738	0.116	7.46	13.5	
	23-Apr-19	0.065	1.75	1.6	57.9	1,788	0.082	7.46	15.6	2.4
	30-Apr-19					1,594	0.0273	7.49	8.1	
	06-May-19	0.059	1.64		63.2	1,853	0.0755	7.54	11.6	2.2
	13-May-19				69.8	1,807	0.0251	7.53	11.6	
	21-May-19	0.073	3.9		73.3	1,808	0.186	7.53	12	4.3
	27-May-19				51.9	1,893	0.0883	7.47	13.2	
	05-Jun-19	0.0163	1.24		80.3	2,090	0.158	7.81	10.9	3.1
	11-Jun-19				76	1,997	0.1439	7.54	12.2	
	17-Jun-19	0.103	3.6		73.8	1,930	0.2241	7.65	11.7	3.1
	24-Jun-19				66.4	1,897	0.1397	7.74	12.8	
	02-Jul-19	0.069	2.9		39.8	1,841	0.034	7.54	11.2	3.2
	08-Jul-19				66.9	1,824	0.1379	7.88	11.9	
	18-Jul-19	0.097	3.5		62.6	1,749	0.0998	7.78	12	3.6
	22-Jul-19				51.5	1,886	0.0683	7.64	11	
	30-Jul-19	0.044	2.3		26	1,852	0.0397	7.54	11.8	4.5
	05-Aug-19				78.4	1,751	0.3187	8.01	11.3	
	12-Aug-19	0.097	2.1		66.5	1,288	0.1954	8	11.7	5.3
	20-Aug-19					1,761	0.1008	7.82	12	
	28-Aug-19	0.077	1.54		66	1,706	0.1121	8.48	12.2	2.2
	02-Sep-19				37	1,698	0.0665	7.87	16.6	
	09-Sep-19	0.054	2.3		15.7	1,679	0.0332	8.6		3.7
	23-Sep-19	0.047	2.4		36	1,648	0.027	8.01	11.3	2.9
	07-Oct-19	0.114	1.3				0.17			2.6
	21-Oct-19	0.099	2.2				0.085			7.2
	05-Nov-19	0.081	1.5		51		0.068		14.5	2.2
	19-Nov-19	0.072	1.72		83.5	1,584	0.188	7.42	12.5	2.8
	25-Nov-19				12.9	1,622	0.103	7.47	12.9	
	02-Dec-19	0.105	2.6		78.6	1,588	0.054	7.88	15.3	2.8
	16-Dec-19	0.105	2.8		74.2	1,642	0.151	7.7	13.9	2.9
	13-Jan-20	0.151	3.6		86.6	1,521	0.37	7.79	12.5	3.8

Appendix 3. Statistic Summary Tables

Table 1: Results from one way analysis of variance and tukey test testing the effect of treatment on iron removal.

Anova Test				
Effect of treatment on: Iron removal	Df	F value	Pr(>F)	
	5	12.38	<0.001	***
TUKEY Test				
	Difference	Lower	Upper	P-Value adjusted
TANK 2 - TANK 1	-21.656030	-37.246562	-6.0654970	0.00121860
TANK 3 - TANK 1	-3.935123	-19.622793	11.7525481	0.97929940
TANK 4 - TANK 1	-16.015251	-31.605784	-0.4247189	0.04020440
TANK 5 - TANK 1	4.292482	-11.115699	19.7006633	0.96724890
TANK 6 - TANK 1	14.968459	-0.528995	30.4659126	0.06506880
TANK 3 - TANK 2	17.720907	2.033236	33.4085777	0.01669100
TANK 4 - TANK 2	5.640778	-9.949755	21.2313107	0.90416760
TANK 5 - TANK 2	25.948512	10.540331	41.3566928	0.00003430
TANK 6 - TANK 2	36.624488	21.127034	52.1219421	0.00000000
TANK 4 - TANK 3	-12.080129	-27.767800	3.6075420	0.23598670
TANK 5 - TANK 3	8.227605	-7.278856	23.7340665	0.64899210
TANK 6 - TANK 3	18.903581	3.308409	34.4987532	0.00769400
TANK 5 - TANK 4	20.307734	4.899553	35.7159147	0.00262940
TANK 6 - TANK 4	30.983710	15.486256	46.4811640	0.00000040
TANK 6 - TANK 5	10.675976	-4.638018	25.9899702	0.34381640

Table 2: Results from one way analysis of variance and tukey test testing the effect of treatment on arsenic removal.

Anova Test				
Effect of treatment on: Arsenic removal	Df	F value	Pr(>F)	
	5	14.51	<0.001	***
TUKEY Test				
	Difference	Lower	Upper	P-Value adjusted
TANK 2 - TANK 1	-24.713340	-36.926475	-12.500205	0.0000003
TANK 3 - TANK 1	-0.606868	-12.896098	11.682362	0.9999919
TANK 4 - TANK 1	-23.764629	-35.977763	-11.551494	0.0000009
TANK 5 - TANK 1	-9.160824	-21.231110	2.909462	0.2508221
TANK 6 - TANK 1	-2.159142	-14.299362	9.981078	0.9957246
TANK 3 - TANK 2	24.106472	11.817242	36.395702	0.0000007
TANK 4 - TANK 2	0.948711	-11.264424	13.161846	0.9999235
TANK 5 - TANK 2	15.552516	3.482229	27.622802	0.0035776
TANK 6 - TANK 2	22.554198	10.413978	34.694418	0.0000032
TANK 4 - TANK 3	-23.157760	-35.446990	-10.868530	0.0000022
TANK 5 - TANK 3	-8.553956	-20.701232	3.593321	0.3323829
TANK 6 - TANK 3	-1.552274	-13.769043	10.664496	0.9991454
TANK 5 - TANK 4	14.603805	2.533518	26.674091	0.0078637
TANK 6 - TANK 4	21.605487	9.465266	33.745707	0.0000095
TANK 6 - TANK 5	7.001682	-4.994821	18.998185	0.5485871

Table 3: Results from one way analysis of variance and tukey test testing the effect of treatment on sulphate removal.

Anova Test				
Effect of treatment on:	Df	F value	Pr(>F)	
Sulphate removal	5	3.994	0.002	**
TUKEY Test				
	Difference	Lower	Upper	P-Value adjusted
TANK 2 - TANK 1	-6.532324	-17.200077	4.1354290	0.49323180
TANK 3 - TANK 1	0.051730	-10.691951	10.7954110	1.00000000
TANK 4 - TANK 1	-7.589055	-18.184484	3.0063730	0.31251870
TANK 5 - TANK 1	4.799761	-5.726691	15.3262130	0.77856800
TANK 6 - TANK 1	3.904365	-6.691063	14.4997940	0.89665340
TANK 3 - TANK 2	6.584054	-4.159627	17.3277350	0.49231770
TANK 4 - TANK 2	-1.056731	-11.652160	9.5386970	0.99973600
TANK 5 - TANK 2	11.332085	0.805633	21.8585370	0.02668660
TANK 6 - TANK 2	10.436689	-0.158739	21.0321180	0.05618750
TANK 4 - TANK 3	-7.640785	-18.312656	3.0310860	0.31295910
TANK 5 - TANK 3	4.748031	-5.855361	15.3514230	0.79150240
TANK 6 - TANK 3	3.852635	-6.819236	14.5245060	0.90451160
TANK 5 - TANK 4	12.388817	1.935667	22.8419660	0.01002970
TANK 6 - TANK 4	11.493420	0.970814	22.0160270	0.02330620
TANK 6 - TANK 5	-0.895396	-11.348546	9.5577540	0.99987510

Table 4: Results from one way analysis of variance and tukey test testing the effect of treatment on Sulphide concentration.

Anova Test				
Effect of treatment on:	Df	F value	Pr(>F)	
Sulphide concentrations	5	3.504	0.007	**
TUKEY Test				
	Difference	Lower	Upper	P-Value adjusted
TANK 2 - TANK 1	-117.309868	-353.334840	118.7151100	0.69518050
TANK 3 - TANK 1	92.637500	-172.999850	358.2748500	0.91025620
TANK 4 - TANK 1	-92.888816	-328.913790	143.1361600	0.85874010
TANK 5 - TANK 1	1.273864	-271.175800	273.7235300	1.00000000
TANK 6 - TANK 1	261.208929	-54.012430	576.4302900	0.16175560
TANK 3 - TANK 2	209.947368	-46.544830	466.4395600	0.17196360
TANK 4 - TANK 2	24.421053	-201.261990	250.1041000	0.99956270
TANK 5 - TANK 2	118.583732	-144.957280	382.1247500	0.77609110
TANK 6 - TANK 2	378.518797	70.964650	686.0729400	0.00720870
TANK 4 - TANK 3	-185.526316	-442.018510	70.9658800	0.29132180
TANK 5 - TANK 3	-91.363636	-381.724240	198.9969600	0.94040590
TANK 6 - TANK 3	168.571429	-162.253240	499.3961000	0.67235660
TANK 5 - TANK 4	94.162679	-169.378340	357.7037000	0.90145440
TANK 6 - TANK 4	354.097744	46.543600	661.6518900	0.01462210
TANK 6 - TANK 5	259.935065	-76.384110	596.2542300	0.22389890

Appendix 4. Photographs

A.

B.

C.

D.

Figure 1. Photographs of the set up of the bioreactors. A: Underdrain pipes being covered with drainage gravel; B: Underdrain pipes being installed; C: Biosolids being delivered to load up area; and D: Truck being loaded with substrates.

A.

B.

C.

D.

Figure 2. Photographs of the bioreactor substrates at load up site. A: front to back: Bark, compost and sawdust; B: Bark inside the digger bucket ready to be loaded; C: sawdust in digger bucket ready to be loaded; and D: compost in digger bucket ready to be loaded.

A.

B.

C.

D.

Figure 3. Photographs of the substates, substrates being mixed and loaded out. A: Mussel shells inside and IBC; B: Biosolids inside of IBC; C: Materials being mixed in the back of dump truck; and D: Substrates being carefully loaded into the tanks.

A.

B.

C.

Figure 4: Photographs of the substrates being mixed and loaded. A: Truck being loaded with sawdust; B: Mixed materials being unloaded into tanks; and C: Materials being mixed in the back of dump truck.

A.

B.

C.

D.

Figure 5: Photographs of the Bioreactor set up and substrate sampling. A:Tank 4 being loaded with materials; B: Materials being raked flat inside the tanks; C: Samples of the substrates for analysis being taken; and D: Feed IBC piping being done just before systems were turned on.

A.

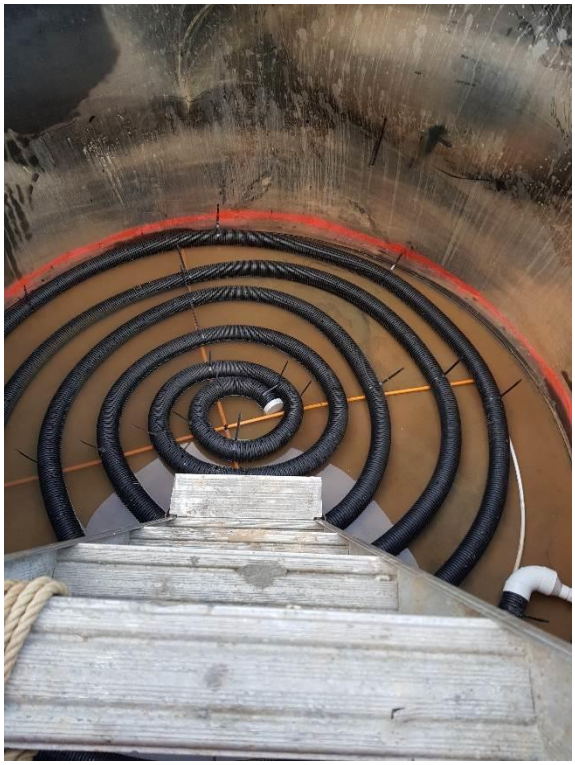

B.

C.

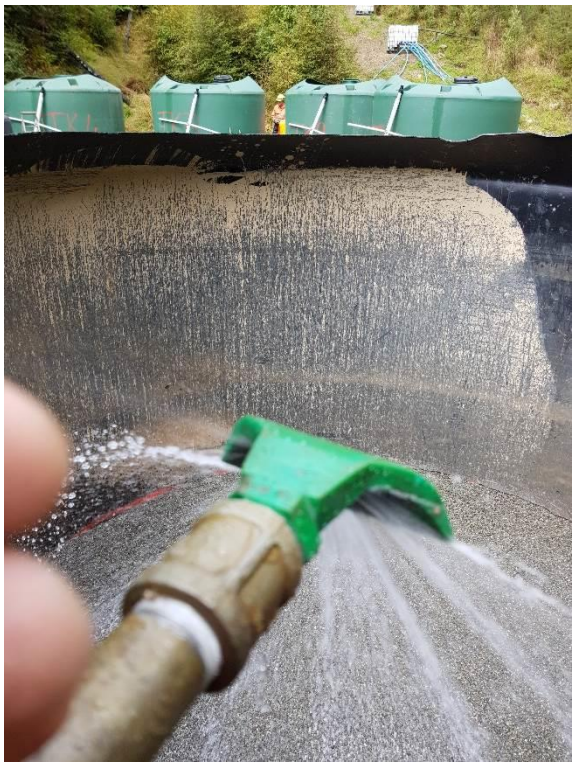

D.

Figure 6: Photographs of the vertical flow reactor set up. A: Installation of underdrain; B: Drainage gravel being placed inside tank by digger; C: Spray nozzle being turned on for the first time; and D: Operational Vertical flow reactor discharging to the sump on the right.

A.

B.

C.

Figure 7: Photographs of samples and the operational bioreactors. A:Samples from the bioreactors; B: Effluent pipes from the bioreactors discharging into sump; and C: IBC feed tank with the inlet lines to the bioreactors.

A.

B.

C.

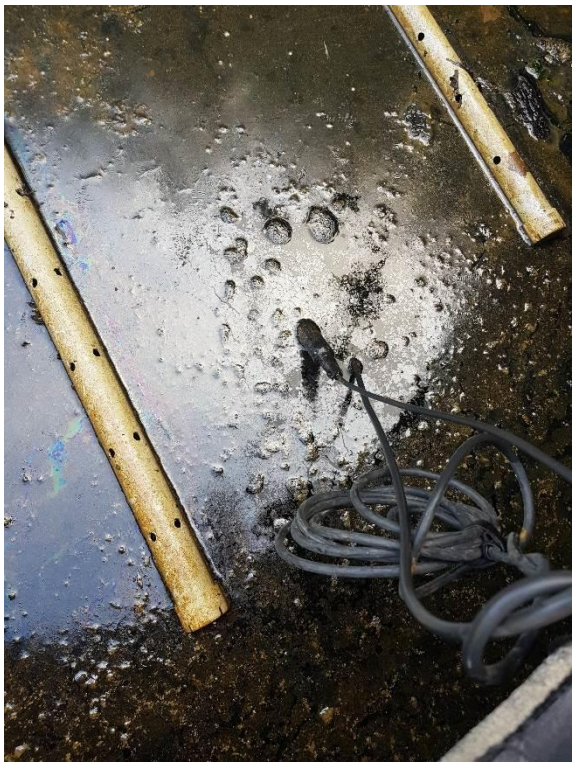

D.

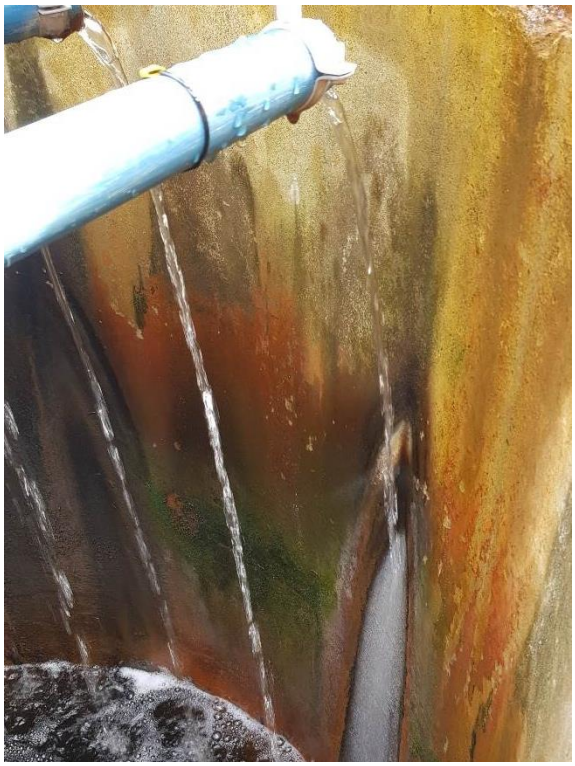

Figure 8: Photographs of the bioreactor sampling and field measurements. A: Sulphide field measurements with the portable spectrometer; B:Suphide field measurements with the portable spectrometer; C:Probes in the free water in the top of the bioreactors measuring physico-chemical properties; and D: Effluent from the tanks where the samples are taken.

A.

B.

C.

Figure 9: Photographs the bioreactor layout, influent feed tank and discharge sump. A: Bioreactor layout, in the foreground from left: Tank 1, Tank 2, Tank 3, and Tanks 4; B: Influent water inside the influent feed tank/IBC; and C: Sampling of the effluent at the collection sump where tanks discharge.

A.

B.

C.

Figure 10: Photographs of the vertical flow reactor. A: The vertical flow reactor with both the RDRN and TSF water influents; B:Vertical flow reactor with just the RDRN water influent; and C:the first round of sludge sampling from the vertical flow reactor.

A.

B.

C.

D.

Figure 11: Photographs of the bioreactor field measurements and of the vertical flow reactor and its sludge. A: Physico chemical field measurements being undertaken on tank 5; B: Ferrous iron field measurements with the portable spectrometer; C: Sludge from the second round of sludge sampling from the vertical flow reactor; and D: the vertical flow reactor overtopping.

A.

B.

C.

Figure 10: Photographs of arsenic speciation and the vertical flow reactor after being drained. A: Sample preparation for arsenic speciation at the CRL Lab in Christchurch; B: Prepped samples for the arsenic speciation; and C: The vertical flow reactor after being drained for the second time prior to sludge sampling.